The Importance of Aquaporins in *Arabidopsis thaliana* Germination and Seedling Establishment

A thesis submitted to
the University of Warwick
for the degree of
Doctor of Philosophy

Charlotte Elizabeth Ella Carroll
School of Life Sciences
University of Warwick
September 2014

Contents

List of Figures

List of tables

Abbreviations

ABA	Abscisic acid
ANOVA	Analysis of variance
APS	Ammonium persulphate
AQP1	Aquaporin 1
ARF-GEF	ADP-ribosylation factor-guanine nucleotide exchange factors
Ar/R	Aromatic/arginine region
ATP	Adenosine triphosphate
BFA	Brefeldin A
BSA	Bovine serum albumin
CaMV	Cauliflower mosaic virus
cDNA	Copy deoxyribonucleic acid
Col-0	*Arabidopsis thaliana* ecotype Columbia
COP	Coat protein complex
C-terminal	Carboxy-terminal
CT reporter	C-terminal tail reporter protein
DAG	Days after germination
DEPC	Diethylpyrocarbonate
DEX	Dexamethasone
dH_2O	Distilled water
DMSO	Dimethyl sulfoxide
DNA	Deoxyribonucleic acid
dNTP	Deoxyribonucleoside 5'-triphosphate
DTT	Dithiothreitol
ECL	Enhanced chemiluminscence
EDTA	Ethylenediaminetetraacetic acid
EGTA	Ethyleneglycoltetraacetic acid
ER	Endoplasmic reticulum
FRET	Fluorescence resonance energy transfer
g	Grams
GFP	Green fluorescent protein
GIP	GlpF-like instrinsic proteins
g/L	Grams per Litre
HIP	Hybrid intrinsic proteins
hr	Hour
HRP	Horseradish peroxidase
IAA	Indole-3-acetic-ccid
L	Litres
LB	Luria-Bertani
LV	Lytic vacuole
M	Molar
mA	Milliamps
MIP	Major intrinsic protein(s)
ml	Millilitres
mM	Millimolar

nm	Nanometres
MPa	Mega Pascals
mRNA	Messenger ribonucleic acid
MS	Murashige and Skoog basal medium
MVB	Multi vesicular body
ng	Nanograms
ng/µl	Nanograms per microlitre
NIP	Nod26-like intrinsic protein(s)
NPA	Asparagine proline alanine
N-terminal	Amino-terminal
OD600	Optical density 600nm
PCR	Polymerase chain reaction
PEG	Polyethylene glycol
PIP	Plasma membrane intrinsic protein(s)
PM	Plasma membrane
PSV	Protein storage vacuole(s)
PVDF	Polyvinylidene fluoride
PVP	polyvinylpyrrolidone
RFP	Red fluorescent protein
rpm	Revolution(s) per minute
s	Seconds
SAV	Sensecence associated vacuole(s)
SDS	Sodium dodecyl sulphate
SDS-PAGE	Sodium dodecyl sulphate-polyacrylamide gel electrophoresis
SIP	Small basic intrinsic protein(s)
SNARE	Soluble NSF attachment protein receptor
SOB	Super optimal broth
SSP	Seed storage proteins
ST	Sialyl transferase
SUC4	Sucrose transporter 4
T_0	Original transformed parent plant
T_1	Offspring of T_0
T_2	Offspring of T_1
TAG	Triglycerides
TBE	Tris/borate/EDTA
TBST	Tris buffered saline with Tween20
TEMED	Tetramethylethylenediamine
TGN	Trans-Golgi network
TIP	Tonoplast intrinsic protein(s)
Tm	Melting temperature
TPK1	Tandem pore potassium channel
U/µl	Units per microlitre
V/cm	Volt per centimetre
v/v	Volume per volume
w/v	Weight per volume

w/w	Weight per weight
YFP	Yellow fluorescent protein
XFP	Miscellaneous (X) fluorescent protein
XIP	Uncategorised X intrinsic proteins
1/s	Cycles per second
°C	Degrees Celcius
µg	Micrograms
µg/ml	Micrograms per microlitre
µl	Microlitres
µM	Micromolar
x g	Times greater than gravity

Amino Acids

Single Letter Code	Amino Acids	Abbreviation
A	Alanine	Ala
C	Cysteine	Cys
D	Aspartic Acid	Asp
E	Glutamic Acid	Glu
F	Phenylalanine	Phe
G	Glycine	Gly
H	Histidine	His
I	Isoleucine	Ile
K	Lysine	Lys
L	Leucine	Leu
M	Methionine	Met
N	Asparagine	Asn
P	Proline	Pro
Q	Glutamine	Gln
R	Arginine	Arg
S	Serine	Ser
T	Threonine	Thr
V	Valine	Val
W	Tryptophan	Trp
Y	Tyrosine	Tyr

Acknowledgements

First and foremost thank you to my supervisor, Dr Lorenzo Frigerio, who has always made time for me and supported the project from the very beginning until the very end. Also, thank you to Professor Bill Finch-Savage for his collaborative efforts and valuable insight within the project.

Thank you to all those who have been a part of the C46 and C30 labs over the last three and a half years for their resources, wisdom, and endless encouragement. Especially Hannah Lee, Roshani Patel, Sarah Smith and Jens Steinbrenner for an outsider's perspective of the project and keeping me smiling!

And finally a big thank you to my family and friends for their endless and unwavering support; particularly Edward Hutchison for always being there at the end of a long day.

Declaration

The data presented in this thesis represent original work conducted by myself, unless otherwise specified, under the supervision of Dr Lorenzo Frigerio at the University of Warwick. The research was funded by a BBSRC Doctoral Training Grant. All sources of information have been acknowledged by means of a reference. None of this work has been used in any previous application for a degree.

Charlotte Elizabeth Ella Carroll

September 2014

Summary

Aquaporins are membrane channels transporting water and small molecules across the membranes of various intracellular compartments. Plant aquaporins constitute the Major Intrinsic Protein (MIP) family, consisting of 35 members in *Arabidopsis thaliana*, all exhibiting expression patterns which are specific in tissue type and developmental timing. Aquaporins are thought to be vital to plant growth, development, and response to drought. However, little work has been done to clarify the exact roles of particular isoforms in each of these aspects.

The MIP isoforms TIP3;1 and TIP3;2 are uniquely localised to both the plasma membrane and tonoplast. In addition, they are the only aquaporins present in the maturing and germinating Arabidopsis seeds. Their potential importance in these developmental processes has therefore been speculated, but is yet to be fully elucidated. In addition, it is suspected that a C-terminal domain unique to TIP3 isoforms is responsible for their plasma membrane localisation. However little has been done to dissect the cellular sorting route they take, or the order in which they reach both membranes.

By misexpressing MIP isoforms, including TIP3, in transgenic Arabidopsis and systematically assessing the resulting effect on germination and seedling growth in water limiting conditions, it was found that increased expression of *Arabidopsis thaliana* aquaporin isoforms at atypical developmental time points can confer drought tolerance in both germination and seedling growth. More specifically, increasing the number of aquaporins at the plasma membrane can enhance tolerance to drought during germination, implying a fundamental role for the dual localisation of TIP3 at this developmental stage.

Fluorescent protein fusions to TIP3 were employed to dissect the order of this isoform's trafficking, and pharmacological techniques confirmed the route. From this, an inducible expression system for TIP3 has been established to study dual sorting, and TIP3 were confirmed to traffic independently of the Golgi complex in embryonic tissues, regardless of the presence or absence of their C-terminal motif.

Chapter 1: Introduction

1.1 Preface

Growth and development of plant cells rely on the vacuole (Rojo *et al.* 2001). The central vacuole, which occupies more than 90% of the protoplasmic cell volume, is responsible for a variety of functions including storage of ions, metabolites and proteins as well as sequestration of toxins and degradation of macromolecules; although, arguably, its most important function is maintaining cell turgor (Marty 1999).

With the discovery of plant aquaporins in the early 1990s, and the finding that they transport water across membranes, the traditional view of cellular water exchanges via osmosis was challenged (Maurel 1997). In fact, the rate of water transport through plant aquaporins is considered to exceed the rate of osmosis across lipid bilayer membranes by ten-fold (Obroucheva 2013). Since then, it has become well established that aquaporins are integral in maintaining water balance, not just at the cellular level, but at the whole plant level too (Li *et al.* 2014). In addition, plant aquaporins have been shown to transport small molecules other than water, including H_2O_2, silicon and CO_2 (Maurel *et al.* 1993, Bienert *et al.* 2013, Ma *et al.* 2006), and are thought to provide vital roles in development, nutrient uptake and stress responses (Li *et al.* 2014).

Expression of aquaporin gene family members is tightly regulated and is specific in tissue location and age within the plant. It is therefore predicted that these proteins are fundamental to key developmental stages and physiological processes. In addition, they have been hypothesised as fundamental to the abiotic stress response, with transcripts of aquaporin family members frequently being reported as upregulated in response to drought and salt stress (Barrieu *et al.* 1999, Lopez *et al.* 2003, Li *et al.* 2007, Jang *et al.* 2013). The primary focus of this project is to investigate the role of some of these aquaporin family members in both early developmental stages and drought conditions.

Aquaporins locate to membranes of various subcellular compartments. In *Arabidopsis thaliana*, those that locate to the vacuolar and plasma membranes are the best characterised. However, how they reach these locations is yet to be fully elucidated, and has relied on expression of aquaporins in tissues to which they are not native. This project addresses this issue by dissecting the targeting route of aquaporins in their endogenous tissues.

1.2 Vacuoles

Vacuoles are the largest organelles within the mature plant cell and incorporate many cellular functions as well as being a driving force for plant growth. The vacuole changes in shape and content during germination, matching its transition from a storage to lytic compartment (Zheng *et al.* 2011). It is imperative to understand when, why and how these changes occur to fully understand the role it plays during this developmental timepoint. Due to the vast size of the vacuole, cellular contents and other organelles often appear very close to the plasma membrane, requiring employment of tonoplast markers of its boundaries to interpret micrographs.

1.2.1 The Protein Storage Vacuole vs the Lytic Vacuole

To accommodate resources for the germinating seed, various organelles within cells of the maturing embryo store metabolites which can later be used for energy. Oil bodies store triglycerides (TAG), plastids store starch and the Protein Storage Vacuoles (PSV) harbour seed storage proteins (Penfield 2006, Mansfield and Briarty 1992, Scarafoni *et al.* 2001). PSV exist as multiple, small storage organs in the embryo of the maturing and dry seed, and in young meristematic plant cells, with a pH varying between 4.9 and 5.5 (Olbrich *et al.* 2007, Gattolin *et al.* 2011, Otegui *et al.* 2006). PSV replace Lytic Vacuoles (LV), at the end of embryogenesis (Hoh *et al.* 1995, Feeney *et al.* 2013), and in turn, PSV fuse to reform the central LV during germination (Zheng *et al.* 2011). In contrast to PSV, LV usually exist as one central large vacuole, containing hydrolytic enzymes and maintaining a pH of 5.5–6 (Martinière *et al.* 2013). The most prominent role of the LV is considered to be cellular expansion driven by its capacity to maintain cell turgor via water uptake.

1.2.2 The Multi-Vacuole Hypothesis

The functional differences between LV and PSV are attributable to the developmental time points at which they are present, however the 'Multi-Vacuole' Hypothesis states that more than one type of vacuole can exist in a single cell. This theory was based on observations by Paris *et al.* (1996) who used antisera raised against the tonoplast markers TIP1;1 and TIP3;1. TIP1;1 is typically located to the LV tonoplast and TIP3;1 to the PSV tonoplast, where they both act as aquaporins. Using immunofluorescence confocal microscopy, these antibodies were shown to localise to tonoplasts of the two different vacuoles within the same cells of *Pisum sativum* (pea) and *Hordeum vulgare* (barley) root tips. However, a repeat of this study using immunogold microscopy, employing antibodies raised specifically to the C terminus of each TIP isoform, did not share this conclusion (Olbrich *et*

al. 2007). The antisera used by Paris *et al.* (1996) were not raised specifically to this C terminal alone, possibly leading to nonspecific labelling. In addition, Olbrich *et al.* (2007) used fixed root tips of pea, barley and Arabidopsis, whereas Paris *et al.* (1996) used root cells isolated by enzymatic maceration. It was reported by Paris *et al.* (1996) that meristematic cells contained one vacuole labelled by both TIP3;1 and TIP1;1; however Olbrich *et al.* (2007) report cells in the root stele did not label with either antibody. These conflicting reports shroud the Multi-Vacuole Hypothesis in doubt (Frigerio *et al.* 2008). Moreover, studies employing fluorescent tag-TIP fusions make the observation that different TIP locate to the same tonoplast (Hunter *et al.* 2007, Gattolin *et al.* 2009, Gattolin *et al.* 2011). In fact, TIP3;1 seemingly replaces TIP1;1 at the tonoplast of the same vacuole post-germination, and in the short time frame for which they are both expressed, they localise to the tonoplast of the same vacuole (Gattolin *et al.* 2011). This suggests TIP labelling of the tonoplast is specific to different tissues and developmental time points, in accordance to type of vacuole present.

Evidence does exist which supports the Multi-Vacuole Hypothesis, but the documented cases are limited cases are very specific. Mesophyll cells of the ice plant *Mesembryanthemum crystallinum* contain two vacuoles - one to sequester salt, and another to store malate (Epimashko *et al.* 2004). Aleurone protoplasts of barley treated with Gibberellins or Abscisic acid (ABA) give rise to smaller vacuoles labelled with TIP3;1 (although no seed storage proteins were found and pH was non-acidic) suspected to have a functional similarity to mammalian lysosomes (Swanson *et al.* 1998). Senescent *Glycine max* (soybean) and Arabidopsis mesophyll and guard cells contained Senescence Associated Vacuoles (SAVs) which contained the senescent-specific cysteine protease SAG12 and have a lower pH, while their tonoplasts do not contain the TIP1;1 isoform that central vacuoles in these cells do (Otegui *et al.* 2005). Most recently, expression of YFP tagged TPK (tandem pore potassium channel) isoforms from rice revealed small PSV-like structures and a large central LV in the same protoplasts from shoots and roots of rice (Isayenkov *et al.* 2011). OsTPKa localised to the tonoplast of the large central LV, co-localising with TIP1;1; whereas OsTPKb did not, and instead located to small vesicular structures which lacked the acidic pH of a LV (Isaykenov *et al.* 2011). Coupled with the evidence that vacuolar identity changes with developmental stage, it is clear that two vacuolar types do exist, however their simultaneous appearance within the same cell appears to be the exception rather than the rule (Frigerio *et al.* 2008).

1.2.3 Imaging the Vacuoles

TIP1;1 and TIP3;1 have been used as markers of the tonoplast since the Multi-Vacuole debate began. Extensive mapping of different TIP translationally fused to fluorescent tags has unveiled high specificity for isoforms to different tissues, and enabled generation of marker lines to visualise the tonoplast at any developmental stage, in any tissue (Hunter *et al.* 2007, Gattolin *et al.* 2009, Gattolin *et al.* 2010, Gattolin *et al.* 2011). Immunolabelling of these specific isoforms can also be used for tonoplast markers in fluorescence or electron microscopy (Olbrich *et al.* 2007). In addition to tonoplast markers, luminal markers exist which can be used to identify the vacuole as LV or PSV by immunolabelling or fluorescent protein fusions. Cysteine protease aleurain is an LV-specific protein (Ahmed *et al.* 2000) whilst *Phaseolus vulgaris* (common bean) Phaseolin or 2S Albumin from Arabidopsis are specific to the PSV (Frigerio *et al.* 1998, Rojo *et al.* 2008). Molecular tools exploiting vacuolar properties can also be employed; LVs can be stained with acidic dyes such as BCECF (2',7'-bis(2-carboxyethyl)-5(6)-carboxyfluorescein) which is a green fluorescent indicator of pH (Viotti *et al.* 2013); and PSV with dyes targeting luminal contents (Di Sansebastiano *et al.* 1998, Swanson *et al.* 1998, Zheng *et al.* 2011). PSV are also autofluorescent when exposed to blue light, which is a useful feature employed heavily within this project.

1.3 The Major Intrinsic Protein (MIP) Family of *Arabidopsis thaliana*

There are 10 isoforms of Tonoplast Intrinsic Proteins (TIP), which belong to the plant aquaporin family of Major Intrinsic Proteins (MIP) in *Arabidopsis thaliana*. The MIP family also contains 13 Plasma Membrane Intrinsic Proteins (PIP), 9 Nod26-like Intrinsic Proteins (NIP) and 3 Small basic Intrinsic Proteins (SIP). Since the first MIP family member, GmNOD26 – soybean NIP, was discovered in 1987 (Fortin *et al.* 1987), the nomenclature and classifications of MIP have changed, in parallel with the genome sequencing of *Arabidopsis thaliana* (Johanson *et al.* 2001, Arabidopsis Genome Initiative 2000).

1.3.1 MIP Nomenclature in *Arabidopsis thaliana*

TIP and PIP are named after their respective tonoplast and plasma membrane localisations, with the exception of TIP3;1 and TIP3;2 which are located to both these membranes in the maturing seed embryo (Gattolin *et al.* 2011). NIP and SIP have varying subcellular localisations; for this reason, their names are derived from other properties. NIP are named

after the first identified member of this family, GmNOD26, which was identified at the peribacteroid membrane of nitrogen-fixing symbiosomes in root nodules (Fortin *et al.* 1987). SIP (small intrinsic proteins) are named after their small molecular size, and basic sequence and properties (Johanson *et al.* 2001).

Each MIP isoform is named after its subfamily and given 2 numbers; the first relates to the group in which it belongs within the subfamily, and the second denotes the individual isoform. This system of nomenclature follows what was already described for *Zea mays* (maize) (Chaumont *et al.* 2001), and replaces the Greek lettering system that was previously used for TIP. The 10 AtTIP isoforms have thus been renamed from γ-TIP to TIP1, δ-TIP to TIP2, α- and β-TIP to TIP3;1 and TIP3;2, ε-TIP to TIP4;1 and ζ-TIP to TIP5;1 (Johanson 2001 and Gattolin 2009). A phylogenetic tree mapping the relationship and grouping of all MIP isoforms in *Arabidopsis thaliana* is shown in figure 1.1. This tree was produced using full-length alignments of all AtMIPs. Even when only the conserved regions within the sequences are used and N and C terminals are omitted, the tree groups MIP isoforms in a similar way, with relative positions of TIP3;1 and TIP3;2 and PIP2;6 changing only slightly (see figure 1.1) (Johanson *et al.* 2001).

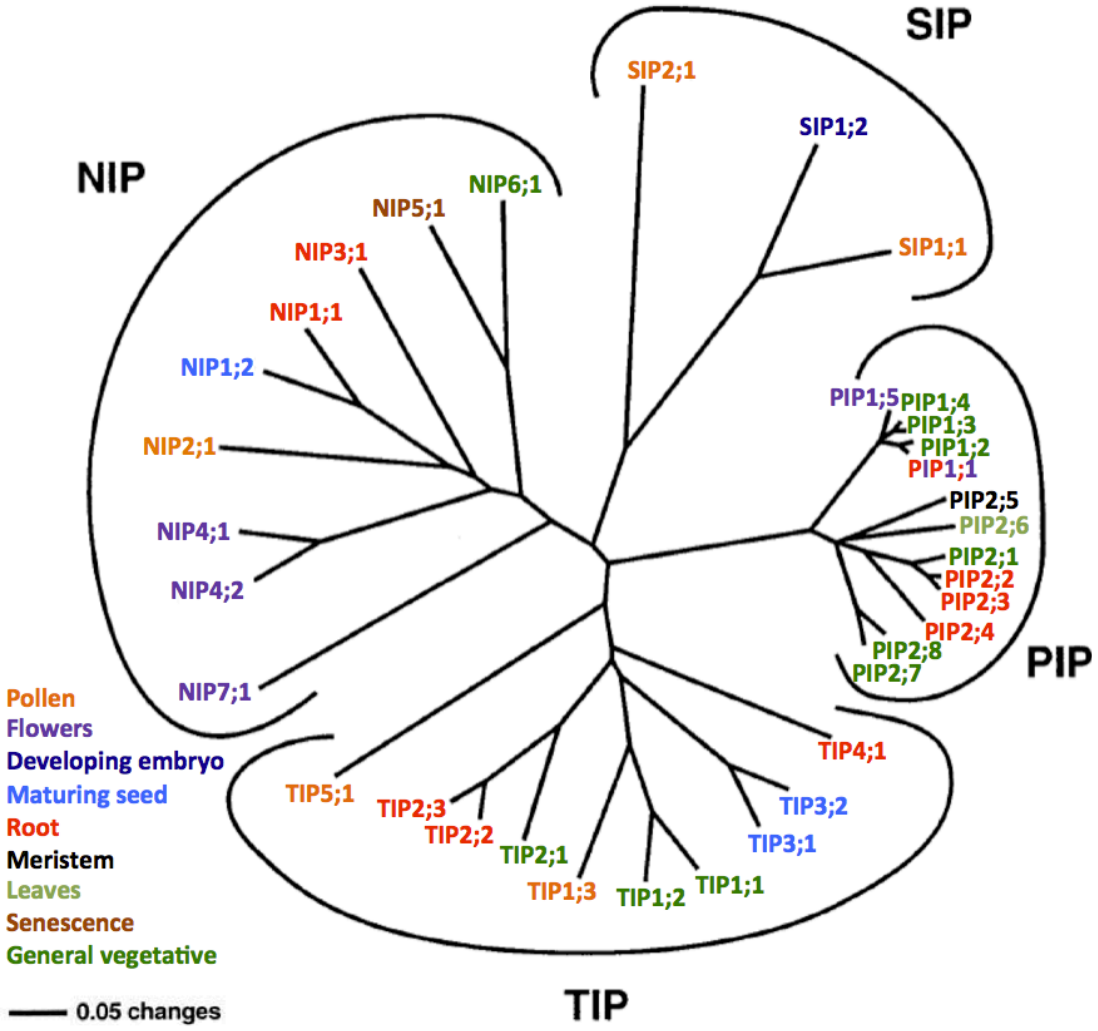

Figure 1.1 The MIP phylogenetic tree of *Arabidopsis thaliana* taken from Johanson *et al.* (2001), and adapted to show primary expression locations of different isoforms (Schmid *et al.* (2005)).
MIP from *Arabidopsis thaliana* are divided into four subfamilies; NIP, SIP, PIP and TIP. The first number given to each isoform denotes the group in which it belongs, and the second is to identify that individual isoform. Isoforms with a maximum of 30% divergence are clustered into monophyletic groups using the whole alignment and distance method. When only conserved regions are used, and N and C termini are omitted, the position of PIP2;6 shifts to form a separate branch between PIP2;4 and PIP2;5, and TIP3;1 and TIP3;2 to between TIP2 and TIP4;1. The scale bar represents changes per amino acid residue, the units for which distance of branches is measured in. Individual isoforms are colour coded according to the tissues in which they are most highly expressed, this information was gathered from Schmid *et al.* (2005) made accessible using eFP browser (Winter *et al.* 2007).

1.3.2 MIP Families Among Different Species

Although there are just four subfamilies of MIP in *Arabidopsis thaliana*, three others do exist in other species. XIP, uncategorised (X) Intrinsic Proteins have been found in several plant species including those of the family Solanaceae, soybean and *Physcomitrella patens* (moss) (Bienert *et al.* 2011, Danielson *et al.* 2008), but is absent from Brassicaceae including Arabidopsis, as well as monocots including maize and rice (Li *et al.* 2014). XIP are not yet as well characterised as other MIP subfamilies, however they have been identified as capable of transporting small, uncharged solutes in Solanaceae (Bienert *et al.* 2011). GlpF-like Instrinsic Proteins (GIP) and Hybrid Intrinsic Proteins (HIP) are the other two subfamilies, but are absent in all vascular plants and are exclusive to mosses and algae (Anderberg *et al.* 2011). Interestingly, these ancestral plants were also found to contain more NIP isoforms, and less TIP isoforms (Anderberg *et al.* 2012). The diverse and abundant group of TIP isoforms are specific to higher plants and are thought to have evolved later than PIP and NIP (apart from NIP2 which is thought to have appeared at the same time as TIP), to accommodate different specialised tissues types which evolved in vascular plants (Anderberg *et al.* 2012). In addition, this increase in TIP divergence was met by a decrease in NIP abundance due to functional overlap and therefore functional redundancy (Anderberg *et al.* 2012). Throughout the evolutionary divergence between MIP family members among the kingdom Plantae, PIP has maintained presence in all land plants, specifically the PIP1 isoforms, highlighting its fundamental role in plant water transport (Anderberg *et al.* 2012).

The MIP family of Arabidopsis contains a similar number to that of maize and rice. Maize have at least 36 aquaporin isoforms, and rice has 34, which are grouped within the same 4 subfamilies as in Arabidopsis (Chaumont *et al.* 2001, Sakurai *et al.* 2005). Despite these similarities, selectivity of the pores in maize and rice aquaporins is different to Arabidopsis, as discussed in section 1.4.4 (Bansal *et al.* 2007), implying they may transport a different variety of solutes. Members of the Brassica genus are evolutionarily closer to Arabidopsis than these crop species, with a genome similarity of 85% (Arabidopsis Genome Initiative 2000). The *Brassica rapa* (Chinese cabbage) genome encodes 53 aquaporin genes, 20 PIP, 14 TIP, 13 NIP and 6 SIP, all of which are orthologues of MIP isoforms in Arabidopsis (Tao *et al.* 2014). *Brassica rapa* has three subgenomes, which were inherited from the same diploid ancestor that Arabidopsis diverged from. However, it is predicted that some inherited genomes were hybridized or fractionated, losing sequences for some MIP isoforms and explaining why there are not 3 orthologues for each of that

found in Arabidopsis (Tao *et al.* 2014, Wang *et al.* 2011). Developments in the understanding of MIP originating from Arabidopsis could therefore be most readily applied to Brassica species.

1.3.3 MIP Expression Patterns

MIP family members have specific expression patterns in both space and time. PIP and TIP mRNA transcript levels are subject to diurnal regulation, with higher abundance shown during the day than night in *Lotus japonicus* (wild legume), *Samanea saman* (rain tree), maize, *Juglans regia* (walnut), *Vitis vinifera* (grapevine) and *Arabidopsis thaliana (*Henzler *et al.* 1999*,* Moshelion *et al.* 2002*,* Lopez *et al.* 2003*,* Cochard *et al.* 2007, Vandeleur *et al.* 2009, Hachez *et al.* 2012*)*. However, Lopez *et al.* (2003) and Hachez *et al.* (2012) report lower amounts of protein in comparison to mRNA transcript levels in the same samples of maize; indicating there may be some differences in turnover rate of RNA and proteins, or post-transcriptional regulation of aquaporins (Hachez *et al.* 2012, Lopez *et al*. 2003). Expression is also tissue specific. Figure 1.1 highlights the spatially and temporally distinct mRNA transcript expression pattern based on microarray experiments to quantify abundance in different tissues and developmental stages (Schmid *et al.* 2005). It should be noted that some of these isoforms have drastically lower levels of mRNA transcripts present than others: for example extremely low levels of NIP1;2 transcripts are found in comparison to TIP3;1 and TIP3;2 at the same developmental time point (Schmid *et al.* 2005). Whilst detection of mRNA transcript levels by microarray can be informative of genes which are upregulated in different tissues at different stages of development, analysis of active protein levels must be quantified to properly map the temporal and spatial specificity of aquaporin proteins. Mapping of MIP proteins using fluorescent tag-protein fusions and immunolocalisation have been used to confirm this (Gattolin *et al.* 2009). In addition, these methods have highlighted subcellular localisation of the different protein isoforms (Gattolin *et al.* 2009, Gattolin *et al.* 2011). In *Arabidopsis thaliana*, TIP are localised to the tonoplast, PIP and some NIP have been localised to the plasma membrane, (Ma *et al.* 2006, Takano *et al.* 2006, Zelazny *et al.* 2007, Bienert *et al.* 2011), whilst other NIP and SIP have been found at the ER (Mizutani *et al.* 2006, Maeshima *et al.* 2008). Some MIP isoforms exhibit dual membrane localization, including AtTIP3;1 and AtTIP3;2 which localize to the tonoplast and plasma membrane in Arabidopsis embryos and NtAQP1 which localize to the plasma membrane and chloroplast inner envelope of tobacco cells, as shown by fluorescent protein fusions and immunogold labelling respectively (Gattolin *et al.* 2011, Uehelin *et al.* 2008). Whilst 8 out of the 10 Arabidopsis

TIP have been mapped using fluorescent protein fusions (Gattolin *et al.* 2009, Gattolin *et al.* 2011), there is yet to be an extensive map covering all Arabidopsis MIP isoforms in both space and time, and thus most predictions of protein expression are based on microarray analysis (Schmid *et al.* 2005).

1.4 Structure and Selectivity of Aquaporins

Plant aquaporins are assumed to be very similar in structure due to conserved motifs within their sequences. The first crystal structure of an aquaporin was obtained for the human isoform AQP1 (figure 1.2A), which was used to model the structural basis for selectivity within the pore. This model is also accepted for plant aquaporins (Murata *et al.* 2000, Chaumont *et al.* 2014). This general structure (figure 1.2B) encompasses 6 membrane spanning α-helices connected by 5 loops, with N and C termini facing the cytosol. The first and only structure specific to plant aquaporins so far, was obtained from crystals of *Spinacia oleracea* (Spinach) SoPIP2;1 tetramers (Tornroth-Horsefield *et al.* 2006). This protein was heterologously expressed in *Pichia pastoris* yeast to enable easy extraction and pure samples to form crystals from (Tornroth-Horsefield *et al.* 2006). Both closed and open structures of the SoPIP1;2 structure were solved (shown in figure 1.2A), enabling assumptions on the assembly, selectivity and gating of plant aquaporins to be made (Chaumont *et al.* 2014, Li *et al.* 2014).

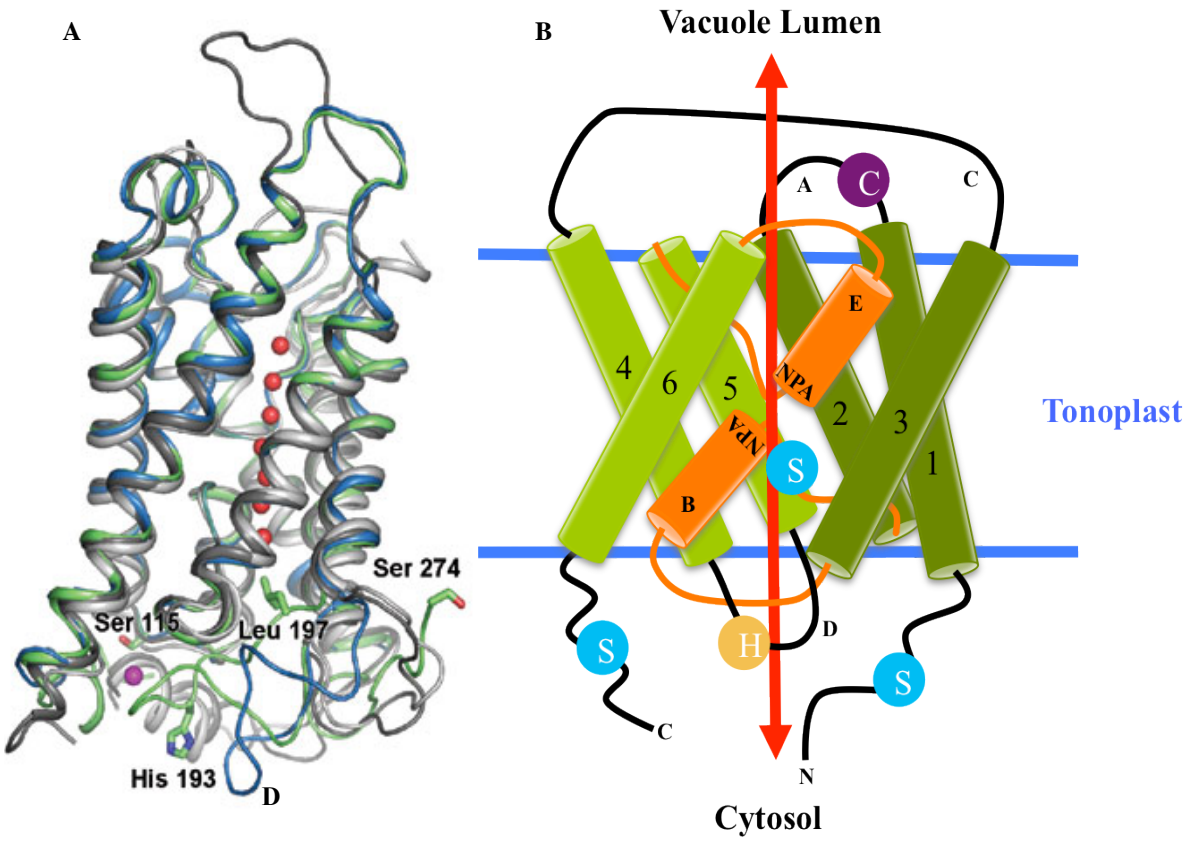

Figure 1.2: Crystal structure of SoPIP2;1, taken from Tornroth-Horsefield *et al.* (2006) and schematic illustration of the topological structure of an aquaporin monomer, taken from Chaumont *et al.* (2014)

A: The crystal structure of AQ1 (grey) is overlaid by the open (blue) and closed (green) structures of SoPIP2;1, as determined by X-ray crystallography (Taken from Tornroth-Horsefield *et al.* 2006). **B**: Aquaporins have 6 tilted membrane spanning α-helices (green) connected by 5 loops (A-E), with N and C termini facing the cytosol. The pore is formed from two short hydrophobic α-helices (orange), these contain conserved Asparagine/Proline/Alanine (NPA) motifs which form a size exclusion zone in the pore. In addition, an aromatic/arginine (Ar/R) region (not shown) formed from residues from helix 2 and 5 and loop E, contributes to a size and charge exclusion barrier (Murata *et al.* 2000). Loop D is responsible for closure of the pore by interacting with N terminal residues, resulting in insertion of a Leucine residue (Leu197) and subsequent blockage of the pore. The histidine (His193) in loop D stabilises this closure when protonated (Tornroth-Horsefield *et al.* 2006). Phosphorylation of serine residues (Ser115 and Ser274) can change aquaporin conformation and re-open the pore (Tornroth-Horesfield *et al.* 2006, Nyblom *et al.* 2009). The cysteine residue in loop A (purple) is involved in disulphide bond formation between monomers to form the tetramers in which aquaporins exist at the membrane (Murata *et al.* 2000, Fetter *et al.* 2004, Bienert *et al.* 2012). As the red arrow indicates, each aquaporin monomer can act as a pore within this tetramer, transporting water and small molecules in both directions across the membrane.

1.4.1 The Aquaporin Structure

The topological aquaporin structure as revealed by Murata *et al.* (2000) resolved individual side chains on the 6 α-helices, guiding the assignment of tilt angles to each and resulting in a topological model, as schematically illustrated in figure 1.2. Each aquaporin functions as a monomer but exists as a tetramer within the membrane; a conserved cysteine residue, shown in purple in figure 1.2 has shown to be involved in disulphide bond formation between monomers (Murata *et al.* 2000, Fetter *et al.* 2004, Bienert *et al.* 2012). The five loops within the structure are termed A-E (figure 1.2), and the pore is formed from two short hydrophobic a- helices from within loops B and E. NPA motifs from within these loops form a size exclusion zone within the pore which is also thought to be responsible for proton exclusion (Tajkhorshid *et al.* 2002), whilst an aromatic/arginine (Ar/R) region (not shown) formed from residues from helix 2 and 5 and loop E, forms a size exclusion barrier and a hydrogen bond environment guiding solutes (Murata *et al.* 2000).

1.4.2 Selectivity of Aquaporin Pores

Whilst Asparagine/Proline/Alanine (NPA) motifs are conserved amongst MIP, aromatic/arginine (Ar/R) regions have been shown to vary, resulting in different sized pores and differences in solutes which can be transported. Based on homology modelling of MIP from *Arabidopsis thaliana*, differences in Ar/R regions between subfamilies are synonymous with the existing grouping which is based on sequence alignments. However, based on diversity of Ar/R regions within the subfamilies, further subcategories can be formed (Wallace *et al.* 2004). PIP are considered to have the most uniform Ar/R pore, consistent with water-specific mammalian AQ1 and are considered 'true' aquaporins, transporting mainly water (Wallace *et al.* 2004). In contrast, TIP are highly diverse in their Ar/R regions, giving rise to 3 main subcategories. All TIP1 are contained in one group, all TIP2, TIP3 and TIP4;1 in the second, although TIP3 and TIP4;1 are thought to be more similar to each other than TIP2, and solo TIP5;1 makes up the third (Wallace *et al.* 2004). NIP and SIP possess two types of Ar/R groups each, enabling each subfamily to contain two subcategories based on this region (Wallace *et al.* 2004). The variety of pore sizes resulting from these differences, is suggested to be much more diverse than those found in animal and microbial species, implies different Arabidopsis MIP could have different functions by transporting different solutes (Wallace *et al.* 2004). In addition to these differences, structural characterization of rice and maize MIP identified that TIP, NIP and SIP from these species have selectivity filters in the Ar/R region that are not found in *Arabidopsis* (Bansal and Sankararamakrishnan 2007).

The catalogue of solutes that are known to be transported through the different MIP isoforms has been documented mainly upon heterologous expression of aquaporins in the *Xenopus* oocyte to measure conductivity of solutes. This was primarily used to show that members of TIP, PIP, SIP and NIP subfamilies can transport water (Maurel *et al.* 1993, Rivers *et al.* 1997, Kammerloher *et al.* 1994, Ishikawa *et al.* 2005), but has also shown that other solutes including glycerol, urea, boric acid, salicylic acid and lactic acid can also be transported (Biela *et al.* 1999, Gerbeau *et al.* 1999, Takano *et al.* 2006, Ma *et al.* 2006, Choi *et al.* 2007), in addition to CO_2 (Uehlein *et al.* 2003, Ma *et al.* 2006, Heckwolf *et al.* 2011). Even within subfamilies and the groups defined by Wallace *et al.* (2004) based on Ar/R regions, different isoforms can exhibit different propensities for what they can transport. Understanding the solute transport capacities of each isoform could aid understanding of MIP functioning in the whole plant. All TIP except TIP2 can transport urea, found by mutating Ar/R sites of AtPIP2;1 using molecular simulations (Dynowski *et al.* 2008). This same simulation method found that no TIP could transport ammonia, despite experimental data showing TIP2;1 expressed in *Xenopus* oocytes can (Holm *et al.* 2005). Therefore, modelling can only make predictions on solute specificity of different Ar/R regions, which must then be verified experimentally. The experimental evidence for the role of Ar/R residues in pore selectivity is patchy. Heterologous expression of OsLsi1 in *Xenopus* oocytes with the serine on helix 5 substituted to isoleucine, showed a reduced ability to transport salicylic acid, boric acid and water in comparison to wild-type. The same mutation decreased boric acid transport of AtNIP5;1, showing an importance for this residue which is not conserved between aquaporin isoforms (Mitani-Ueno *et al.* 2011). Wild type AtNIP5;1 is unable to transport salicylic acid, and when this isoform is mutated to include the NPA and Ar/R regions of OsLsi1 (which can transport salicylic acid), it is still unable to transport this solute (Mitani-Ueno *et al.* 2011). These results suggest that the transport substrate selectivity may be due to regions other than just NPA and Ar/R, however so far no further structural features have been identified as responsible. Recently, there has been a call to specifically explore structure-function relationships of TIP isoforms due to this subfamily's wide variety in Ar/R regions (Azad *et al.* 2011). Heterologous expression of *Tulipa gesneriana* (tulip) TgTIP1;1 and TgTIP1;2 in the methylotrophic yeast *Pichia pastoris,* has shown transport of urea and hydrogen peroxide by these aquaporins; a feature which is lost when the alanine in loop E is substituted for glycine. This substitution results in an Ar/R region mimicking that of Arabidopsis TIP1, and highlights the requirement for this residue in solute specificity (Azad *et al.* 2012). Despite these revelations, expression of native AtTIP1;2 in yeast showed an ability to take up

ammonia, whilst PIP2;1 mutants with an identical TIP-like selectivity filter did not, emphasising the limitations of mutation-based techniques to assess pore selectivity (Dynowski et al 2008). There is still little conclusive evidence as to the exact roles for Ar/R regions in pore selectivity and requires more experimental data in order to determine the full extent of their importance.

1.4.3 Gating of Aquaporins

Given the closed and open structures for SoPIP1;2 which have been revealed, it has been possible to model the mechanism of aquaporin gating (Tornroth-Horsefield *et al.* 2006). Using dynamics simulation modelling, Nyblom *et al.* (2009) have highlighted the importance of loop D in open and closed conformations. In the closed formation, loop D inserts Leu197 into the pore, blocking the cytoplasmic opening. This is achieved through loop D linking to part of the N-terminal region via ionic interactions and hydrogen bonds (Tornroth-Horsefield *et al.* 2006). The histidine labelled in yellow on loop D in figure 1.2, is in part responsible for stabilization of this closed state once it becomes protonated (Tornroth-Horsefield *et al.* 2006). This has been experimentally demonstrated by expressing wild type and mutated PIP in *Xenopus* oocytes incubated in acidic solutions (Tournaire-Roux *et al.* 2003). Indeed, closure of several PIP isoforms has been reported in Arabidopsis suspension cells, isolated plasma membrane vesicles from *Beta vulgaris* (sugar beet), and in reconstituted proteoliposomes under H^+ treatment, as well as $Ca2^+$ treatment which also induces a conformational change of loop D (Gerbeau *et al.* 2002, Alleva *et al.* 2006, Verdoucq *et al.* 2008).

Aquaporins can be artificially closed with intracellular propionic acid which leads to protonation of the histidine in loop D (Tournaire-Roux *et al.* 2003, Alleva *et al.* 2006). But a more common method to halt aquaporin activity is to block the pore with mercury chloride (Preston *et al.* 1993). This compound binds to cysteine residues within the pore to block exit and entry of solutes, and is reversible using reducing agents such as mercaptoethanol (Rivers *et al.* 1997). $HgCl_2$ can also bind to the cysteine residues responsible for disulphide bond formation between monomers (Preston *et al.* 1993, Bienert *et al.* 2012). This was shown to inhibit activity of maize ZmPIP1;2 and ZmPIP2;5 when coexpressed in *Xenopus* oocytes to form heterotetramers (Biernet *et al.* 2012). However, caution is necessary when employing this technique as its specificity to aquaporin proteins and ability to completely block them is often questioned (Li *et al.* 2014, Chaumont 2014, Maurel 2009).

Phosphorylation of serine residues (shown in blue in figure 1.2) is considered to be responsible for reopening of this closed state (Tornroth-Horesfield *et al.* 2006, Nyblom *et al.* 2009). Phosphorylation was first shown to activate TIP3;1 by injecting *Xenopus* oocytes with wild-type and mutated mRNA transcripts (Maurel *et al.* 1995). Mutated mRNA transcripts were changed from wild-type by site-directed mutagenesis, replacing serine residues (Ser7, Ser23 and Ser99, seen as potential phosphorylation sites within the primary amino acid sequence) with alanine. Expression of wild-type TIP3;1 lead to increased water flux across the membrane, whereas those with mutated phosphorylation sites didn't (Maurel *et al.* 1995). In addition, exposing fractionated membranes of these oocytes expressing TIP3;1 to cAMP-dependent protein kinase revealed TIP3;1 phosphorylation (Maurel *et al.* 1995). Similar experiments were replicated with soybean GmNod26 (NIP isoform) and spinach SoPIP2;1 to show phosphorylation opens aquaporin pores (Guenther *et al.* 2003, Johansson *et al.* 1998).

Environmental cues have also been found to affect aquaporin gating. In soybean, an increase in NIP phosphorylation leading to pore opening was observed under conditions of drought and high salinity (Guenther *et al.* 2003). In contrast, SoPIP2;1 was shown to be dephosphorylated in drought conditions (Johansson *et al.* 1998), whilst salt stress decreased but H_2O_2 increased phosphorylation of AtPIP2;1 (Prak *et al.* 2008). From this, it is clear that phosphorylation can act as a response to abiotic change, which may be specific to different aquaporins according to their function, but perhaps the exact response is dependent on other factors such as quantity of aquaporins expressed.

1.5 The Role of Aquaporins in Plant Physiology

Water uptake is essential at all stages of the plant life cycle and is crucial to vascular plants for many physiological processes. Typically, movement of water is driven by its potential; i.e. water molecules move from a region of high water potential to low water potential, typically where a higher ratio of solutes to water molecules are found. Transpiration, the process in which water evaporates from the leaf through open stomata, drives water uptake through the xylem towards the leaves. In turn, the xylem draws water from the soil via the root system (Steudle *et al.* 2001). On a smaller scale, water must be balanced within the cell, a part most obviously played by the vacuole which is accountable for maintaining cell turgor. Cell turgor is responsible for driving cellular expansion and stomatal opening. Water is transported at the cellular level by three pathways; the apoplastic route around

protoplasts, the symplastic route through plasmodesmata and the transcellular pathway across cell membranes (Steudle *et al.* 1998). The transcellular pathway is mediated by PIP; their expression positively correlates with apoplastic barriers (Suga *et al.* 2003, Hachez *et al.* 2006, Hachez *et al.* 2008, Hachez *et al.* 2012).

1.5.1 A Role for Aquaporins in Germination

Arabidopsis thaliana seeds are subject to desiccation before being released from the dehiscing silique, and require rehydration before germination can occur. This process is referred to as imbibition and is a necessary trigger for rapid germination and subsequent tissue growth (Welbaum *et al.* 1998, Finch-Savage *et al.* 1993, Bewley *et al.* 2013). This initial stage of rapid water uptake during imbibition is referred to as phase I of germination. Phase II is a plateau phase in which little or no water is taken up prior to germination whilst the seed metabolically prepares for germination. Phase III describes the final stages of water uptake into the seed which results in seedling emergence. Live cell imaging of Arabidopsis embryos constitutively expressing a GFP-tagged AtTIP2 isoform revealed that expansion of the hypocotyl is responsible for pushing the radicle out of the testa (seed coat) resulting in the germinated seed (figure 1.3C) (Silwinska *et al.* 2009). Radicle emergence from the endosperm layer is considered to constitute the final stage of germination, which is a two-step process in Arabidopsis, the first being rupture of the testa (Liu *et al.* 2005).

Aquaporins are known to be expressed in the developing and germinating seeds; with TIP3 isoforms reported to be expressed strongly at this time point in pea, rice, soybean and *Arabidopsis thaliana* (Hoh *et al.* 1995, Li *et al.* 2007, Melroy *et al.* 1991, Vander Willigen *et al.* 2006 and Gattolin *et al.* 2011). Due to the time point at which it is expressed, TIP3 expression accompanies not only deposition of storage proteins, oligosaccharides and phytins to PSV but also the PSV to LV transition (Maurel *et al.* 1997, Zheng *et al.* 2011, Gattolin *et al.* 2011). The active role for TIP3 in the germinating seed has been implied by use of the aquaporin blocker, mercury, which slows germination at the later stages in Arabidopsis, pea and broad bean (*Vicia faba*) (Willigen *et al.* 2006, Veselova *et al.* 2003, Novikova *et al.* 2014). TIP3 gene expression halts shortly after germination, once the LV is established (Feeney *et al.*, 2013; Novikova *et al.* 2014), which coincidently is when expression of other TIP, including TIP1;1, and PIP, including PIP1;1 and PIP2;2, begin to appear, presumably to take over roles of water transport in the establishing seedling (Gattolin *et al.* 2011, Vander Willigen *et al.* 2006).

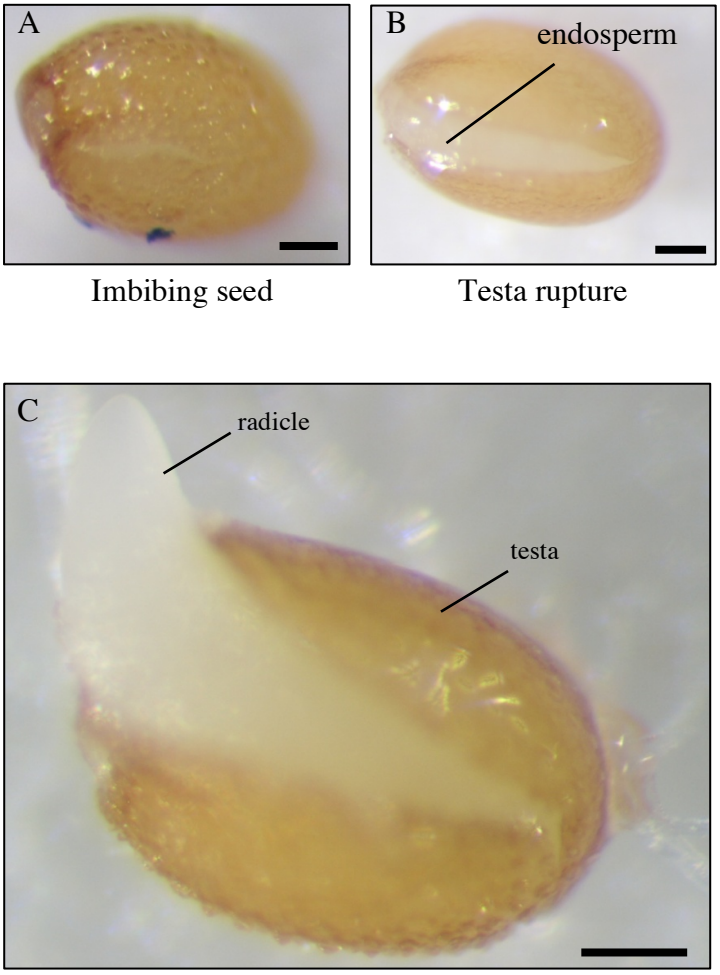

Figure 1.3: The triphasic water uptake and proper germination of an *Arabidopsis thaliana* seed

A: Imbibing seed and phase I of germination, in which rapid water uptake occurs. Phase II follows, in which little or no water is taken up by the seed. **B**: Phase III begins in which further water uptake causes the testa (seed coat) to rupture although the endosperm layer remains intact, constitutive the first stage of Arabidopsis germination. **C**: The endosperm layer is ruptured leading to the second and final stage of Arabidopsis germination, in which the radicle emerges. Scale bars = 1mm.

1.5.2 A Role for Aquaporins in Plant Growth

Post-germination, tissues of the emerged seedling must expand rapidly for successful seedling establishment. Seedling establishment is defined as the period between germination and when an autotrophic lifestyle is achieved, meaning when the seedling is no longer dependent on seed storage reserves (Raven *et al.* 2005). AtTIP1;1 expression begins during seedling establishment, seemingly replacing TIP3;1 and TIP3;2, as shown by fluorescent protein fusions and confocal microscopy in germinating Arabidopsis embryos (Gattolin *et al.* 2011). In mature plants, AtTIP1;1 promoter transcripts reveal localisation to roots, hypocotyls, leaves and flower stems using promoter-GUS fusions (Ludevid *et al.* 1992). Gus activity was not detected in meristematic or older tissues, and instead correlated most strongly with tissues undergoing cell enlargement, consistent with the proposed role for aquaporins in driving plant growth (Ludevid *et al.* 1992).

AtTIP1;1 expression is in part regulated by growth hormones; spraying Arabidopsis plants with gibberellic acid induced upregulation of transcripts for this gene, whereas exposure to Indole-3-acetic acid (IAA) auxin, lead to a reduced number of transcripts detected (Phillips *et al.* 1994, Peret *et al.* 2012). Profiling of all 13 PIP and 4 TIP isoforms during lateral root development showed repression in root primordia at a time when auxin levels are known to be high in this tissue (Peret *et al.* 2012). However, transcriptional and translational fusions revealed PIP2;1 was highly expressed in stele tissues and *pip2;1* knockouts and overexpressing lines exhibited a delay in lateral root emergence (Peret *et al.* 2012). It is therefore clear that aquaporins play a complex role in root growth and development. More specifically, several TIP and PIP isoforms have been found to localise to particular tissues within the root; high expression of aquaporins is observed in the inner cortex, endodermis, stele and around xylem vessels (Hachez *et al.* 2006, Vandeleur *et al.* 2009, Sakurai-Ishikawa *et al.* 2011, Gambetta *et al.* 2013, Vandeleur *et al.* 2014, Gattolin *et al.* 2009). However, unique and specific patterns of expression for different isoforms can also be observed in specific cell types among these tissues. For example, Maize ZmPIP2;5 is found to be most highly expressed in the exodermis, with expression fading towards the cortex (Hachez *et al.* 2012). AtTIP2;2 and AtTIP2;3 are highly expressed in the pericycle, but low in the endodermis whilst no TIP were located to the meristem or root vasculature using fluorescent protein tag fusions (Gattolin *et al.* 2009). The heavy presence of aquaporins in these tissues indicates an essential role for water uptake in the root. In addition, their specific localisation patterns suggest specific roles for different isoforms.

There is also evidence to suggest aquaporins are important in water transport within leaf tissues, particularly in recovery from drought. Leaf hydraulic conductance decreases in mercury treated *Helianthus annuus* (sunflower), due to blocking of aquaporin pores and thus reduced levels of functional MIP (Nardini *et al.* 2005). Whilst there was no difference noted in leaf hydraulic conductivity in antisense *pip1;2* and *pip2;3* Arabidopsis lines in normal conditions, hydraulic conductance and transpiration rates recovered faster in wild type plants than these mutants (Martre *et al.* 2002). This indicates that PIP may also be responsible for recovery of leaf water balance after drought

As aquaporins are implicated in leaf hydraulic conductance, a tentative role for them in transpiration can be postulated. In fact, PIP and TIP are highly expressed in guard cells, and are predicted to play a role in stomatal conductance (Kaldenhoff *et al.* 2008). Turgor changes in guard cells result in opening and closing of the stomata, driven by ion fluxes. Employment of immunolabelling for SoPIP1;1 has discovered its presence is specifically confined to guard cells (Fraysse *et al.* 2005). In addition, Arabidopsis and broad bean PIP1 isoforms have been located to guard cells (Kaldenhoff *et al.* 1995, Sun *et al.* 2001). Aquaporins at these locations could be providing the high membrane water permeability necessary for rapid opening and closing of stomata. Indeed, changed stomatal conductance was observed in both NtAQP1 antisense and overexpressing tobacco plants (Uehlein *et al.* 2003). Stomatal conductance is considered to positively correlate to photosynthetic rate as they both increase in the presence of elevated CO_2 (Ainsworth *et al.* 2007). Uehlein *et al.* (2003) also highlighted the ability of NtAQP1 to transport CO_2 across membranes. The ability to transport CO_2 suggests aquaporins may have a role in photosynthesis at the cellular level. Supporting this theory, overexpression of AtPIP1;2 in tobacco increased photosynthetic efficiency as measured by plant growth rate, transpiration rate, stomatal density, and photosynthetic efficiency (Aharon *et al.* 2003). In addition, rice overexpressing HvPIP2;1 (barley) exhibited higher CO_2 assimilation rates and increased stomatal conductance (Hanba *et al.* 2004).

Plant aquaporins are vital in several key processes which are integral to plant growth, and are not just limited to water transport within the cell. These key processes include cell enlargement, water uptake in the root, leaf water balance, stomatal conductance, CO_2 assimilation and therefore photosynthesis.

1.5.3 Aquaporins in the Drought Response

Land plants, as sessile organisms, must be able to intrinsically respond to stress. Stresses can occur in the form of drought, flooding, temperature extremes, high salinity as well as pathogenic infections. It is thought that aquaporin expression, and possibly their gating, can be regulated in response to stress, with a large proportion of the literature dedicated to the aquaporin-mediated response to drought. ABA is a drought-induced hormone promoting stomatal closure and increasing water flux in roots (Zhang *et al.* 1995, Aroca *et al.* 2006). ABA deficient tomatoes exhibit lower root hydraulic conductance and lower leaf water potential and turgor (Nagel *et al.* 1994) and plants overproducing ABA have higher root hydraulic conductance (Thompson *et al.* 2007). Application of ABA to roots of tobacco increased transcript levels and protein abundance of NtAQP1 and NtPIP1;1. In addition, application of ABA to maize roots resulted in increases in ZmPIP1;2, ZmPIP2;1 and ZmPIP2;5 transcript levels and protein abundance in drought conditions. Consequently in both instances, osmotic root hydraulic conductivity was increased (Mahdieh *et al.* 2009, Ruiz-Lozano *et al.* 2009). Therefore it appears that ABA can increase water flux in roots by upregulating aquaporins localised to root tissue.

Root hydraulic conductance, as well as leaf water potential has also been shown to decrease in tobacco exhibiting antisense inhibition of NtPIP1 isoforms (Siefrietz *et al.* 2002). However, in Arabidopsis antisense inhibition of AtPIP1 and AtPIP2 did not modify these two measures of water flux, until the plants were subjected to drought conditions (Martre *et al.* 2002). Upon re-watering post-drought, these antisense lines has lower leaf water potential and lower plant hydraulic conductivity than wild type lines. Together, these data indicate that PIPs can play an important role in drought recovery, by acting on root water transport and re-mobilizing water in dehydrated leaves.

Transcripts of aquaporin family members have frequently been reported as upregulated in response to drought in species including sunflower, *Brassica oleracea* (cauliflower), maize, *Jatropha* (physic nut), rice and *Arabidopsis thaliana* (Sarda *et al.* 1999, Barrieu *et al.* 1999, Lopez *et al.* 2003, Jang *et al.* 2013, Li *et al.* 2007, Alexandersson *et al.* 2005). Jang *et al.* (2013) was the only study out of this group which also measured protein abundance; they confirmed this transcriptional upregulation was also observed at the protein level in *Jatropha*. As such, overexpression of aquaporin genes has been employed in an attempt to confer drought tolerance. This has in some cases been reported to successfully induce higher resistance to water deficit (Peng 2007, Liu *et al.* 2007, Zhou *et*

al. 2012, Sade 2009, Lian 2004, Zhang 2013) but, in some instances, to actually increase sensitivity (Aharon 2003, Katsuhara 2003, Wang 2011). Among the successful cases are important crop species including rice (Liu *et al.* 2007) and tomato (Sade *et al.* 2009), which showed increased germination and yield respectively. Cumulatively, these results indicate aquaporins could indeed be a target for engineering drought resistance. However further understanding of their transcriptional responses to water deficit, and a systematic approach to detailing the advantages of their employment in aiding drought tolerance is required.

1.6 Sorting of MIP the Secretory Pathway

Correct localization of proteins is crucial to their function. Sorting through the secretory pathway is achieved through vesicle carriers trafficking proteins between endomembrane compartments. MIP are thought to be co-translationally translocated into the ER to have their final topology established before export via vesicles delivering them to their destination. However the route they take, and the signal motifs directing this journey is yet to be fully understood. Small steps have been made to begin elucidating these pathways; so far, two discrete sorting motifs and heteromerization have been identified as important for ER export of PIP. While sorting signals from TIP are yet to be elucidated, pharmacological approaches have identified targeting to the tonoplast does not require transport through the Golgi and thus routes for different isoforms can be either Golgi dependent or Golgi independent (Rojas-Pierce 2013).

1.6.1 PIP Targeting to the Plasma Membrane

PIP are exported from the ER in tetramers via COPII vesicles. Initially, expression of maize PIP1 and PIP2 isoforms in *Xenopus* oocytes suggested that interactions between the two are important for trafficking to the plasma membrane, as co-expression led to enhanced membrane water permeability (Fetter *et al.* 2004). More recently, the importance of this interaction was confirmed using live FRET (Fluorescence Resonance Energy Transfer) imaging of transfected maize mesophyll protoplasts (Zelazny *et al.* 2007). This technique shows ZmPIP1;2 and ZmPIP2;1 form heterotetramers at the PM. Moreover, when ZmPIP1;2 was expressed alone, it was retained within the ER whereas ZmPIP2;1 was able to reach the PM, suggesting PIP1;2 trafficking is reliant on PIP2;1 (Zelazny *et al.* 2007).

Diacidic motifs are thought to be responsible for recruiting PIP into budding ER COPII vesicles. These diacidic export signals have been studied in both maize ZmPIP2;4 and ZmPIP2;5, in addition to Arabidopsis AtPIP2;1 (Hachez *et al.* 2012). AtPIP2;1-GFP with the D-X-E motif mutated to D-X-D was retained in the ER of Arabidopsis epidermal cells. Moreover, when it was co-expressed with wild type AtPIP1;4-mCherry, both proteins were retained in the ER, whereas when wild type AtPIP2;1-GFP was used, both proteins reached the PM (Sorieul *et al.* 2011). Despite this, the diacidic motif is not conserved between PIP2 family members. The observation that ZmPIP2;1 cannot reach the PM even when a diacidic motif is fused to its sequence (Zelazney *et al.* 2009), indicates that there must be other export signals. Indeed, most recently the LXXXA motif in the third transmembrane domain of ZmPIP2;5 has been found to be necessary for trafficking to the plasma membrane (Chevalier *et al.* 2014). Unlike the diacidic motif, this sequence is conserved in ZmPIP2, but not found in ZmPIP1. In addition, this LXXXA motif is not found in TIP3;1 or TIP3;2, the only TIP dually targeted to both tonoplast and PM (Gattolin *et al.* 2011). Therefore export signals other than the diacidic and LXXXA motifs must exist in aquaporin sequences for ER export and subsequent plasma membrane targeting to occur.

Upon export from the ER, PIP are trafficked through the Golgi and TGN, as demonstrated by colocalisation of fluorescent protein-tagged ZmPIP2;5 with a Golgi resident fluorescent marker line ST-YFP (sialyltransferase) and TGN fluorescent marker line VTI12 (SNARE protein) (Hachez *et al.* 2013). For correct PIP insertion into the PM, SNARE complexes are thought to be necessary. SNARE proteins from vesicle and target membranes come together to form SNARE complexes mediating the fusion of donor carriers or endosomal compartment with target organelle membranes. These SNAREs are specific to particular vesicles and compartments (Fujimoto *et al.* 2012). The SNARE protein SYP121 is required to interact with ZmPIP2;5 for delivery of this PIP to the PM of maize mesophyll protoplasts (Besserer *et al.* 2012), and more recently, AtPIP2;7 has been found to interact with SYP61 in addition to SYP121 for delivery to the PM in Arabidopsis, as demonstrated with confocal microscopy (Hachez *et al.* 2014).

1.6.2 TIP isoforms Take different Routes to the Tonoplast

Targeting of TIP to the tonoplast is not as well understood as PIP targeting to the PM. However, early studies found that the sixth (last) transmembrane domain and cytosolic tail of TIP3;1 were sufficient for targeting to the tonoplast (Hofte *et al.* 1992). The C terminus of TIP3;1 has also been shown as sufficient to direct the transmembrane domain of the

plant vacuolar sorting receptor, BP-80, to the tonoplast via a Golgi independent route, however this chimeric protein did colocalise with TIP3;1 C-terminal reporter proteins at Multi Vesicular Bodies (MVB) when both were expressed in protoplasts (Jiang *et al.* 1998). This was the first example of TIP being sorted to the tonoplast through two routes, and has led to a series of experiments to confirm this model, depicted in figure 1.4.

Brefeldin A has widely been used as an inhibitor of Golgi-dependent trafficking in *Arabidopsis thaliana*. This drug specifically inhibits ARF-GEFs (ADP-ribosylation factor-guanine nucleotide exchange factors) which are required for COPI coat formation on vesicles trafficking from Golgi to ER (retrograde). As a consequence, ER to Golgi traffic is inhibited due to the redistribution of Golgi membranes, and therefore proteins targeting to the tonoplast are retained within the ER. This pharmacological approach has so far been used to demonstrate that OsTPK1 (tandem pore potassium channel 1) (Dunkel *et al.* 2008, Maitrejean *et al.* 2011), OsTPKa (tandem-pore potassium channel a) from rice (Isayenkov *et al.* 2011), INT1 (inositol transport1), SUC4 (sucrose transporter 4) (Wolfenstetter *et al.* 2012) and TIP1;1 (Rivera-Serrano *et al.* 2012) transport through the Golgi before reaching their final destination at the tonoplast.

Using Brefeldin A treatment, TIP3;1 (from *Phaseolus vulgaris*) has been shown to avoid the Golgi by transient expression in tobacco and Arabidopsis protoplasts (Gomez *et al.* 1993, Park *et al.* 2004), alongside TIP2;1 in Arabidopsis hypocotyl cells (Rivera-Serrano *et al.* 2012) and OsTPKb in rice protoplasts (Isayenkov *et al.* 2011). Furthermore, this Golgi independent route to the tonoplast has been demonstrated by taking advantage of glycan modifying enzymes in the Golgi. These enzymes modify N-glycans making them resistant to digestion by endoglycosidase H (EndoH). In contrast, glycans from the ER are sensitive to this recombinant glycosidase. By expressing a modified version of TIP3;1 to contain an N-glycosylation site from the phaseolin C-terminal region, it was shown that Endo H treatment produced a smaller protein as detected by western blot. This indicated that the modified TIP3;1 contained glycans which were sensitive to cleavage by Endo H, and thus had not been subjected to Golgi processing, suggesting that the protein did not travel through this organelle (Park *et al.* 2004). However, TIP3;1 has been found to localise to Golgi stacks in soybean embryos by immunolocalisation studies (Melroy *et al.* 1991). This highlights the importance of investigating TIP trafficking in the actual tissues in which they are endogenously expressed, something which is yet to be achieved for TIP3 isoforms.

Other tools which could be used to decipher a Golgi-dependent trafficking route are the recently identified drug C834, which was shown to retain TIP3;1 and TIP2;1 in the ER, but not affect the trafficking of TIP1;1 in Arabidopsis hypocotyl cells (Rivera-Serrano *et al.* 2012). It has therefore been proposed that this drug inhibits the ER-to-MVB transport step, although how this occurs is yet to be elucidated (Rivera-Serrano *et al.* 2012). The MVB, also known as the Pre-Vacuolar Compartment (PVC) or late endosome, is implicated in trafficking of TIP3;1 as demonstrated by mutating members of the Rab5 family (Bottanelli *et al.* 2011). Members of the Rab5 family are GTPases involved in membrane fusion between endocytic vesicles and MVB compartments (Olkkonen *et al.* 2007). Coexpression of the Rab5 members Rha1 and Ara6 with an Asn-to-Ile substitution (NI) in the nucleotide binding domain, alongside TIP3;1-YFP in tobacco, resulted in the accumulation of this TIP to punctate structures. This indicates fusion of endocytic vesicles carrying TIP3;1 with the MVB is required for proper trafficking (Bottanelli *et al.* 2011). In addition, coexpressing TIP3;1-YFP with the mutated Rab11, a GTPase involved in vesicle fusion at the TGN (early endosome), resulted in normal trafficking of TIP3;1-YFP to the tonoplast, showing that the TGN is not implicated in the Golgi-independent traffic route (Bottanelli *et al.* (2011).

The SNARE protein SYP21 which localises to the MVB and tonoplast, has been shown to be involved in inserting TIP1;1 into the tonoplast. This was achieved by coexpressing a soluble fragment of this SNARE, which acts as a dominant negative mutant, with TIP1;1-YFP in Tobacco epidermal cells (Tyrrell *et al.* 2007). The model so far proposed does not take into account the dual sorting of TIP3 isoforms to the tonoplast and plasma membrane (Gattolin *et al.* 2011). It could be assumed that TIP3 is trafficked in the same way to the plasma membrane as to the tonoplast, but how the same sequence targets to different locations post-MVB remains puzzling.

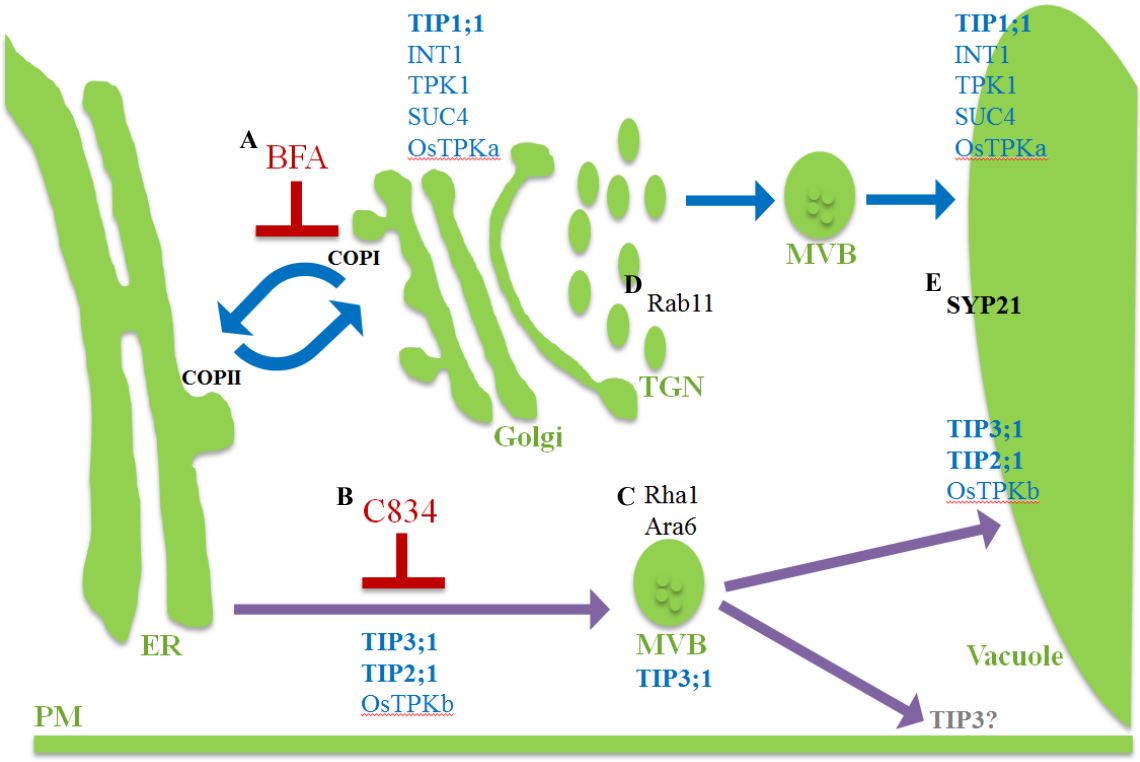

Figure 1.4 Targeting TIP to the tonoplast, taken from Rojas-Pierce (2013)
TIP isoforms are trafficked to the tonoplast from the ER via a (blue) Golgi dependent or (purple) Golgi independent route (Jiang *et al.* 1998). **A**: Brefeldin A (BFA) inhibits retrograde transport of COPI vesicles from Golgi to ER, causing Golgi membranes to be relocalised and proteins trafficking via the Golgi-dependant route to be retained in the ER. Proteins targeted via this route include: TIP1;1, INT1, TPK1, SUC4 and OsTPKa (Dunkel *et al.* 2008, Maitrejean *et al.* 2011, Isayenkov *et al.* 2011, Wolfenstetter *et al.* 2012, Rivera-Serrano *et al.* 2012). The same drug has shown TIP3;1, TIP3;2 and OsTPKb traffics Golgi independently as these proteins are trafficked normally under treatment (Viotti *et al.* 2013, Rivera-Serrano *et al.* 2012, Isayenkov *et al.* 2011). **B**: TIP3;1 trafficking is also insensitive to the drug C834, which inhibits the ER to MVB step (Rivera-Serrano *et al.* 2012). **C**: The MVB has been shown to be required for TIP3;1 trafficking using Rha1 and Ara6 mutants which are required from fusion of endocytic vesicles with the MVB (Bottanelli *et al.* 2011). **D**: The Golgi-independent route does not require the TGN as shown by Rab11 mutants not affecting TIP3;1 targeting (Bottanelli *et al.* 2011). **E**: The SNARE protein SYP21 is involved in TIP1;1, and possibly other TIP isoforms incorporation into the tonoplast by aiding fusion of vesicle and tonoplast membranes (Tyrell *et al.* 2007, Rojas Pierce 2014).

1.7 Project Introduction and Aims

Considering the likely importance of aquaporins in key developmental stages of plant development, there has been relatively little work to systematically identify exact roles for different isoforms. TIP3 isoforms have uniquely been found to locate to both plasma membrane and tonoplast in cells of the maturing and germinating seed (Gattolin *et al.* 2011). TIP3 are the only aquaporins highly expressed at these developmental time points, and mercury treatment has been shown to slow germination (Vander Willigen *et al.* 2006). Thus it has been postulated that TIP3 provides the major inlet for water through the plasma membrane, driving tissue expansion and subsequent growth for germination.

In addition, reports in the literature are mixed regarding the implication and potential use for aquaporins in the drought stress response. This has the potential to be addressed by methodically reviewing both overexpression and reduced expression of aquaporin isoforms in drought conditions.

Moreover, little work has been done to confirm the targeting route for TIP3 isoforms in their endogenous tissues, whilst considering their newly found dual membrane localisation. Understanding how these isoforms are sorted to their dual membrane localisations could increase understanding of how they aid water uptake during germination.

This project aims to assess the importance of TIP3 in germination, and systematically review the potential of TIP and PIP to confer drought resistance at both this time point, and during seedling establishment. Finding out how TIP3 reaches both plasma membrane and tonoplast is also valuable in understanding its role. Therefore the main experimental aims of this work are:

- To determine the effect of TIP and PIP overexpression on seed germination and seedling establishment in conditions of water stress.
- To investigate the importance of TIP3 in germination by employing RNAi technology to reduce transcripts in Arabidopsis seeds.
- To characterise the route TIP3 follow to their dual plasma membrane and tonoplast locations in embryos from maturing and germinating seeds.

Chapter 2: Materials and Methods

2.1 Suppliers of Chemicals and Reagents

3M (UK): Micropore tape

AgfaPhoto (Germany): Developer, fixer

Bayer (Germany): BASTA (Kaspar (150g/L glufosinate ammonium))

BDH (UK): 40% Acrylamide solution, Bisacrylamide (NN'-methylene bis-acrylamide)

Biorad (UK): BSA standards

Biotium (USA): GelRed Nucleic Acid Stain

Difco (USA): Bacto-agar, Bacto-tryptone

Expedeon (UK): Instant Blue

Fisher Scientific (UK): SDS (sodium dodecyl sulphate), Sodium hypochlorite (bleach)

GeneScript (USA): Custom anti-TIP3 polyclonal antibody

Invitrogen (UK): 1kb Plus DNA ladder , Cloned AMV Reverse Transcriptase, FM4-64, Restriction endonucleases, REact™ buffers, T4 DNA ligase, T4 DNA ligase buffer

Kodak (UK): Biomax MR-1 X-ray film.

Loveland Industries (UK): Silwet L-77

Miltenyi Biotec (USA): Anti-GFP-HRP

New England Biolabs (USA): ColorPlus Prestained Protein Marker (7-175KDa)

Pierce (UK): 660nm Protein Assay

Promega (USA): Anti-rabbit-HRP, ECL western blotting substrate

Qiagen (Germany): QIAprep Spin Plasmid kit, QIAprep Gel Extraction kit, RNeasy columns

Roche) (UK): Complete protease inhibitor cocktail tablets, proteinase K.

Santa-Cruz (USA): Anti-myc polyclonal antibody

Sigma-Aldrich (UK): Acetosyringone, agarose**,** ammonium persulphate (APS), β-mercaptoethanol, boric acid, brefeldin A (BFA), bromophenol blue, calcium chloride, calcium nitrate, custom oligos, diethylpyrocarbonate (DEPC), dexamethasone, dithiothreitol (DTT), dimethyl sulfoxide (DMSO), ethylenediaminetetraacetic acid (EDTA), ethanol, ethyleneglycoltetraacetic acid (EGTA), gentamycin, glycerol, glycine, hydrochloric acid, hygromycin, kanamycin, lithium chloride, magnesium chloride, magnesium sulphate, mannitol, methanol, MES, Murashige and Skoog basal medium (MS), polyethylene glycol 8000 (PEG), polyvinylpyrrolidone (PVP), potassium acetate, potassium chloride, potassium hydroxide, rifampicin, RNase AWAY (decontamination reagent for RNase), sodium acetate, sodium chloride, sodium deoxycholate, sodium tetraborate decahydrate, sodium phosphate tribasic dodecahydrate, spectinomycin, tetramethylethylenediamine (TEMED), tetracycline, Triton X-100, Tween-20, yeast extract

Tesco (UK): Marvel dried milk powder.

ThermoScientific (UK): Agarose, PVDF (Polyvinylidene fluoride) transfer membrane, 2X ReddyMix PCR Master Mix

Thistle Scientific (UK): Metal beads

Whatman (UK): 3MM chromatography paper, filter paper

2.2 Culture, preparation and transformation of competent *Escherichia coli* and *Agrobacterium tumefaciens*

2.2.1 Culture of competent *Escherichia coli* and *Agrobacterium tumefaciens* strains

The *E.coli* strains DH5α and DB3.1 and *A. tumefaciens* strains C58 and GV3101 were grown on Luria-Bertani (LB) agar (10g/l bacto-tryptone, 5g/l yeast extract, 10g/l sodium chloride, 2% (w/v) bacto agar) supplemented with the appropriate antibiotics (table 2.1 and 2.2) at 37°C overnight or 28°C for 2-4 days respectively. 5ml overnight cultures, with appropriate antibiotics, were inoculated with individual *E.coli* or *A. tumefaciens* colonies and incubated at 37°C or 28°C shaking overnight at 200rpm for approximately 16 hours. A glycerol stock was made with 1:1 ratio of overnight culture to sterile 80% (v/v) glycerol, mixed using the vortex until thoroughly mixed, flash frozen in liquid nitrogen and stored at -80°C.

2.2.2 Preparation of competent *E.coli* DH5α and DB3.1 cells

Cells (in 50mM $CaCl_2$, 20% (v/v) glycerol) were inoculated in 5ml of LB medium and incubated for 16 hours at 37°C shaking at 250rpm. This culture was used to inoculate 500ml of SOB (2.0% tryptone, 0.5% yeast extract, 10mM NaCl, 2.5mM KCl), supplemented with 5ml of sterile Mg solution (1M $MgCl_2$ and 1M $MgSO_4$), in a 2L flask. Cells were grown to an OD600 (Biochrom Ultrospec 3300 Pro Spectrophotometer) between 0.4 and 0.6 and subsequently chilled on ice for 10 minutes. The cell culture was decanted evenly across two 500ml centrifuge bottles and pelleted at 4000 x g (Beckman J2-21MIE) for 5 minutes at 4°C. The supernatant was removed and pellet gently re-suspended in 36ml of cold CMG buffer (50mM $CaCl_2$, 50mM $MgCl_2$). Cells were transferred to a 50ml falcon tube and incubated on ice for 15 minutes. 1.26ml of high grade DMSO was added and the sample was incubated on ice for a further 5 minutes. A further 1.26ml of DMSO was added, mixed and incubated on ice again for 5 minutes. The suspension was aliquoted in a 4°C cold room at volumes of 100µl into 1.5ml microcentrifuge tubes, flash frozen in liquid nitrogen and stored at -80°C.

2.2.3 Transformation of competent *E.coli* DH5α and DB3.1 cells

Approximately 5ng of DNA was added to a 100µl aliquot of cells which had been thawed on ice for 15 minutes. The cells were subsequently left on ice for a minimum of 15 minutes before being heat shocked at 42°C for 42 seconds, and being returned to ice for 2 more minutes. 1000µl of LB was then added to the tube which was then incubated at 37°C,

shaking at 200rpm for 1 hour. Cells were harvested by centrifugation at 5000rpm (Eppendorf bench microfuge) for 2 minutes. 800µl of supernatant was discarded and pellet re-suspended in the remaining broth. The suspension was then plated on LB-agar plates supplemented with appropriate antibiotics and incubated at 37°C overnight.

2.2.4 Preparation of chemically competent *A. tumefaciens* C58 and GV3101 cells

Cells (in 20mM $CaCl_2$, 20% (v/v) glycerol) were inoculated in 5ml of LB medium and incubated overnight at 28°C shaking at 200rpm. 2ml of this culture was used to inoculate a 100ml culture in a 250ml conical flask. Cells were grown to an OD600 (Biochrom Ultrospec 3300 Pro Spectrophotometer) between 0.5 and 1.0. The culture was then chilled on ice for 30 minutes and pelleted at 4000 x g (Beckman J2-21MIE) for 10 minutes at 4°C. The supernatant was discarded and pellet was gently re-suspended in 2ml of ice cold 20mM $CaCl_2$. Cells were aliquoted in a 4°C cold room in 50µl volumes into 1.5ml microcentrifuge tubes, flash frozen with liquid nitrogen and stored at -80°C.

2.2.5 Transformation of chemically competent *A. tumefaciens* C58 and GV3101 cells

0.1-1ug of plasmid DNA was added to a 50µl aliquot of frozen cells before thawing at 37°C for 5 minutes. Cells were then flash frozen in liquid nitrogen for at least 1 minute before being incubated again at 37°C for a further 5 minutes. 1ml of LB was then added to the cells which were subsequently incubated at 28°C for 4 hours. Cells were harvested by centrifugation at 3000rpm (Eppendorf bench microfuge) for 5 minutes at 4°C. 800µl of the supernatant was discarded and the pellet was re-suspended in the remaining liquid. Cells were plated on LB-agar supplemented with appropriate antibiotic selection and incubated for 2-4 days at 28°C.

2.3 Nucleic acid techniques

2.3.1 Preparation of genomic DNA for PCR analysis from *Arabidopsis thaliana* leaves

50µg of leaf tissue was cut from the plant and placed in a 1.5ml microcentrifuge tube before being flash frozen in liquid nitrogen. 2 metal beads were added to tubes and samples were ground in a Retsch MM300 tissue grinder for 2 minutes at 30 cycles per second (1/s). 400µl of DNA extraction buffer (200mM Tris-HCl pH7.5, 250mM NaCl, 25mM EDTA, 0.5% SDS) was added and tissues were ground for a further 2 minutes. Tubes were centrifuged at 14,000rpm for 1 minute at 4°C (Eppendorf bench microfuge) and the

supernatant transferred to a sterile 1.5ml microcentrifuge tube. 300µl of isopropanol was added to the supernatant, mixed and left on ice for 20 minutes. Samples were centrifuged for a further 5 minutes at 14,000 rpm 4°C to pellet DNA. Supernatent was discarded and pellets were dried by leaving tube lids open for 5 minutes. Pellets were resuspended in 50µl of sterile dH_2O by gentle shaking. Extracts can be stored at -4°C for up to two days.

2.3.2 Amplification of DNA by PCR

DNA fragments were amplified from plant genomic DNA or from a vector containing the desired fragment of interest using conventional PCR. 2X ReddyMix PCR Master Mix containing Taq DNA Polymerase, dNTPs, and inert dye was used to perform PCR reactions using a Biometra T3000 Biocycler. A typical PCR reaction contained 0.5ng of template DNA, 0.5µM of each custom oligo primer, 12.5µl of 2X ReddyMix PCR Master Mix and dH_2O to 20µl volume. Reactions were heated to 94°C for 1 minute and typically underwent 25-30 cycles of PCR (94°C (denaturing) for 30 seconds, 50-55°C (annealing) for 30 seconds and 72°C (extension) 1min/1kb). The final extension took place at 72°C for 10 minutes. Amplicons were analysed via agarose gel electrophoresis. Precise times and temperatures varied depending on the length of the expected PCR product and primer Tm.

2.3.3 Preparation of plasmid DNA from *E. coli* and *A. tumefaciens*

The QIAprep Spin Plasmid Kit was used to isolate plasmid DNA. A 2ml LB culture of the plasmid-containing *E. coli* or 10ml of *A. tumefaciens* with the appropriate antibiotic was incubated for 16 hours at 37°C or 28°C respectively, shaking at 200rpm. Cells were harvested by centrifugation at 13,000rpm (Eppendorf mini-spin) for 5 minutes. The supernatant was discarded and DNA extracted from pellet according to manufacturer's protocol. DNA was eluted in 30-50µl of dH_2O and stored at -20°C.

2.3.4 Digestion of DNA using restriction endonucleases

DNA fragments for construct generation were prepared, or DNA constructs produced through cloning were checked using restriction endonucleases. Approximately 500ng DNA was incubated with 1µl of the appropriate enzyme(s) (5U/µl) and corresponding REact™ buffer (1x final concentration) made up to a total volume of 10µl with dH_2O at the recommended temperature for 1 hour. Digested fragments were separated by agarose gel electrophoresis.

2.3.5 Agarose gel electrophoresis of DNA

Depending on the size of the band expected, agarose gels were made with 0.5-1% (w/v) agarose dissolved in 1x TBE buffer (89mM Tris, 89mM H_3BO_3, 20mM EDTA pH8.0) containing GelRed Nucleic Acid Gel Stain at 1x from 10,000X stock. DNA not from PCR, which used the dye-containing 2X ReddyMix PCR Master Mix, was mixed with 6× DNA sample buffer (40% (w/v) sucrose, 0.25% (w/v) bromophenol blue. DNA was electrophoresed at 100 V/cm submerged in 1x TBE until the band and DNA ladder (Invitrogen 1kb Plus DNA ladder) was 2cm from the end of the gel. DNA was visualised using a short wave ultra-violet trans-illuminator, with digital images recorded using a GDS8000 Documentation and Analysis system.

2.3.6 Extraction of DNA from an agarose gel

Agarose gels were illuminated on a short wave ultra-violet trans-illuminator in order for bands to be visualised and excised from the gel using a scalpel. The small piece of agarose gel containing the desired DNA product was transferred to a 2ml microcentrifuge tube and DNA was extracted using QIAquick Gel Extraction Kit before being eluted in 30µl of sterile dH_2O and stored at -20°C.

2.3.7 Ligation of DNA fragments

After their appropriate restriction digest, DNA fragments of interest were ligated into desired vectors using T4 DNA ligase. A typical ratio of 4:1 vector to insert was used in a mix containing 4µl of 5x T4 DNA Ligase buffer (250mM tris.HCL pH 7.6, 50mM $MgCl_2$, 5mM ATP, 5mM DTT, 25% (w/v) polyethylene-glycol 8000) and 1µl of T4 DNA ligase (1U/µl), made up to a total volume of 20µl with dH_2O. This mixture was incubated at room temperature overnight. Ligated DNA was transformed in *E. coli* DH5α cells.

2.3.8 Constructs and cloning

All constructs made in this study were generated using oligonucleotide primers (Appendix Table A1) to amplify and engineer fragments by PCR from existing constructs. These fragments were either ligated directly into their destination vector by conventional cloning techniques, or via lambda-based recombination using Gateway cloning. Constructs were sequenced (see section 2.3.9) to exclude missense, nonsense and frameshift mutations prior to plant transformation.

Table 2.1 Competent cells used for cloning and *Arabidopsis thaliana* transformation

Line	Helper Plasmid	Selection
DH5α	n/a	n/a
DB3.1	n/a	n/a
C58	pSOUP	Rifampicin (10 μg/ml) and Gentamycin (50 μg/ml)
GV3101	pMP90	Rifampicin (10 μg/ml) and Tetracycline (50 μg/ml)

Table 2.2 Vectors used for generation of constructs

Vector	Application	Selection	Reference
pGreenII-0029	Plant Transformation	Kanamycin (50 μg/ml)	Hellens *et al.* 2000
pDONR207	Gateway Donor	Gentamycin (50 μg/ml)	Invitrogen
pFAST-R03	Gateway Silencing Destination	Spectinomycin(50 μg/ml) /Hygromycin (50 μg/ml)	Shimada *et al.* 2010
pDEX GW	Gateway Dexamethasone inducible	Kanamycin (50 μg/ml) /BASTA	Jens Steinbrenner and Jim Beynon, University of Warwick

Table 2.3 Constructs generated and used in this project

Construct	Vector	Description
35S:mycTIP3;1	pGreenII-0029	Genomic sequence of TIP3;1 (1389bp) fused in frame with myc epitope tag (30bp) at N terminus 35S promoter = 1379bp
TIP3;1pro: mEoSFP-TIP3;1	pGreenII-0029	Full genomic sequence of TIP3;1 (1389bp) fused to photoconvertible protein mEoSFP (741bp) at N terminus (TIP3;1 promoter = 789bp)
pFAST::TIP3	pFAST-R03	386 base pair region from TIP3;1 cDNA sequence inserted twice either side of an intron
pDEX: TIP3;1-YFP	pDEX GW	Full genomic sequence of TIP3;1 (1389bp) fused to YFP (723bp) at the C terminus

Table 2.4 Primers used for cloning constructs in table 2.3 (continued overleaf)

Purpose	Name	Sequence (restriction sites)	Description
TIP3;1pro: mEoSFP-TIP3;1	EoSFP FWD	CAGATAGGATCCATGGACTACAAAGACGATGACG	to add BamHI and XbaI sites to mEoSFP sequence
	EoSFP RVS	CAGATATCTAGATCGTCTGGCATTGTCAGGCAATCC	
35S: myc TIP3;1	MYCTIP3;1 FWD	CAGATATCTAGAATGGAGCAGAAACTCATCTCTGAAG AGGATCTGGCAACATCAGCTCGTAGAGCATACGG	fusion of myc tag onto TIP3;1 using PCR
	TIP3;1 RVS 3'	CAGATATCTAGACTAGTAATCTTCAGGGGCCAAGGGC	
	35S FWD	CAGATAGCTATCATTCAAGATGCCTCTGCC	Sequencing and genotyping (Highlighted colours correspond to primer sets described in figure 3.9, section 3.2.6)
	MYC RVS	CAGATACAGATCCTCTTCAGAGATGAG	
	MYC FWD	GGAGCAGAAAC TCATCTCTGAAGAGG	
	attB TIP3;1 FWD	GGGGACAAGTTTGTACAAAAAAGCAGGCTTC ATGGCAACATCAGCTCGTAG	for addition of attB sites to TIP3;1 and YFP to form insert by PCR
	attB YFP RVS	GGGGACCACTTTGTACAAGAAAGCTGGGTC CTAGATCACCTTGTACAGCTCG	
pDEX: TIP3;1 -YFP	TIP3;1 MID FWD	GTAGCGTTGGCTCATGC	Sequencing and genotyping
	TIP3;1 MID RVS	GCATGAGCCAACGCTAC	
	YFP MID RVS	GTGTTCTGCTGGTAGTG	
	YFP MID FWD	CACTACCAGCAGAACAC	
	attB TIP3 PFAST FWD	GGGGACAAGTTTGTACAAAAAAGCAGGCCTTCCCGCCA ATGCCAGTTGGTTTCCGTCTAGC	for addition of attB sites to selected TIP3;1 motif by PCR
	attB TIP3 PFAST RVS	GGGGACCACTTTGTACAAGAAAGCTGGGTC GTAATCTTCAGGGGCCAAGG	

Table 2.4 continued

pFAST::TIP3	PFAST Vec FWD 1	CTCAACACATGAGCGAAAC	Sequencing and genotyping
	PFAST Vec FWD 2	CATAACTCAGCACACCAG	
	PFAST Vec RVS 1	GAATTTGATGGCCATAGG	
	PFAST Vec RVS 2	CATTTGGAGAGGACTGCAG	
	TIP3.1-N term FWD	CGATGAGGCTACACACCCTG	RTPCR (Sequence position of highlighted yellow primers are shown in figure 4.2, and used to produce figure 4.4, as described in section 4.2.2).
	TIP3.1-N term RVS	ACTCTGCCTCCAACAAGAGC	
	TIP3.2-N term FWD	ATGGATTCGGGAGAGCTGAC	
	TIP3.2-N term RVS	GGCAAGCCTCAACAAGAGAC	
	TIP3.1 RNAi FWD	**TGTTAAGGCTCACAACAAACGGC**	
	TIP3.1 RNAi RVS	**AGCAGTGGTGACATGAGGAAAGTTC**	
	TIP3.2 RNAi FWD	**TTGTTGAGGCTTGCCACTAATGG**	
	TIP3.2 RNAi RVS	**ACCCTCTACATGAAGACTGCTCCG**	

Table 2.5 Constructs used in this project which were generated previously

Construct	Vector	Description	Reference
TIP3;1pro: TIP3;1-YFP	pGreenII-0029	Genomic sequence (1389bp) fused in frame with YFP (723bp) at C terminus (TIP3;1 promoter = 789bp)	Paul Hunter, University of Warwick UK
TIP1;1pro: YFP-TIP1;1	pGreenII-0029	Genomic sequence (TIP1;1=1398bp, PIP1;2=1688bp , TIP3;1=1389bp, TIP3;2=1603bp, fused in frame with YFP (723bp) at N terminus (TIP1;1 promoter=935bp, TIP3;2 promoter=816bp, TIP3;1 promoter=789bp)	Stefano Gattolin, University of Warwick UK
TIP3;2pro: YFP-PIP1;2	pGreenII-0029		Stefano Gattolin, University of Warwick UK
TIP3;1pro: YFP-TIP3;1	pGreenII-0029		Stefano Gattolin, University of Warwick UK
TIP3;2pro: YFP-TIP3;2	pGreenII-0029		Stefano Gattolin, University of Warwick UK
TIP3;2pro: YFP-TIP3;2ΔC	pGreenII-0029	Truncated genomic sequence, final C terminal 23 amino acids removed (1534bp), fused to YFP (723bp) at N terminus (TIP3;2 promoter=816bp)	Stefano Gattolin, University of Warwick UK
TIP3;1pro: Dendra2-TIP3;1	pGreenII-0029	Full genomic sequence (TIP3;1=1389bp, Calnexin=2690bp) fused to photoconvertible protein Dendra2 (690bp) or mEoSFP (741bp) at N terminus (TIP3;1 promoter=789bp, Calnexin promoter=851bp)	Stefano Gattolin, University of Warwick UK
Calnexinpro: mEoSFP:Calnexin	pGreenII-0029		Dr. Jaideep Mathur, University of Guelph
VHA-a1pro: YFP-VHA-a1	pGreenII-0029	Full length CDS sequence (2454bp) fused in frame with YFP (723bp) at N terminus (VHA-a1 promoter = 870bp)	Mathias Sorieul, University of Warwick UK
35S: TIP1;1-YFP	pGreenII-0029	Full length CDS (TIP1;1=756bp, TIP3;1=807bp) fused in frame with YFP (723bp) at the C terminus (35S promoter = 1379bp)	Paul Hunter, University of Warwick UK
35S: TIP3;1-YFP	pGreenII-0029		Paul Hunter, University of Warwick UK

2.3.9 Automated sequencing of plasmid DNA

Automated sequencing was outsourced to GATC Biotech, Konstanz, Germany and used Sanger ABI 3730xl. Samples sent contained 80 - 100ng/µl of plasmid DNA or 20-80 ng/µl of PCR product and primers at a final concentration of 5µM.

2.3.10 Gateway cloning

2.3.10.1 *att* site primers

Primers were designed with attB site sequences added in order to engineer their addition to the 5' and 3' ends of the fragment of interest by PCR (as recommended by Invitrogen Gateway® recombination cloning technology). This fragment was extracted from the agarose gel on which PCR products were electrophoresed. The extracted fragment did not require any other downstream modifications before addition to the BP reaction.

2.3.10.2 Propagation of Gateway vectors

Gateway vectors that have not been recombined to contain the fragment of interest contain the lethal ccdB gene and so were transformed into and DNA propagated in DB3.1 competent cells which are resistant.

2.3.10.3 BP reaction

~15-150ng total attB-PCR product was mixed with 150ng/µl Donor vector and made up to a final volume of 8µl with dH_2O in a 1.5ml Eppendorf tube at room temperature. 2 µl of BP Clonase™ II enzyme mix was added, which had been thawed on ice and mixed by vortex prior to addition. Reactions were mixed thoroughly by vortexing and incubated overnight at 25°C. 1µl of the provided Proteinase K solution was added to terminate the reaction at 37°C for 10 minutes. DH5α competent cells were transformed with 1µl of reaction, and plated on LB agar plates supplemented with the appropriate selection. Entry clones were isolated from 2ml cultures inoculated with positive colonies as described in section 2.3.3.

2.3.10.4 LR reaction

50-150 ng of Entry clone was mixed with 150 ng/µl Destination vector and made up to a final volume of 8µl with dH_2O in a 1.5ml Eppendorf tube at room temperature. 2 µl of LR Clonase™ II enzyme mix was added, which had been thawed on ice and vortexed

prior to addition. Reactions were mixed thoroughly using a vortex and incubated overnight at 25°C. 1µl of the provided proteinase K solution was added to terminate the reaction at 37°C for 10 minutes. DH5α competent cells were transformed with 1µl of reaction, and plated on LB agar plates supplemented with the appropriate selection. Destination clones were isolated from 2ml cultures inoculated with positive colonies as described in section 2.3.3. These were then transformed into GV3101 competent cells as described in section 2.2.4.

2.3.11 RNA extraction from seeds

Prior to, and throughout different stages of extraction, gloves, bench and equipment were sprayed with RNase AWAY (Sigma). 700µl of extraction buffer (0.2M Sodium tetraborate decahydrate, 30mM EGTA, 1% w/v SDS, 1% w/v sodium deoxycholate, pH9) was heated to 80°C and added to a 2ml Eppendorf containing 14mg polyvinylpyrrilidone (PVP) and 1.1mg dithiothreitol (DTT). Meanwhile, dry seeds were frozen in liquid nitrogen and homogenised using metal beads and the Retsch MM300 tissue grinder for 2 minutes at 30 cycles per second (1/s). 500µl of extraction buffer which had been heated to 80°C was added and seeds were homogenised for a further 30 seconds. Homogenate was transferred to a pre-chilled 2ml Eppendorf containing 0.35mg Proteinase K. A further 200µl 80°C extraction buffer was added to the tube containing any residual homogenate, so that this could also be added to the pre-chilled Eppendorf. These Eppendorfs were then incubated for 90minutes at 42°C. 56µl 2M KCl was then added (to give final concentration 60mM KCl) and tubes were incubated at 4°C for 1 hour. Following incubation, tubes were centrifuged (Eppendorf benchtop centrifuge) at 14,000rpm for 20 minutes at 4°C. Supernatent was decanted and pellet discarded, before enough 8M LiCl to make a final concentration of 2M was added to the supernatant (approximately 1/3 of the supernatant volume) and tubes were incubated overnight at 4°C. Samples were centrifuged at 14,000rpm for 20 minutes at 4°C. Supernatents were discarded and the pellets washed twice in ice-cold 2M LiCl. Pellet was then resuspended in 300µl DEPC water by vortexing. Undissolvable material was removed by centrifugation at 14,000rpm for 10 minutes at 4°C. Supernatent was transferred to a clean Eppendorf and 30µl ice-cold 2M KAc was added before incubation on ice for 15 minutes. Tubes were further centrifuged at 14,000rpm for 10 minutes at 4°C to remove undissolvable material and supernatant was transferred to a clean Eppendorf. 990µl ice-cold ethanol was added and samples were left to precipitate at -80°C for up to 3 hours. RNA was pelleted by centrifuging at 14,000rpm for 30 minutes at 4°C, and washed with ice-cold 70% ethanol.

Pellet was left to dry and resuspended in 40µl DEPC water. RNA was precipitated with 4µl 3M NaAc and 132µl ice-cold ethanol for 2 hours at -20°C. Tubes were centrifuged at 14,000rpm for 20 minutes at 4°C, and were washed once more with ice-cold 70% ethanol. Pellet was dried and resuspended in 50µl DEPC water, before finally cleaning up using a Qiagen RNeasy column.

2.3.12 Reverse transcriptase PCR

Reverse-transcriptase PCR was carried out using the Invitrogen Cloned AMV Reverse Transcriptase Kit. All quantities of RNA, reagents and PCR parameters were followed as per the manufacturer's instructions. Full parameters are discussed alongside results.

2.4 Protein separation and detection

2.4.1 Protein extraction and quantification

Protein from seed and leaves was extracted directly into Laemmli loading dye in instances where it was not quantified prior to loading (0.5 M Tris-HCl pH 6.8, 4.4% (w/v) SDS, 20% (v/v) glycerol, 0.036% bromophenol blue in dH_20). The reducing agent β-mercaptoethanol was added at a concentration of 2% (v/v) to all samples unless otherwise indicated. Samples were ground with metal beads in the Retsch MM300 tissue grinder for 5 minutes at 30 cycles per second (1/s) and homogenate was centrifuged at 15,000g for 10 minutes at 4°C. Supernatent was loaded directly onto SDS-polyacrylamide gels (see section 2.4.2). When there was a requirement for protein to be quantified, seed and leaves were collected in 1.5ml Eppendorf tubes and flash frozen in liquid nitrogen. Tissue was ground with metal beads in the Retsch MM300 tissue grinder for 2 minutes at 30 1/s. Homogenisation buffer (0.2M NaCl, 1mM EDTA, 2% β-mercaptoethanol, 0.2% Triton X-100, 0.1M Tris-HCl pH 7.8, complete protease inhibitor cocktail tablet) was then added to tissue at a ratio of 6:1 before grinding for a further 2 minutes at 30 1/s. Homogenate was centrifuged at 15,000g for 10 minutes at 4°C and supernatant collected. To quantify total protein extracted, 10µl sample (from collected supernatant) was added to 150µl Pierce 660nm Protein Assay reagent in a flat bottom 96 well plate. Samples were mixed well and incubated for 5 minutes before reading at 660nm with a ThermoScientific Varioskan Flash plate reader. Values were retrieved from SkanIt Software 2.4.3. Amount of protein was calculated using BSA standards.

2.4.2 Separation of proteins by SDS-polyacrylamide gel electrophoresis (SDS-PAGE)

SDS-polyacrylamide gels were cast and run using the Bio-Rad Protean II gel electrophoresis system, according to the manufacturer's instructions. 15% acrylamide gels (15% (w/v) acrylamide, 0.15% (w/v) bisacrylamide, 375 mM Tris.HCl pH 8.8, 0.1% (w/v) SDS, 0.05% (w/v) APS and 0.005% (v/v) TEMED) were used to resolve proteins and stacking gels consisted of 4.5% (w/v) acrylamide, 0.8% (w/v) bisacrylamide, 50 mM Tris.HCl pH 6.8, 0.o4% (w/v) SDS, 0.045% (w/v) APS and 0.0045% (v/v) TEMED.

2.4.3 Coomassie staining of SDS-polyacrylamide gels

SDS-PAGE gels were incubated with Expedeon Instant Blue for ~1 hour shaking. Gels were rinsed with dH_2O until bands were clearly visible.

2.4.4 Western blotting of SDS-polyacrylamide gels

Proteins separated on SDS-PAGE gels were transferred to PVDF membrane using Sigma-Aldrich techware Semi-dry blot apparatus under a constant current of 200mA for 2 hours. Prior to assembly, the PVDF membrane was briefly soaked in methanol and chromatography paper soaked in transfer buffer (25 mM Tris, 192 mM glycine, 20% methanol)). The membrane was then blocked by gentle shaking in tris-buffered saline (50 mM Tris-Cl pH 7.5, 150 mM NaCl)) containing 0.1% Tween-20 (TBST) and 5% (w/v) skimmed milk powder for 1 hour at room temperature, or at 4°C overnight. Blocking solution was removed and membrane was incubated with primary antibody in 20 ml TBST with 5% milk for 1 hour shaking at room temperature. The membrane was then rinsed in TBST (three quick rinses followed by three subsequent incubations of 10 minutes, and a further two quick rinses) before incubation in 20 ml TBST with 5% milk containing a horseradish peroxidase-conjugated secondary antibody for 1 hour shaking at room temperature. The membrane was washed again with TBST as before, and detection of immunoreactive bands was performed using the Promega ECL Western Blotting Substrate according to the manufacturer's instructions, and recorded by exposing to X-ray film (Fujifilm Super RX) in a light-proof cassette for up to 5 minutes. Films were developed using an Agfa Curix 60 automatic developer, with conditions and protocols recommended by the manufacturer.

2.4.5 Antibodies

The antibodies used for western blotting in this project are described in table 2.6

Table 2.6 Antibodies

Antibody	Animal, Class	Antigen	Dilution	Reference
Anti-GFP-HRP	Rabbit, polyclonal	GFP, YFP	1/6,666	Miltenyi Biotec
Anti-myc	Rabbit, polyclonal	Myc-epitope (EQKLISEEDL)	1/5,000	Santa Cruz
Anti-TIP3	Rabbit, polyclonal	TIP3 (CHQPLAPEDY)	1/2,000	GenScript
Anti-Rabbit	Rabbit, HRP conjugate	Rabbit	1/5,000	Promega (USA)

2.4.6 TIP3 custom antibody

Anti-TIP3 raised in rabbit, was ordered from GenScript USA inc based on the epitope described in Juah *et al.* (1999). Upon arrival, the affinity-purified antibody was resuspended in sterile distilled water upon arrival to make a 1mg/ml stock. The antibody was used for immunoblots with the method described in section 2.4.4. Using dilutions in the range of 1/750 to 1/7500 to provide final concentrations between 1.5µg/ml – 0.15 µg/ml, it was found that the 1/2000 dilution (0.5 µg/ml final concentration) is optimal as a primary antibody for TIP3 detection (as described in section 3.2.1). The secondary anti-rabbit antibody was used at a concentration of 0.2 µg/ml as already established in previous lab protocols.

2.5 Growth and maintenance of *Arabidopsis thaliana and Nicotiana benthamiana*

2.5.1 *Arabidopsis thaliana* ecotype

The *Arabidopsis thaliana* ecotype Columbia (Col-0, used in the Arabidopsis Genome Initiative, 2000) was used exclusively in this work. Col-0 ecotype plants with a *gnl1* knockout background, making them susceptible to brefeldin A treatment, were transformed with selected vectors for experiments described in section 5.2.6.

2.5.2 *Arabidopsis thaliana* seed sterilisation and sowing

Seeds were sterilised using either sodium hypochlorite (bleach) and sterile dH_2O or chlorine gas. To use bleach, seeds were shaken for 5 minutes in 1ml of 30% bleach and tween in a 1.5ml Eppendorf. They were then pelleted at 16,000 x g for 20 seconds and rinsed in sterile dH_2O. This step was repeated twice more before 900µl sterile dH_2O was removed after the final spin, and seeds were plated directly onto petri dishes containing ½

MS-agar (Murashige and Skoog (MS) basal medium (4.4g/l), adjusted to pH5.8 with 1M KOH, and containing 0.8% (w/v) bacto agar and a selective antibiotic if desired). To use chlorine gas, less than 100 seeds were placed into an open 1.5ml Eppendorf which was then placed into a rack inside a large plastic lidded box within the fume hood. 100ml of sodium hypochlorite was added to a glass beaker within this box, and 3ml of 35% hydrochloric acid was added slowly. The lid was immediately placed over the box and seeds were incubated overnight. Once sterile, seeds were aerated for 10 minutes in a flow hood. Seeds were then sterile and ready to be sown at any time.

2.5.3 Maintenance of *Arabidopsis thaliana*

½ MS-agar plates (containing appropriate antibiotics for selection as necessary) were sealed with micropore tape and typically subjected to 24-48 hours of stratification at 4°C before being transferred to a 24 hour light chamber at 25°C. Seedlings were transferred to Arabidopsis-mix soil (University of Warwick) 14 D.A.G and cultivated in a designated transgenic glasshouse facility with conditions at 16 hours light / 8 hours dark and 18°C.

2.5.4 Transformation of *Arabidopsis thaliana*

The primary stem of Arabidopsis plants was removed once the plants had bolted in order to encourage further stems and increased number of flowers. Plants were deemed ready for transformation once 20-50% of the flowers were open. At this point, a 10ml culture of LB supplemented with the appropriate antibiotic was inoculated with *Agrobacterium tumefaciens* containing the plasmid of interest, and was incubated at 28°C, shaking at 200rpm for 18-24 hours. This was decanted into 100ml of LB and incubated for a further 6 hours before pelleting cells at 3,000rpm for 15 minutes (Beckman J2-21MIE). The supernatant was discarded and the pellet re-suspended in sterile dH_2O containing 5% (w/v) sucrose. Silwet L-77 was added to a final concentration of 0.01%. Flowers of the plants were submerged in the suspension for 30 seconds. The suspension was then shaken and foam was pipetted onto the flowers. Plants were incubated in sealed plastic sleeves for 24 hours and left to dry. Dry seeds were collected, sterilised and plated on ½ MS-agar plates containing appropriate antibiotics for selection.

2.5.5 *Arabidopsis thaliana* seed collection

Plants were left to dry once lowest siliques began dehiscing. Once dry, stems were cut from the base of the stem and left for a further 1 week before these were placed into

paper bags. Bags were folded over and left for at least 1 week for seeds to completely dry before collection.

2.5.6 BASTA selection of transgenic *Arabidopsis thaliana* seedlings

T_1 and T_2 seeds were sown directly onto Arabidopsis-mix soil (2:1 potting mix to perlite) soaked in BASTA (Kasper, 150g/L glufosinate ammonium, Bayer, Germany) diluted 1/1000 with H_2O, and subjected to 2 days in the dark at 4˚C. Trays of seedlings were given a second BASTA treatment two weeks after this, with regular watering in between. Positive transformants were transferred to larger pots three weeks after sowing and brought to seed.

2.5.7 Seed preparation for germination and seedling growth assays

Prior to these assays, all seeds were grown in a Panasonic MLR-352-PE cabinet at the same time in the same conditions. They were first subjected to a 2 day 4˚C dark treatment, then grown at 16hr 22˚C days and 18˚C night. This was reduced after flowering to 18˚C day and 10˚C night for enhanced dormancy. Seeds were collected at silique dehiscing and left to dry for 1 week before being desiccated in calcium nitrate for 7 days to bring seeds to 8-10% moisture. They were then stored at -20˚C.

2.5.8 Germination experiment set up and data analysis

Sterilised seeds were evenly spaced on a layer of fine mesh which lay on filter paper dampened with 10ml sterile dH_2O. This was contained within lidded plastic boxes, and subjected to a 3 day cold treatment at 4°C for 24 hours in the dark. After this, the mesh with seeds on was transferred to a box of the same set up but containing 25ml of polyethylene glycol (PEG) solution at the desired drought condition (MPa), as described in table 2.5 and based on Michel *et al.* 1973. Boxes were kept at 15°C with 24 hour light for 14 days. Seeds were checked for germination using a stereomicroscope at the same time each day. The point of germination was defined as emergence of radicle. Results were analysed using a Two-Way ANOVA in GenStat, and calculating confidence intervals in Microsoft Excel.

2.5.9 Seedling establishment experiment set up and data analysis

Sterilised seeds were plated on ½ MS-agar for a 3 day cold treatment at 4°C in 24 hours dark. Plates were then transferred to 15°C 24 hours light for 2 days to germinate. Germinated seeds were transferred to ½ MS-agar plates containing varying amounts of

mannitol to create different drought conditions, as described in table 2.4. Seedlings were grown at 20°C for 14 days in 24 hour light. Seedling length (radicle, hypocotyl and lateral roots) was measured using electronic callipers for 35S promoter lines, and in Image J for native promoter lines. Results were analysed using a Two-Way ANOVA in GenStat.

Table 2.7 Amount of PEG or mannitol added to create levels of drought (Bill Finch-Savage, University of Warwick)

Nominal Water Potential (MPa)	-0.4	-0.6	-0.8
Polyethylene Glycol 8000 (g)	66.5	82.8	96.6
Mannitol (g)	29.1	43.8	58.3

2.5.10 Growth and maintenance of *Nicotiana benthamiana*

Seeds were sown onto a mix of 50% soil and 50% vermiculite. These were germinated and grown in conditions of 16 hours light / 8 hours dark and 18°C. After 5-6 weeks of growth plants were typically ready for infiltrations.

2.5.11 Transformation of *Nicotiana benthamiana* leaves by infiltration with *Agrobacterium tumefaciens*

A 5 ml culture of *A. tumefaciens* containing the plasmid of interest was grown overnight to an OD of 0.5–1.5 at 28°C, shaking at 200 rpm. 1.5ml of this culture was centrifuged at room temperature in a 2ml Eppendorf tube at 1000×*g* for 10 minutes (Eppendorf bench microfuge). The supernatant was discarded and pellet re-suspended in 1ml of infiltration media (50 mM MES, pH5.6; 0.5% glucose (w/v); 2mM Na_3PO_4; 100μM acetosyringone (1M in DMSO stock)). This was repeated to wash cells. Further infiltration buffer was added as necessary to reach OD_{600} 0.05-0.5. A wound was made with a small needle on the lower epidermis of a younger leaf and the cell suspension was injected using a 1 ml disposable syringe. Plants were left at room temperature for 3 days until tissue collection.

2.6 Microscopy

2.6.1 Isolation of *Arabidopsis* embryos

Embryos of varying developmental stages were isolated from their seed coats using fine forceps (Sigma-Aldrich No.5). A small incision was made at the micropyle, and gentle pressure applied at the opposite end, enabling the embryo to slide out.

2.6.2 Stereomicroscope imaging

Arabidopsis thaliana seeds and seedlings were screened and imaged using a Leica MZ-FLIII. It could be used to visualise YFP and RFP using the filter sets described in table 2.7. Images were taken using the Nikon Digital Sight DS-Fi2.

Table 2.8 Excitation and emission filter values on Leica MZ-FLIII

Fluorophore	Filter Excitation (nm)	Filter Emission (nm)
YFP	480/40	510
RFP	546/10	590

2.6.3 Confocal microscopy

Arabidopsis thaliana embryos, seedlings and mature leaves and infiltrated *Nicotiana benthamiana* leaf sections were imaged using a Leica TCS SP5 confocal microscope. Images were collected with a 10x or 63x water objective lens and samples were mounted onto slides in sterile dH_2O with a long coverslip. Fluorophores were excited and detected at their excitation/emission peaks as shown in table 2.7. Image processing was performed with Leica Advanced Fluorescence (LAS-AF) software (Leica GmbH, Germany). And cellular measurements for data described in 3.2.5 were performed in ImageJ, and subsequently analysed in GenStat with a One-Way ANOVA.

Table 2.9 Excitation and emission values of fluorophores and auto-fluorescent compartments

Fluorophore	Excitation (nm)	Emission (nm)	Type	Reference
eYFP	514	519 - 590	Protein	Clontech Laboratories, Palo Alto, CA
RFP	561	592 - 635	Protein	Clontech Laboratories, Palo Alto, CA
Dendra2	488 (unconverted)	508 - 535	Protein	Clontech Laboratories, Palo Alto, CA
	405 conversion			
	543 (converted)	560 - 650		
mEoSFP	488 (unconverted)	490 - 530	Protein	Dr. Jaideep Mathur, University of Guelph
	405 conversion			
	543 (converted)	570 - 620		
Storage metabolites	405	450 - 510	Autofluorescent material in protein storage vacuoles	Hunter *et al.*., 2007

2.6.4 Photoconversion of photoconvertible proteins

Isolated embryos were mounted directly into dH_2O on glass slides with a long coverslip. A region of interest was selected and 405nm light directed on it for long enough to photoconvert the fluorophore (approximately 20 seconds). This was detected real time in a sequential channel.

2.6.5 Photobleaching

Isolated embryos were mounted directly into dH_2O on glass slides with a long coverslip. A region of interest was selected and 405nm light directed on it for long enough to completely eradicate any YFP signal (between 30 seconds and 1 minute).

2.6.6 BFA incubation

Isolated embryos and seedlings were submerged in ½ MS 0.5% sucrose supplemented with 50µM Brefeldin A (from a 5mM stock made in DMSO) or dH_2O for 3 hours. They were mounted directly into dH_2O on glass slides with a long coverslip.

2.6.7 FM4-64 incubation

Isolated embryos and seedlings were submerged in 8nM FM4-64 (diluted with dH_2O from a stock made in DMSO) for 20 minutes and rinsed twice in dH_2O before mounting in dH_2O on glass slides with a long coverslip.

2.6.8 Dexamethasone induction

Sterilised dry *Arabidopsis* seeds, isolated embryos or seedlings containing the pDEX GW vector were plated onto ½ MS agar plates supplemented with dexamethasone (DEX) at a final concentration of 30μM. DEX stock was made to 30mM with DMSO.

Chapter 3: The effect of TIP and PIP overexpression on germination and seedling establishment

3.1 Introduction

Water uptake during seed imbibition is a trigger for seed germination, and is essential for tissue expansion and subsequent growth (Bewley *et al.* 2012). TIP3 are the only aquaporins expressed in the developing *Arabidopsis thaliana* embryo (Vander Willigen *et al.* 2006, Schmid *et al.* 2005), yet little is known about the exact role they play in the maturing and germinating seed, or the longer term effects they may have on establishment of seedlings. There is now gathering evidence to suggest the importance of TIP3 in these developmental stages. Treating germinating seeds with mercury, an aquaporin blocker, has been shown to significantly delay the later phases of germination, but has no effect on the earlier stages (Vander Willigen *et al.* 2006). In addition, TIP3;1 and TIP3;2 have been uniquely identified as having dual localisation, locating to both the plasma membrane and tonoplast (Gattolin *et al.* 2011). In combination, these conclusions have lead us to hypothesise that TIP3 has an important role to the seed in germination, and may provide a lasting effect into seedling establishment.

Many studies have analysed transcript levels of PIP and TIP in response to drought. In some cases, the response is a downregulation of TIP and PIP transcripts. MIP2 and MIP3 (TIP homologues) and MIP4 (PIP homologue) transcripts from *Nicotiana glauca* decreased in drought conditions (Smart *et al.* 2001), and *Arabidopsis thaliana* plants not watered for 12 days exhibited decreases in PIP1;3, PIP1;5, PIP2;2, PIP2;3, TIP1;1, TIP1;2, TIP2;1 and TIP2;2 transcripts (Alexandersson *et al.* 2005). In contrast, Alexandersson *et al.* (2005) also reports an increase in PIP1;4 and PIP2;5 in the same plants. A similar situation was reported by Sarda *et al.* (1999) whereby transcript abundance of SunTIP18 from Sunflower (*Helianthus annuus)* decreased in roots deprived of water for 24 hours, but SunTIP7 increased (Sarda *et al.* 1999). In fact, upregulation of TIP and PIP transcripts in response to drought is reported in numerous species. In *Jatropha*, JcPIP1 transcripts increased during the recovery from water stress while JcPIP2 transcripts increased as an early response (Jang *et al.* 2013). In cauliflower (*Brassica oleracea*) slices, BobTIP26 mRNA increased dramatically upon dessication (Barrieu *et al.* 1999). ZmTIP2;3 transcripts increased in maize (*Zea mays*) seedlings (Lopez *et al.* 2003), and OsTIP1;1 OsTIP1;2, OsTIP4;1 and OsTIP4;2 in rice (Oryza sativa) seedlings (Li *et al.* 2007) upon PEG (polyethylene glycol) treatment. These studies have lead the scientific community to the consensus that aquaporin regulation is

carefully controlled in response to water stress, and that the upregulation of particular isoforms as a stress response could confer targets for drought tolerance.

From this hypothesis, numerous studies have employed overexpression of specific aquaporin isoforms in an attempt to increase germination and growth rates in drought conditions. However, once again, there have been conflicting results published as to the success of these transgenic plants. 3 week old *Arabidopsis thaliana* seedlings overexpressing *Glycine soja* GsTIP2;1 showed increased dehydration speed, and struggled to germinate and survive on mannitol plates replicating an environment of drought (Wang *et al.* 2011). Similarly, overexpression of the *Arabidopsis thaliana* PIP1;2 in transgenic tobacco resulted in wilting under water stress sooner than in wild-type plants (Aharon *et al.* 2003). Despite these two reports, there have been examples where overexpression of an aquaporin has actually conferred drought tolerance. Sade *et al.* (2009) demonstrated this in a 3 year long commercial glasshouse trial in which tomato plants (*Solanum lycopersicum)* overexpressing SlTIP2;2 were able to switch their water use from an isohydric to anisohydric strategy. The former is characterised by reduced stomatal conductance whereas in the latter state plants constantly transpire, even to a reduced leaf water potential, a strategy seen as risky but beneficial in mild drought conditions (Sade *et al.* 2012). The change of strategy resulted in tomato plants with significant increases in fruit yield, harvest index and plant mass when under water defecit (Sade *et al.* 2009). In addition, overexpression of OsPIP1;3 in rice promoted germination (Liu *et al.* 2007) and tobacco plants transformed to overexpress the wheat (*Triticum aestivum*) TaAQP7 grew better in conditions of drought (Zhou *et al.* 2012). Lastly, Arabidopsis overexpressing the *Panax ginseng* PgTIP1 showed tolerance to water stress when grown in deep (45cm) pots (Peng *et al.* 2007).

Based on these studies, it is not possible to make a general conclusion as to whether overexpression of aquaporins enhances drought tolerance in plants. To date there has not been a comprehensive study in which a single species overexpressing their native aquaporins, at their developmentally relevant time points, has been assessed for increased drought tolerance. This chapter aims to address this by assessing seed germination and seedling establishment of *Arabidopsis thaliana* transgenic lines overexpressing AtTIP3;1, AtTIP3;2, the truncated TIP3;2 termed TIP3;2ΔC, AtTIP1;1 and AtPIP1;2 in different levels of water stress.

3.1.1 Aims and Experimental Approach

- To overexpress TIP1;1, TIP3 and PIP1;2 in seeds of transgenic lines.
- To determine the effect of overexpression of TIP1;1 and TIP3;1 on seed germination and seedling establishment in conditions of water stress.
- To investigate the effect of TIP3;1 overexpression on tissue development.
- To determine the effect of introducing additional TIP3;2 and non-native PIP1;2 on seed germination and seedling growth in conditions of water stress.

TIP3, TIP1;1 and PIP1;2 were detected by immunoblot in samples from dry, imbibed and germinating transgenic seeds using a custom anti-TIP3 peptide antibody and anti-GFP. The impact of overexpression of TIP1;1, TIP3;1, TIP3;2 and PIP1;2 on early plant development was determined by measuring germination rates and counts, and seedling length as a representative parameter for seedling establishment. These experiments were performed in water stress conditions mimicking drought to confer any increased or decreased tolerance of transgenic lines. Confocal microscopy was used to confirm localisation of PIP1;2 to the plasma membrane and to image cells of seedlings overexpressing TIP3;1.

3.1.2 Constructs

Figure 3.1 shows the schematic diagrams of the constructs used in this chapter, their designated shorthand names and their expected localisation.

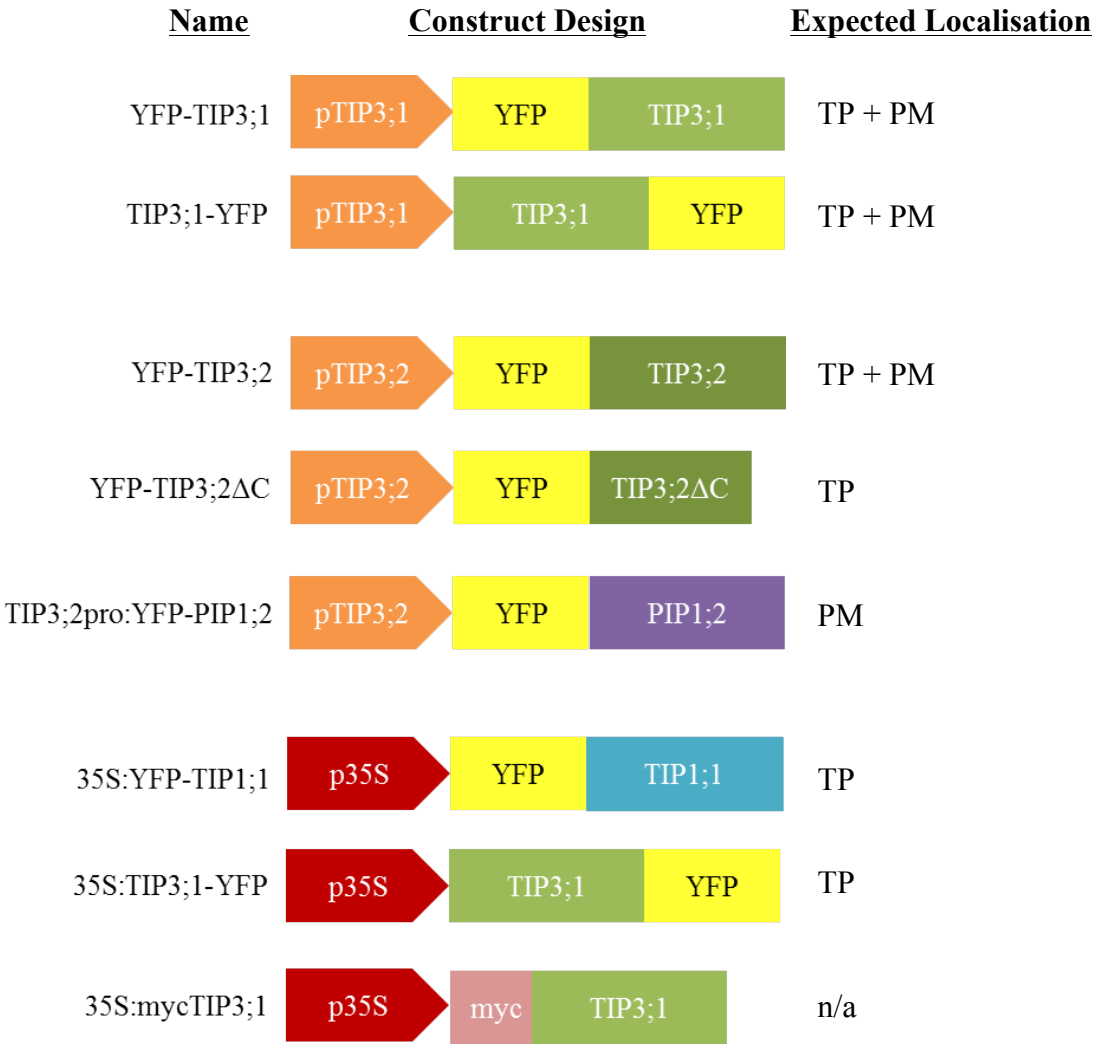

Figure 3.1: Schematic representation of the constructs transformed into Col-0 ecotype *Arabidopsis thaliana* used to produce the results in Chapter 3
Full length promoter and genomic sequences (as detailed in tables 2.3 and 2.5, materials and methods) for TIP3;1, TIP3;2, TIP1;1, PIP1;2 and the truncated sequence of TIP3;2 with 75 base pairs removed to give TIP3;2ΔC, were cloned into pGreen-0029 with YFP; except for 35S:mycTIP3;1 where the myc sequence was fused onto the TIP3;1 genomic sequence using PCR. 35S:mycTIP3;1 was not visualised and so localisation is not listed. Lists of constructs cloned previously to this work are listed in methods table 2.5. TP=Tonoplast, PM=Plasma Membrane.

3.2 Results

3.2.1 TIP3 antibody optimization

A custom antibody was designed on one previously reported in the literature, first used in Jauh *et al.* (1999). In this work it was found that raising an antibody against the C terminal sequence, HQPLAPEDY, of *Arabidopsis thaliana* TIP3;1 is sufficient to allow specific recognition of the protein for immunoblot analysis. Given that TIP3;2 has the same C terminal sequence as TIP3;1, this antibody will recognise both isoforms. The affinity-purified antibody, made in rabbit, was ordered from GenScript USA Inc. Total protein extract from 20 wild-type Col-0 and TIP3;1pro:YFP-TIP3;1 expressing dry *Arabidopsis thaliana* seed was separated by SDS-PAGE and blotted onto nitrocellulose. The anti-TIP3 antibody was diluted in 5% milk TBST (as per standard protocol, methods section 2.4.4) to produce range of final concentrations between 1.5µg/ml – 0.15 µg/ml (detailed in methods section 2.4.6). Figure 3.2 illustrates the resulting blots treated with an enhanced chemiluminescence kit (ECL Western Blotting Substrate**,** Promega USA) and detected upon exposure to X-ray film which was then developed. TIP3;1 translationally fused to YFP is ~45kDa and native TIP3 25.6kDa in size; both proteins migrate to an estimated size similar to their calculated molecular weight (as indicated by <). Bands indicated by * are thought to be breakdown products of TIP3. In order to achieve a balance between detecting all the available TIP3 protein, and avoiding non-specific binding, it was concluded that the 1/2000 dilution to give 0.5 µg/ml final concentration should be used for TIP3 detection with this antibody in future experiments (figure 3.2)

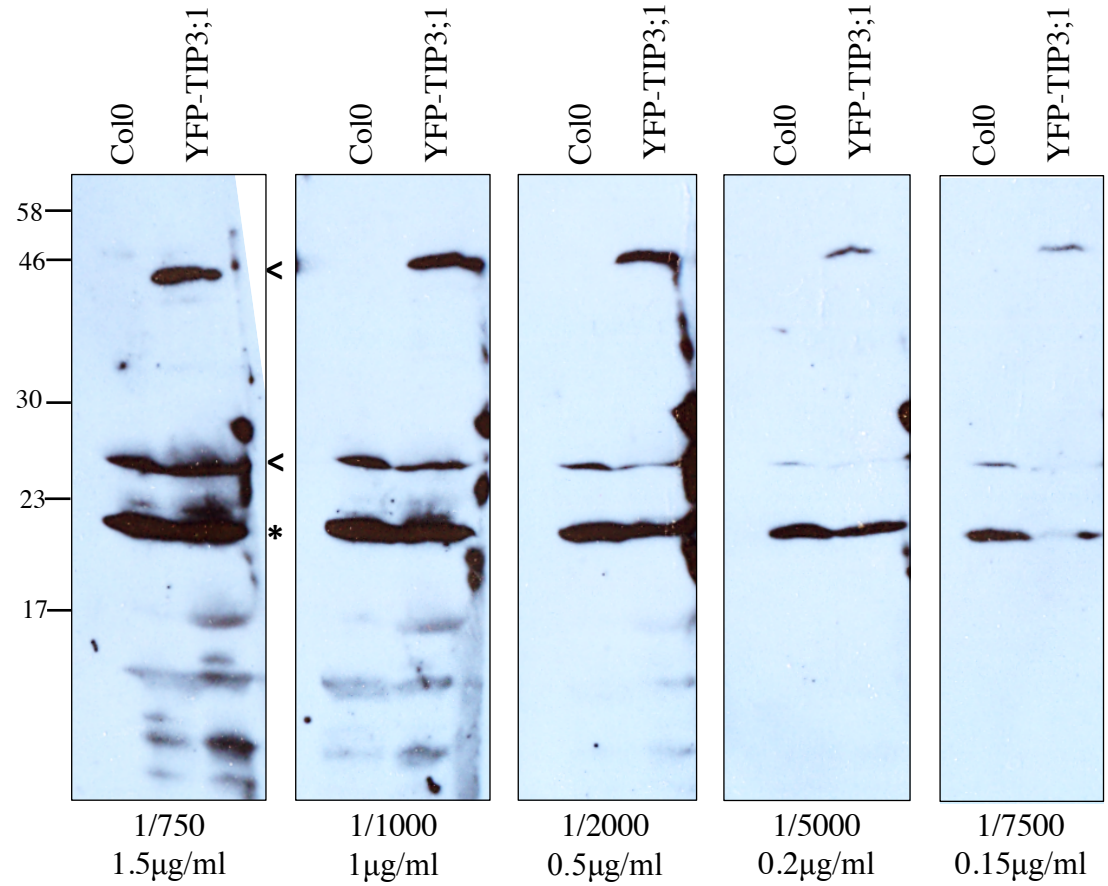

Figure 3.2: Custom made TIP3 polyclonal antibody optimisation
The antibody was raised against the TIP3 C terminal peptide HQPLAPEDY in rabbit. It was tested using total protein extract from 20 wild-type Col-0 and TIP3;1pro:YFP-TIP3;1 expressing dry *Arabidopsis thaliana* seed. For use as a primary antibody, anti-TIP3 is best used at a concentration of 0.5µg/ml in 5% milk TBST for 1 hour at room temperature. Molecular weight of the marker bands is given in kDa.

3.2.2 Expression of TIP can be detected by immunoblot

The anti-TIP3 antibody and an anti-GFP antibody (Miltenyi Biotec) were used to confirm expression of TIP3;1-YFP and YFP-TIP3;1, YFP-TIP3;2 and YFP-TIP3;2ΔC (in which the last 23 amino acids are removed, abolishing plasma membrane localisation as discussed in section 5.2.2), along with YFP-TIP1;1 and YFP-PIP1;2 in transgenic lines (described schematically in figure 3.1). 20 dry (figure 3.3A and B), imbibed (figure 3.3C and D) or germinating (figure 3.3E and F) seeds from each transgenic line were selected by fluorescence using a stereomicroscope and homogenised directly into 2x Laemmli buffer (methods section 2.4.1) to provide total protein extracts which were separated by SDS-PAGE. Positive seeds were selected by fluorescence stereomicroscopy prior to homogenisation to ensure no negative seeds were used. In addition, seeds of the segregating heterozygous line 35S:TIP3;1-YFP were separated based on fluorescence intensity. Homozygous seeds appeared brighter than heterozygous seeds, an observation discussed in more detail in section 3.2.4.

Each sample was detected by both anti-TIP3 and anti-GFP antibodies. Anti-TIP3 recognises proteins containing the epitope HQPLAPEDY, meaning both endogenous TIP3 (indicated by arrows (> <) in figure 3.3 A, C and E) and introduced TIP3 sequences (indicated by *) are detected. TIP3;2ΔC, TIP1;1 and PIP1;2 are not detected by this antibody as they do not contain this C-terminal motif, however they are detected by anti-GFP (indicated by * in figure 3.3. B, D and F) as they are translationally fused to a YFP tag (figure 3.1). YFP and GFP are similar enough in sequence that the anti-GFP antibody will recognise YFP. Col-0 ecotype seeds were used as a negative control for anti-YFP and positive control for anti-TIP3.

Despite using the same amount of starting material in each blot, total protein was not normalised before loading as these immunoblots were produced only to confirm protein expression. Gels were stained with coomassie post-blotting (not shown), and showed roughly equal loading. However, due to the extremely high quantities of proteins in seed tissues it was also difficult to make exact discrepancies between lanes. To make direct comparisons, standardised loading would be necessary and so conclusions comparing protein abundance should be made with caution in this instance.

Blots presented in figure 3.3 are not identical in exposure time and instead are representatives of a collection of exposure times for each blot. This selection of blots was chosen to best indicate the range of introduced YFP-tagged proteins expressed. The signal for these bands is much lower than native TIP3 bands.
TIP3;1 and TIP3;2 translationally fused to YFP migrate to ~45kDa, whilst the truncated YFP-TIP3;2ΔC is smaller due to the removal of the last 23 residues, and YFP-TIP1;1 is slightly smaller due to the smaller molecular weight of TIP1;1 (boxed in figure 3.3F). All proteins therefore appear smaller than their expected molecular weights (TIP3 are 25.6kDa, TIP1;1 25.6kDa and YFP 26.4kDa). This is most likely due to their electrophoretic properties as membrane proteins (Rath *et al.* 2009).

Expression of full length YFP-TIP3;2, YFP-TIP3;1, and TIP3;1-YFP expressed under their native promoters is detected at each stage of seed development. The signal of YFP-TIP3;1, and TIP3;1-YFP does appear to diminish in germinating seeds (figure 3.3. E and F). The inclusion of TIP3;1-YFP on these immunblots, the only line which is not used is germination and establishment assays discussed later in this chapter, is to show that TIP migration and size is not affected by the terminus to which YFP is appended (shown clearest in figure 3.3 panels A-D).

Expression of YFP-TIP1;1 and TIP3;1-YFP under the 35S promoter should theoretically be detected at all three developmental seed stages. However YFP-TIP1;1 is only detected in germinating seeds (figure 3.3F). This is most likely due to differences in expression between the dry and imbibed seed (Nakabayashi *et al.* 2005). This is likely to also be the case for the 35S:TIP3;1-YFP lines, in which expression appears most prominent in imbibed seeds (figure 3.3 C and D). Within these lines, the difference in expression between heterozygous and homozygous seeds is evident, with signal for TIP3;1-YFP in heterozygous seeds appearing approximately 2-fold lower than homozygous. Despite this, there appears to be an overall lower signal than in seeds from TIP3;1 and TIP3;2 promoter-driven lines. This is most likely a result of not normalising total protein concentration before gel loading.

PIP1;2 expression is visible under the stereomicroscope but is too low in abundance to be detected by immunoblot. We confirm the expression of PIP1;2 in maturing and germinating seeds by confocal microscopy later in this chapter.

Protein samples were heated to 95˚C prior to gel loading. In some instances it has been recorded that this can cause aggregation of membrane proteins (Robinson 2011). However, inclusion of the reducing agent β-mercaptoethanol in the denaturation buffer used here reduces the likelihood of this occurrence. In addition, no protein aggregates were found in the stacking gel. It is therefore fair to conclude that the higher bands detected in the lanes for YFP-TIP1;1 and YFP-TIP3;2 expressing seeds (see Δ in figure 3.3 A, E, B and F) are a result of protein dimers. This conclusion can be made on the basis that there are larger bands on the blots which are double the size of the detected monomers, this is already been reported in the literature for TIP in several species (Johnson *et al.* 1989, Jauh *et al.* 1998). Breakdown products also appear in later stages of seed development for almost all lines, most probably due to protein turnover (see filled arrow heads in figure 3.3.F).

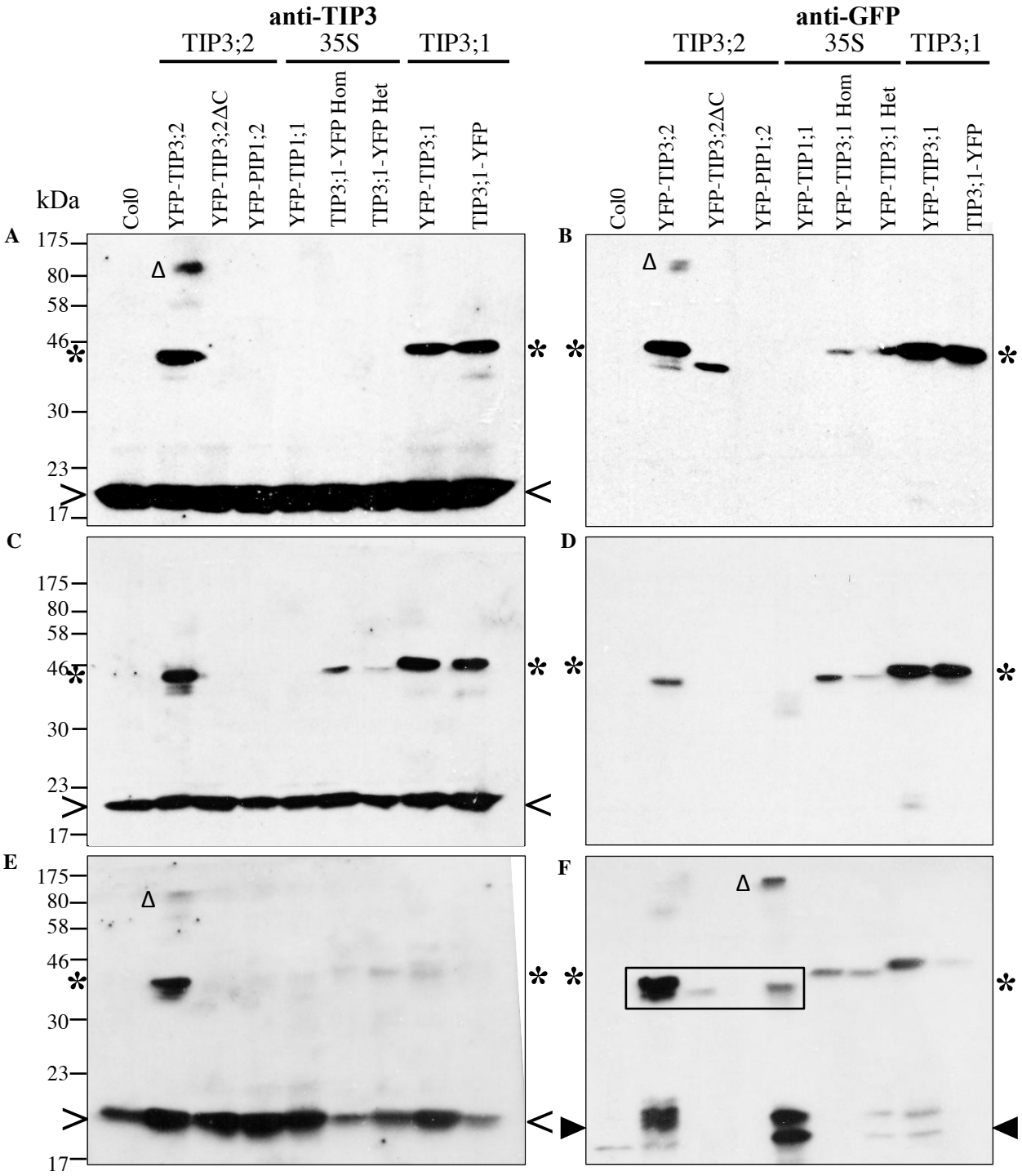

Figure 3.3: TIP3;1-YFP, YFP-TIP3;1, YFP-TIP3;2, YFP-TIP3;2ΔC and YFP-TIP1;1 protein is expressed in dry, imbibed and germinating seed of transgenic lines
Total protein extracted from 20 (**A-B**) dry, (**C-D**) imbibed or (**E-F**) germinating seed of Col-0 and transgenic lines containing TIP3;1, TIP3;2, TIP3;2ΔC, TIP1;1 or PIP1;2 translationally fused to YFP under the TIP3;2, 35S or TIP3;1 promoters. Seeds were selected by fluorescence using a GFP filter on a stereomicroscope. PIP1;2 expression is visible under the stereomicroscope but is too low in abundance to be detected by immunoblot. Protein was detected with (**A,C,D**) anti-TIP3 or (**B,D,E**) anti-GFP. anti-TIP3 confirms presence of endogenous TIP3 (> <). TIP3;1-YFP, YFP-TIP3;1, YFP-TIP3;2, YFP-TIP3;2ΔC and YFP-TIP1;1 protein was detected by both antibodies (*). Dimers (Δ) and breakdown products also noted (▶◀). Molecular weight of the marker bands is given in kDa. (TIP3 are 25.6kDa, TIP1;1 25.6kDa and YFP 26.4kDa). Blots are representatives of a collection of exposure times, to maximise variety of proteins detected

3.2.3 Overexpression of TIP3;1 and TIP1;1 is detrimental to germination of *Arabidopsis thaliana* seeds in water stress conditions

Germination counts and rates of transgenic seeds overexpressing TIP3;1-YFP or YFP-TIP1;1 under the 35S promoter were compared to the Col-0 wild type, at varying degrees of water stress. Seeds of all lines were produced at the same time, in the same conditions, as described in materials and methods section 2.5.7, to ensure comparability. Water stresses were created using different concentrations of polyethylene glycol (PEG) 8000 to make nominal osmotic pressures measured in Mega Pascals (MPa) (Finch-Savage B. and Footitt S., unpublished; based on Michel *et al.* 1973). Osmotic pressures of -0.4, -0.6 or -0.8 (MPa) were used to create water stress conditions which correspond to varying levels of drought. -0.4MPa is the condition with the most water available to the seed, and -0.8MPa the least, therefore -0.8MPa is the condition with the highest water stress, and highest level of drought.

Germination experiments were conducted on evenly spaced, dry-sterilised seeds placed on a layer of fine mesh. Seeds must be evenly spaced to avoid influences of neighbouring seeds on germination speed (Baskin and Baskin 2014), and must be dry-sterilised to avoid microbial growth. The fine mesh on which the seeds were positioned was initially placed on top of filter paper dampened with dH_2O, within an enclosed box. Boxes were then kept in the dark for 3 days at 5°C to stratify seeds. After this, the fine mesh on which seeds lay was transferred to an identical box, which additionally contained a plastic grid, piece of gauze and filter paper wetted with the appropriate PEG solution (figure 3.4A). These boxes were termed 'germination boxes', and were additionally sealed within plastic bags to provide a controlled environment. The layers within the box were used in order to maintain seed contact with the filter paper, but also to ensure seeds do not become submerged, causing oxygen depletion. Oxygen depletion, or anoxia, has a widely reported negative effect on germination (Finch-Savage *et al.* 2005, Mattana *et al.* 2007). Boxes were kept at 15°C with 24 hour light for 14 days. Seeds were checked for germination using a stereomicroscope at the same time each day. The point of germination was defined as emergence of radicle, as in accordance with the definition provided in Weitbrecht *et al.* (2011).

Experimental design included 3 technical replicates of each line in each osmotic condition. In each box ~50 seeds were analysed, leading to a total of 1800 seeds being manually scored for a germination time.

Figure 3.4B shows the total number of seeds which germinated in each line, in each condition, and figure 3.4C shows the length of time it took for these seeds to germinate. Percentages of seeds which germinated were calculated and transformed to arcsine to convert the binomial distribution into a normal distribution, before being analysed by a Two-Way ANOVA. From this output, the Least Significant Difference (LSD) between the numbers of Col-0 seeds which germinated, and the number of 35S:YFP-TIP1;1, heterozygous 35S:TIP3;1-YFP or homozygous 35S:TIP3;1-YFP seeds which germinated within each condition of water stress was compared to the *actual differences* recorded. The actual differences must be greater than the LSD for there to be a significant difference ($P<0.05$). The same analysis, was conducted for data scoring the time it took for seeds to germinate, without need for transformation.

A significantly lower amount of seeds overexpressing TIP3;1-YFP at the homozygous level germinate in each water stress condition in comparison to Col-0. In addition, the same seeds were significantly slower to germinate at -0.4MPa and -0.6MPa. It could therefore be concluded that constitutive overexpression of TIP3;1 is detrimental to germination in water stress conditions. This detrimental effect of overexpression is also witnessed in seeds overexpressing YFP-TIP1;1. Here, seeds were significantly slower to germinate than Col-0 at -0.6MPa and -0.8MPa.

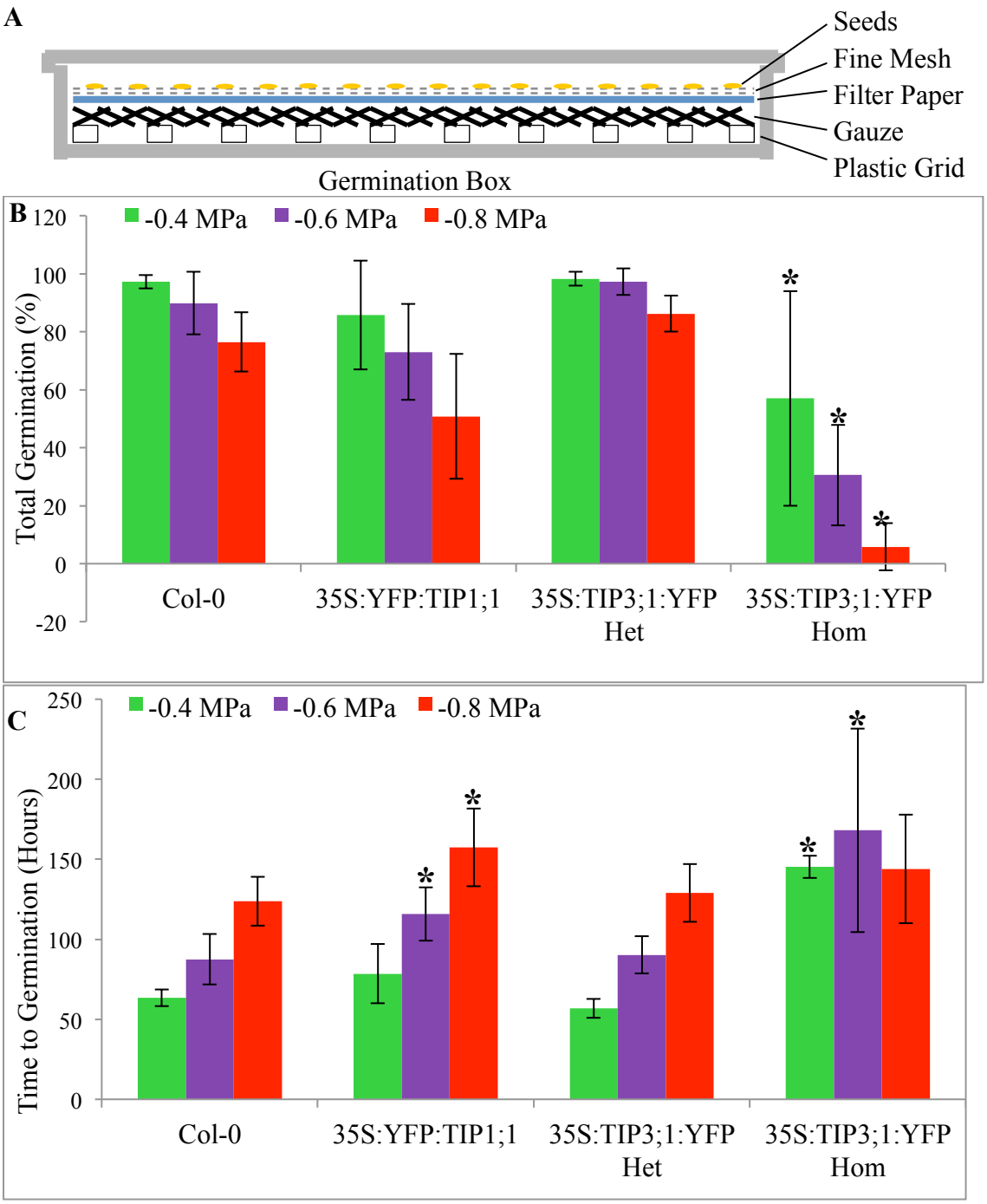

Figure 3.4: Overexpression of TIP3;1 and TIP1;1 is detrimental to germination of *Arabidopsis thaliana* seeds in water stress conditions

(**A**) *Arabidopsis thaliana* seeds were germinated in boxes to create a controlled environment. Filter, gauze and grid layers were used to ensure seeds would not come into contact with PEG medium used to create water stress. Water stress was measured in MPa, with -0.8MPa being the highest level water stress, mimicking the highest level of drought. (**B**) Total number of seeds which germinated in water stress conditions within a 2 week period. Total number of seeds which germinated was significantly reduced in lines overexpressing TIP3;1 at the homozygous level. (**C**) Each seed was manually assigned a time point by which it had germinated. Seeds overexpressing TIP3;1 and TIP1;1 took significantly longer to germinate than wild-type Col-0. Significance was based of Least Significant Differences (LSD) generated from Two-Way ANOVAs. Error bars are standard error between technical replicates. n= between 50-200 seeds for each lines in each condition (which be explain variability in error bars)

3.2.4 The effect of overexpression of TIP3;1 on *Arabidopsis thaliana* seedling establishment in water stress conditions is dose dependent.

Seedling establishment is described as the period from which seed storage reserves are exhausted post-germination until establishment as an independent organism is achieved; during this phase seedlings are most vulnerable to stress (Raven *et al.* 2005). Seeds of the same lines overexpressing TIP3;1-YFP or YFP-TIP1;1 under the 35S promoter, as described in section 3.2.4, were used to assess the effect of TIP overexpression on *Arabidopsis thaliana* seedling establishment in water stress conditions.

To do this, sterilised seeds were evenly dispersed onto a layer of fine mesh on ½ MS-agar plates and subjected to stratification at 4°C for 3 days. Seeds were germinated in 24 hours light at 15°C, and 2 days after germination (D.A.G.), the fine mesh was transferred to ½ MS-agar plates supplemented with mannitol. Different mannitol concentrations were used to create the same osmotic pressures described in section 3.2.5; -0.4, -0.6 and -0.8MPa. Full methods are available in section 2.5.9. Mannitol was used because it is has a lower molecular weight than PEG and is thus more easily incorporated into agar (van der Weele *et al.* 2000).

Seedlings were grown upright at 20°C for 14 days in conditions of 24 hour light, before the radicle, hypocotyl and lateral roots for each seedling were measured individually using electronic callipers. Seedling length at 16 D.A.G (exposed to water stress for 14 days) was used as a measure of seedling establishment.

Each plate had ~10 seedlings, and there were 20 technical replicates for each of the 4 lines in each of the 3 conditions. In total, ~2400 seeds were plated, however due to inevitable losses through microbial contamination, ~1200 seedlings were measured in total.

Seedlings overexpressing TIP3;1 at the homozygous level have a significantly reduced total seedling length (total sum of radicle, hypocotyl and lateral roots) than wild-type Col-0 in water stress conditions ($P<0.05$) whereas heterozygous seedlings are significantly larger than wild-type Col-0 in water stress conditions ($P<0.05$) (figure 3.5). Significance was calculated using Least Significant Differences (LSD) generated from a Two-Way ANOVA, in the same way as described in the previous section 3.2.3. This suggests overexpression of TIP3;1 has a dose-dependent effect on seedling establishment

in water stress conditions, as it confers drought tolerance until a particular threshold amount of TIP3;1 protein is reached.

Seedlings overexpressing TIP3;1-YFP at the homozygous and heterozygous level also appear to exhibit the same phenotypes in optimal conditions, as in water stress conditions (figure 3.6A and B).

35S:TIP3;1-YFP seedlings were identified as homozygous or heterozygous according to level of fluorescence visualised with the GFP filter on a stereomicroscope, coupled with their strong growth phenotypes (figure 3.6A and B). This was confirmed using ratio counts. Approximately 25% of seedlings were very small with a uniform pattern of YFP signal, 50% of seedlings were fluorescent but much larger, and the other 25% did not exhibit any true fluorescent signal. These observations were analysed with Chi^2 to confirm that seeds of the line 35:TIP3;1-YFP segregate in a 1:2:1 ratio (negative:heterozygous:homozygous). Calculated Chi^2 values ($\chi 2$, table 3.1) were smaller than the critical value (5.99, using the Degrees of Freedom of 3) and thus ratios of seedlings were no different to that expected of a segregating line $P<0.05$.

Table 3.1: Four different seed batches from a confirmed 35S:TIP3;1-YFP transgenic plant were analysed with Chi^2 to confirm they segregate as a heterozygous line. Chi^2 values ($\chi 2$) were smaller than the critical value (5.99, using Degrees of Freedom as 3)

Progeny	Not fluorescent	Large and fluorescent	Small and fluorescent	Total	$\chi 2$	Sig. Difference ($P<0.05$)
1	16	25	10	51	1.43	No
2	21	36	16	73	0.70	No
3	18	34	10	62	2.65	No
4	22	32	11	65	3.74	No

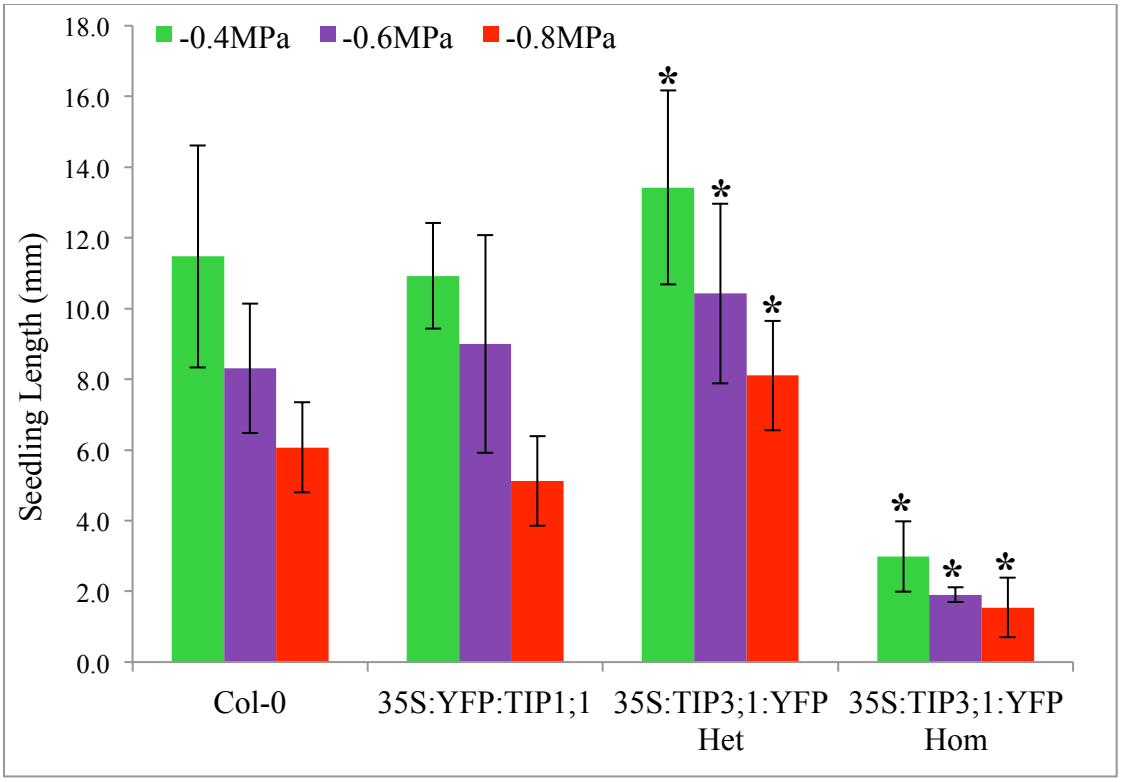

Figure 3.5: Homozygous overexpression of TIP3;1 is detrimental to *Arabidopsis thaliana* seedling establishment in water stress conditions, but heterozygous overexpression is beneficial

Arabidopsis thaliana seeds were germinated under normal conditions and transferred to water stress conditions after 2 days. These conditions were created using Mannitol in ½ MS 0.8% Agar medium. Water stress was measured in MPa, with -0.8MPa being the highest level of water stress, mimicking the highest level of drought. Each seedling was measured by hand from root tip to the top of the hypocotyl, including lateral roots, 14 days after transfer. Seedlings overexpressing TIP3;1 at the homozygous level have a significantly reduced seedling length than wild-type Col-0 in water stress conditions whereas heterozygous seedlings are significantly larger. Significance was worked out using Least Significant Differences (LSD) generated from a Two-Way ANOVA. Error bars are standard error between technical replicates. n=80-120 seedlings for each line in each condition.

Figure 3.6: Wild type, heterozygous and homozygous seedlings overexpressing TIP3;1-YFP are easily distinguished by fluorescence, and homozygous seedlings appear to be developmentally delayed

Fluorescence of 10 D.A.G. *Arabidopsis thaliana* overexpressing TIP3;1-YFP under the 35S promoter. Seedlings grown on ½ MS 0.8% Agar. **A: i**=Negative control seedling, (green root tip most likely cell wall autofluorescence. **ii**=Heterozygous, **iii**=Homozygous. **B:** Homozygous seedlings. Homozygous seedlings appear to be developmentally delayed in comparison to negative and heterozygous expressing seedlings. Green = YFP, Red = autofluorescence. Scale bar = 1mm

3.2.5 Overexpression of TIP3;1 affects cell morphology

Given the strong phenotypes in both homozygous and heterozygous seedlings expressing TIP3;1-YFP, the effect of overexpression on cell morphology was explored.

Firstly, it was confirmed that the 35S promoter drives expression of TIP3;1-YFP constitutively accross tissues in both heterozygous and homozygous seedlings (figure 3.7A-B). Using FM4-64 to label plasma membranes, it was identified that TIP3;1-YFP localises to the tonoplast in seedlings of both types (figure 3.7 B-C). This is in contrast the dual plasma membrane-tonoplast localisation demonstrated in embryos of these lines (discussed in more detail in chapter 5).

Imaging cells of heterozygous and homozygous seedlings at the same age and at the same magnification identified clear differences (figure 3.8). Leaf size is reduced in homozygous seedlings in comparison to homozygous seedlings (figure 3.8 panels A and D), in addition, the cellular morphology appears to be different between the seedlings (figure 3.8 B and E). From images of a higher magnification (figure 3.8 panels C and F), it is apparent that the curvature of digits (the interlocking curved extensions typical of an *Arabidopsis* leaf epidermal, or pavement cell) is reduced.

Based on this initial observation, 3 cells each from either 3 homozygous or heterozygous 4 D.A.G. seedlings (36 cells in total) were analysed in ImageJ for differences in area, perimeter and circularity. These measurements were then analysed for significance using a One Way ANOVA.

Initially, it was thought that perimeter would be reduced in cells of homozygous embryos due to their lack of curvature, however it has recently been shown that cell area and cell perimeter can be widely variable between cells of the same leaf, as well as cells between seedlings at the same developmental age (Staff *et al.* 2012). Staff *et al.* (2012) therefore suggest alternative geometric measurements to compare between cells. It is suggested that the calculated area:perimeter ratio could be a good measurement for cell circularity (Staff *et al.* 2012). Circles have a high area:perimeter ratio, therefore the higher the ratio, the more rounded and less prominent digits a cell will have. Cells of homozygous 35S:TIP3;1-YFP seedlings have a significantly higher area:perimeter ratio ($P=0.029$) than cells of heterozygous seedlings (figure 3.8G). In addition, ImageJ calculated circularity as

a measure of how well the cells fit a circular shape, with a measure of 1 indicating a perfect circle (calculated using $4\pi\times[\text{Area}]/[\text{Perimeter}]^2$). Cells of homozygous seedlings exhibited a significantly higher circularity ($P<0.001$) than heterozygous cells (figure 3.8H). Therefore cells of homozygous 35S:TIP3;1-YFP seedlings can be concluded as more circular in shape, with less prominent and reduced curvature of digits.

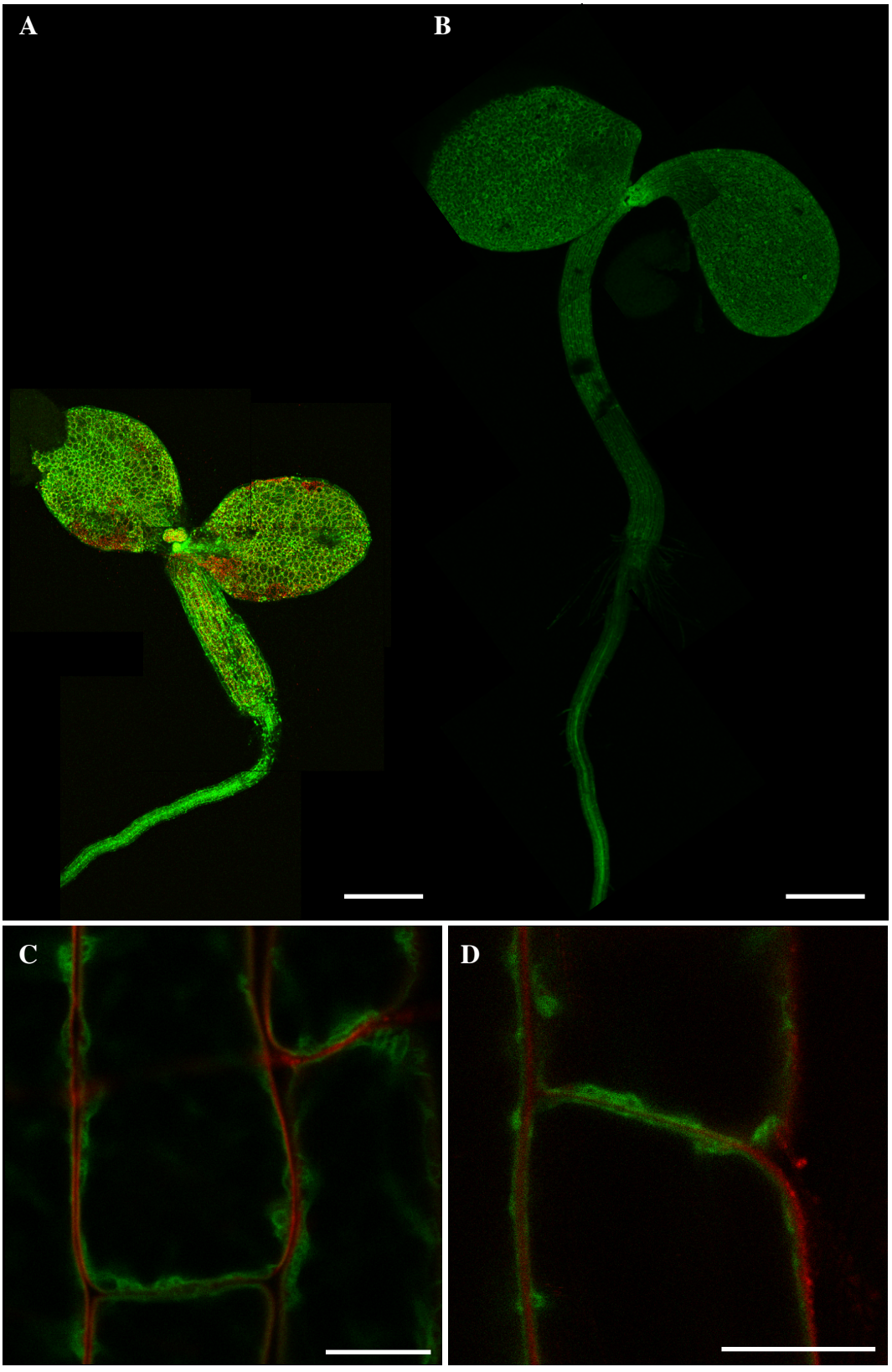

Figure 3.7: TIP3;1-YFP is expressed in all tissues of seedlings and localised to the tonoplast when driven by the 35S promoter
Arabidopsis thaliana seedlings 14 D.A.G overexpressing TIP3;1-YFP **A:** Homozygous seedling **B:** Heterozygous. Green = YFP, Red = autofluorescence. Scale bars = 100µm. TIP3;1-YFP is localised at the tonoplast in **C**: homozygous and **D**: Heterozygous seedlings. Green = YFP, Red = FM4-64. Scale bars = 10µm

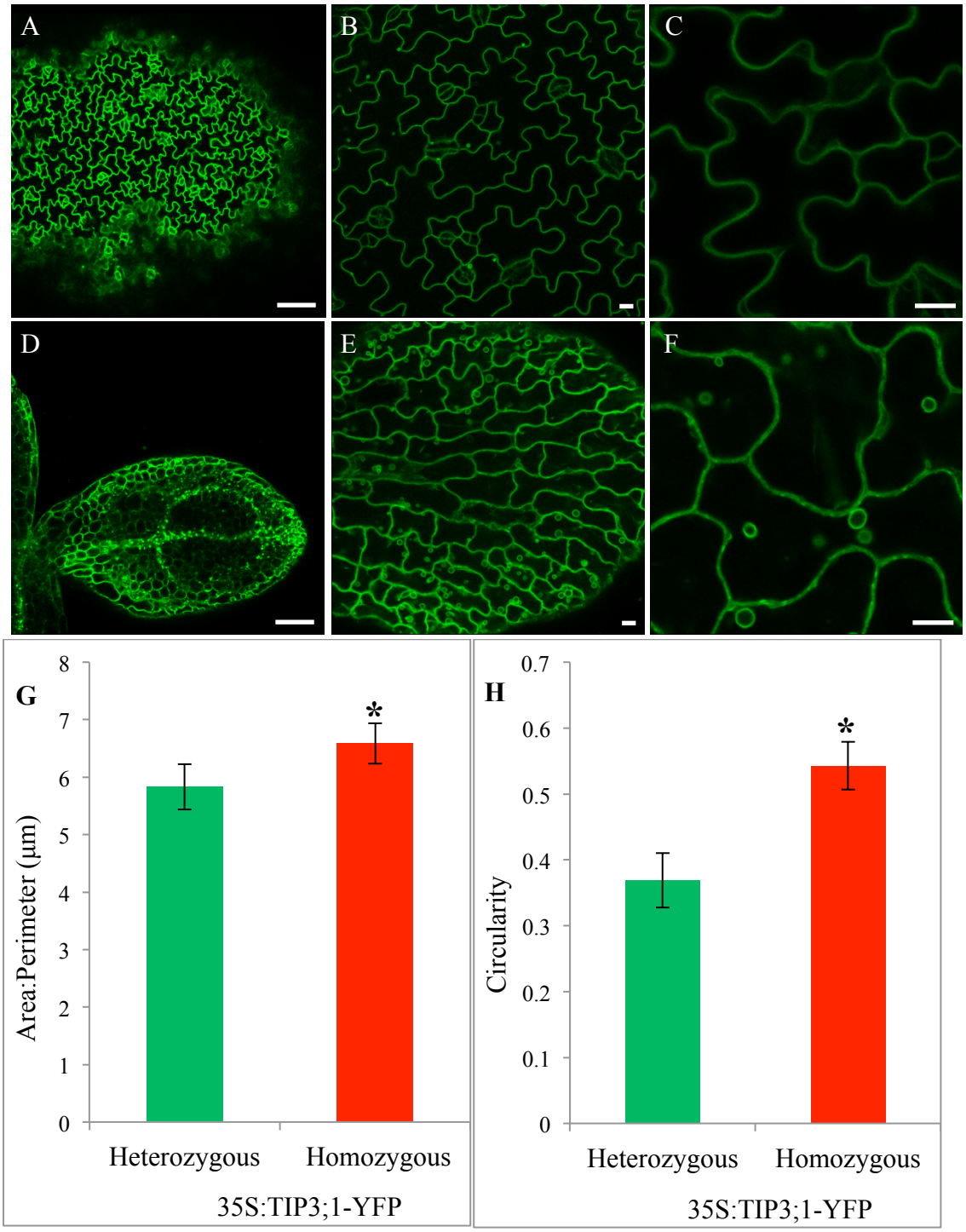

Figure 3.8: Epidermal cell shape is affected in seedlings overexpressing TIP3;1-YFP at the homozygous level.
4 DA.G. *Arabidopsis thaliana* seedlings (**A-C**) heterozygous and (**D-F**) homozygous for the overexpression of TIP3;1-YFP under the 35S promoter. Leaf size is altered between (**A**) heterozygous (**D**) and homozygous seedlings. Cell shape is altered between (**B**) heterozygous (**E**) and homozygous seedlings. The curvature of a typical epidermal cell digit is maintained within (**C**) heterozygous seedlings, but lost in (**F**) homozygous. Scale bars, **A** & **D** = 100µm, **B-C** & **E-F** = 10 µm. (**G**) Cells of homozygous seedlings have a significantly higher area:perimeter ratio (P=0.029), (**H**) and a significantly higher circularity (P<0.001) than cells of heterozygous seedlings of the same age. Therefore cells of homozygous seedlings are more circular, and digits are less prominent in comparison to heterozygous cells.

3.2.6 mycTIP3;1 is not detectable in transgenic *Arabidopsis thaliana* or infiltrated *Nicotiana benthamiana*

The phenotypes of 35S:TIP3;1-YFP seeds and seedlings are unlikely to be due to overexpression of an aquaporin, as 35S:YFP-TIP1;1 lines do not exhibit these cellular or growth changes. To ascertain that the phenotypes of homozygous and heterozygous 35S:TIP3;1-YFP seeds and seedlings were independent of the presence of YFP, a myc-epitope tagged version of TIP3;1 was generated. The nucleotide sequence ATG GAG CAG AAA CTC ATC TCT GAA GAG GAT CTG translating into the myc epitope tag MEQKLISEEDL, was fused to the TIP3;1 sequence taken from the 35S:TIP3;1-YFP vector. This fragment was cloned back into the 35S:pGreenII-0029 vector (see materials and methods 2.3.8), to produce 35S:mycTIP3;1 (figure 3.1).

Arabidopsis thaliana Col-0 ecotype plants were transformed with this vector (materials and methods 2.5.4) and DNA was extracted from leaf tissue from T3 generation plants for PCR screening. Primers were designed to target both the 35S:myc region (red arrows in figure 3.9A) to produce a fragment 260 base pairs long, and the mycTIP3;1 region (blue arrows in figure 3.9A), producing an 840 base pair long fragment. Primer sequences can be found in table 2.4, materials and methods. The 35S:mycTIP3;1 construct is confirmed to be in samples 1a and 1c, 2b, 3a and 3b, 4a and 4b, and 5b and 5c; 9 out of the 11 plants sampled (figure 3.9 B).

Consequently, RNA was extracted from leaves of some of these same plants, and was used for RTPCR (figure 3.9C). At this stage, transcripts for mycTIP3;1 were only detectable in plant 3a.

Total protein was extracted from leaves of two replicates of T3 generation transgenic 35S:mycTIP3;1 plants and separated by SDS-PAGE. Immunoblots were performed using anti-myc (Santa-Cruz). anti-myc bound to the epitope of MYC-14-3-3β purified fusion protein from HEK293T cells (Holly Baum and Jurgen Mueller, University of Warwick), but could not detect mycTIP3;1 (figure 3.10).

Since mycTIP3;1 could not be detected in stably transformed lines, leaves of *Nicotiana benthamiana* were agroinfiltrated (materials and methods 2.5.11) to determine whether the 35S:mycTIP3;1 construct can translate detectable mycTIP3;1 in a transient expression

system. Total protein was extracted from these leaves, and used for immunblots (figure 3.11). GFP-HDEL and TIP3;1-YFP were used as a positive control for infiltration, and detected with anti-GFP whilst purified MYC-14-3-3β was used as a positive control for anti-myc. All positive controls were detected, however no myc-TIP3;1 was found (figure 3.11). It was therefore concluded that mycTIP3;1 either cannot be detected or is not translated from transcripts *in vivo*.

At the time this work was conducted, anti-TIP3 was not available and so no further attempts were made to detect plants expressing mycTIP3;1. The puzzling results observed are unlikely to be due to silencing in *Arabidopsis thaliana*, as the same construct was not able to express the protein in *Nicotiana Benthamiana.* In addition, the construct was fully sequenced (methods section 2.3.9) and confirmed to be correct. Given more time, it would be interesting to see if using a different plasmid to host the 35S:mycTIP3;1 insert could lead to protein expression.

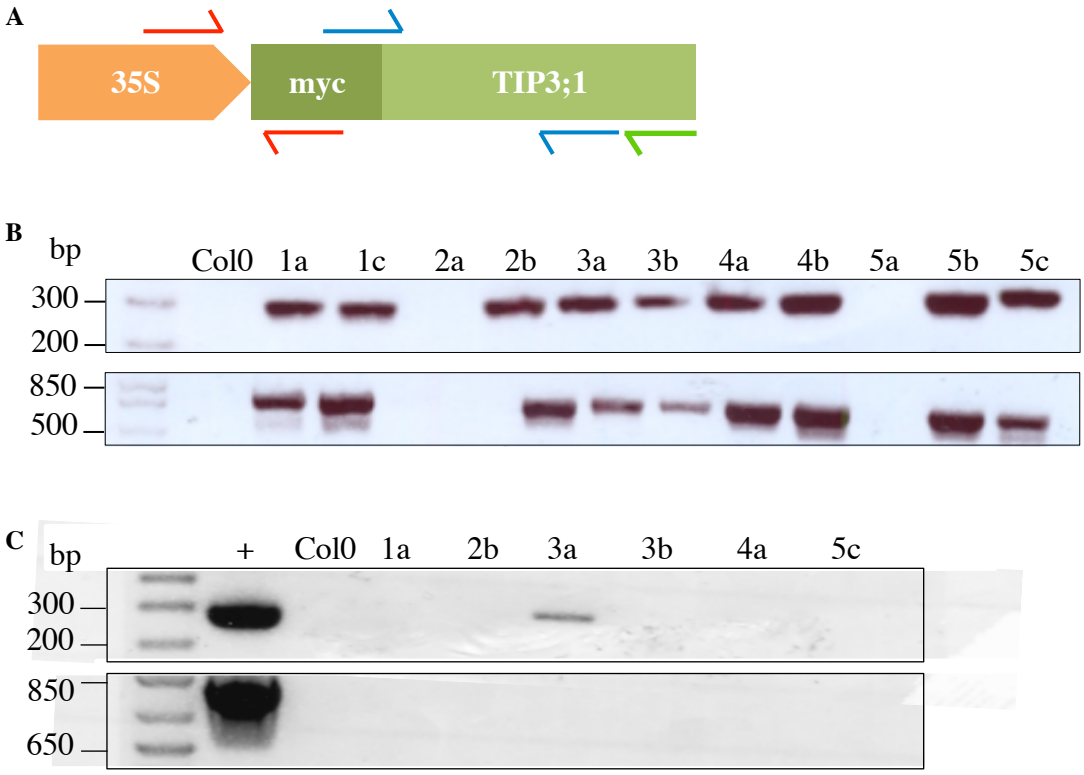

Figure 3.9: Detection of 35S:mycTIP3;1 DNA and RNA transcripts
(**A**) Primers used for DNA PCR which either targeted the region between the 35S promoter and myc sequences (red) to give a band of ~260bp or the region between the myc and TIP3;1 sequence (blue) giving a band of ~840bp. (**B**) DNA from T3 generation *Arabidopsis thaliana* plants was screened by PCR for the presence of the 35S:mycTIP3;1 construct. Its presence is confirmed in 9 lines. 1-5 correspond to T2 plants, a-c correspond to T3 plants. (**C**) RNA from T3 generation *Arabidopsis thaliana* seed was reverse transcribed for RTPCR screening. cDNA was quanitifed for each reaction to contain approximately 50ng of genetic material under 28 cycles. A DNA mini prep of 35S-myc-TIP3;1 was used for the positive control. Forward primer used in all reactions was that shown in blue in (**A**). The top gel used the reverse primer shown in blue (**A**) to give an estimated band size of ~290bp and the bottom gel used a primer flanking the 3' end (green, **A**) to give a band of ~840bp. Although the transgene is present in most plant lines, transcripts were only detectable in line 3a. Molecular weight of the marker bands is given in base pairs (bp). Primer sequences available in table 2.4, materials and methods.

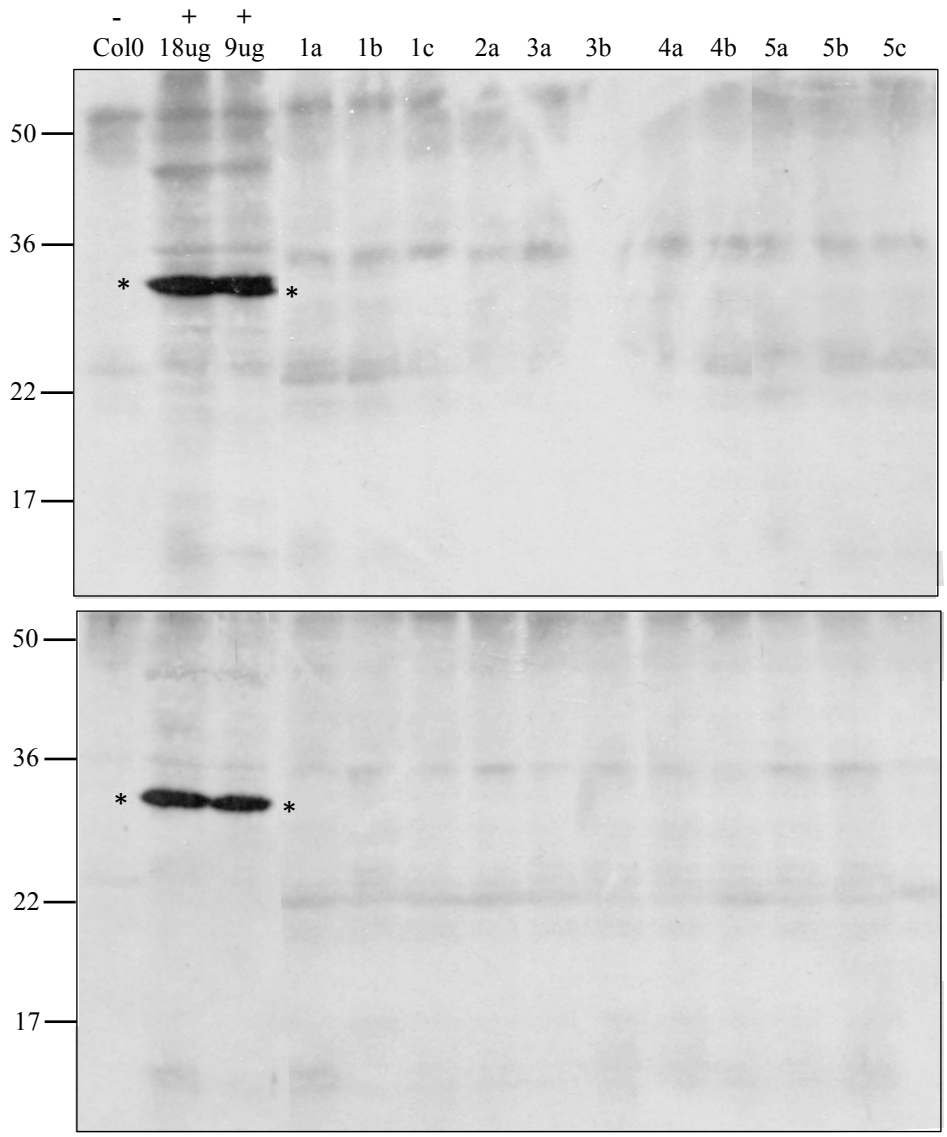

Figure 3.10: mycTIP3;1 protein is not detectable in transgenic *Arabidopsis thaliana* leaf protein extracts

20µg of total protein extracts from leaves (as determined by Pierce 660nm Protein Assay reagent described in methods section 2.4.1) of T3 generation *Arabidopsis thaliana* plants containing the transgene were subjected to reducing SDS-PAGE and blotted with anti-myc (Santa Cruz). Positive control (*) is MYC-14-3-3β fusion protein from HEK293T cells, expected size 30kDa (Holly Baum and Jurgen Mueller, University of Warwick). No mycTIP3;1 protein, expected size ~27KDa, was detected. Molecular weight of the marker bands is given in kDa.

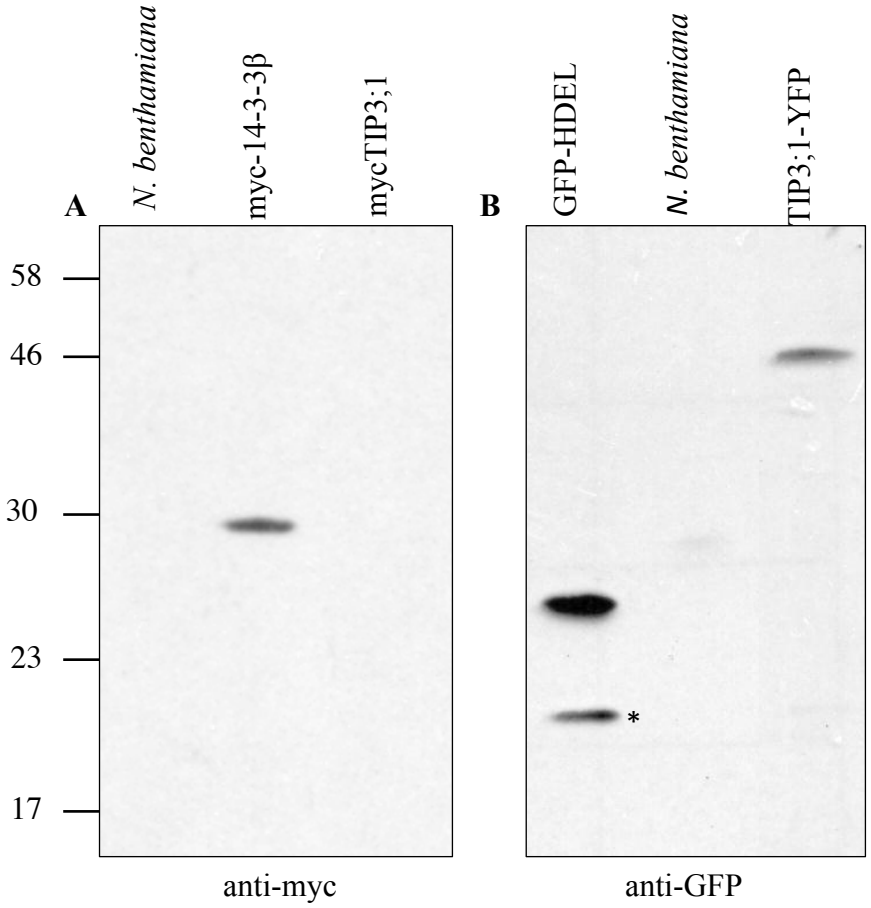

Figure 3.11: mycTIP3;1 is not detectable in *Nicotiana benthamiana* leaf extracts
20μg of total protein extracts from leaves of *Nicotiana benthamiana* plants agroinfiltrated with the mycTIP3;1 construct (as determined by Pierce 660nm Protein Assay reagent described in methods section 2.4.1) were subjected to reducing SDS-PAGE and blotted with anti-myc (**A**) or anti-GFP (**B**). Positive control is MYC-14-3-3β fusion protein from HEK293T cells (expected size 30kDa, Holly Baum and Jurgen Mueller, University of Warwick). No mycTIP3;1 protein (expected size ~27kDa) was detected in tissues infiltrated with 35S-mycTIP3;1 however TIP3;1-YFP (expected size ~50kDa, running a little lower at 46kDa due to their membrane protein properties) and GFP-HDEL (expected size ~25kDa) were detected during the same round of infiltrations. A breakdown product of GFP-HDEL is marked by *. Molecular weight of the marker bands is given in kDa.

3.2.7 PIP1;2 localises to the plasma membrane when expression is driven under the TIP3;2 promoter

YFP-PIP1;2 is not detected in dry, imbibed or germinating seeds by immunoblot (figure 3.3), but seeds do appear to be fluorescent under the GFP filter of a stereomicroscope. Seeds which appeared brightest were subjected to a confocal microscopy time course was conducted with TIP3;2:YFP-PIP1;2 embryos. YFP-PIP1;2 is not visible in embryos from dry seeds, but was visualised during seed maturation (figure 3.12 A-B) and germination (figure 3.12 C-D). It therefore appears YFP-PIP1;2 is expressed during maturation, and is turned over before its new synthesis in the germinating seed, suggesting that its half life in this tissue is considerably shorter than that of TIP3.

To confirm cellular localisation, PSV were visualised by autofluorescence and FM4-64 was used to stain plasma membranes. These tools show YFP-PIP1;2 is separate from PSV in maturing embryos, and lies only at the plasma membrane (figure 3.12 A-B), as indicated by its colocalisation with FM4-64 at the plasma membrane in cells of germinating embryos (figure 3.12 C-D).

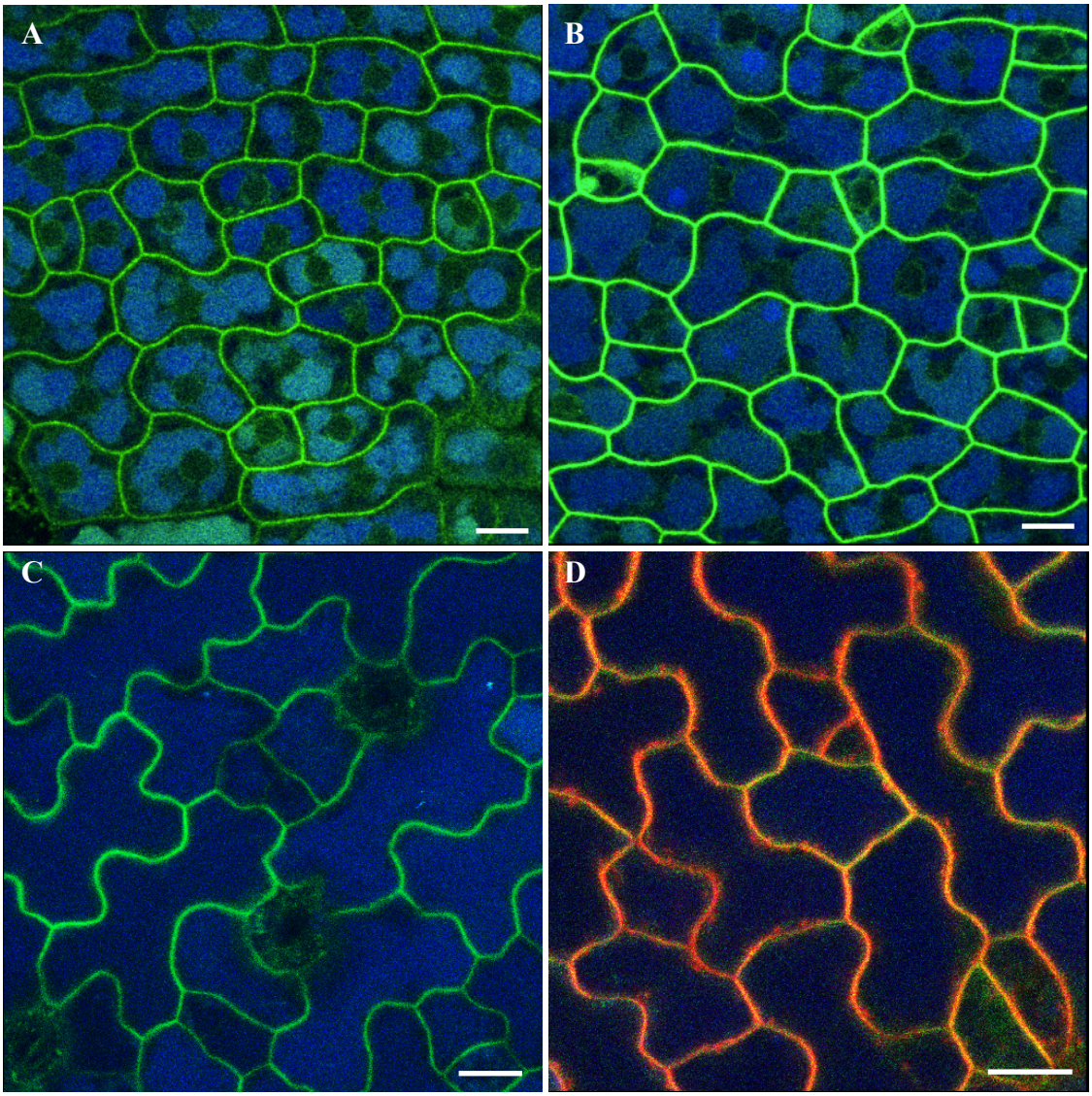

Figure 3.12: YFP:PIP1;2 is expressed at the plasma membrane in embryos of maturing and germinating seeds under the TIP3;2 promoter.
YFP:PIP1;2 localises to the plasma membrane under control of the TIP3;1 promoter. This is confirmed by the colocalisation with FM4-64 (**D**). It can be visualised by confocal microscopy throughout seed maturation (**A-B** late torpedo stage) and germination (**C-D** radicle fully emerged). Green is YFP and Red is FM4-64 dye. Scale bar = 10µm.

3.2.8 Overexpression of PIP1;2 and TIP3;2 (under the TIP3;2 promoter) is beneficial to germination of *Arabidopsis thaliana* seeds in drought

Total numbers of germinated seeds and the time it took for germination to occur were recorded in transgenic seeds expressing YFP-PIP1;2, YFP-TIP3;2 and YFP-TIP3;2ΔC under the TIP3;2 promoter. Due to the wild-type Col-0 background of transformed plants (rather than PIP1;2 or TIP3;2 knockouts), the seeds and seedlings analysed in this section and 3.2.9 are described as overexpressing the introduced aquaporin, as they are in addition to native aquaporin levels. Counts and rates were compared to Col-0 wild type seeds, in a range of water stress conditions. In this instance, a 0MPa water stress, in which no PEG was present, was included, and -0.4MPa, -0.6MPa and -0.8MPa were used for water stress conditions. The germination boxes were set up and treated in the same way as described in section 3.2.3.

Experimental design included approximately 60 seeds of each line in 4 different conditions, 0MPa, -0.4MPa, -0.6MPa and -0.8MPa. Unfortunately, no seeds at -0.8MPa germinated, most likely due to the high level of dormancy maintained by storing seeds at -20°C for a 4 months prior to the experiment (Finch-Savage *et al.* 2006). It is more difficult for seeds to germinate in high water stress conditions, an effect which is exasperated by high dormancy. In total 960 seeds were manually scored for a germination time at the same time each day for 21 days. This is longer than the 14 days of the previous experiment as it was thought seeds at -0.8MPa may germinate within the extra 7 days allowed.

In this experiment, seeds were treated as replicates rather than germination boxes, meaning a Two-Way ANOVA could not be performed on the germination count data. Instead, the upper and lower 95% confidence intervals were calculated for this binomial distributed data set. This confidence interval calculates the upper and lower number of seeds predicted to germinate, with a confidence of 95%, based on the data available. If the confidence intervals of the transgenic lines in each treatment do not fall within the same range as the Col-0 seeds in each treatment, it is deemed as significantly different ($P<0.05$). All seeds in all lines germinated at 0MPa and so these were eliminated from the analysis. As there were 6 comparisons made (i.e. Col-0 at -0.4MPa versus TIP3;2pro:YFP:PIP1;2 at -0.4MPa, Col-0 at -0.6MPa versus TIP3;2pro:YFP:PIP1;2 at -0.6MPa, Col-0 at -0.4MPa versus TIP3;2pro:YFP:TIP3;2 at -0.4MPa etc), the Bonferroni

principle was applied. This states that the more comparisons which are made, the more the confidence level is reduced. And so to calculate a 95% confidence interval for each comparison, a 99.2% confidence interval was calculated ($P<0.08$). This number arises from subtracting the division of the usual $P<0.05$ by the number of comparisons (0.05/6), and converting this to a percentage (0.8%), which is then subtracted from 100% to reveal the confidence interval of 99.2%.

Using this analysis, figure 3.13A shows that total number of germinating seeds was found to be significantly increased in lines overexpressing PIP1;2 at -0.4MPa and -0.6MPa, TIP3;2 at -0.6MPa and TIP3;2ΔC at -0.6MPa, in comparison to Col-0 seeds in the same condition ($P<0.008$). However numbers of seeds which germinated in the line overexpressing TIP3;2ΔC at -0.4MPa were found to be significantly decreased ($P<0.008$).

The same analysis was conducted as in section 3.2.3 for time it took for seeds to germinate (figure 3.13B). This Two-Way ANOVA was possible by using individual seeds as replicates, as time measurements form a normal distribution. Seeds overexpressing PIP1;2 germinated in significantly less time than Col-0 at -0.8MPa ($P<0.05$), but seeds overexpressing TIP3;2ΔC took significantly longer to germinate than Col-0 at 0MPa (figure 3.13B).

It therefore appears overexpressing PIP1;2 at the plasma membrane of embryos using the TIP3;2 promoter increases germination speed and count in water stress conditions, and overexpressing TIP3;2 at the tonoplast and plasma membrane increases germination count in high water stress conditions. However the effect of overexpressing TIP3;2ΔC on germination speed and count is highly dependent on the condition in which the seeds are kept.

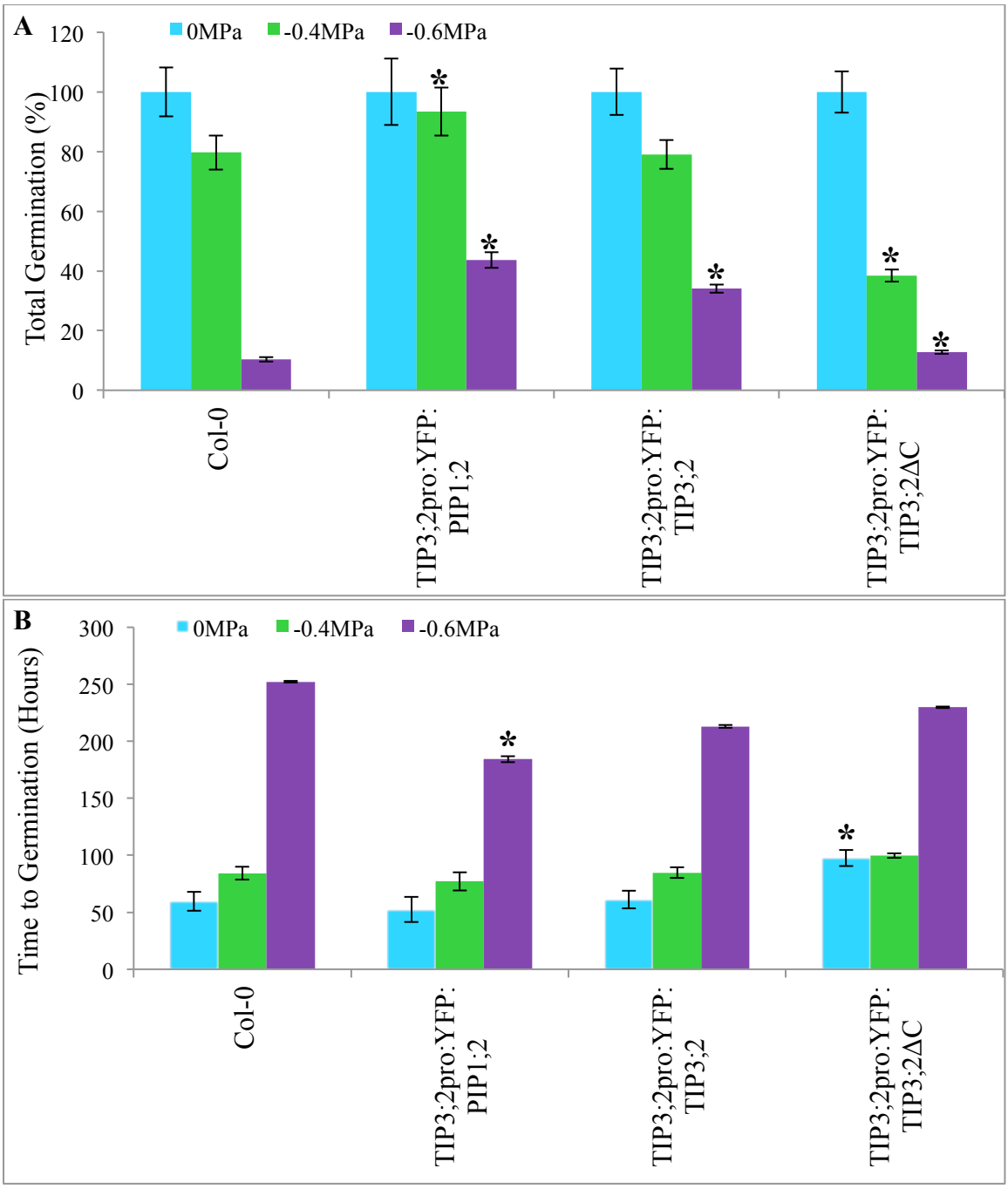

Figure 3.13: Overexpression of PIP1;2 and TIP3;2 the TIP3;2 promoter is beneficial to germination of *Arabidopsis thaliana* seeds in drought

Arabidopsis thaliana seeds were germinated in boxes as described in figure 3.4A. Drought was measured in MPa, with -0.6MPa being the highest level of drought in this instance. 0MPa conditions did not contain any PEG. (**A**) Total number of seeds which germinated in drought conditions within a 2 week period. Total number of germinating seeds was significantly increased in lines overexpressing PIP1;2, TIP3;2 and TIP3;2ΔC at -0.6MPa, but significantly decreased in lines expressing TIP3;2ΔC at -0.4MPa ($P<0.008$). Significance was calculated using calculated 95% confidence intervals. (**B**) Seeds overexpressing PIP1;2 germinated in significantly less time than Col-0 at -0.6MPa ($P<0.05$), but seeds overexpressing TIP3;2ΔC took significantly longer to germinate than Col-0 at 0MPa. Significance was calculated using a Two-Way ANOVA. Error bars are standard error between seeds. n=~80 for each line in each treatment.

3.2.9 Overexpression of TIP3;2 and PIP1;2 (under the TIP3;2 promoter) does not improve *Arabidopsis thaliana* seedling establishment in water stress conditions

The protocol described in 3.2.5 was used to measure establishment of seedlings overexpressing YFP-PIP1;2, YFP-TIP3;2 and YFP-TIP3;2ΔC under the TIP3;2 promoter.

In this experiment, each plate had around 20 seedlings (seedlings spaced in the same way as previous). There were 6 box replicates for each of the 4 lines in 4 conditions, 0MPa (½ MS-agar), -0.4MPa, -0.6MPa and -0.8MPa, made with mannitol as before (materials and methods section 2.5.9). In total 1920 seeds were plated and ~1400 seedlings were measured in total. In this instance, plates were scanned using a flatbed scanner connected to a computer and images were saved as TIF files. From these images, hypocotyl, radicle and lateral root measurements were taken by tracing the roots with the free hand line tool in Image J.

Significance was calculated using Least Significant Differences (LSD) generated from a Two-Way ANOVA, in the same way as described previously. From this analysis it was found that only TIP3;2pro:YFP-TIP3;2ΔC seedlings in 0MPa conveyed a significantly longer seedling length, and therefore establishment, than Col-0 (figure 3.14). Whereas overexpression of TIP3;2 and PIP1;2 under the TIP3;2 promoter did not affect seedling establishment in any conditions (figure 3.14). This suggests overexpression of TIP and PIP at the plasma membrane does not have a lasting effect on seedling establishment.

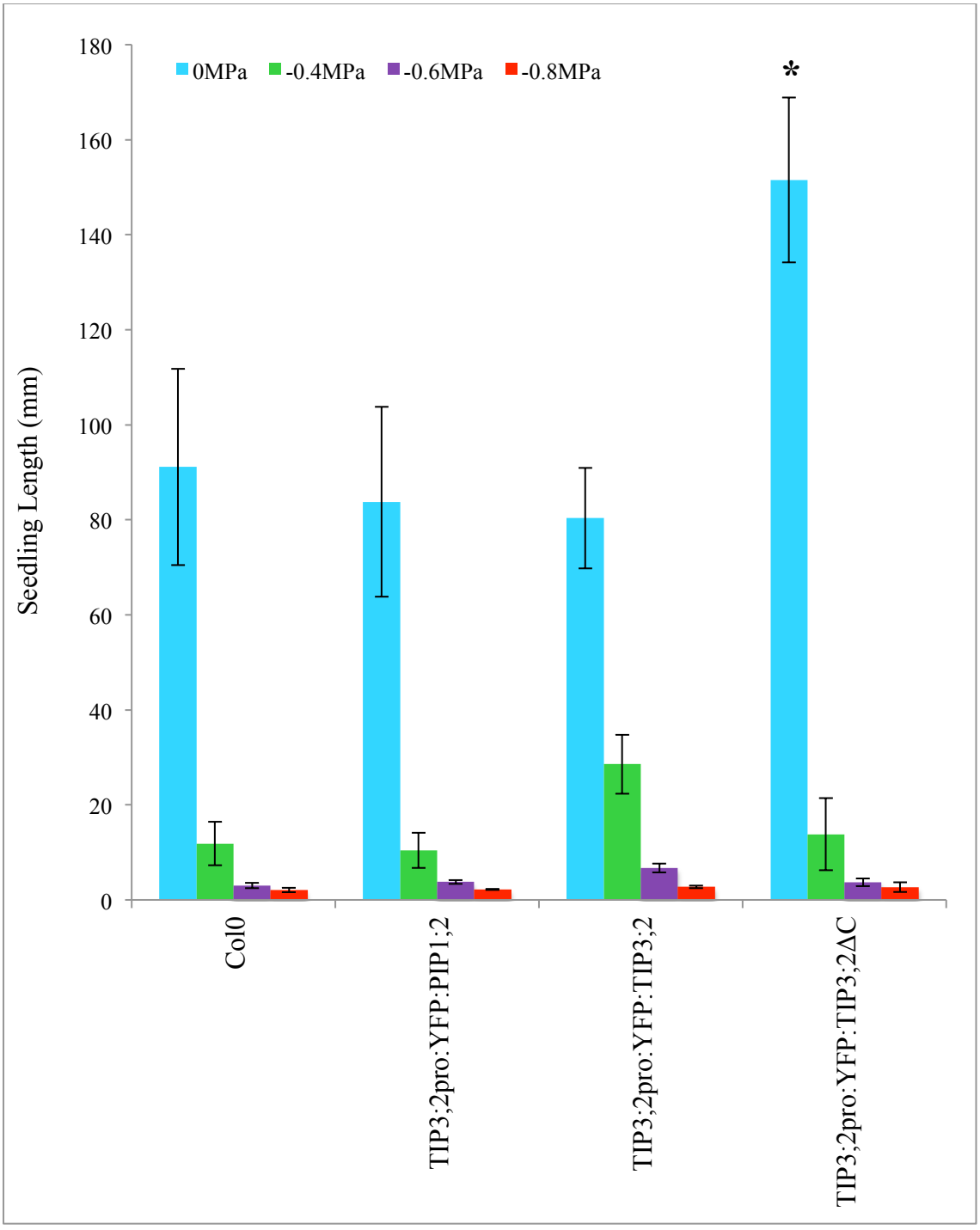

Figure 3.14: Overexpression of TIP3;2 and PIP1;2 under the TIP3;2 promoter does not affect *Arabidopsis thaliana* seedling establishment in water stress conditions
Arabidopsis thaliana seeds were germinated under normal conditions and transferred to water stress conditions after 2 days. Water stress was measured in MPa, with -0.8MPa being the highest water stress condition conferring the highest level of drought. These conditions were created using mannitol in ½ MS 0.8% agar medium, except 0MPa where mannitol was omitted. Each seedling was measured in ImageJ from root tip to the top of the hypocotyl, including lateral roots, 14 days after transfer. Seedlings expressing TIP3;2ΔC under the TIP3;2 promoter, grown in 0MPA are the only line significantly longer than wild-type Col0. Significance was based of Least Significant Differences (LSD) generated from Two-Way ANOVA. Error bars are standard error between boxes. n=70-90 for each line in each treatment.

3.3 Discussion

A combination of immunoblots and confocal microscopy successfully confirms the expression of TIP3;1, TIP3;2, TIP3;2ΔC, TIP1;1 and PIP1;2 translationally fused to YFP in transgenic lines used in this chapter. All proteins detected by immunblot migrate to a point which suggests a molecular size smaller than that expected. This is most likely due to their helix-loop-helix structure and abundance of hydrophobic residues as membrane proteins, which leads to incomplete denaturation by SDS, and a migration distance which can ultimately be 30% higher or 10% lower than their true size (Rath *et al.* 2009).

Breakdown products of TIP are prominent in samples from germinating seeds, as detected by anti-GFP (figure 3.3F). It is possible that the same breakdown products are not as obvious in the blots probed with anti-TIP3 antibody because they migrate to the same place as native TIP3. However it is more likely that cleavage has removed the C terminal motif to which the anti-TIP3 antibody is raised, and any breakdown product containing this sequence is too small to detect. Due to the different intensity and sizes of breakdown product bands between samples it is highly unlikely that they are a result of non-specific antibody binding, and given that protease inhibitors and constant incubation of samples on ice were employed here, it is unlikely that these products have been formed as a result of sample degradation during preparation. Instead I postulate that these breakdown products are a result of high protein turnover. Maitrejean *et al.* (2011) report the tonoplast protein TPK1 (Tandem Pore Potassium channel 1) as having a half life of around 24 hours, possibly due to strong 35S overexpression (Maitrejean *et al.* 2011a). Bean TIP3;1 expressed in tobacco protoplasts is reported to have a longer half life than this (Gomez *et al.* 1993). Due to the prominence of these breakdown products in germinating tissues, it could be assumed that TIP3;1 has a longer half-life than that recorded of TPK1, and that breakdown products are caused by degradation of older proteins (Maitrejean and Vitale 2011). In addition, internalisation of TIP3 into the vacuole for degradation has been previously been recorded in germinating soybean (Melroy *et al.* 2011) and tobacco (Zheng *et al.* 2011) by immunolabelling in electron microscopy. Both Maitrejean et al. (2011) and Gomez et al. (1993) make their conclusions on the half-lives of TPK1 and TIP3;1 based on how long radioactively-labelled proteins can be detected for during pulse-chase experiments. To determine the half-life of YFP-tagged TIP proteins, a cycloheximide treatment could be used on seedlings. Cycloheximide inhibits protein synthesis; thus treated seedlings could be used

for immunoblot detection of TIP at fixed time points post-treatment, enabling estimation of TIP half-life.

Transcript expression levels change during seed maturation, imbibition and germination. Around half the *Arabidopsis thaliana* genome is stored as mRNA in dry seeds; approximately 35% of these transcripts decrease during imbibition, the majority of which are transcripts encoding proteins for late-embryogensis (Nakabayashi *et al.* 2005). These huge differences in expression were detected by microarray experiments, using RNA extracted from seeds which were dry or imbibed for a duration of 6, 12 or 24 hours. The dramatic decrease in transcripts involved in late-embryogenesis was found to occur as early as 6 hours after the start of imbibition, which in turn correlates with the appearance of new transcripts thought to be involved in germination (Nakabaysahi *et al.* 2005). These changes in expression could explain some results visualised in the immunoblot in figure 3.3 of this chapter. It is known that TIP3;1 and TIP3;2 expression begins during late-embryogenesis, therefore these transcripts could draw parallel with patterns described in Nakabayashi *et al.* (2005), explaining why less protein, as driven by the native TIP3;1 or TIP3;2 promoters is visible at germination. However, it is also known that TIP3 protein is present until approximately 4 D.A.G. (Gattolin *et al.* 2011) and therefore I suggest that the blots reflect a downregulation of promoter activity and therefore reduced protein levels, rather than the complete degradation. In addition the bands corresponding to TIP3;1-YFP under the 35S promoter remain constant over the developmental stages, particularly when detected by anti-GFP, a finding consistent with the constitutive expression this promoter provides. The band intensity of proteins expressed under the 35S promoter appear to be weaker than what is detected under control of the TIP3;1 and TIP3;2 promoters. Given that this immunoblot is not strictly quantitative, this is most likely a result of unequal loading. However, it is worth considering that the TIP3 promoters, which are highly active during seed maturation, are stronger than the 35S promoter in this instance. Indeed, comparison of overexpression promoter activity has shown differences between promoters, and between lines using the same promoter (Holtorf *et al.* 1995). This could be due to silencing of the transgene resulting in changes in level and location of expression (Wilkinson *et al.* 1997). It has been proposed that this silencing could be caused by the location of transgene insertion within the genome or by cells recognising transgenes as foreign and deactivating them (Wilkinson *et al.* 1997, Palauqui *et al.* 1996, Potenza *et al.* 2003). There is also no evidence in the literature to suggest native promoters can exhibit higher activity than CaMV35S. However, in this

work, microscopy confirms expression driven by the 35S promoter results in TIP3;1-YFP in all tissues. In order to compare 35S promoter strength with that of the TIP3 promoter, it will be necessary to produce quantitative immunoblots of several lines transformed with either 35S:TIP3;1-YFP or TIP3;1pro:TIP3;1-YFP. Despite the blots in figure 3.3 not being quantitative, it does show that in dry, imbibed and germinating seeds, transgenic lines used in the germination and seedling establishment assays reliably express their inserted transgenes.

The transgenes are expressed during germination in all lines, and so germination assays were conducted to understand the impact of overexpression on this developmental time point (summarised in table 3.2). In addition, seedling establishment assays were performed to gain insight into effects 35S overexpression or lasting impact TIP3;2 promoter-driven expression has on this later developmental stage (summarised in table 3.3). Following reports of aquaporin overexpression being beneficial to plants in water stress conditions (Sade *et al.* 2009, Liu *et al.* 2007, Zhou *et al.* 2012, Peng *et al.* 2007), both the germination and seedling establishment assays were conducted in similar environments. Water stresses are referred to in units of pressure (MegaPascals) to make the different PEG 8000 and mannitol concentrations comparable between germination and establishment assays. -0.4MPa, -0.6MPa and -0.8MPa were selected based on preliminary data collected as part of an undergraduate dissertation supervised by Prof Bill Finch-Savage and Dr Lorenzo Frigerio at the University of Warwick, which used an even wider range of water stresses. When comparing our data to other experiments in which seeds and plants overexpressing aquaporins are grown in water stress, it is necessary to consider the range of conditions used. Most experiments which use seedlings more than 4 weeks old, simply withhold water to produce drought conditions (Peng *et al.* 2007, Sade *et al.* 2009, Aharon *et al.* 2003). However Liu *et al.* (2007) use 15% PEG 6000, similar to our range of 16.6-24.1% PEG 8000 to create stresses between -0.4MPa and -0.8MPa water. However, most experiments which report using mannitol, used concentrations in the range of 100-300mM, whereas we used 400, 600 and 800mM. Whilst our concentrations are higher than previously reported, van der Weele *et al.* (2000) only state water stresses higher than -0.8MPa are classed as extreme stress, and Vallejo *et al.* (2010) class -0.6MPa as moderate stress. In our particular case we were interested in how water stress slows germination speed, reduces count and decreases seedling growth without debilitating these developmental processes. This is also in agreement with Vallejo *et al.* (2010) who theorise that employing moderate stresses in experimental designs will prove

more informative to understanding germination in conditions of water and salt stress. Therefore the range of water stresses used here are representative of levels of stress faced in the environment, without compromising seed and seedling viability.

By overexpressing TIP3;1-YFP using the 35S promoter, a segregating transgenic population is achieved. Prior to these germination and seedling growth experiments, this had already been confirmed using ratio counts of growth phenotypes and YFP expression (section 3.2.4). It was noticeable at that time that homozygous seedlings, easily visually identified by their higher level of YFP expression, were remarkably smaller than heterozygous plants, and could not produce viable seed. These observations, alongside reports in the literature, spurred us to assess the performance of these lines in germination and seedling establishment.

Heterozygous 35S:TIP3;1-YFP seeds were faster to germinate in comparison to Col-0 at -0.6MPa and -0.8MPa, and exhibited an increased seedling length in all three water stress conditions. However, few homozygous seeds germinated in all water stress conditions and those that did were slower than Col-0 at -0.4MPa and -0.6MPa; seedling length in all three water stress conditions was also severely affected. Therefore it appears that increasing TIP3;1-YFP expression is beneficial to the plant and seedlings until a certain threshold protein concentration is reached. 35S:YFP-TIP1;1 seeds were also slower to germinate in the two highest water stress conditions, however seedlings did not appear to be affected. Taken together, these results suggest homozygous overexpression is detrimental to germination and seedling establishment, whereas heterozygous expression is actually beneficial. Therefore there appears to be a threshold effect caused by amount of protein. Most overexpression studies reported employ the CaMV 35S promoter, including the two papers reporting lower drought tolerance, Wang *et al.* (2011) and Aharon *et al.* (2003) as well as two of four publications reporting enhanced drought tolerance, Zhou *et al.* (2012) and Peng *et al.* (2007). It is assumed that all reports focus their results on homozygous lines, and so differences in drought tolerance reported are not due to transgene dosage. As previously discussed, there have been differences in strength of 35S activity reported (Holtolf *et al.* 2005). Therefore, without proper quantification, it could be assumed that the 35S promoter lines used in Wang *et al.* (2011) and Aharon *et al.* (2003) could be exhibiting stronger activity than in Zhou *et al.* (2012) and Peng *et al.* (2007). In contrast, Sade *et al.* (2009) uses the EVO205 promoter to drive constitutive expression, and Liu *et al.* (2007) uses SWPA2. Both of these reports found

overexpression inferred drought tolerance (an improved growth yield or speed over wild-type grown in the same drought conditions), therefore it would be interesting to compare expression levels of these lines with those employing 35S promoters to distinguish if the amount of protein translated is on par.

Given the drastic effect that TIP3;1-YFP overexpression has on phenotype, cell morphology was assessed using confocal microscopy. Cells of homozygous seedlings were found to be more rounded, with a loss of digit prominence. Embryo cells did not exhibit the same phenotype, as they are not yet matured into their puzzle-like epidermal cell shape. No obvious cell phenotypes were observed in imbibed or germinating seeds of this line. The area:perimeter ratio was chosen to show the loss of digit prominence in seedlings because it is comparable between cells of the same leaf, and between seedlings (Staff *et al.* 2012). Area:perimeter ratio does increase with age, as shown in 10, 17 and 24 day old seedlings in Staff *et al.* (2012) and circularity has been shown to decrease with age (Zhang *et al.* 2011), therefore it could be that this ratio is higher in heterozygous seedlings because homozygous seedlings are simply developmentally delayed. To identify if this is the case, plants would need to have developmental time points compared rather than age time points used here. Another possibility is that this cellular morphology is an effect of increased water uptake, caused by the increased quantity of TIP3;1-YFP at the tonoplast. It is well known that water balance is responsible for cell turgour, with the central vacuole being responsible for water uptake. During growth, water uptake into the vacuole increases due the difference in water potential between the protoplastic and apoplastic spaces, and the cell wall becomes less tensile to accommodate the resulting cellular enlargement (Schopfer *et al.* 2006). Homozygous 35S:TIP3;1-YFP seedlings may effectively be taking up more water into the vacuole, within the same time frame as heterozygous seedlings due to increased aquaporin number at the tonoplast. This could be causing rapid cell growth, faster than the rate at which the cell wall can increase tension and inhibit growth, leading to a loss of distinct pavement shape (Schopfer *et al.* 2006). In turn, this could be causing cellular function to be compromised, as cells become ‘waterlogged’ leading to a deformed phenotype. In contrast, cells of heterozygous seedlings may exhibit improved germination and seedling growth as they are able to maintain regular functions in the presence of more TIP and therefore increased water uptake and growth.

Within this work, it has been assumed that introduced aquaporins have remained functional despite high expression levels and YFP tagging. However, it cannot be excluded that the phenotypes observed are a result of aquaporin function being blocked. Aquaporins are known to be gated, a function regulated by phosophorylation, protons and divalent cations (Li *et al.* 2003). X-ray structures of the open and closed version of the spinach aquaporin SoPIP2;1 reveal that ionic and H-bond interactions between residues within a loop positioned in the cytosolic pore (termed loop D) can prevent passage of water, a feature which is tightened when this loop is protonated or divalent cations binds to N terminal residues. In contrast phosphorylation of C terminal residues or loop 'B' found outside the pore, can unfold loop D resulting in an open pore (Tornroth-Horsefield *et al.* 2005). Gating of TIP is not as well characterised, however it could be assumed they are regulated in a similar manner as when PvTIP3;1 from pea is expressed in *Xenopus* oocytes, these aquaporins are shown to be phosphorylated by Protein Kinase A, affecting activity of water transport (Maurel *et al.* 2005). It would be valuable to assess functionality of these overexpressed aquaporins *in situ* by either expressing TIP-YFP fusions in *Xenopus* oocytes to rule out interference of fluorescent tags on solute transport, or by quantitative mass spectrometry to assess the extent of phosphorylation, and therefore 'open' TIP.

To confirm the observed phenotypes were caused by TIP3;1 overexpression rather than the larger TIP3;1-YFP translational fusion, an attempt was made to create a myc-tagged TIP3;1. The c-myc tag in 1.2kDa as opposed to the 26.4kDa YFP. However, for reasons as yet unknown, the protein was unable to be detected using anti-myc in both stable *Arabidopsis thaliana* transformants and transient expression in *Nicotiana benthamiana*. Attempts to detect this tag could, however, be repeated with our custom anti-TIP3 antiserum described in section 3.2.1, which was unavailable at the time this work was performed. Had the 35S:mycTIP3;1 construct worked, it is assumed that positive transformants would produce the same segregating heterozygous lines as 35:TIP3;1-YFP. On this basis, this line would have also been used in germination and seedling establishment assays, in addition to seedling cell morphology analysis through immuno-labelling in confocal micrographs. This would enable us to rule out phenotypic effects being caused by YFP translational fusions.

Although not detected by immunoblot, YFP-PIP1;2 was visualised at the plasma membrane in both maturing and germinating seeds. The protein therefore appears to

exhibit rapid turnover between the phases of seed drying and imbibition when expressed under the TIP3;2 promoter. This could also suggest that TIP3 may be upregulated in the maturing seeds and downregulated during imbibition, as suggested earlier based on the observations of Nakabayashi *et al.* (2005), but could also begin to be upregulated again during germination. TIP3;2pro:YFP-PIP1;2 seeds were imaged approximately 24 hours after germination, whereas germinating seeds used in the blots were harvested just before testa rupture was about to occur, therefore immunoblots could be showing the point of downregulation, whereas confocal images could show its upregulation. This would fit in with the observation of TIP3;1-YFP at the tonoplast and plasma membrane as early as the bent cotyledon stage embryos, but as late as 4 D.A.G (Gattolin *et al.* 2011). Quantitative immunoblot detection of proteins at regular time intervals between seed maturation and germination could be used to map changes in protein expression during these stages.

Results from germination and establishment assays using lines overexpressing YFP-PIP1;2, YFP-TIP3;2 and YFP-TIP3;2ΔC under the TIP3;2 promoter, further solidify conclusions made regarding amount of protein being beneficial to germination (summarised in table 3.2). The amount of seeds which germinated in water stress conditions increased for lines expressing YFP-PIP1;2 and YFP-TIP3;2 whilst germination was also quicker for seeds overexpressing YFP-PIP1;2. This is in agreement with the finding that heterozygously overexpressing TIP3;1-YFP under the 35S promoter enhances drought tolerance; as it would be predicted that the TIP3 promoter exhibits less expression that a 35S in a homozygous line, but could be relatively close to that of heterozygous seeds. To further interpret these results, it is also essential to consider localisation of the protein overexpressed. YFP-TIP1;1 and YFP-TIP3;2ΔC are localised to the tonoplast and they do not exhibit drought tolerance (apart from total seeds germinating at -0.6MPa for TIP3;2pro:YFP-TIP3;2ΔC, a possible anomaly given that it does not fit with the general trends observed for this line). TIP3;1-YFP is expressed at the plasma membrane and tonoplast in germinating seeds under the 35S promoter, along with YFP-TIP3;2. Heterozygous 35S:TIP3;1-YFP and TIP3;2pro:YFP-TIP3;2 seeds both exhibit enhanced drought tolerance in germination. Finally seeds overexpressing YFP-PIP1;2, which localises to the plasma membrane only, also exhibits enhanced drought tolerance. Taken together these results indicate that it is the plasma membrane localisation of aquaporins which can confer increased ability to germinate in water stress conditions, and suggests our hypothesis that TIP3 plays a key role in water uptake of the germinating seed holds true.

In contrast, the patterns of subcellular aquaporin localisation do not appear to be as important in conferring water stress tolerance during seedling establishment. While YFP-PIP1;2 is the only aquaporin to be solely expressed at the plasma membrane, all TIP3 under study overexpressed localise to the tonoplast only in seedlings (summarised in table 3.3). TIP3;2pro:YFP-TIP3;2ΔC seedlings were significantly longer than Col-0 in 0MPa but aside from this, no other significant changes were observed. This could be due to the TIP3;2 promoter only being active until 72 hours post germination (Gattolin *et al.* 2011).

In conclusion, there is a clearly a strong requirement for members of the wider aquaporin family to be developmentally and spatially regulated, as interference with their expression levels can drastically effect their ability to germinate and grow in both normal, and water stress conditions. However, it can be observed here that overexpressing an aquaporin at the plasma membrane of seeds can enhance drought tolerance during germination, until a particular threshold amount of protein is reached (table 3.2). In addition, this threshold effect could also enhance drought tolerance of seedlings during establishment (table 3.3), although in this case aquaporins can be localised to tonoplast, and we are yet to assess the effect of constitutive overexpression of a PIP during this timepoint.

Table 3.2: A summary of the effects of overexpressing aquaporins on germination (✖=negative effect ✔=positive effect)

Promoter	Protein	Embryo Localisation	0MPa	-0.4MPa	-0.6MPa	-0.8MPa
35S	TIP1;1	Tonoplast	N/A	-	✖	✖
35S	TIP3;1 (het)	Tonoplast + Plasma Membrane	N/A	-	-	-
35S	TIP3;1 (hom)	Tonoplast + Plasma Membrane	N/A	✖	✖	✖
TIP3;2	PIP1;2	Plasma Membrane	-	✔	✔	N/A
TIP3;2	TIP3;2	Tonoplast + Plasma Membrane	-	-	✔	N/A
TIP3;2	TIP3;2ΔC	Tonoplast	-	✖	✔	N/A

Table 3.3: A summary of the effects of overexpressing aquaporins on seedling establishment (✖=negative effect ✔=positive effect)

Promoter	Protein	Seedling Localisation	0MPa	-0.4MPa	-0.6MPa	-0.8MPa
35S	TIP1;1	Tonoplast	N/A	-	-	-
35S	TIP3;1 (het)	Tonoplast	N/A	✔	✔	✔
35S	TIP3;1 (hom)	Tonoplast	N/A	✖	✖	✖
TIP3;2	PIP1;2	N/A	-	-	-	N/A
TIP3;2	TIP3;2	N/A	-	-	-	N/A
TIP3;2	TIP3;2ΔC	N/A	✔	-	-	N/A

Chapter 4: Characterisation of TIP3 downregulation by RNAi

4.1 Introduction

From the findings that overexpression of TIP3 and PIP can have beneficial effects on seed germination and seedling establishment in drought conditions (as discussed in Chapter 3), we hypothesise TIP3 could be a major conduit for water movement in seeds during maturation and germination, the only developmental time points at which they are expressed. Following the use of loss and gain of function mutants to discover the importance of PIP1;3 in rice germination (Liu *et al.* 2007), I aimed to generate a TIP3 knockdown line to be used in physiology assays.

It is thought that due to the 85% homology in protein sequences, and virtually identical expression patterns, TIP3;1 and TIP3;2 are functionally redundant (Li *et al.* 2013). Indeed, the *tip3;2* knockout alone does not exhibit an obvious phenotype (Gattolin, Carroll and Frigerio unpublished). Other examples of functional redundancy between TIP isforms are found in Schussler *et al.* (2008), who identified an *Arabidopsis* transposon insertion line *tip1;1-1* devoid of any TIP1;1 protein, and created a *tip1;1tip1;2* knockout line, and Beebo *et al.* (2009) who also isolated a *tip1;1* knockout. Both studies found that all mutants grew normally with no changes in water status, indicating other TIP may be fulfilling the role of those missing (Schussler *et al.* 2008). TIP3 are the only aquaporins present in the maturing and germinating embryos, therefore functional redundancy provided by other isoforms is not possible. Consequently, lines exhibiting reduced TIP3 expression could provide valuable insight into the role these aquaporins play in seed development. At the time this work was performed, only a TIP3;2 T-DNA insertion knockout line was available (The Nottingham Arabidopsis Stock Centre (NASC), and so a double TIP3;1TIP3;2 knockout was not possible. Therefore a double TIP3 knockdown line was generated instead.

Transgenic lines downregulating expression of TIP3 were created using the GATEWAY™ vector pFAST-RO3 to induce gene silencing by RNAi (Kirimi *et al.* 2002, Shimada *et al.* 2010). This vector uses short hairpin RNA technology whereby the short sequence from the targeted gene inserted into the vector is transcribed into a hairpin loop. This hairpin loop is then spliced remove the intron, resulting in double stranded RNA (dsRNA) (Fire *et al.* 1998) complementary to the mRNA of the target transcripts (Hamilton *et al.* 1999). A protein complex containing the nuclease Dicer processes these dsRNAs into double stranded, small interfering RNA (siRNA) fragments (Bernstein *et al.* 2001). The resulting 21-23 nucleotide siRNAs (Zamore *et al.* 2000) trigger the formation of RNA-Induced

Silencing Complexes (RISC) including the protein Argonaute (Fagard *et al.* 2000). Helicases in the RISC separate the two strands of siRNA, and Argonaute cleaves one of the strands, which is subsequently degraded (Mello *et al.* 2004). The remaining single-stranded siRNA which is complementarily base paired with the target mRNA, directs the RISC complex to this transcript, inducing Argonaute to cleave and degrade the target mRNA resulting in decreased protein expression (Hammond *et al.* 2000, Meister *et al.* 2004, Valencia-Sanchez *et al.* 2006).

The GATEWAY™ vector pFAST-RO3 also contains the sequence for OLE1-tagRFP under the OLE1 promoter. By expressing OLE1-tagRFP in the pFAST-RO3 vector, transgenic seeds become selectable by fluorescence using a green light-equipped stereomicroscope. In addition, the intensity of fluorescent signal is stronger in homozygous, and weaker in heterozygous seeds, allowing rapid selection for homozygous lines (Shimada *et al.* 2010). This provides a quicker way to isolate transgenic plants and avoids the use of antibiotic or herbicide selection. The use of OLE1-tagRFP as a selectable marker was based on Shimada *et al.* (2010) finding that the OLE-GFP fusion protein expressed under the OLE1 promoter in seeds could be visualised through the seed coat by stereomicroscopy. Immunoelectron microscopy confirmed the OLE-GFP localisation to oil body membranes and confocal microscopy highlighted it's presence on a network-like formation corresponding to oil body membranes (Shimada *et al.* 2010).

OLE1 is the most abundant oleosin in *Arabidopsis* seeds (Shimada *et al.* 2008) and is embedded within the phospholipid membranes of oil bodies, organelles accumulating storage lipids (Abell *et al.* 1997, Huang 1992). At present, the only known physiological function of oleosins, besides shaping the oil body, is to confer freezing tolerance in the seed (Shimada *et al.* 2008). However oleosins have been found to function in size regulation of oil bodies in *Arabidopsis* (Siloto *et al.* 2006). Electron and confocal microscopy of knockdown and knockout lines of OLE1 exhibited oil bodies of around 5µm in diameter (Siloto *et al.* 2006). This is in stark contrast to the narrow range of 0.5-2µm diameters measured from electron micrographs of a broad range of wild-type background species: *Brassica napus* (rape), *Brassica juncea* (mustard), *Gossypium hirsutum* (cotton), *Usitatis simum* (flax), *Zea mays* (maize), *Arachis hypogaea* (peanut) and *Sesamum indicum* (sesame)) (Tzen *et al.* 1993). In addition, it was reported that reduction in expression of OLE1 caused a delay in germination and affected the organisation of PSV (Siloto *et al.*

2006). To date, there has been no further investigation of the effect of modulating OLE1 expression levels on PSV.

By using the pFAST-RO3 vector it should be possible to create transgenic lines exhibiting Post Transcriptional Gene Silencing (PTGS) of TIP3, which are selectable by fluorescence as early as the T1 generation.

4.1.1 Aims and Experimental Approach

- To create a double TIP3;1 and TIP3;2 knockdown line using the GATEWAY™ gene silencing binary vector pFAST-RO3
- To characterise the extent and the effect of the reduction in TIP3 in mature seeds
- To assess the impact of the pFAST::TIP3 on PSV organisation

To address these aims a 393 base pair region of the TIP3;1 sequence, having 77% homology with TIP3;2, was cloned into the GATEWAY™ pFAST-RO3 vector via lambda recombination using GATEWAY™ technology as outlined in methods section 2.3.10. The pFAST-RO3 vector omitting this sequence was used as a control. Stereomicroscopy was employed to screen for positive transgenic seeds, and confocal microscopy used to image PSV and OLE1-tagRFP. Transformed lines were characterised by RT-PCR and immunoblot analysis.

4.1.2 Constructs

Figure 4.1A is a map of the GATEWAY™ pFAST-RO3 vector used to create the lines pFAST::empty and pFAST::TIP3, schematically illustrated in figure 4.1B. Both constructs were transformed into Col-0 ecotype *Arabidopsis thaliana.*

GATEWAY™ cloning uses lambda phage recombination events to transfer DNA fragments, flanked by specific recombination sites, into vectors with compatible sites. The first reaction places the desired fragment of DNA with *attB* sites into an donor vector, in this case pDONR207 (Invitrogen), with *attP* sites, leading to the formation of *attL* sites in the recombined entry clone. The second reaction transfers this fragment with *attL* sites into the destination vector, in this case pFAST-RO3 (Shimada *et al.* 2010) which contains *attR* sites (figure 4.1A), to produce the expression clone containing *attB* sites. In both the entry and destination vectors, upon successful recombination, the DNA fragment of interest replaces a ccdB gene which produces the lethal bacterial toxin (Figure 4.1A and B). This enables confident selection of transformed bacteria. Full methods are outlined in section 2.3.10.

A

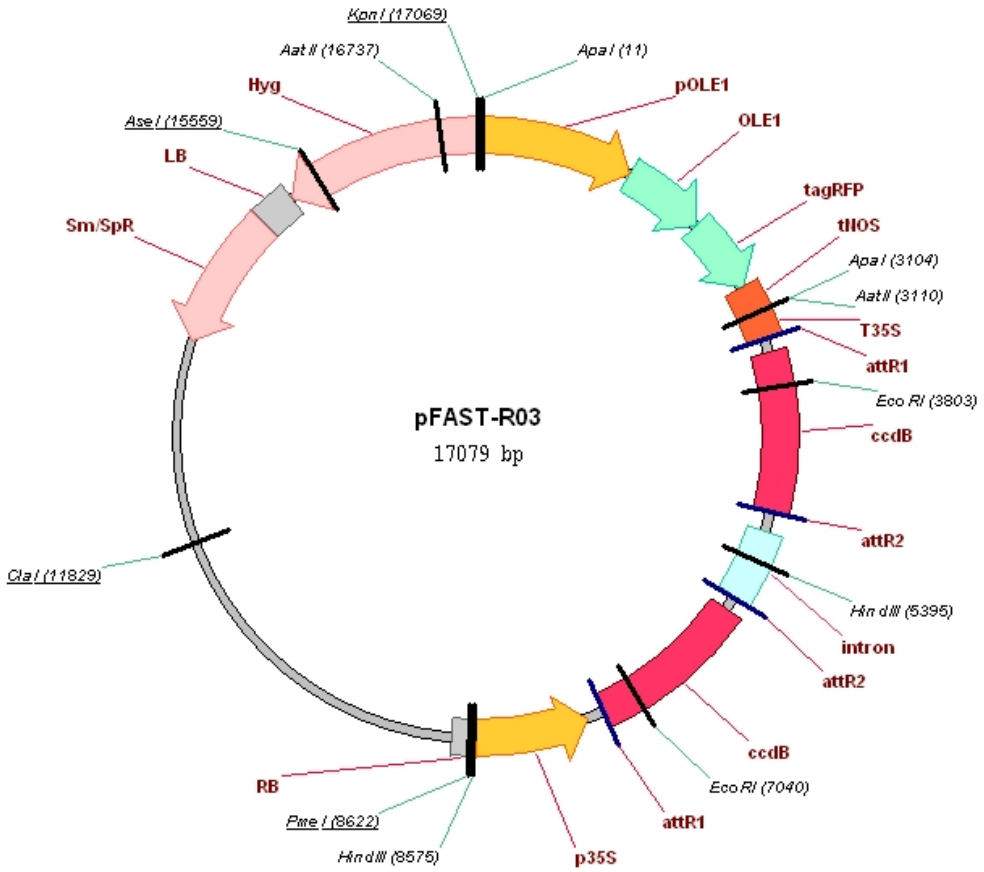

B

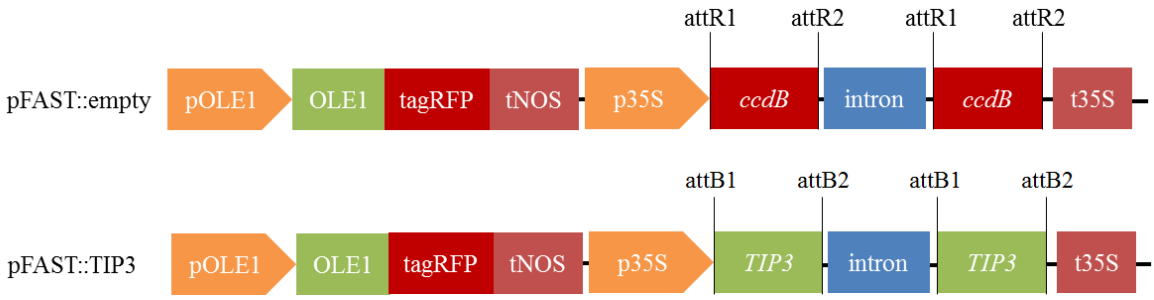

Figure 4.1: Schematic representation of the GATEWAY™ **pFAST-RO3 vectors used in Chapter 4**

Using GATEWAY™, a 386 base pair region from the third exon of the TIP3;1 cDNA sequence was cloned into the (**A**) binary pFAST-RO3 vector (Shimada *et al.* 2010, Karimi *et al.* 2002). This sequence has 77% homology with TIP3;2, which is sufficient to recognise mRNA transcripts for both TIP3. (**B**) This construct is referred to throughout the chapter as 'pFAST::TIP3'. The inserted sequence takes the place of the ccdB gene, which remains in the vector used as a control, 'pFAST::empty'

4.2 Results

4.2.1 Generating the pFAST TIP3 RNAi construct

A 393 base pair region from the third exon of the TIP3;1 cDNA sequence was selected to form the hairpin loop for RNAi knockdown. In this case it was desirable to target both TIP3;1 and TIP3;2 transcripts simultaneously. Figure 4.2 shows that the region selected from the TIP3;1 sequence shares 77% homology with that of TIP3;2. This should be sufficient to target mRNA transcripts of both genes given that it is advised that 8 contiguous base pairs shared between sequences can result in targeting of both transcripts for knockdown (Jonchere *et al.* 2013). In addition to ensuring the region selected was similar between TIP3;1 and TIP3;2 sequences, the sequence was submitted to BLAST to identify any other similar sequences. The selected sequence was shown to have 73% similarity with TIP1;1 and TIP4;1 and below 70% for other TIP isoforms. This unavoidable occurrence caused by high sequence similarity between TIP isoforms will not impact studies on the effect of TIP3 downregulation on seed physiology as TIP3 are the only aquaporins expressed in the maturing and germinating embryo (Vander Willigen *et al.* 2006). No other TIP are expressed during seed development and so any unlikely off-target effects that reduce transcript levels of other TIP isoforms will not present a phenotype until later vegetative growth stages.

Longer stretches of dsRNA have been shown to be more effective at reducing mRNA transcript levels than shorter ones. A *Drosophila in vitro* assay showed dsRNAs between 505 and 957 base pairs in length were more efficient in inducing mRNA degradation (75-80% reduction) than those 149 base pairs long (~50% reduction) (Tuschl *et al.* 1999). The length of the region chosen for this knockdown is in accordance with accepted practice in the field of plant research, which indicates that dsRNAs are most effective in decreasing mRNA transcript levels when they are 300-700 base pairs in length (Engelke 2004).

The 393 base pair sequence was inserted into the pFAST-RO3 vector (figure 4.1A) by GATEWAY™ cloning (Shimada *et al.* 2010, Karimi *et al.* 2002) to produce pFAST::TIP3 (figure 4.1B). This sequence replaces both ccdB genes either side of an intron which causes the hairpin loop.

Figure 4.3 demonstrates that OLE-tagRFP was visible through the dry *Arabidopsis* seed coat by stereomicroscopy within T1 seeds successfully transformed with the pFAST-RO3

vector. Fluorescent seeds were selected and taken to T2, from which heterozygous and homozygous seeds are identifiable by differences in fluorescent signal intensity, which is in accordance with Shimada *et al.* (2010). Suspected T2 generation homozygous seeds were selected and T3 populations from these were screened for uniform seed fluorescence to confirm homozygous lines.

Figure 4.2: A sequence with 77% homology between TIP3;1 and TIP3;2 was chosen to create RNAi knockdown lines.

A 386 base pair region from the TIP3;1 cDNA sequence (highlighted in blue), which has 77% homology with the TIP3;2 cDNA sequence was chosen to be cloned into the silencing vector pFAST R03. The high level of homology between sequences means both transcripts will be targeted. Primers recognising both the N terminal (highlighted yellow) and C terminal regions (underlined in bold) of TIP3 transcripts were used to detect TIP3 RNA transcripts in knockdown lines (discussed in 4.2.2).

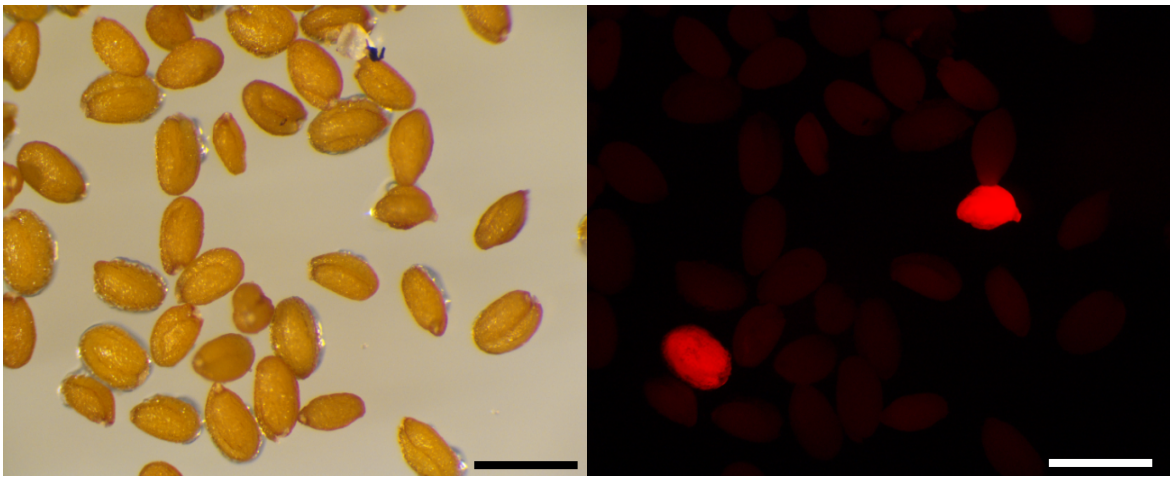

Figure 4.3: The pFAST RO3 vector (Shimada *et al.* 2010) contains OLE1pro:OLE1-tagRFP, enabling transgenic seeds to be fluorescently selectable.
Transgenic seeds from a T1 population containing this vector are selectable by red fluorescence due to the expression of OLE1-tagRFP under the seed specific oleosin (OLE1) promoter. Scale bar = 1mm

4.2.2 Characterising pFAST TIP3 RNAi lines

Four independent homozygous T3 lines expressing pFAST-RO3 with (pFAST::TIP3 a, b , c or d) and two control lines containing empty vector (pFAST::empty 1 and 2) were characterised for TIP3 expression. PCR was performed on 50µg of cDNA made from seed extracted RNA. This showed a reduced level of transcripts for both TIP3;1 and TIP3;2 in pFAST::TIP3 compared to pFAST::empty (figure 4.2). Primers recognising both the N terminal (sequences highlighted yellow in figure 4.3, resulting PCR fragments shown in figure 4.4C) and C terminal regions (primer sequences shown underlined in bold in figure 4.2, resulting PCR fragments in figure 4.4D) of TIP3 transcripts were used for 27 cycles of PCR. This was to rule out potential artefacts from the region of which the hairpin loop was designed. In addition, primer sequences were designed to ensure they would not bind to the hairpin loop itself or the dsRNA made from it. Primer sequences are available in table 2.4, materials and methods.

Primers for specific control housekeeping gene transcripts were selected based on the published recommendation of Czechowski *et al.* (2005), who suggest At4g34270 coding for TIP4;1-like protein is a reliable *Arabidopsis* reference gene; and Dekkers *et al.* (2012) who have found At4g12590 (unknown protein), At4g02080 (ASAR1) and At3g25800 (PP2AA2) are stable expressed genes in *Arabidopsis* seeds. It was found in our experiments that transcripts for At4g02080 and At3g25800 were most uniform among samples (figure 4.4B), most likely because these are seed specific in expression. In contrast, we have found that At4g34270 and At4g12590e may not be reliable reference genes for Arabidopsis seeds. Further investigation using the eFP browser (Winter *et al.* 2007) has enabled us to identify that these genes are not solely expressed in seeds, and exhibit an uneven expression pattern throughout Arabidopsis development (Schmid *et al.* 2005). This may provide an explanation for the variability between samples depicted in figure 4.4A. All four reference primer sets were subjected to 38 cycles of PCR. RTPCR was performed several times with the same PCR conditions, but varied cycle numbers, to optimise transcript levels for visualisation.

Based on all four primer sets targeting TIP3;1 and TIP3;2 transcripts, it is evident that in particular, lines c and d of pFAST::TIP3 have a reduced level of transcripts in comparison to a and b as well as the pFAST::empty samples.

A more quantitative method to show reduced transcript levels would be to employ QPCR. For this, primers for At4g02080 and At3g25800 reference genes (figure 4.4B) would be most suitable. In addition, the inclusion of a *tip3;2* knockout sample could confirm the specificity of TIP3;1 and TIP3;2 primers. In this instance, these samples would exhibit no TIP3;2 transcripts, but would have TIP3;1 transcripts amplified.

In the interest of time, QPCR was not performed, and on the basis that some lines exhibited reduced transcript levels, immunoblots were performed on the same seed batches. Amount of protein does not always reflect transcript expression and thus this experiment was given priority. TIP3 protein levels were detected using anti-TIP3 (described in chapter 3). This antibody is raised to the motif HQPLAPLEDY, which is unique to TIP3;1 and TIP3;2, therefore accurately detecting only these two TIP isoforms (optimisation discussed in section 3.2.1).

Total protein from 20 dry seeds showed PFAST::TIP3 samples to contain less TIP3 than pFAST::empty (Figure 4.5 top panel). More accurately, using 100ug of total protein from dry seeds (as normalised by Pierce 660nm Protein Assay, described in methods section 2.4.1) also showed reduced levels of TIP3 (figure 4.5 bottom panel), particularly in samples c and d. 100ug of total protein was used to detect TIP3 due to the smaller proportion of this protein in relation to the vast amount of seed storage proteins in these tissues. The inclusion of a protein sample from *tip3;2* knockout seeds demonstrates lines c and d have a similar quantity of TIP3 protein. Together, these results indicate RNAi silencing of TIP3 in pFAST::TIP3 seed.

Since the amount of TIP3 in the strongest silenced lines pFAST::TIP3 c and d is equal to that found in *tip3;2*, no further phenotypic analysis was pursued. On the basis that *tip3;2* has no apparent phenotype (Gattolin, Carroll and Frigerio unpublished), it is extremely unlikely that these knockdown lines have sufficiently reduced TIP3 to provide a phenotype or clues into the role of TIP3 in maturing and germinating seeds. Furthermore, a *tip3;1* knockout line has recently become available (The Nottingham Arabidopsis Stock Centre (NASC), and so efforts are now being focussed on creating a double *tip3;1tip3;2* knockout line.

The immunoblots additionally suggest that the amount of TIP3;2 in Col-0 and pFAST::empty seeds is greater than TIP3;1, given that the intensity of the band in *tip3;2* is

less than half of the control lines. It is also apparent that band intensity is increased in pFAST::empty in comparison to Col-0, suggesting expression of OLE1-tagRFP by this vector may influence TIP3 expression levels.

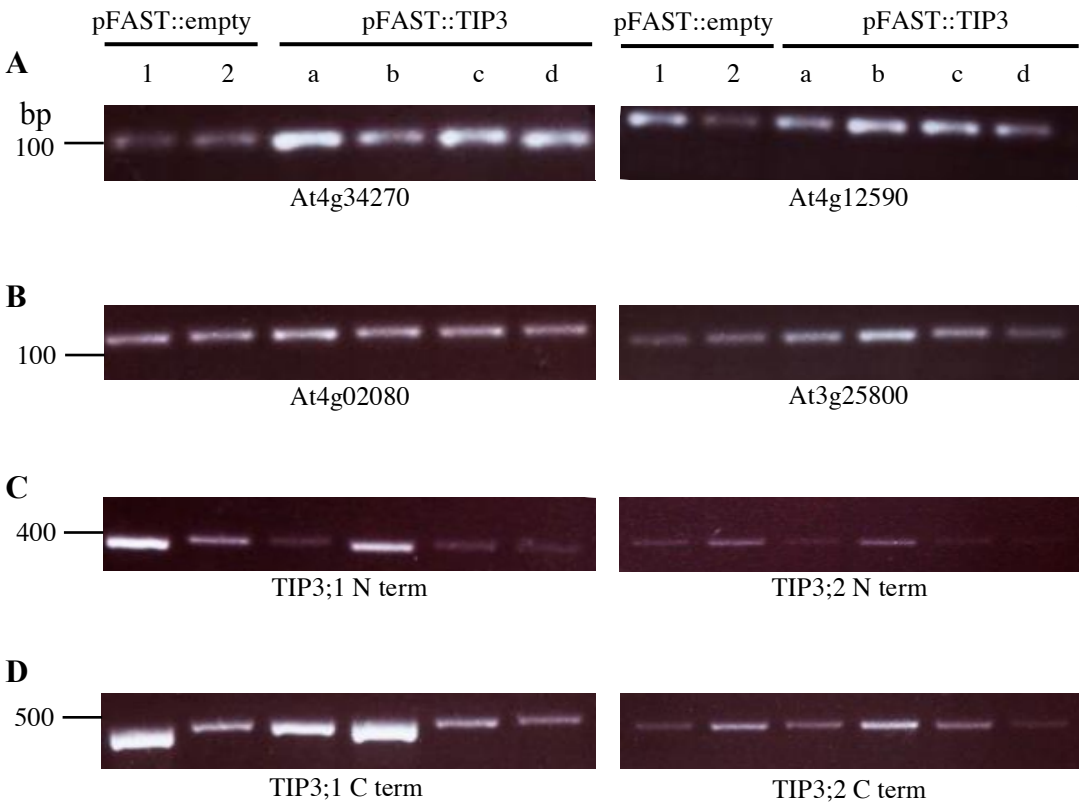

Figure 4.4: RTPCR shows reduced mRNA transcripts in pFAST TIP3 RNAi transgenic seeds.

RNA was extracted from transgenic seed containing the empty pFAST vector (samples 1 and 2) or the pFAST vector containing the TIP3 sequence (samples a-d). 50µg of cDNA made from this RNA was used in each reaction to make results as quantitative as possible (**A-B**) Four sets of control primers targeting different stable expressed genes were used for 38 cycles of PCR. At4g34270 is an *Arabidopsis* reference gene coding for TIP4;1-like (Czechowski *et al.* 2005), while At4g12590, At4g02080 and At3g25800 are stable expressed genes in *Arabidopsis* seeds coding for an unknown protein, ASAR1 and PP2AA2 respectively (Dekkers *et al.* 2012). (**B**) Transcripts for At4g02080 and At3g25800 were most uniform among samples whilst (**A**) At4g34270 and At4g12590e produced varying results, and may not be reliable as seed-specific reference genes. (**C-D**) To amplify TIP3;1 and TIP3;2 transcripts, primers targeting the N terminal region and the C terminal RNAi target area were used for 27 cycles of PCR. Molecular weight of the marker bands is given in base pairs (bp). Sequences for custom primers (Not those from Czechowski *et al.* 2005 and Dekkers *et al.* 2012) are available in table 2.4, materials and methods.

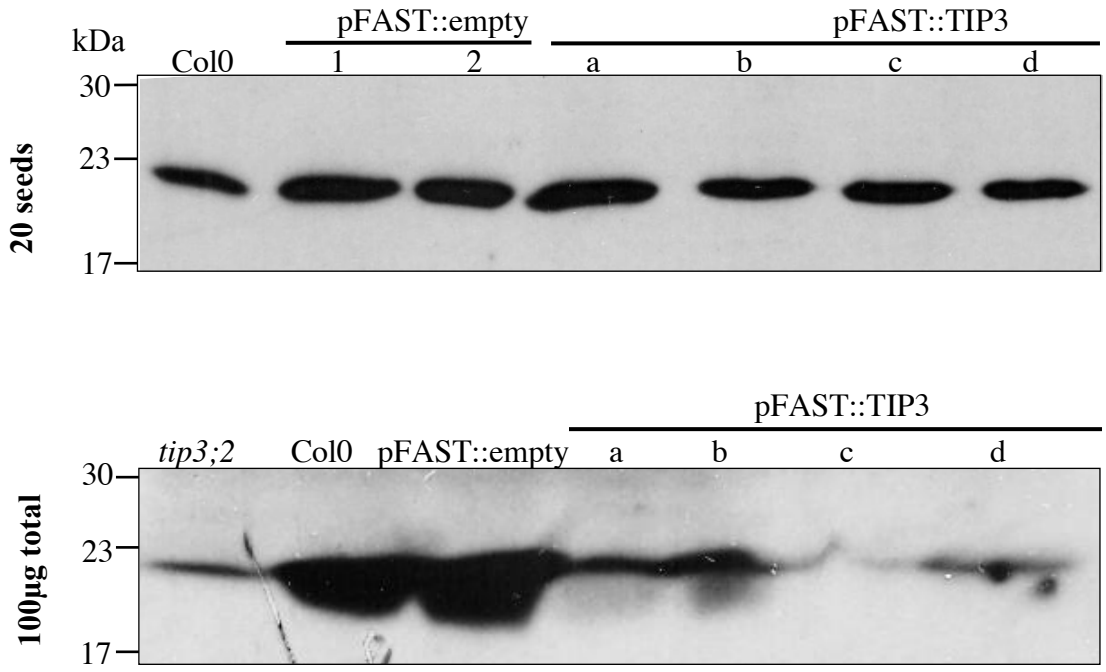

Figure 4.5: pFAST TIP3 RNAi seed show reduced amounts TIP3
Total protein extracted from seeds of *TIP3;2*, Col0, pFAST:empty or pFAST:TIP3 *A. thaliana* T3 plants were subjected to reducing SDS-PAGE and blotted with anti-TIP3. pFAST:empty plants/seeds contain the empty vector whereas pFAST:TIP3 contain selected region of TIP3 sequence. Protein from 20 seeds (top panel) showed small differences in protein quantity. Despite the same amount of starting material, total protein was not normalised before loading. Loading a normalised 100µg (bottom panel) of total protein indicated much clearer that pFAST:TIP3 has reduced amounts of TIP3 and is a successful RNAi knockdown line. Molecular weight of the marker bands is given in kDa.

4.2.3 Expression of OLE1-tagRFP alters Protein Storage Vacuole organisation

Embryos from dry seeds expressing the pFAST RO3 vector were screened by stereomicroscopy and imaged by confocal microscopy. OLE1-tagRFP was confirmed to localise to oil body membranes (figure 4.6) which appeared to be large and abundant in both pFAST::TIP3 and pFAST::empty lines. It is difficult to detect distinctly separate oil bodies, however it is deducible from the scale bar that oil bodies appear larger and less rounded than the expected 0.5-2µm wild type (figure 4.6 A-B) (Tzen *et al.* 1993, Siloto *et al.* 2006), a finding also reported in Shimada *et al.* (2010).

In addition to OLE1-tagRFP, autofluorescence of PSV was imaged to determine whether reduced amounts of TIP3, or indeed expression of OLE1-tagRFP affected PSV organisation. Figure 4.6 panels C and E show the typical organisation of PSV in Col0 wild type embryo cotyledons and radicles respectively. pFAST::TIP3 lines a-d (figure 4.6 panels C-H, and K-N) do not exhibit this PSV organisation. More importantly, pFAST::empty PSV (figure 4.6 panels D and J) also display this change in PSV shape and size. This suggests OLE1-tagRFP expression alters PSV organisation.

To identify whether the change in PSV organisation by OLE1-tagRFP was long term, embryos from imbibed and germinated seeds were imaged by confocal microscopy (figure 4.7). OLE1-tagRFP remains abundant in imbibed seeds (figure 4.7 panel A), but reduces significantly post-germination (figure 4.7 panel D). This is in agreement with reports that the OLE1 promoter is active during seed maturation (Kim *et al.*., 2002) and OLE1-GFP can been observed from the mature embryo stage of the developing seed until 3 days post-germination (Shimada *et al.* 2010). In parallel to this expression pattern, altered PSV organisation persists in embryos of the imbibed seed (figure 4.7 panel B). However once germinated, PSV shape and size returns to wild type (figure 4.7 panels E and F).

Transgenic seeds expressing pFAST RO3 germinated and grew normally in these experiments, and in studies by Shimada *et al.* (2010). Therefore it is assumed that the change in PSV orientation caused by OLE1-tagRFP is not detrimental to seed development or germination.

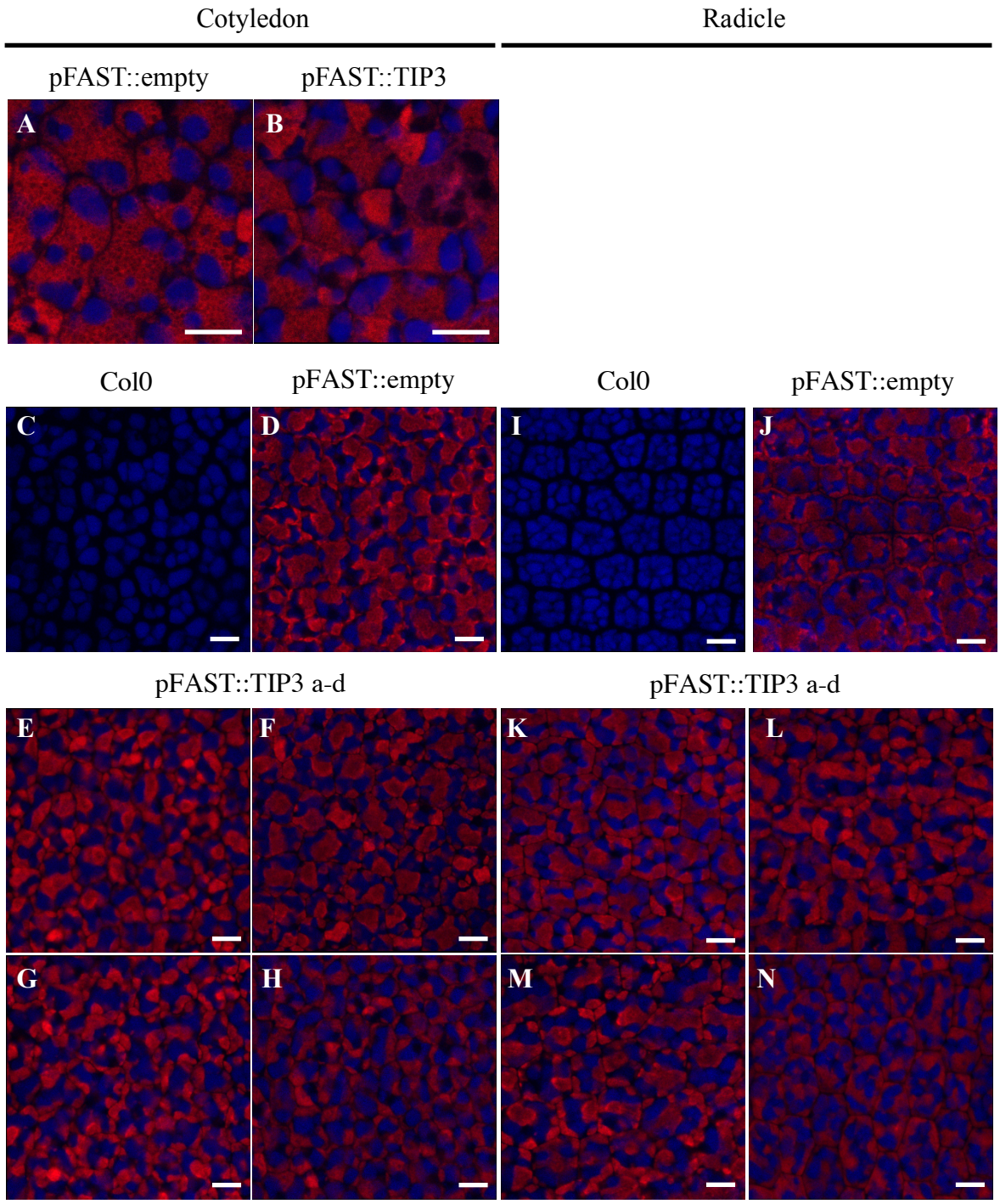

Figure 4.6: Protein Storage Vacuole shape is altered in mature embryos of seeds expressing the pFAST RO3 vector.

Transgenic seeds expressing the pFAST vector are selectable by red fluorescence using tagRFP translationally fused to the oil body protein oleosin1, expressed under the OLE1 promoter. (**A-B**) High magnification images showing lack of distinct separate oil bodies which are larger and less rounded than reported in the literature (Tzen *et al.* 1993, Siloto *et al.* 2006). (**D,J**) PSV of embryos from dry seed expressing this construct, and therefore accumulating OLE1-tagRFP, are altered in shape in comparison to (**C,I**) wild type. (**E-H**, **K-N**) Cells from embryos of the TIP3 RNAi knockdown lines (pFAST vector containing the targeting TIP3 sequence) exhibit a similar phenotype. E-H and K-N correspond to pFAST:TIP3 samples a-d respectively. Red is OLE1-tagRFP and blue is PSV autofluorescence. Scale bar = 10μm.

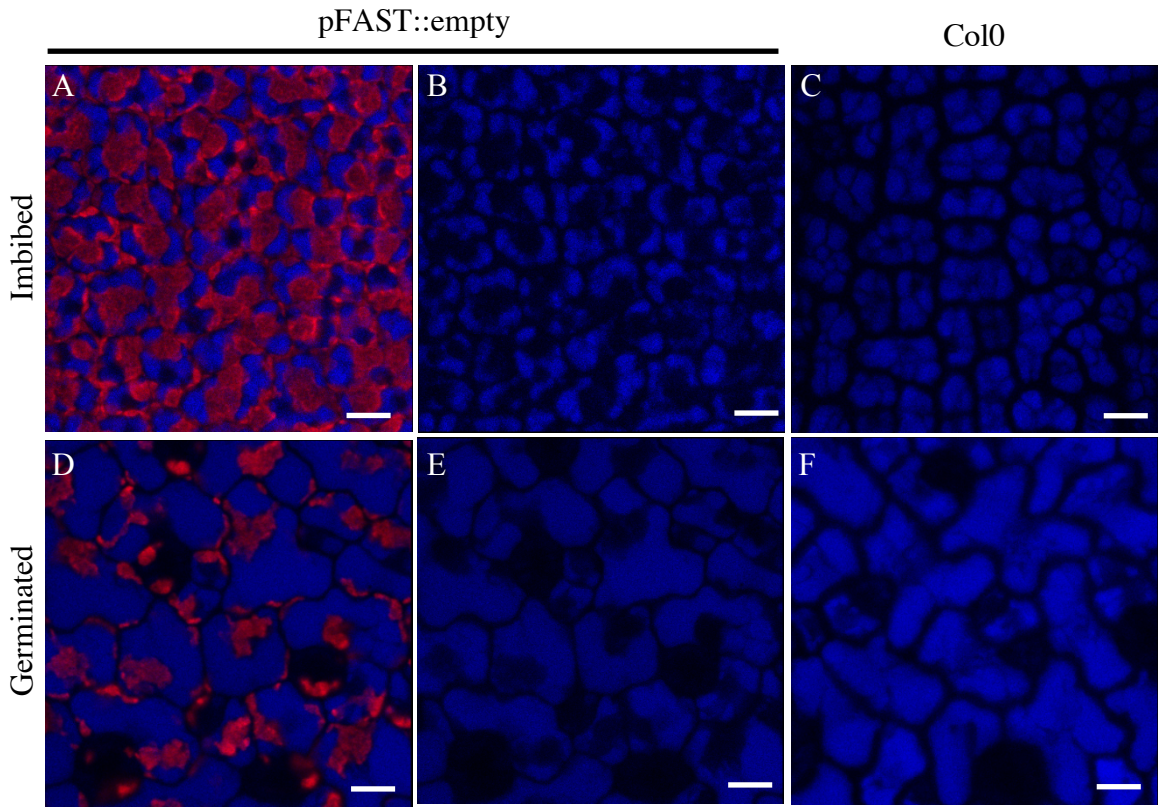

Figure 4.7: Protein Storage Vacuole shape returns to wild-type shape in embryos of seeds expressing OLE1-tagRFP.

(**A-B**) Protein Storage Vacuoles (PSVs) of imbibed embryos (B is identical to A, with OLE-tagRFP signal removed) expressing the pFAST vector exhibit an altered shape in comparison to (**C**) wild type due to accumulation of OLE1-tagRFP. (**D**) Post-germination, expression of this protein under the OLE1 promoter is reduced and reduction in quantity leads to (**E**) return of (**F**) wild type PSV shape, during which it is undergoing transition into a LV. (E is identical to D, with OLE-tagRFP signal removed) Red is OLE1-tagRFP and blue is PSV autofluorescence. Scale bar = 10μm.

4.3 Discussion

GATEWAY™ cloning was successfully employed to generate a construct targeting TIP3;1 and TIP3;2 transcripts for PTGS. The selected 386 base pair region of TIP3;1 sequence recombined into the pFAST-RO3 vector was effective in producing transgenic lines with reduced amounts of TIP3 in dry seeds. However immunoblots showed the amount of TIP3 within these lines remains equal to, or more than, that in *tip3;2.* Thus, efforts have since been redirected to creating a double *tip3;1tip3;2* knockout line.

PIP and TIP knockout mutants of *Arabidopsis thaliana* have already been used to begin unravelling the role these aquaporins play in plant water uptake. *pip2;2* (Javot *et al.* 2003) and *pip1;2* knockouts (Postaire *et al.* 2010) have shown reduced hydraulic conductivity of roots, while *pip1;2*, *pip2;1*, and *pip2;6* exhibit a decrease in hydraulic conductivity within rosettes (Prado *et al.* 2013) and relative water flux within leaves was estimated to have decreased in *pip2;1* and *pip2;2* based on deuterium tracing to fit a model (Da Ines *et al.* 2010). Deuterium is a heavy hydrogen isotope which can be located and quantified from plants that take it up via a hydroponic growth media, therefore indicating how much and where water flux has occurred. In addition to unmasking the function of PIP in plant water balance, knockouts have shown transport of other solutes are reliant on these channels; *pip1;2* has shown CO_2 transport depends on this particular PIP isoform (Uehlein *et al.* 2012). Conclusions from these *pip* mutants have been based on moderate phenotypes, a possible side effect of functional redundancy between isoforms.

The few studies that use TIP knockout lines highlight the importance of targeting multiple isoforms for PTGS to conduct functional studies. Functional redundancy of TIP has been reported in *Arabidopsis tip1;1* and *tip1;2* lines, which did not exhibit any growth defects (Schussler *et al.* 2008, Beebo *et al.* 2009). This is most likely due the spatiotemporal expression pattern of TIP1;1 and TIP1;2 overlapping strongly with TIP2;1, another uniformly expressed TIP in vegetative tissues, and other isoforms such as TIP4;1, TIP2;3 and TIP2;2, which are strongly expressed in the roots (Schmid *et al.* 2005; Gattolin *et al.* 2009). However, a *tip1;3tip5;1* double knockout, resulted in an abnormal rate of barren siliques, highlighting the requirement for TIP1;3 and TIP5;1 in normal plant reproduction (Wudick *et al.* 2014). Strikingly, single *tip1;3* or *tip5;1* single knockouts had no apparent phenotype (Wudick *et al.* 2014). Given that these are the only two TIP isoforms present in mature pollen (Schmid *et al.* 2005), this work emphasises the importance of removing all

isoforms expressed within the tissues or developmental stage being studied, to avoid artefacts through functional redundancy. TIP3 are the only aquaporins present is the maturing and germinating embryo (Vander Willigen *et al.* 2006) and so the *tip3;1tip3;2* double knockout lines will be sufficient to study the impact of these water channels on these developmental processes.

The pFAST-RO3 vector was chosen for its ease of selection for positive transformants. Without the fluorescent marker of OLE-tagRFP, seeds of many possibly successful TIP3 RNAi lines would need RNA extracted from; a very time consuming and tricky task in these tissues (see methods section 2.3.11 for seed RNA extraction protocol). Whilst imaging embryos expressing OLE-tagRFP, it became apparent that oil body size was enlarged and irregularly shaped in comparison to what normally reported in the literature (Tzen *et al.* 1993, Siloto *et al.* 2006). Oleosins, including OLE1 are reported to have an important function in regulating oil body size (Siloto *et al.* 2006). *Arabidopsis thaliana* knockdown and knockouts of OLE1 displayed heterogeneously sized oil bodies in electron micrographs and confocal images where the organelles were stained with Nile Red (Siloto *et al.* 2006). The double knockout *ole1ole2* also exhibits enlarged and irregular oil bodies in electron micrographs (Shimada *et al.* 2008). It is predicted these enlarged irregular shapes are formed from cohesion of several oil bodies, as oleosin has been shown to provide steric hindrance between individual compartments (Tzen *et al.* 1992, Tzen and Huang 1992, Shimada *et al.* 2008). In wild type plants, it is postulated that these individual compartments provide a larger surface area to lipases for degradation of essential lipids during germination (Siloto *et al.* 2006). Surprisingly, overexpression of OLE1-GFP also increased the size of oil bodies (Shimada *et al.* 2010), suggesting any change to the amount of oleosin expressed could affect oil body organisation. In this context, it is not surprising that introduction of OLE1-tagRFP to seeds resulted in enlarged and irregular shaped oil bodies.

In addition to the changes seen in oil body shape and size, PSV organisation was also altered in seeds expressing OLE1-tagRFP. Shimada *et al.* (2010) does not report a vacuolar phenotype in seeds expressing OLE1-GFP, however PSV in mature embryos were found to be irregular in comparison to wild type in the *ole1* knockdown lines by electron microscopy (Siloto *et al.* 2006). Caleosin (CLO1), another oil body membrane anchored protein expressed at the same time as oleosin, has been identified as participating in oil body – vacuole interactions (Poxleitner *et al.* 2006). This conclusion was made based on

electron micrographs from Arabidopsis embryos 48 hours after germination, showing that PSV in *clo1* knockout mutants do not interact as frequently with oil bodies. PSV and oil body membranes have been shown to lie in close proximity, with a maintained fixed distance between them in electron micrographs (Poxleitner *et al.* 2006). In addition, immunogold labelling has highlighted TIP3;1 at the PSV tonoplast surrounding oil bodies, and similarly PSV tonoplast has been shown to be internalised by oil bodies using immunofluorescence microscopy in both *Arabidopsis thaliana* and *Brassica napus* (Poxlietner *et al.* 2006, Naested *et al.* 2000). It has previously been suggested that oil bodies associate with vacuoles in order for oil body membranes to be broken and lipases to enter for triglyceride degradation during germination (Huang *et al.* 1996). However more recently, and much more likely in light of observed membrane internalisations, it is suggested that this association is to function in oil body breakdown and tonoplast turnover during PSV to LV remodelling post germination (Poxleitner *et al.* 2006). Regardless, given the observed relationship between the two organelles, and the effect expression changes have on oil body morphology, PSV changes are unsurprising. Despite the different time points in development that these pictures were taken, it is evident that oleosin and caleosin are both involved in maintaining PSV integrity and possibly mediate interactions between oil bodies and PSV. On this basis it is completely feasible that increasing amount of OLE1 expression, as the pFAST:RO3 vector does, will impact PSV morphology.

Immunoblots showed an increase in the amount of TIP3 detected in protein extracts from dry seed transformed with the pFAST:RO3 vector in comparison to wild type Col-0. The OLE1 promoter contained within the pFAST:RO3 vector to drive OLE1-tagRFP expression, is active during seed maturation (Kim *et al.* 2002), coinciding with TIP3 expression and deposition of storage proteins, oligosaccharides and phytins to PSV (Maurel *et al.* 2007). In parallel to this, when amount of OLE1 diminishes in embyros, TIP3 expression is replaced with TIP1;1 (Gattolin *et al.* 2011) and PSV fuse to transition into LV (Zheng *et al.* 2011). Therefore changes in OLE1 expression is intrinsically linked to TIP3 expression and vacuolar identity within these transgenic seeds. It could be hypothesised that TIP3 expression increases upon OLE1-tagRFP expression, in attempt to remedy the altered PSV organisation given the importance of its storage role in these cells. Regardless of the reason this occurs, analysis of transgenic lines produced using pFAST vectors should be careful to include the untransformed pFAST vector as a control.

Despite the effects that OLE1-tagRFP expression have on PSV morphology and TIP3 expression, there did not appear to be a long-lasting effect on seedlings or plants. Although we did not systematically test germination here, no abnormalities were noted, and Shimada *et al.* (2010) also report seeds germinate normally and seedlings and plants develop as expected. In contrast, OLE1 knockdown and *ole1* knockout seeds did exhibit a delay in germination. However, those on media supplemented with sucrose germinated normally, indicating the delay is most probably due to availability of carbon resources than a change in PSV organisation (Siloto *et al.* 2006). Shimada *et al.* (2008) report a similar phenotype in single *ole* knockout lines but found that double *ole1ole2* or *ole1ole3* seeds exhibited more severe germination defects with as few as 10 and 50% germinating respectively. Shimada *et al.* (2008) conclude that enlarged oil bodies due to oleosin deficiency cause germination defects. Conversely, it appears enlarged oil bodies due to increased oleosin levels do not cause germination defects (Shimada *et al.* 2010). It could be concluded on the basis of sucrose rescuing mild germination defects, that oleosin mutants do not have sufficient stores to germinate efficiently, and whilst providing a source of sugar can remedy this in single knockouts, double knockouts are too depleted for this to be possible (Siloto *et al.* 2006). Poxleitner *et al.* (2006) found *clo1* seeds had reduced amounts of storage lipids available during germination, and that these seeds also contained a higher level of total protein, suggested to be in compensation for these lipids. However, sucrose and starch content remained the same (Poxleitner *et al.* 2006). Germination counts and rates were not measured in *clo1* mutants, just as storage lipid, protein and carbohydrate contents were not measured in oleosin mutants. To understand if these phenotypic effects are mutually exclusive between mutants of the closely associated oleosin and coleosin would enable a more solid conclusion as to what extent enlarged oil bodies, or indeed the impact of this on PSV size, is responsible for these germination defects. It would be interesting to perform germination assays discussed in chapter 3 on our lines containing pFAST-RO3 to confirm enlarged oil bodies due to excess OLE1 do not cause germination defects. Despite these germination defect phenotypes, development of *ole1* and knockdown OLE1 seedlings is reported to be normal (Siloto *et al.* 2006).

Had TIP3 knockdown seeds been phenotypically characterised, it is unlikely that a dramatic effect on germination would have been observed. Treating germinating seeds with mercury (the aquaporin blocker) slows germination, but does not inhibit it (Vander Willigen *et al.* 2006). Now that a double TIP3 knockout is in the pipeline, it is imperative that seeds of this line are used to analyse the extent of this aquaporin's role in germination.

Chapter 5: Targeting routes of TIP3 to the plasma membrane and tonoplast

5.1 Introduction

TIP3 localise to both tonoplast and plasma membrane (PM), the two cellular endpoints of the plant secretory pathway (Gattolin *et al.* 2011). Both TIP expression and localisation are developmentally regulated during seed maturation and germination (Gattolin *et al.* 2011). TIP3 has been visualised at both membranes by confocal microscopy from early torpedo stage embryos through to seed germination, although presence of TIP3 at the PM is reduced in the drying seed (Gattolin *et al.* 2011). Dual localisation of TIP3 has also been reported in developing pea cotyledons using immunological detection (Robinson *et al.* 1996).

The sixth (last) transmembrane domain and cytosolic tail of TIP3;1 was able to reach the tonoplast when fused to a signal peptide for translocation into the ER followed by a cytosolic bacterial enzyme (Hofte and Chrispeels 1992). Recently, we have found that removing the distal C- terminal 23 amino acids of TIP3;2 (TIP3;2ΔC) abolishes PM localisation (Gattolin, Carroll and Frigerio, unpublished). There must therefore be information in this final part of the TIP3 primary sequence, which is responsible for targeting to both tonoplast and PM. However, the specific sequence is yet to be elucidated, as is whether targeting to tonoplast and PM occurs simultaneously or whether the protein trafficked vectorially from PM to tonoplast.

Tonoplast proteins are thought to be co-translationally inserted into the membrane of the endoplasmic reticulum (ER) before being sorted through the secretory pathway to reach their destination via the Golgi-dependent or -independent routes (Jiang and Rogers 1998). TIP3;1 has already been reported to reach the tonoplast via the Golgi independent pathway (Park *et al.* 2004). Park *et al.* (2004) showed in *Arabidopsis* protoplasts that TIP3;1 modified to contain the phaseolin C terminus N-glycosylation site, is not altered by Golgi resident glycan modifying enzymes until Brefeldin A treatment re-localises these enzymes to the ER. Brefeldin A (BFA) prevents the formation of COPI vesicles responsible for retrograde traffic from Golgi to ER, disrupting protein transport and causing Golgi proteins to be retained within the ER (Nebenfuhr *et al.* 2002). This pharmacological tool has been used to show that TIP3;1 traffics Golgi independently through its persistent tonoplast localisation in the presence of BFA. This has been shown both by immunodetection of the protein in vacuole extracts from transformed tobacco protoplasts (Gomez *et al.* 1993), and confocal microscopy visualising overexpressed TIP3;1 at the tonoplast in *Arabidopsis*

hypocotyls (Rivera-Serrano *et al.* 2012). However to date, TIP3 trafficking has not yet been studied in its native tissues under quasi-native expression levels.

5.1.2 Aims and Experimental Approach

- To identify whether targeting of TIP3 to the PM and tonoplast is as a result of dual sorting or of a novel tonoplast trafficking route that uses PM as an intermediary station;
- to unravel the trafficking route by which TIP3 takes to reach these membranes.

Various TIP3-fluorescent protein fusions were visualised using confocal microscopy to confirm dual localisation and the role of the TIP3 C-terminus in PM localisation. Photoconversion, photobleaching and dexamethasone induced expression of TIP3-fluorescent tag fusions were employed as techniques to visualise dual or sequential targeting while BFA treatment was used to establish trafficking routes through the secretory pathway.

5.1.3 Constructs

Figure 5.1 shows the diagrams of the constructs and the genetic background of the *Arabidopsis thaliana* lines used in this Chapter. Photoconvertible proteins Dendra2 and mEoSFP were used as an approach to decipher order of TIP3 trafficking to the plasma membrane and tonoplast (as discussed in section 5.2.3). These particular photoconvertible proteins were available from a collaborator (Dr. Jaideep Mathur, University of Guelph), and so a tried and tested method was available. The mEoSFP-calnexin fusion was used as a positive control given its reported success Mathur *et al.* (2010).

To investigate the Golgi dependent and independent pathways of TIP proteins, *gnl1* background Arabidopsis lines were used. As described in sections 1.6.2 and 5.1, Arabidopsis GNL1 is insensitive to Brefeldin A (BFA), the drug used to disrupt trafficking via the Golgi. Therefore, using a knockout background renders these plants susceptible and enables BFA treatment to disrupt this pathway. VHA-a1, the subunit of Arabidopsis V-ATPase, is known to traffic to the TGN via the Golgi and is thus a suitable control for these experiments (Viotti et al. 2013).

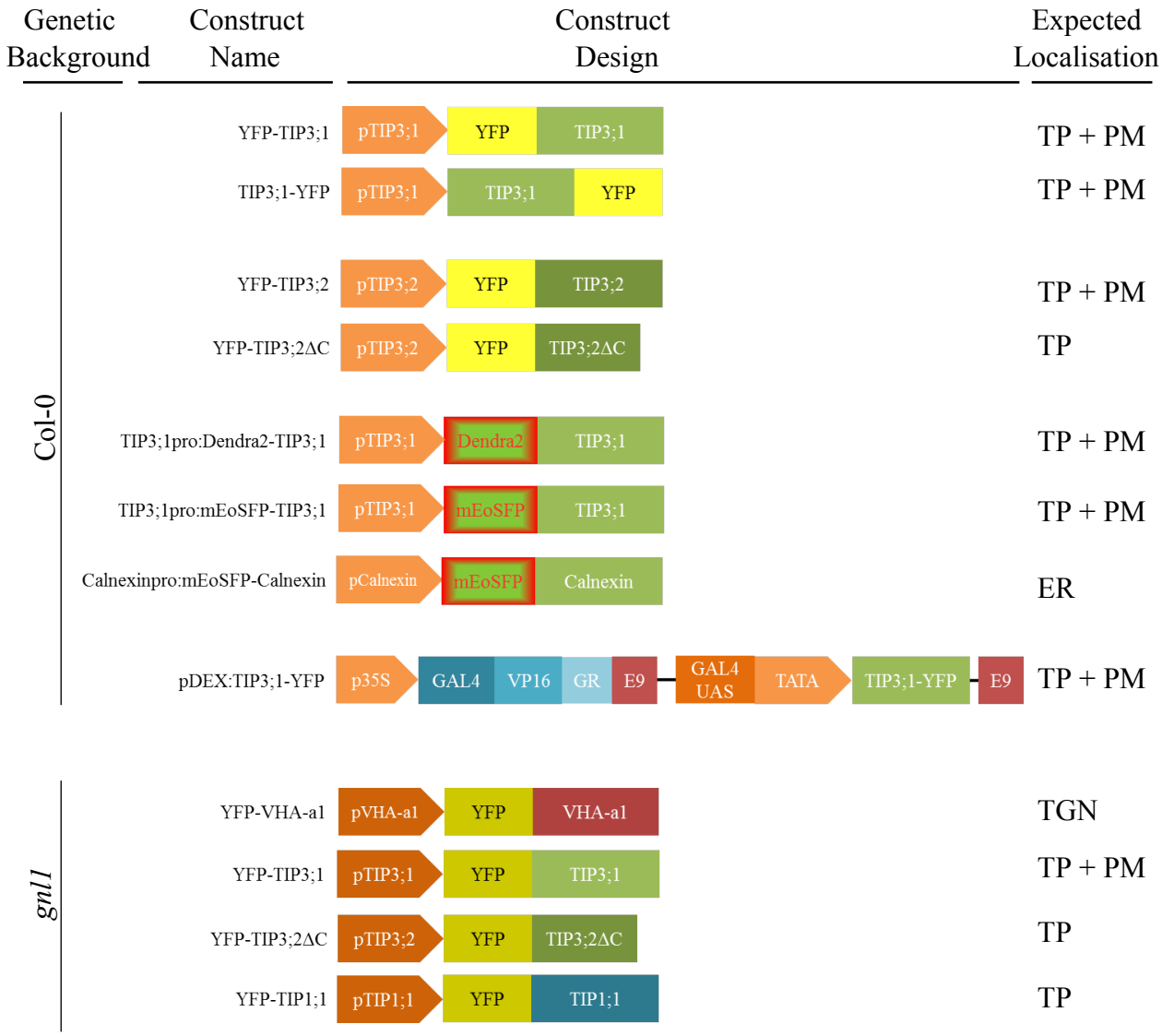

Figure 5.1: Schematic representation of the constructs used to produce the results in Chapter 5

Full genomic sequences for TIP3;1, TIP3;2, TIP1;1, Calnexin or VHA-a1 were cloned into pGreen-0029 with YFP or photoconvertible proteins Dendra2 or mEoSFP; apart from in the case of pDEX:TIP3;1-YFP where it was cloned into the Gateway pDEX vector (Dr Jens Steinbrenner and Professor Jim Beynon, University of Warwick). Some constructs were used to transform *gnl1* background plants in order to convey sensitivity to Brefeldin A treatment. A list of constructs cloned previously to this body of work is listed in table 2.4. TP=Tonoplast, PM=Plasma Membrane, ER=Endoplasmic Reticulum, TGN=Trans Golgi Network.

5.2 Results

5.2.1 TIP3 locates to tonoplast and plasma membrane independently of the position of the fluorescent protein tag

Dual localisation of TIP3 to the tonoplast and PM was shown to be independent of XFP position in Gattolin *et al.* (2011). To confirm this is independent of YFP being fused to the N or C terminus of TIP3;1, embryos expressing TIP3;1-YFP and YFP-TIP3;1 were imaged by confocal microscopy (figure 5.2A-B). It is difficult to capture the PM by confocal microscopy in these embryos during imbibition, as amount of TIP3;1-YFP or YFP-TIP3;1 at the tonoplast is so high that signal becomes saturated at a low laser power. At this low laser power visualising the signal at the PM, which is approximately 10-fold lower in fluorescent signal, is problematic. Nevertheless, in combination with the results from Gattolin *et al.* (2011) (C-D), it is clear that dual localisation is maintained regardless of the position XFP is fused to.

From these results, it is deducible that XFP does not mask an essential sorting signal causing TIP3 to be redirected. In addition, PM localisation has already been found not be an artefact of overexpression by expressing tip3;2pro:TIP3;2-YFP in TIP3;2 tDNA knockout lines mutant lines (*tip3;2*) (Gattolin *et al.* 2011). Furthermore, use of the TIP3;2 promoter to drive expression of YFP-TIP1;1 in *tip3;2* has confirmed that PM localisation is due to a sorting signal contained within the TIP3 sequence itself, as this construct results in TIP1;1 localisation only to the tonoplast (Gattolin *et al.* 2011).

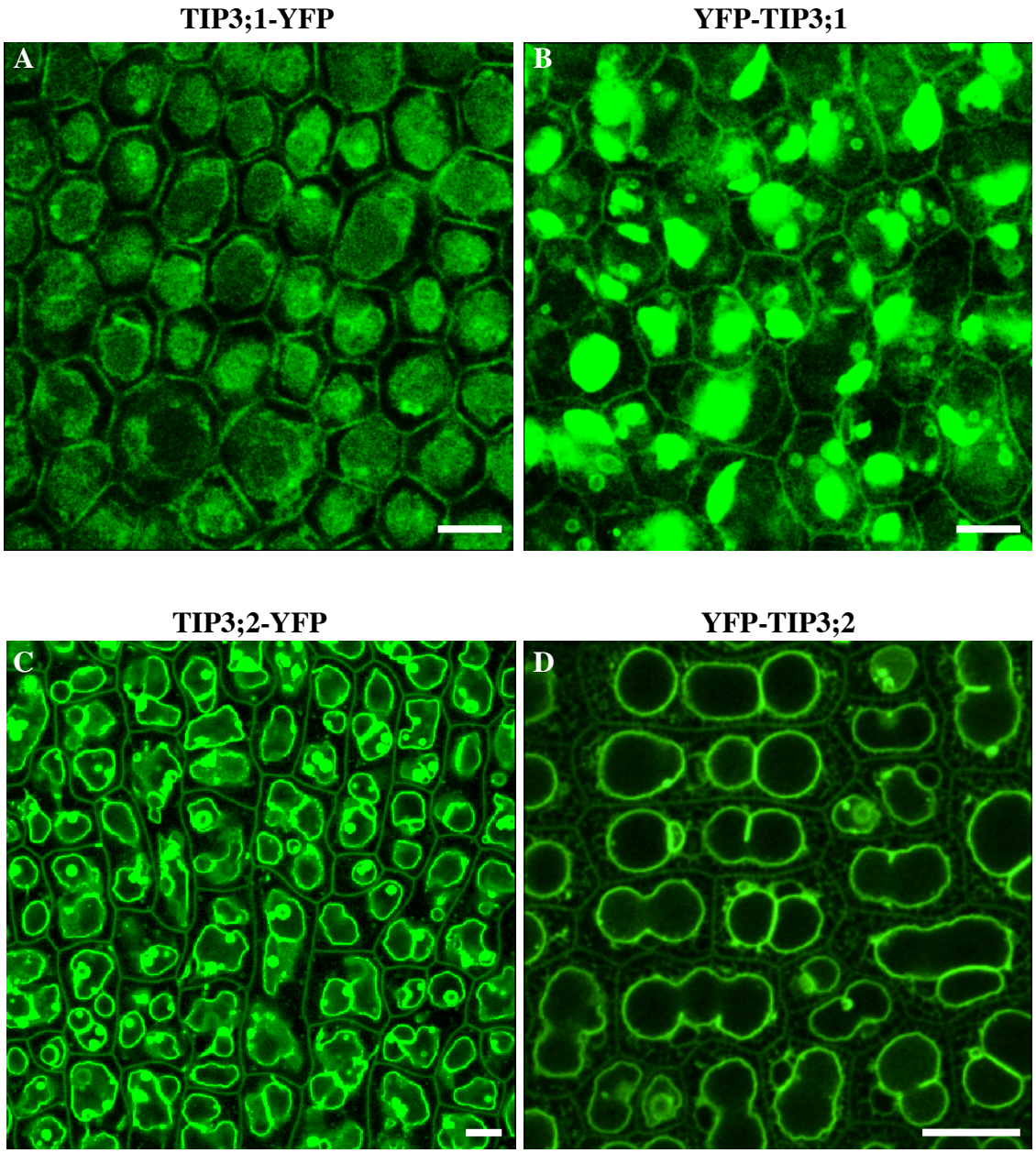

Figure 5.2: TIP3;1 and TIP3;2 translationally fused to YFP localises to the tonoplast and plasma membrane independently of N or C terminal position
(**A**) TIP3;1-YFP and (**B**) YFP-TIP3;1 expressed under their native TIP3;1 promoters are localised to the PM and tonoplast in mature embryos. These images are of embryo cotyledons which have been imbibed for 24 hours. Image B was acquired at high detector gain in order to visualise PM, resulting in several overexpressed fluorescent structures. (**C**) TIP3;2-YFP and (**D**) YFP-TIP3;2 expressed under their native TIP3;2 promoters are also localised to PM and tonoplast in mature embryos (**C-D** taken from Gattolin *et al.* 2011). Scale bars = 10μm.

5.2.2 Deletion of the C terminus abolishes plasma membrane localization

Alignment of *Arabidopsis* TIP sequences reveals that TIP3;1 and TIP3;2 harbour an additional sequence at their C terminus in comparison to other isoforms (figure 5.3). Deletion of the final 23 amino acids of the C-terminus of TIP3;2 has revealed that this sequence is necessary for targeting to the PM, as these YFP-TIP3;2ΔC fusions locate to the tonoplast only (figure 5.4). This also suggests PM targeting of TIP3 is not a prerequisite for tonoplast localisation.

PM localisation of TIP3 is seed-specific; overexpressing TIP3;1 with the CaMV 35S promoter leads to dual labelling in embryos and germinating seeds but tonoplast- only localisation in vegetative tissues (figure 5.5).

Further dissection of the C terminus is essential in order to determine its role in trafficking of TIP3 to the PM, but this will need to be considered in context of the relevant seed specific machinery to be fully understood.

The region which is deleted in YFP-TIP3;2ΔC contains 2 serine residues. As discussed in section 1.4.3 (introduction), phosphorylation of serine residues results in opening of the aquaporin pore. Expression of TIP3;1 in *Xenopus* oocytes with Ser7, Ser23 or Ser99 residues mutated to alanine, resulted in reduced water transport in comparison to wild-type TIP3;1 (Maurel *et al.* 1995). The residues removed in YFP-TIP3;2ΔC have so far not yet been implicated in aquaporin function. Moreover, the same C-terminal portion of the TIP3;1 primary sequence does not contain these 2 serine residues. Given that these two isoforms are considered to be functionally identical, this infers that deletion of the C terminal tail will not affect protein function.

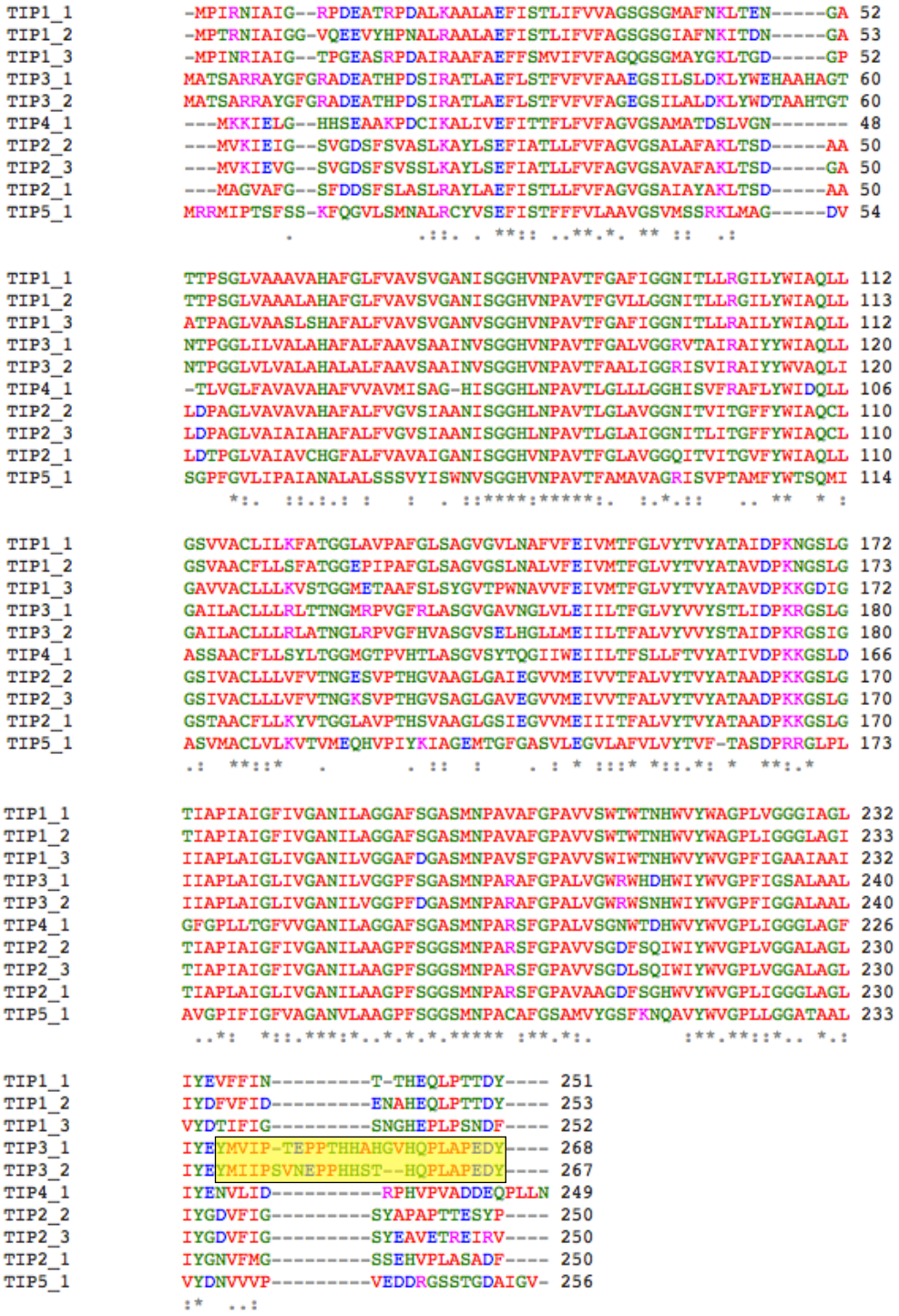

Figure 5.3: Alignment of *Arabidopsis thaliana* TIP isoform primary sequences show extra C terminal motif at the C terminus of TIP3;1 and TIP3;2

A. thaliana TIP isoform primary sequence alignment reveals that TIP3;1 and TIP3;2 have additional residues at their C terminus. Highlighted in yellow is the C terminal region deleted in YFP-TIP3;2ΔC transgenic lines. Colours correspond to physiochemical properties of residues; RED=small hydrophobic, BLUE=acidic, MAGENTA=basic, GREEN=hydroxyl, sulfhydryl, amine and G, GREY= unusual. Results from ClustalW2, EMBL-EBI.

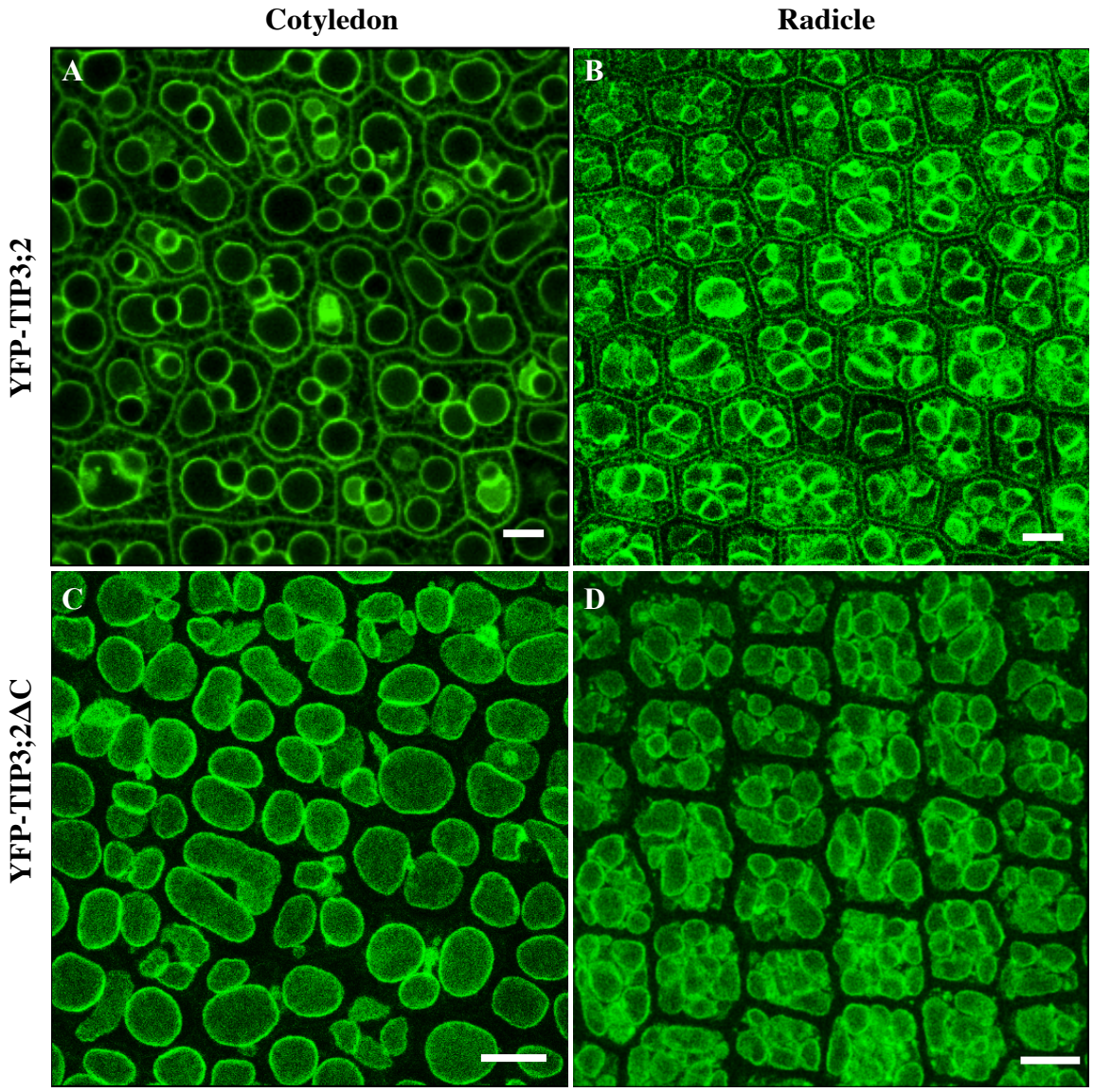

Figure 5.4: Deletion of the C terminus of TIP3 abolishes plasma membrane localization

(**A-B**) TIP3;2 translationally fused to the N-terminus of YFP expressed under the native TIP3;2 promoter localises to the PM and tonoplast in embryos of mature seeds. (**C-D**) TIP3;2ΔC has its 23 C-terminal amino acid residues deleted. This translational fusion is localised to the tonoplast only. Scale bars = 10μm.

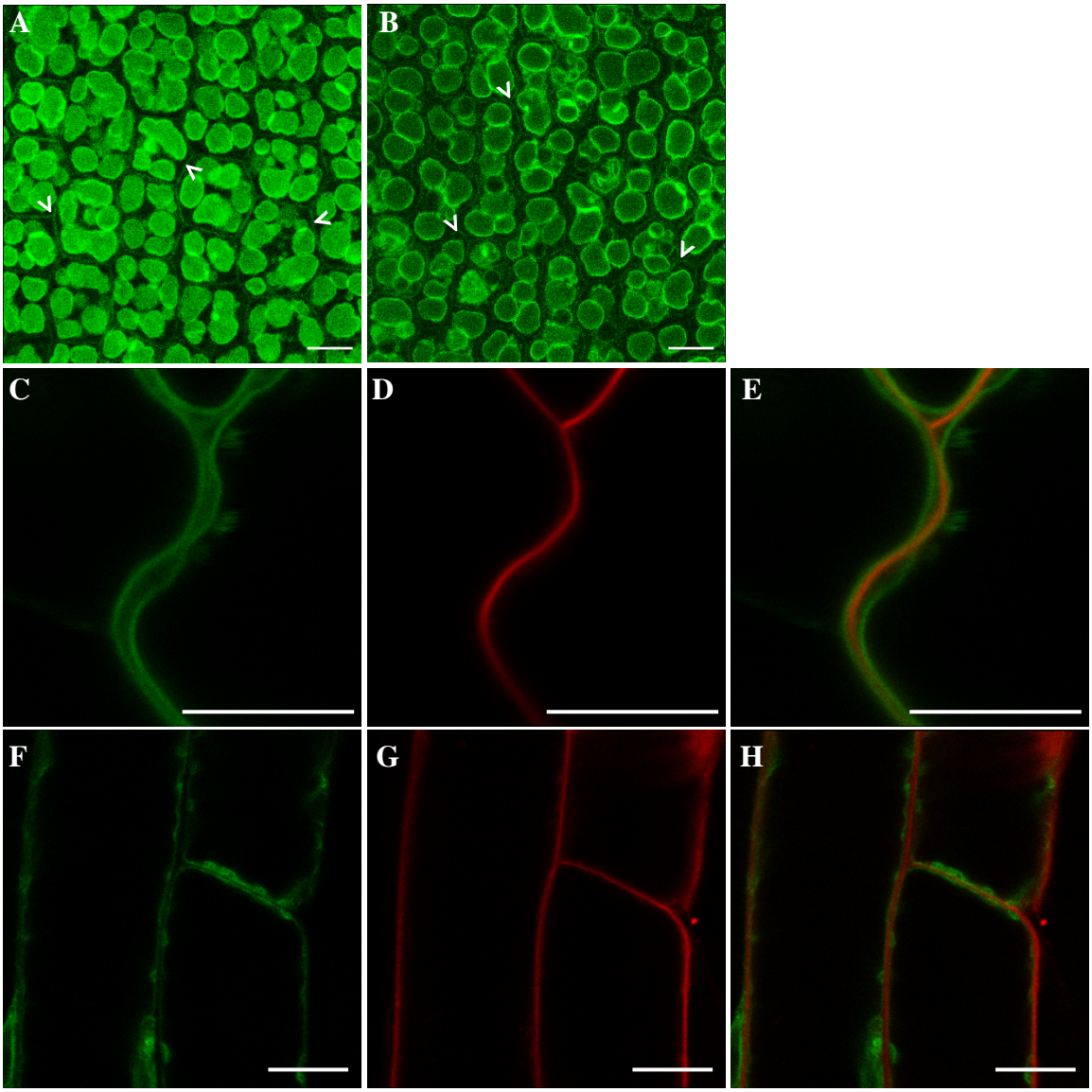

Figure 5.5: 35S:TIP3;1-YFP localises to the plasma membrane and tonoplast in embryos but only to the tonoplast in seedlings.
(**A-B**) TIP3;1 with YFP translationally fused to the C-terminus expressed under control of the 35S promoter localises to the PM and tonoplast in radicle (A) and cotyledon cells (B) of mature embryos. The PM is indicated by arrows. (**C-H**) In seedlings, TIP3;1-YFP is only localised to the tonoplast. This is true for cells of the cotyledon (**C-E**) and root (**F-H**). (**D**,**G**) Tonoplast-only localisation was confirmed by labelling of the PM with the FM4-64 dye (red), and (**E**,**H**) overlaying this with YFP signal (green). Scale bars = 10µm.

5.2.3 Photoconvertible proteins Dendra2 and mEoSFP are unsuitable for visualising TIP3 in *A. thaliana* embryos

With the knowledge that a C terminal truncation of TIP3 abolishes PM localisation, it is next logical to question in which order this protein reaches its destinations. It could be assumed that TIP3 is sequentially targeted, being sent first to the PM before being endocytosed and trafficked to the tonoplast. However, dual localisation is a more likely possibility given that TIP3 reaches only the tonoplast without its C terminus and when expressed in non-seed tissues, highlighting the fact that PM targeting is not a requirement for TIP3 targeting to the tonoplast.

To address this, photoconvertible proteins, Dendra2 and mEosFP (Gurskaya *et al.* 2006; Wiedenmann *et al.* 2004) were employed to visualise TIP3 trafficking. Both Dendra2 and mEoSFP are photoconvertible monomers which emit fluorescence within the green light spectrum (490-535nm) in their native state, until they are photoconverted with blue 405nm light. Upon this irreversible photoconversion, covalent modifications occur and the fluorescent proteins' emission spectra are shifted to a red emission peak (560-650nm) (Nienhaus *et al.* 2006). Exact excitation and emission spectra are outlined in methods table 2.8. These fluorescent tags were translationally fused to the N terminus of TIP3;1 and their expression driven under control of the native promoter sequence. Within *Arabidopsis* embryos, at this timepoint, the PSV are sufficiently spatially separated from the PM that a region of interest on just the PM can be photoconverted without interference on the tonoplast. In addition, protein diffusion at the PM is slower than at the tonoplast (Martinière *et al.* 2012) so visualization should be possible before the photoactivated protein at the PM is laterally diffused among inactivated protein.

As illustrated schematically in figure 5.6, if dual targeting occurs there would be no colocalisation of the photoconverted with unphotoconverted protein given that TIP3 had already been successfully targeted to both the PM and tonoplast at the same time. However if sequential targeting occurs, the photoconverted protein (red) at the PM which is endocytosed and targeted to the tonoplast would colocalise with the (green) non-photoconverted proteins (orange).

Dendra2, enhanced from the original Dendra (Gurskaya *et al*. 2006), was translationally fused to the N terminus of TIP3;1. Expression under the native TIP3;1 promoter showed

localisation only at the tonoplast (figure 5.7). Excitation laser power was high (>40%) in comparison to what is needed for YFP (typically 2-4%) visualisation in this construct, indicating its weak fluorescence. Although the detectable protein was successfully photoconverted (Fig. 5.7, B) using 20-50% laser power (as recommended by Evrogen, Russia), Dendra2 was deemed unsuitable for visualising TIP3 trafficking in *A. thaliana* embryos because it was not visible at the PM.

mEoSFP, a photoconvertible protein with reportedly brighter fluorescent signal, was then used in the same way as Dendra2 (figure 5.7) (Wiedenmann *et al.* 2004). Our control, mEoSFP translationally fused to calnexin, an ER targeted protein (Huang *et al.* 1993, Runions *et al.* 2006, Mathur *et al.* 2010), was bright and targeted efficiently (Fig. 5.7, E-F). mEoSFP-TIP3;1 was also only visible at the tonoplast, in the same way as Dendra2-TIP3;1 is and in addition, photoconversion rates were extremely low. The low level of fluorescent emission coupled with a low photoconversion rate, led to this system also being unsuitable for visualising TIP3 targeting in *A. thaliana* embryos.

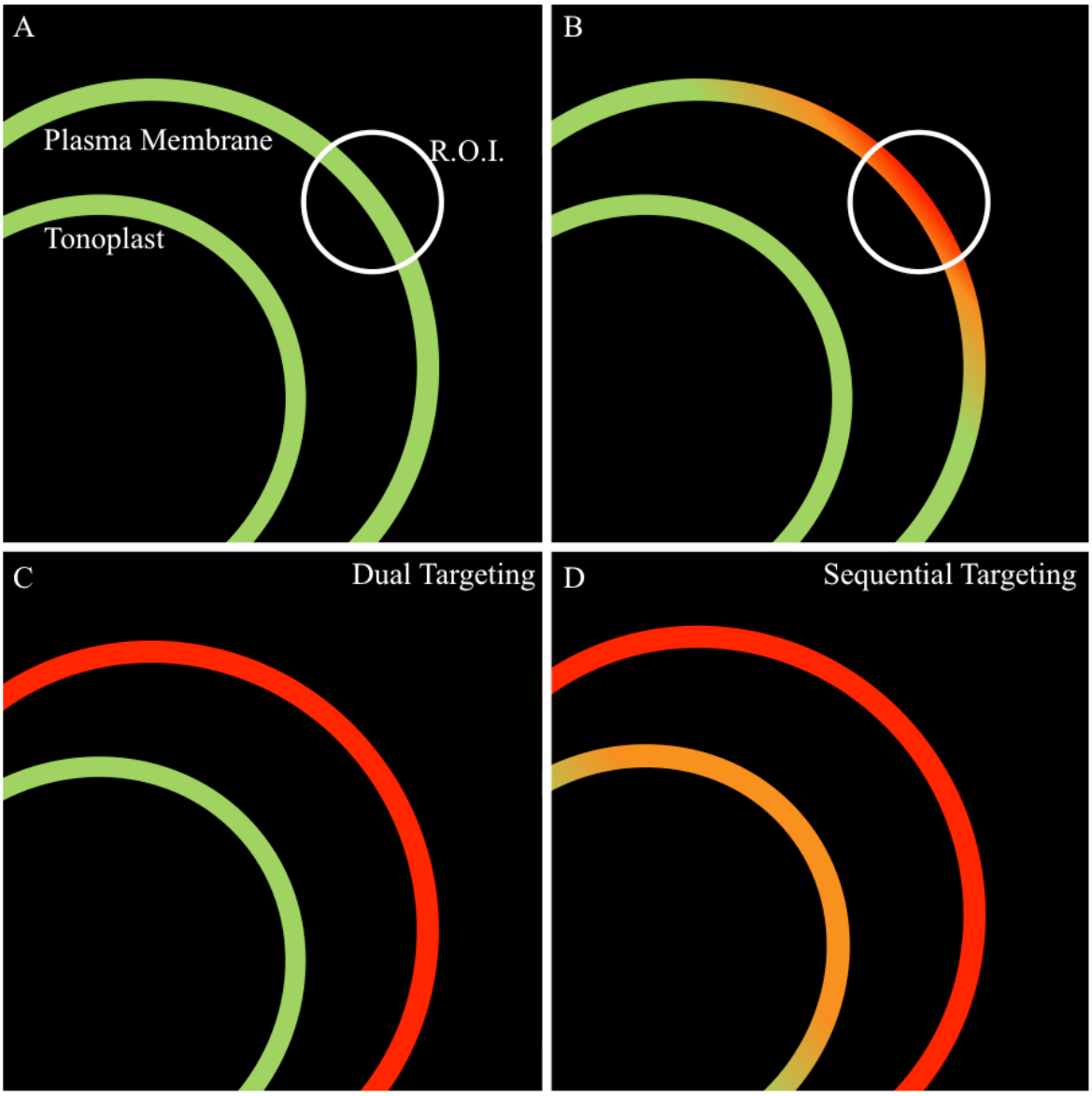

Figure 5.6: A strategy to determine the targeting route TIP3 takes to reach the plasma membrane and tonoplast using photoconvertible proteins.
Photoconvertible fluorescent proteins can have their emission spectra shifted by activation with blue (405 nm) light. (A-B) By activating regions of interest (R.O.I.), it would be possible to photoconvert an entire membrane and visualise protein targeting to subsequent locations. TIP3;1 was translationally fused to Dendra2 or mEoSFP in order determine whether targeting to PM and tonoplast occurred simultaneously (dual targeting, C) or subsequently (sequential targeting, D).

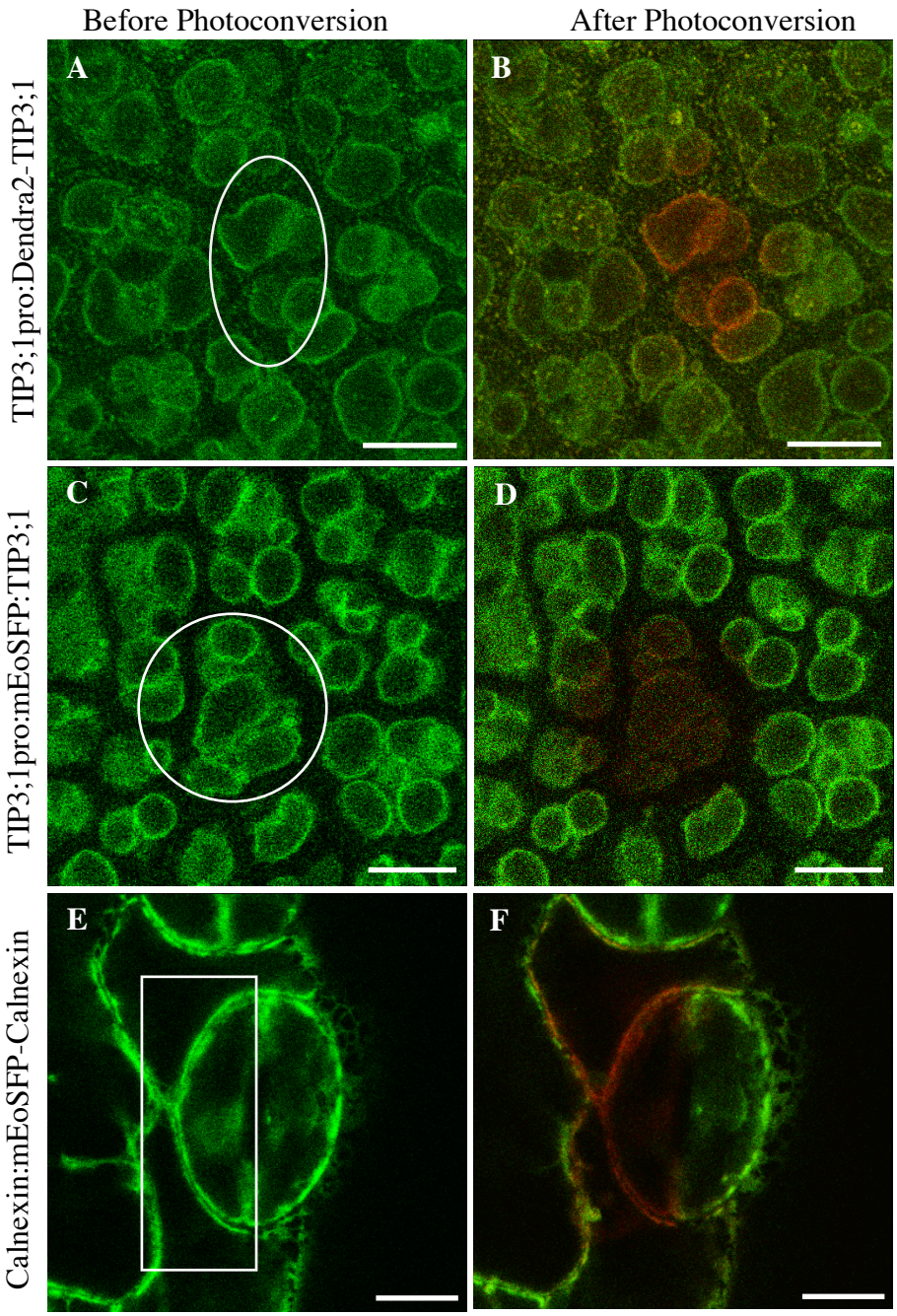

Figure 5.7: The photoconvertible proteins Dendra2 and mEoSFP are unsuitable for visualising TIP3 targeting between tonoplast and plasma membranes.
(**A**) Dendra2 was translationally fused to the N terminus of TIP3;1, and visualised in embryos from dry seeds. (**B**) Photoconversion was effective with blue light at 405nm, however overall fluorescent signal is weak. (**C**) mEoSFP was translationally fused to the N terminus of TIP3;1 and imaged in embryos from dry seeds. (**E**) As a control, mEoSFP translationally fused to calnexin (from Dr. Jaideep Mathur, University of Guelph) was visualised in young seedlings. (**F**) EoSFP photoconversion was effective with blue light at 405nm when fused to Calnexin, (**D**) but not sufficient to study targeting when fused to TIP3;1. Green is pre-photoconversion and red is post-photoconversion. Scale bars = 10µm.

5.2.4 Long-term photobleaching is detrimental to embryos

As an alternative to photoconvertible fluorescent proteins, we attempted to use photobleaching as a method to determine whether TIP3 is targeted dually or sequentially to the PM and tonoplast. By using high-intensity 405 nm blue light from a diode laser directed to a large region of interest encompassing several cells, we were able to completely eradicate fluorescent emission in sections of embryos expressing YFP-TIP3;1 (figure 5.8a). By removing all traces of signal, it was thought that by imaging the embryo's recovery overnight, we would be able track the localisation of newly synthesised YFP-TIP3;1. Should this newly synthesised protein be visualised at the PM first, it would indicate sequential sorting whereas new synthesised TIP3;1-YFP at both tonoplast and PM would indicate dual sorting.

In order to completely obliterate all YFP signal, which is extremely high in this line, very high doses of 405nm light were targeted over a shallow Z section of the embryo (figure 5.8b). After overnight imaging, there was barely any signal of TIP3;1-YFP, with no detectable recovery (figure 5.8c). Parts of the embryo which were not photobleached appeared to maintain TIP3;1-YFP expression, albeit at lower levels than prior to photobleaching. As only the photobleached section of the embryo was exposed to the laser overnight, it was unclear as to whether long-term exposure of this region to the 514nm excitation laser, or photobleaching itself had caused irreversible damage to cells, and possibly the entire embryo.

Embryos were therefore imaged overnight without prior photobleaching in order to determine the effect of this method on embryo health (figure 5.8 d-e). There was a decrease in fluorescence intensity of YFP due to prolonged exposure to the 514nm laser; however a clearly detectable signal was still present. Therefore it is most likely that photobleaching with 405nm light irreversibly damaged the regions of interest within the embryos. These results also indicate that the time required for the new synthesis, sorting and accumulation of TIP3;1-YFP far exceeds our overnight window of observation. In order to observed fluorescence recovery (if possible), it will be necessary to employ a perfusion chamber in order to maintain the embryos alive under the confocal microscope for a longer period of time.

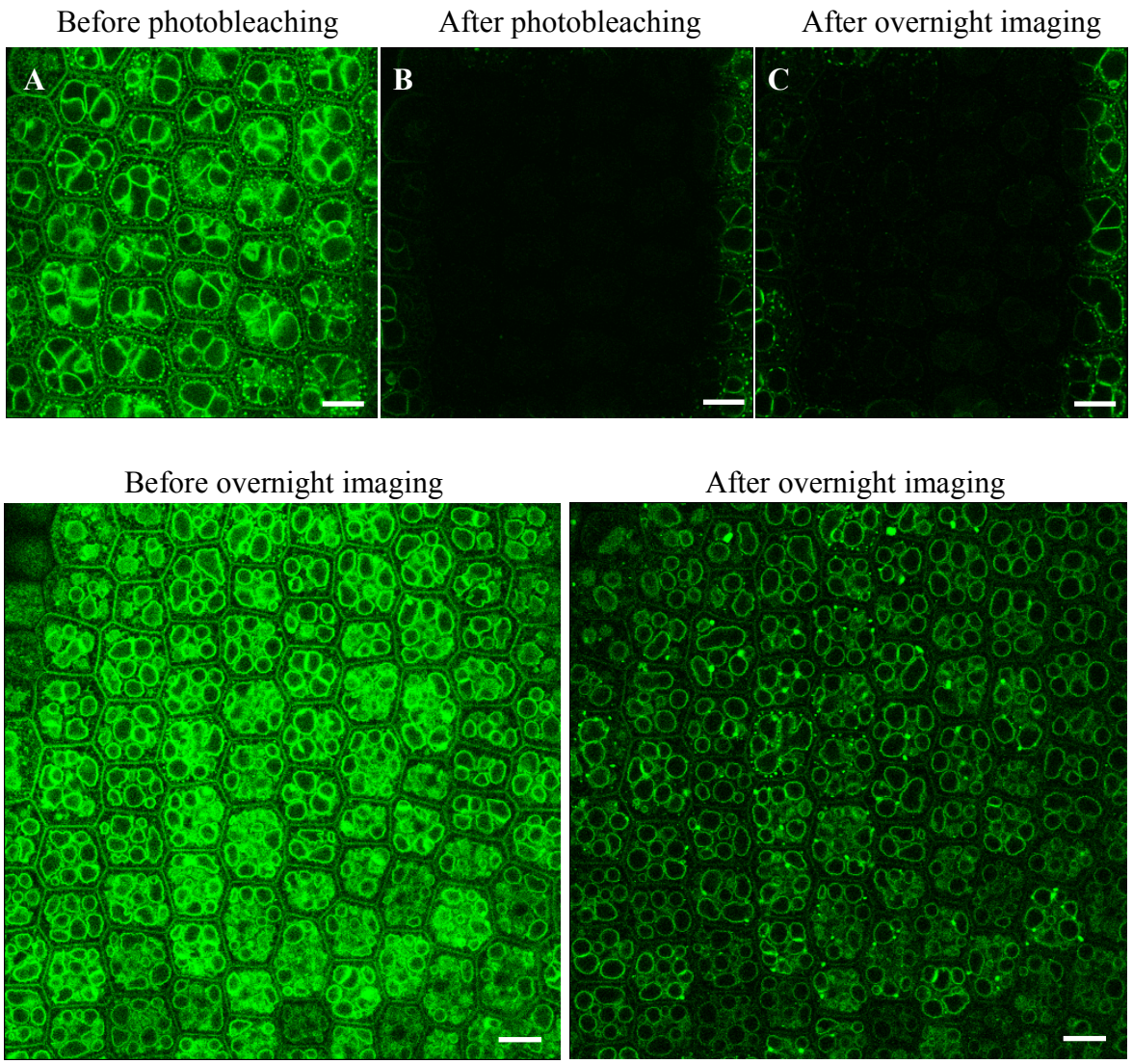

Figure 5.8: Photobleaching of embryos expressing TIP3;1-YFP is lethal.
A region of 24-hour imbibed embryos expressing TIP3;1-YFP (**A**) were bleached (**B**) to determine order of targeting to PM and tonoplast. A prolonged exposure of high intensity 405nm light was required to completely photobleach the tissue. After overnight imaging with the 514nm excitation laser, YFP fluorescence was not recovered (**C**). To determine whether this effect was caused by overnight laser exposure or tissue damage caused by UV light, we imaged embryos expressing TIP3;1-YFP (**D**) overnight. There is a significant decrease in fluorescence intensity of YFP due to prolonged exposure of 514nm light; however embryos tissues maintained integrity (**E**). Therefore it is most likely that photobleaching with 405nm light is detrimental to embryo tissues. Scale bars = 10μm

5.2.5 Expression of TIP3;1-YFP can be induced using the pDEX Gateway vector

Since it was not possible to study targeting of TIP3;1 using photoconvertible proteins or photobleaching, an *ad hoc* induction system of TIP3;1-YFP was devised. Using the pDEX Gateway plasmid, (Dr Jens Steinbrenner and Prof Jim Beynon, University of Warwick) expression of the inserted gene can be controlled by dexamethasone (DEX) treatment. This pDEX Gateway vector is derived from the DEX inducible plant promoter vector pTA7001 originally described by Aoyama & Chua (1997). The plasmid contains a transacting synthetic GVG transcription factor, which is expressed under the control of the cauliflower mosaic virus 35S promoter and flanked by the polyadenylation signal of the pea ribulose bisphosphate carboxylase small subunit rbcS-E9. Using Gateway cloning, the sequence for TIP3;1-YFP was inserted into the vector, flanked by the polyA sequence of the pea rbcS-3A and under the control of a cis- acting element containing 6 Gal4 upstream activating sequences (UAS) and the -46 to +1 region of the 35S promoter (Aoyama *et al.* 1997). Figure 5.9 illustrates this setup schematically.

The constitutively expressed synthetic GVG transcription factor contains the hormone binding domain (HBD) of vertebrate glucocorticoid receptor, the transactivation domain of herpes virus VP18 and the DNA binding domain of yeast Gal4 TF. In the absence of its ligand DEX, interactions of the GR-HBD with cytosolic chaperones hold GVG in the cytosol. In the presence of DEX, GVG can enter the nucleus. The Gal4-DNA binding domain of GVG interacts with the Gal4 UAS elements of the promoter activating transcription of the inserted gene; TIP3;1-YFP.

The induction system was initially tested in stably transformed *Arabidopsis thaliana* seedlings. Testing the system in these tissues enabled us to explore methods and time course of induction as well as concentration of DEX required, without potential complication of the effects of germination on induction or the potential negative effects of DEX on induction on germination. Seedlings germinated and grown on ½ MS agar plates for five days were transferred to plates supplemented with 1μM (Bhorgi *et al.* 2010) or 30μM DEX (Lewis, 2012). After 24 hours, strong TIP3;1-YFP signal was detected in seedlings subjected to 30μM DEX (figure 5.10 A-B). Fluorescence of seedlings from these plates was significantly brighter than those exposed to 1μM DEX, indicating that induction of TIP3;1-YFP expression is responsive to DEX concentration. From this point onwards, a 30μM DEX concentration was used.

Figure 5.9: TIP3;1-YFP expression is induced using a hybrid transcription factor 'GVG' as activated by Dexamethasone.
To induce TIP3;1-YFP expression, the translational fusion was cloned into the pDEX Gateway vector (Jens Steinbrenner and Jim Beynon, University of Warwick). This vector is based on the pTA7001 binary vector as outlined in Aoyama and Chua 1997. The 'GVG' hybrid transcription factor, comprised of the DNA-binding domain of the yeast transcription factor GAL4, transactivating domain of the herpes viral protein VP16 and HBD of the rat glucocorticoid receptor (GR), is constitutively expressed. In the presence of dexamethasone (DEX), GVG can enter the nucleus and activate expression of TIP3;1-YFP by binding to GAL4 UAS fused to a small region of the CaMV 35S promoter (TATA). *Adapted from Aoyama and Chua 1997.*

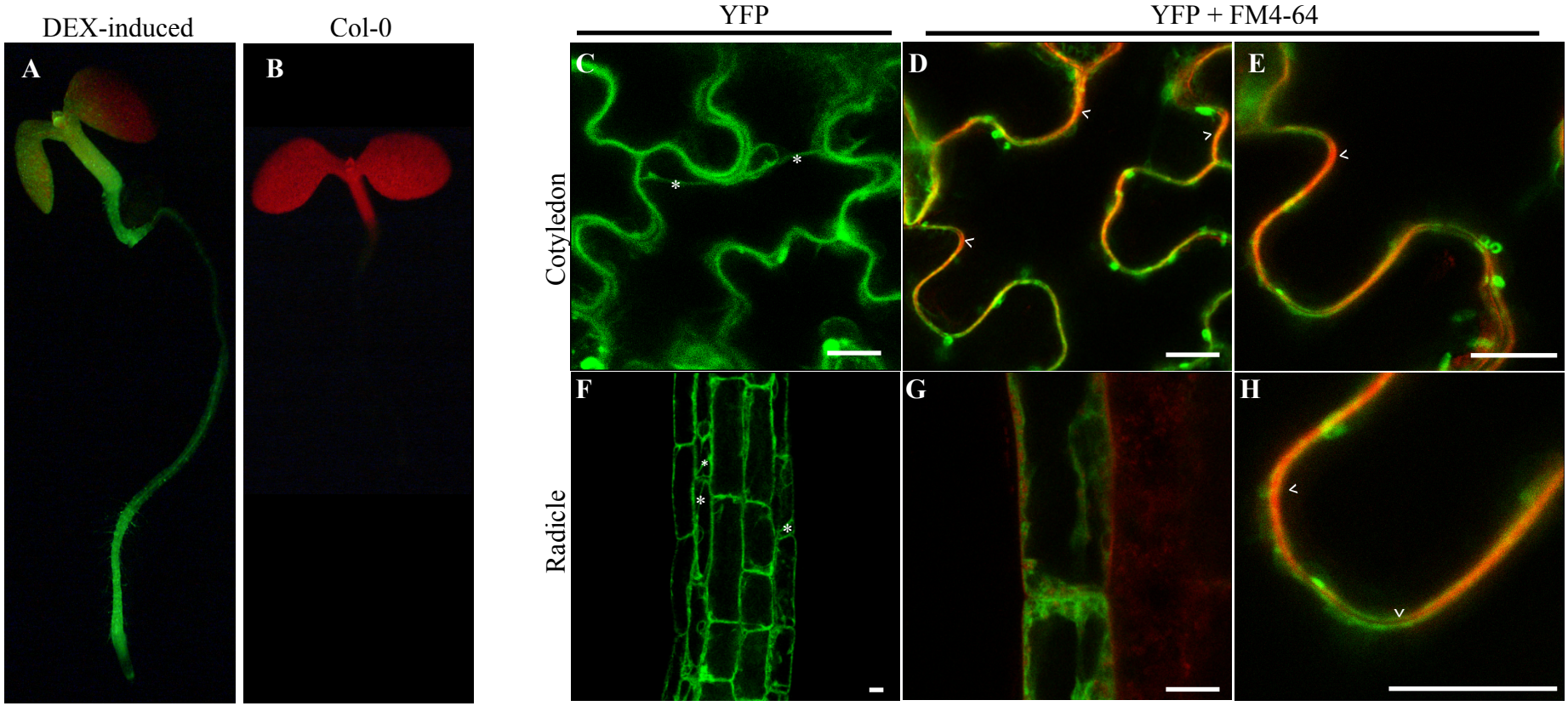

Figure 5.10: TIP3;1-YFP expressed under dexamethasone-inducible promoter localises to the ER and tonoplast in 7 day old seedlings.
5 day old seedlings germinated and grown on ½ MS 0.8% agar plates were transferred to plates supplemented with 30µM dexamethasone (DEX) for 24 hours. (**A**) After 24 hours of exposure to DEX, TIP3;1-YFP was clearly visible using a stereomicroscope in comparison to (**B**) wild type. (**C-H**) Confocal microscopy confirmed the localisation of TIP3;1-YFP to the tonoplast, as indicated by transvacuolar strands (*) and (**G**) ER but not (**D-E, G-H**) the PM as there is no colocalisation with FM4-64 styryl dye, as shown with arrows. Green is TIP3;1-FP and Red is autofluorescence in (**A-B**) and FM4-64 PM dye in (**D-H**). Scale bars = 10µm

After two days of DEX exposure, seedlings were imaged by confocal microscopy to study TIP3;1-YFP cellular localisation. TIP3;1-YFP was visualised at the tonoplast in both root and cotyledons, as indicated by the presence of transvacuolar strands (figure 5.10 C and F), transvacuolar strands highlighted with asterisks). These transvacuolar strands could be confirmed in future experiments by using GFP-fABD2, a marker line for actin. In this line, GFP is fused to the sequence for ABD2 (actin binding domain 2) of the Arabidopsis fimbrin AtFIM1, which binds to actin filament bundles (Sheahan *et al.* 2004). Actin forms part of the structure of transvacuolar strands. The styryl PM dye FM4-64 was used to delineate the plasma membrane (figure 5.10 D-E, F-H, with arrows) from the tonoplast. The lack of consistent colocalisation at the cell perimeter confirms that TIP3;1-YFP is localised only to the tonoplast in these induced seedlings. Orange patches (figure 5.10D) can be explained by the fact that FM4-64 is endocytosed from the PM and can subsequently be incorporated into other organelle membranes, including the tonoplast. These observations match our previous observation that dual localisation of TIP3 to PM and tonoplast occurs only in maturing and germinating embryos.

Once the DEX concentration and time course of induction were established, sterilised dry seed of the same transgenic line were plated directly onto ½ MS agar containing 30μM DEX. This would allow us to observe TIP3;1-YFP localisation at a developmental time point when dual localisation to the tonoplast and PM is expected. Initial observations indicated that seeds did not fluoresce until after radicle emergence from the seed coat, roughly 48 hours following imbibition. At this point, TIP3;1-YFP is localised solely within the endoplasmic reticulum (ER), just as the PSV are in transition to becoming LV (figure 5.11 A-D). Once LV are formed, and take up most of the cellular space, the tonoplast lies directly adjacent to the PM, making it very difficult to distinguish clearly between the two. In addition, post-germination, TIP3 is not targeted to the PM. Imaging beyond this developmental time point is therefore uninformative, yet necessary in order to determine where TIP3;1-YFP localises following exit from the ER.

In order to decrease the time taken for TIP3;1-YFP induction to occur, and maximise the window for observation of targeting, dry embryos were removed from their seed coat and placed on ½ MS agar 30μM DEX to imbibe and induce. Less than 24 hours after plating, TIP3;1-YFP was expressed in embryos and localised to the ER (figure 5.11 E-F). This ER localisation was maintained for almost 72 hours following this observation, at which point PSV transition to LV and tissues develop into that of a germinated seedling.

Throughout the window of observation for these different time points, embryos were continually incubated on ½ MS agar 30μM DEX. In some places large aggregates of fluorescent protein were apparent, which could be an indication of stress. In addition, it was thought that TIP3;1-YFP may be retained in the ER as a result of continual exposure to DEX and therefore stress caused by excessive expression.

To test if retention of TIP3;1-YFP in the ER was a result of stress by prolonged exposure to DEX, embryos extracted from seed coats and plated directly onto ½ MS agar 30μM DEX were transferred to ½ MS agar-only plates 24 hours later, which is when TIP3;1-YFP expression has been induced. TIP3;1-YFP fluorescence was still clearly visible by stereomicroscopy 24 hours after transfer, however TIP3;1-YFP was still observed only at the ER (figure 5.11 G-H). 45 hours after transfer, fluorescence had substantially decreased and a low signal of YFP was observed to be maintained at the ER. Further to this observation, a small number of aggregates were once again observed; the Frigerio group has observed similar structures to these in numerous live embryo or seedling samples subjected to extended observation time by confocal microscopy. Whilst the identity of these structures is unknown, these structures may be an artefact of prolonged exposure to the excitation laser during imaging. It can therefore be concluded that stress to the embryo from prolonged exposure to DEX, is not responsible for the retention of TIP3;1-YFP in the ER.

In order to determine whether TIP3;1-YFP does eventually leave the ER, a time frame of at least 72 hours is required from the point of induction. To ensure PSV and PM are sufficiently spatially separated, it is necessary to image developing, rather than mature embryos found in the dry seed (Bowman and Mansfield 1993). Excising mature green embryos from their developing seed coat, and plating them on ½ MS agar 30μM DEX was found to induce expression of TIP3;1-YFP embryos within 24 hours. With this knowledge, embryos from even earlier developmental stages than the mature green embryo stage will be induced and observed. Figure 5.12 outlines which main stages of *Arabidopsis* embryo development have been used so far, and those that will be used in future experiments.

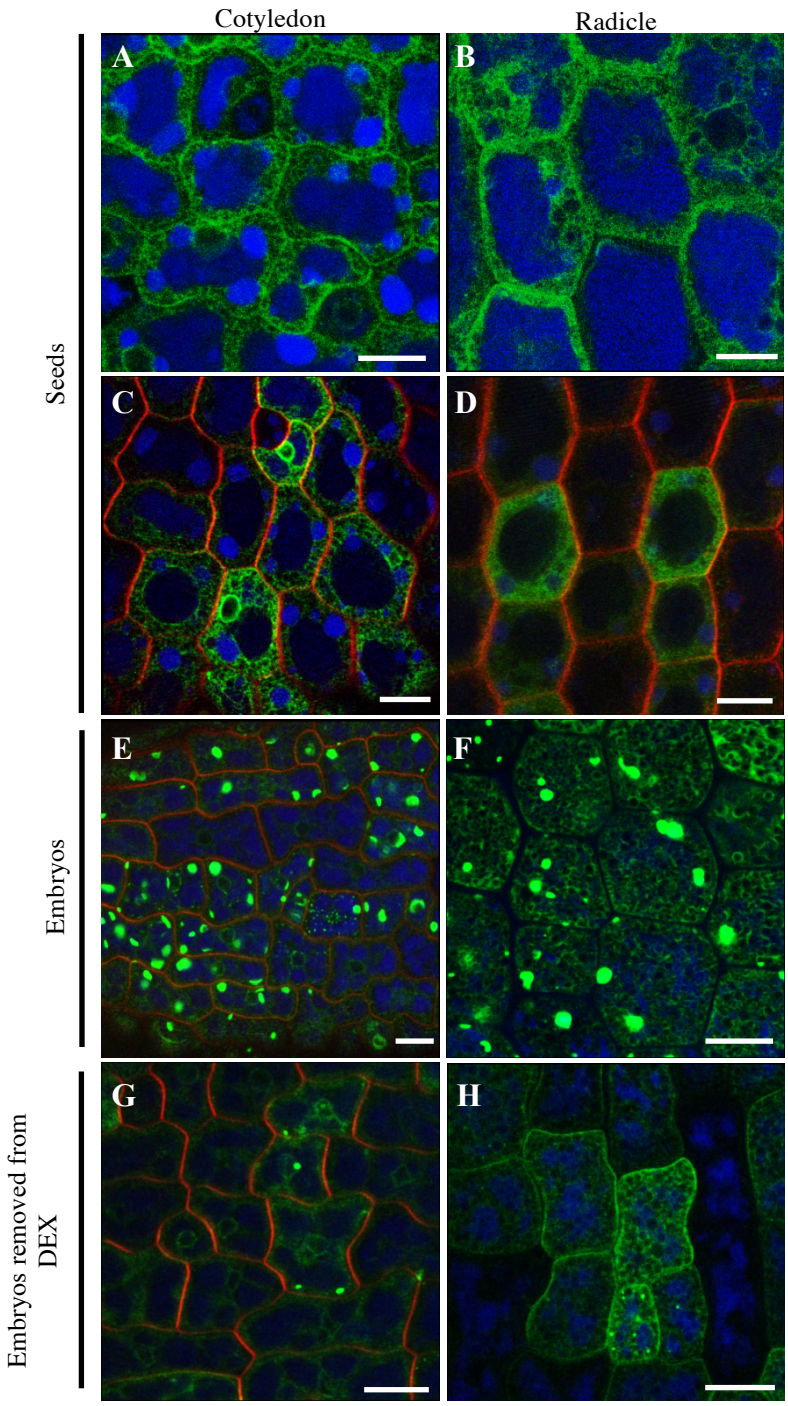

Figure 5.11: TIP3;1-YFP expressed under a dexamethasone inducible promoter localises to the ER in germinated seedlings and mature embryos.
(**A-D**) Dry seeds were plated on media supplemented with 30µM dexamethasone (DEX) and imbibed for 48 hours. Once seeds had germinated, TIP3;1-YFP was localised to ER. (**E-F**) Embryos extracted from seed coat after 1 hour imbibition were plated on media containing 30µM DEX. Between 21 and 70 hours after exposure to DEX, TIP3;1-YFP was localised to ER in embryos. (**G-H**) Embryos which were exposed to 30µM DEX for 20 hours, and subsequently transferred to media without DEX, expressed TIP3;1-YFP for a further 48hours where it was localised at the ER. Green is TIP3;1-YFP, blue is autofluorescence of PSVs and red is PM FM4-64 dye. Scale bars = 10µm

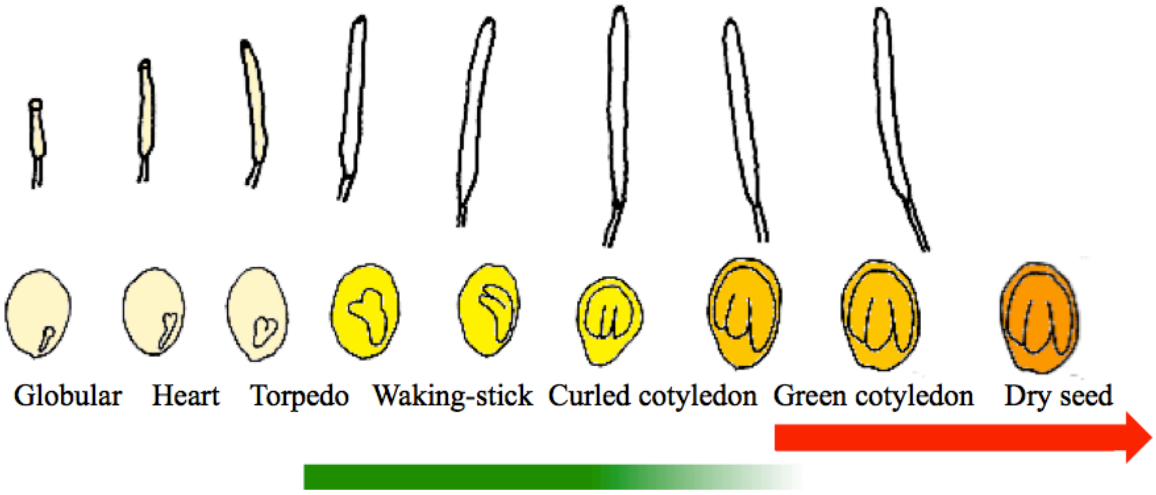

Figure 5.12 TIP3;1-YFP expression will need to be induced by DEX in early developmental stages of *Arabidopsis thaliana* embryos
Copied from eFP browser (Winter *et al.* 2007), the developmental stages of *A. thaliana* embryo development and their respective silique sizes. The red arrow indicates the earliest stages of embryo development which were used in these experiments. Since TIP3 is expressed from late torpedo stage, embryos from earlier developmental stages, indicated with the green bar, will be used in future experiments. This will enable imaging of the PSV for a longer period of time.

5.2.6 TIP3 sorting is insensitive to Brefeldin A treatment

Tonoplast proteins are known to be trafficked from the ER to their destination by either a Golgi dependent or a Golgi independent route (Pedrazzini *et al.* 2013). TIP3;1 and TIP1;1 have previously been used in part to demonstrate this differential targeting in a number of heterologous expression systems, however there is yet to be conclusive evidence for how both proteins are trafficked in their native state and tissues (Jiang and Rogers 1998, Oufattole *et al.* 2005, Rivera-Serrano *et al.* 2011, Bottanelli *et al.* 2007, Park *et al.* 2004).

Brefeldin A (BFA) binds to complexes formed by the ADP ribosylation factor (ARF) GTPase and its guanine nucleotide exchange factor (ARF-GEF). Nucleotide exchange by ARF-GEF is required to recruit the COPI vesicle coat, BFA binding prevents this and thus disrupts formation of vesicles responsible for retrograde traffic between the Golgi and ER (Nebenfuhr *et al.* 2002). The result of this disruption is typically fusion of Golgi and ER membranes to form BFA 'compartments' (Robinson *et al.* 2008). However *Arabidopsis* roots uniquely possess the ARF-GEF GNOM-LIKE1 (GNL1), which is resistant to BFA treatment (Richter *et al.* 2007). Whilst hypocotyl cells are susceptible to BFA treatment (Rivera-Serrano *et al.* 2012), embryos, the native tissue to study TIP3 trafficking, are not. Therefore *gnl1* mutant lines of *Arabidopsis thaliana* (Richter *et al.* 2007, Teh and Moore 2007) were transformed with fluorescent tag-gene fusion constructs in order to visualise the effects of BFA treatment on protein trafficking. Employing this pharmacological tool offered the opportunity to study TIP3 and TIP1;1 trafficking in its native tissues. BFA sensitive tissues would result in a breakdown of Golgi under treatment, and so proteins which would normally be targeted via this organelle would become retained in the ER (Robinson *et al.* 2008).

It has already been documented that the subunit of H^+-ATPase, VHA-a1 is targeted to the Trans-Golgi Network (TGN), and has been used in previous studies as a positive control for BFA treatment (Dettmer *et al.* 2006, Viotti *et al.* 2013). Therefore *gnl1* YFP-VHA-a1 was used as a control in these experiments. In order to study TIP3 trafficking to both the tonoplast and PM, YFP-TIP3;1 and the truncated YFP-TIP3;2ΔC fusions expressed under their native promoters, were transformed into *gnl1* background lines. In addition, YFP-TIP1;1 was also studied in seedlings.

Mature embryos from dry *gnl1* seeds expressing YFP-VHA-a1, YFP-TIP3;1 or YFP-TIP3;2ΔC were extracted from their seed coats and incubated in DMSO or BFA for 3 hours at room temperature. As shown in figure 5.13, targeting and localisation of YFP-TIP3;1 (E-H) and YFP-TIP3;2ΔC (I-L) were unaffected by BFA treatment whereas the control VHA-a1 (A-D) was retained within the ER in both radicle and cotyledon cells. Therefore TIP3 traffics to the tonoplast and PM through the Golgi independent pathway. Localisation of TIP3 with or without their C terminus was equally unaffected, indicating that this motif does not play an obvious role in determining their trafficking route.

To study the TIP1;1 trafficking route at its correct the developmental stage, 2-week old seedlings expressing YFP-TIP1;1 and YFP-VHA-a1 were incubated in DMSO or BFA for 3 hours at room temperature. As demonstrated in figure 5.13 panels M-P, both YFP-VHA-a1 and YFP-TIP1;1 were retained in the ER after BFA treatment. Therefore TIP1;1 is trafficked to the tonoplast via the Golgi. These results are in accordance with Rivera-Serrano *et al.* (2012).

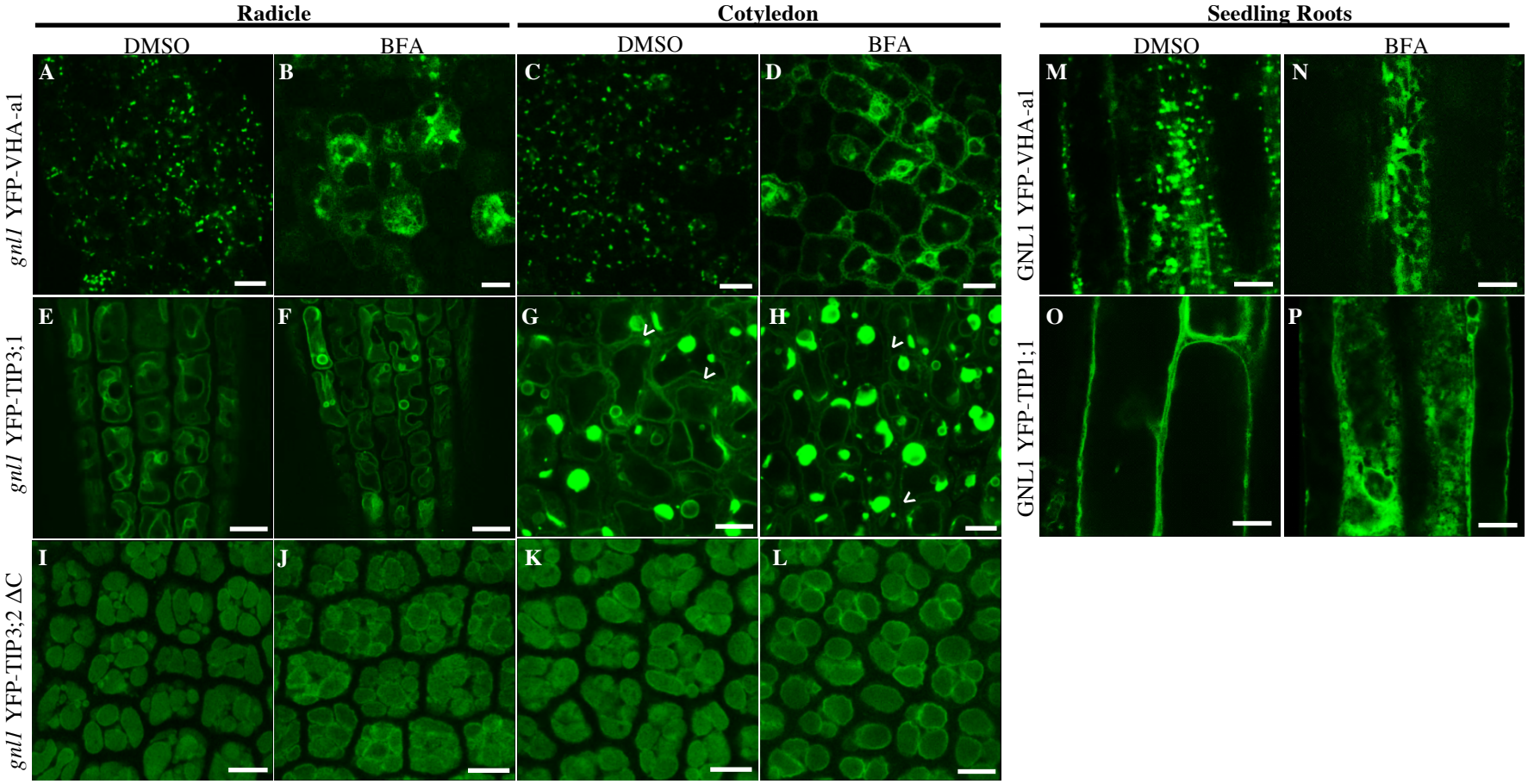

Figure 5.13: TIP3 traffics to the tonoplast and plasma membrane independently of the Golgi but TIP1;1 traffics to the tonoplast via the Golgi. (**A-D**, **M-N**) VHA-a1, (**E-H**) TIP3;1, (**I-L**) TIP3;2ΔC and (**O-P**) TIP1;1 translationally fused to YFP were expressed in *gnl1* background *Arabidopsis* Mature embryos or 2 week old seedlings were exposed to DMSO or Brefeldin A (BFA) for 3 hours. (**A**,**C**,**M**) VHA-a1 traffics to the TGN (punctate structures) via the Golgi; as disruption with BFA leads to ER retention (**B**,**D**,**N**). (**E**,**G**) TIP3;1 trafficking to the tonoplast and PM (white arrows) is not disrupted with BFA treatment (**F**,**H**) and is therefore Golgi independent. (**I**,**K**) TIP3;2ΔC traffics to the tonoplast independently of the Golgi (**J**,**L**), therefore the C terminus is not responsible for the Golgi-independent route of TIP3. (**O**) TIP1;1 is trafficked to the tonoplast via the Golgi (**P**) Scale Bar = 10μm

5.5 Discussion

TIP3 locates to tonoplast and plasma membrane independently of fluorescent protein tag position. XFP therefore does not appear to mask a sorting signal causing mislocalisation. Given the same dual membrane localisation of TIP3;2-YFP in *tip3;2* background, it is also possible to rule out that dual localisation is an overexpression artefact. In light of this, fluorescent protein markers were used throughout this chapter, with confidence that no artefacts would be caused.

The sequence homology between TIP3;1 and TIP3;2 is 85%. They localise to the same membranes at the same developmental time points, and they are thought to be redundant in function. It has therefore been assumed in this chapter that TIP3;1 and TIP3;2 are targeted to the tonoplast and PM in the same way, and so these isoforms have been used interchangeably in accordance with the convenience of constructs already available.

Alignment of the different TIP isoforms sequences reveals that TIP3;1 and TIP3;2 harbour an extra sequence at their C terminus. Deletion of the final 23 amino acids at the C terminus of TIP3;2 abolishes plasma membrane localization. TIP3-YFP fusions are much easier to visualise at the tonoplast than at the PM, however even when tonoplast signal is saturated from using a combination of high laser power, line average and gain, the PM is unable to be visualised. The C terminus of TIP3 contains a tyrosine based sorting motif (YMVI in TIP3;1 and YMII in TIP3;2), which is a known signal for recruitment into clathrin-coated vesicles for protein transport (Dhonukshe *et al.* 2007). Clathrin coated vesicles are involved in membrane protein endocytosis (Bonifacino and Traub 2003) and could in part explain a mechanism by which TIP3 is first targeted to the PM, before being endocytosed and vectorially targeted to the tonoplast. However, TIP3;2ΔC maintains tonoplast localisation, showing PM targeting of TIP3 is not a prerequisite for tonoplast localisation. Moreover, mutation of the TIP3;2 motif to AMAA had no affect on PM localisation of YFP-TIP3;2 (Gattolin unpublished). To conclude TIP3 is not endocytosed and targeted to the tonoplast after reaching the PM first, an endocytosis inhibitor such as TE1 could be used (Paudyal *et al.* 2014). If TIP3 is dually targeted as we predict, TE1 treatment of a TIP3;1-YFP expressing line would show no effect on localisation. However, in the unlikely case that TIP3 is sequentially targeted (first to PM, then tonoplast), tonoplast localisation of newly synthesised TIP3;1-YFP would be abolished.

In addition to the tyrosine based sorting motif, the TIP3 C terminus contains the sequence PTEPPTHH, aligning with *Phaseolus vulgaris* PIEPPPHH sequence. This sequence was believed to be responsible for trafficking to PSV compartments as TIP3;1 missing this motif was thought to locate to a different vacuolar destination within the same cell (Oufattole *et al.* 2005). However this conclusion was made at a time when the multi-vacuole hypothesis, which states more than one type of vacuole can exist in a single cell, was still widely accepted. Confocal immunofluorescence was initially used to show TIP3;1 and TIP1;1 as markers labelling the tonoplasts of the PSV and LV respectively, within the same meristematic cells of pea and barley seedling roots (Paris *et al.* 2003). However using fluorescent protein fusions; a more specific and therefore reliable method than immunolabelling, it has since been shown that these two TIP isoforms (along with TIP4;1), all localise to the same tonoplast of a single vacuolar compartment in *Arabidopsis* at different developmental stages, (Hunter *et al.* 2007). The multi-vacuole hypothesis therefore appears to be the exception rather than the rule, and conclusions made using the PIEPPPHH sequence in tobacco suspension culture cell protoplasts would not stand true in light of this, alongside our findings that TIP3;2 ΔC can still reach the PSV tonoplast.

The question as to which part of the C terminal sequence of TIP3 is responsible for PM localisation remains unanswered, however we do know that whatever it is, is not sufficient for this targeting. Fusing the final 23 amino acids of the TIP3 C terminus to the C terminus of YFP-TIP1;1 results in tonoplast-only localisation of the fusion protein. Thus, the C terminus is necessary but not sufficient to target TIP to the PM (Gattolin and Frigerio, unpublished data). TIP3;1-YFP expression under control of the CaMV 35S promoter also results in tonoplast only localisation. This indicates that whatever the signal motif is, contained within this region of the sequence, must be recognised by the seed tissue sorting machinery. Moreover, the result is found not to depend on the use of the TIP3 promoter, as TIP4;1-YFP expression driven this way is also localised to the tonoplast only (Gattolin and Frigerio, unpublished data). There is therefore now a need to study in depth the C terminal sequence of TIP3 in its native tissues during seed maturation and germination.

Here, employment of photoconvertible proteins and photobleaching are shown to be unsuitable methods to study TIP3 targeting in mature *Arabidopsis* embryos (summarised in table 5.1). Due to such low fluorescence emissions of both Dendra2 and mEoSFP when translationally fused to the N terminus of TIP3;1, it was impossible to visualise the PM which typically has a signal over 10 times lower than that of the tonoplast. Given that

YFP-TIP3;1 emits a much brighter fluorescent signal, it is much easier to visualise the PM using this construct. Photobleaching a region of interest was thought to allow tracking of newly synthesised YFP-TIP3;1 during overnight imaging (summarised in table 5.1). The flaw with using this bright fluorophore was that a large amount of 405nm laser was necessary to achieve complete photobleaching of a very shallow Z section. Given that a similar technique, Fluorescence Recovery After Photobleaching (FRAP), has previously been used successfully to study MIP trafficking with GFP, a similar fluorescent tag to YFP (Luu *et al.* 2012, Takano *et al.* 2010), it was surprising that tissues became so damaged. However these studies did not require the use of embryos and it is already well documented that UV radiation and can induce production of reactive oxygen species (ROS) in plants (Bartosz 1997, Foyer at al 2006). In particular it has been found that longer exposure to a high intensity of laser can saturate scavenging and downregulating mechanisms which could otherwise allow cells to recover under mild photooxidative stress (Dixit and Cyr 2003). Due to the irreversible damage caused to *Arabidopsis* embryo cells in photobleaching, it was impossible to visualise newly synthesised YFP-TIP3;1. A future experiment could be to replace YFP with a fluorophore of less intense signal such as RFP, thus lower levels of 405nm laser would be necessary to completely photobleach samples and tissues may not become as damaged.

The DEX inducible system can be successfully used to control the onset of expression of TIP3;1-YFP, providing opportunity to study *ab initio* sorting of TIP3 (summarised in table 5.1). Conditions of induction were developed that gave rise to TIP3;1-YFP expression sufficient for the observation of localisation within cellular compartments. TIP3;1-YFP was successfully induced by DEX in five day old seedlings, embryos from germinating seeds, embryos from dry mature seeds and mature green embryos from developing seeds.

In seedlings, TIP3;1-YFP was localised to the tonoplast only, drawing parallel with TIP3;1-YFP expressed under the control of the 35S promoter. Given that these seedlings were imaged less than 48 hours after exposure to DEX, and that PM localisation of TIP3 in seeds persists for more than 48 hours, it is unlikely that TIP3;1-YFP was first targeted to the PM before being endocytosed and sent to the tonoplast in this short time frame. Therefore it was imperative to study the system within the tissues and time frame native to when TIP3 is expressed. Induced TIP3;1-YFP in embryos of germinating seeds, dry seeds and maturing seeds localised to the ER in all cases. Time course imaging of embryos from germinating and dry seeds showed TIP3;1-YFP was retained in the ER until up to 72 hours

post induction, which is consequently also the time point in *Arabidopsis* development that PSV fuse to become LV (Zheng *et al.* 2011). Once LV are formed, it is no longer relevant and it becomes technically challenging to continue imaging and distinguish between the tonoplast and PM.

As TIP3;1-YFP is retained in the ER for such a lengthy period of time, it was questioned whether DEX induction had stressed the ER resulting in retention of TIP3;1-YFP, or whether DEX itself was harmful to the tissues. Embryos removed from DEX post-induction, continued to show ER localisation of TIP3;1-YFP until the protein was degraded. Embryos incubated on DEX also develop into healthy seedlings, therefore DEX is unlikely to cause ER stress. However, it remains unknown the strength at which the DEX inducible system works at. Overexpression of YFP-TIP3;1 under the activation of its CaMV 35S promoter (TATA) may be so high that the ER, which may already be stressed by synthesis of significant amounts of storage proteins, becomes overloaded to the point at which YFP-TIP3;1 export is blocked. It has already been shown that overexpression of a recombinant protein (alpha antitrypsin, OsrAAT) in rice endosperm induces ER stress which is dependent on expression level (Zhang *et al.* 2013). It could be useful for future work to understand the capacity at which this DEX system induces protein expression in comparison to other promoters, and indeed whether decreasing concentration of DEX for induction can decrease the amount of TIP3;1-YFP expressed (Aoyama *et al.* 1997).

Inducing embryos from a developmental stage as early as the late torpedo stage, when TIP3 expression begins, will allow a longer time frame in which the targeting of TIP3;1-YFP can by imaged successfully (Gattolin *et al.* 2011). It would also be essential to consider inducing embryos whilst they are still in siliques as extracting embryos at these developmental stages would be technically challenging. Embryos are fragile and small at these early developmental stages, making manual extraction (described in methods section 2.6.1) extremely difficult. In addition, there are plans to put the pDEX:TIP3;1-YFP construct into transgenic plants expressing fluorescent organelle markers. These marker lines include RFP-HDEL, HDEL is an ER retention signal, ST-RFP, where ST (sialytransferase) is a Golgi-resident enzyme, TIP1;1-RFP expressed under the 35S promoter to label tonoplast of PSV and LV, and RFP-Rab F2b (also known as ARA7), a Rab5 family member localising to the MVB. This will enable more precise mapping of TIP3 trafficking from when it is co-translated in the ER, to its final plasma membrane and tonoplast locations.

The current model for how tonoplast proteins reach their destination suggests they can either be trafficked through the Golgi, TGN and MVB, in the same way that all soluble vacuole proteins have so far found to be trafficked; or Golgi independently, perhaps through PVC or directly to the tonoplast (Pedrazzini *et al.* 2013). It has previously been reported that only some TIP isoforms traffic via a BFA insensitive, Golgi independent pathway, namely TIP3;1 (Gomez *et al.* 1993, Rivera-Serrano *et al.* 2012). In addition, TIP3;1 targeting was shown to be COPII dependent by inhibition of COPII assembly, through overexpression of the exchange factor of the COPII GTPase Sec12p, leading to the disruption of TIP3;1 expression (Bottanelli *et al.* 2011). Furthermore, the addition of an N-linked glycosylation site to TIP3;1 results only in ER-type N-glycan moiety; reiterating that TIP3;1 does not traffic via the Golgi (Park *et al.* 2004). The PVC have however been shown to be part of the TIP3;1 trafficking route to the tonoplast through mutation of Rab GTPases (Botanelli *et al.* 2011). Asn-to-Ile substitution in the nucleotide binding domain of the tonoplast localized Rab7, TGN localized Rab11 and PVC localized Rab5 family members Ara6 and Rha1 were used to dissect routes vacuolar proteins take through the secretory pathway. Specifically the Rab7 mutant produced motile clusters independent from the Golgi (marked using YFP-ST) which were shown to colocalize with the PVC marker RFP-VSR2, TGN YFP-SYP61 and vacuole lumen Aleu-RFP. Moreover, the size of these structures is concurrent with what is expected from PVC (Bottanelli *et al.* 2011, Foresti *et al.* 2006).

All these experiments were performed with no consideration of the prospect of TIP3;1 being targeted to both the PM and the tonoplast. Most studies were also carried out at stages of development in which PM localisation of TIP3 does not occur. This therefore opened opportunity to image TIP3 trafficking in embryos of dry seeds, a developmentally relevant time point. TIP3;2 and TIP3;2ΔC trafficking to the tonoplast and PM was BFA insensitive, reconfirming reports in the literature and additionally demonstrating that the C terminus does not play a role in determining this route.

AP-3 belongs to the family of ADAPTER PROTEIN complexes, composites of clathrin coat of vesicles. AP-3 is specifically localised to the vesicles trafficking proteins to lysosome-related organelles in animals, and has been reported to be part of the Golgi-dependent trafficking pathway to the tonoplast in plants (Robinson 2004, Wolfenstetter *et al.* 2012). It is therefore a new priority to use an *ap-3* mutant line as background to image

the same constructs used in these experiments. This should confirm our findings of a Golgi-independent pathway for TIP3 trafficking, by having no affect on the localisation of YFP-TIP3;1 or YFP-TIP3;2ΔC.

Table 5.1: Summary of strategies used to decipher dual or sequential TIP3 targeting to plasma membrane and tonoplast		
Strategy	**Tissue Type**	**Result**
Photoconvertible Dendra2	Embryos of dry and imbibed seeds	Not visible at plasma membrane
Photoconvertible EosFP	Embryos of dry and imbibed seeds	Not visible at plasma membrane, insufficient photoconversion
Photobleaching of TIP3;1-YFP embryos	Embryos of imbibed seeds	No newly synthesised TIP3;1-YFP 0-24hours after photobleaching, YFP intensity decreases due to prolonged laser exposure overnight
Dexamethasone-inducible TIP3;1-YFP expression	Seedlings	TIP3;1-YFP reached tonoplast only less than 24 hours after exposure of tissues to dexamethasone
	Dry Seeds	TIP3;1-YFP was only expressed once seed had germinated and radicle exposed to dexamethasone
	Embryos from 1 hour imbibed seeds	21-70 hours after DEX exposure, TIP3;1-YFP was retained in ER (after this point, LV is formed and TIP3;1-YFP no longer locates at PM)
	Embryos from 1 hour imbibed seeds	Embryos exposed to DEX for 20hours, retained TIP3;1-YFP in ER for further 48 hours (after this point, LV is formed and TIP3;1-YFP no longer locates at PM)
	Green cotyledon stage embryos from mature green seeds (from green siliques)	Embryos exposed to DEX for 20hours, retained TIP3;1-YFP in ER for further 48 hours (after this point, LV is formed and TIP3;1-YFP no longer locates at PM)

Chapter 6: Discussion

6.1 Expression of aquaporin isoforms at atypical developmental time points can confer drought tolerance in *Arabidopsis thaliana* germination and seedling growth

Aquaporins can have a large influence on cell water dynamics within the plant, helping to regulate processes such as guard cell movement, responses to drought, and cellular turgor and volume (Maurel *et al.* 2001, Li *et al.* 2014). As TIP3 isoforms are the only aquaporins found in the maturing and germinating seed and dually locate to the PM and tonoplast, a role for these proteins in germination has been postulated (Vander Willigen *et al.* 2006, Gattolin *et al.* 2011, Novikova *et al.* 2014). To assess the importance of TIP3 in germination and seedling establishment, *Arabidopsis thaliana* lines overexpressing YFP-tagged TIP3;1, TIP3;2, TIP3;2ΔC, TIP1;1 and PIP1;2 were assayed for rates of germination and seedling growth at these developmental time points. In addition, following reports of MIP overexpression conferring drought tolerance (Sade *et al.* 2009, Liu *et al.* 2007, Zhou *et al.* 2012, Peng *et al.* 2007), these assays were performed under conditions of water stress mimicking drought.

It has previously been proposed that heterologous expression of aquaporins does not support stress tolerance (Li *et al.* 2014). In particular, AtPIP1;2 expressed in tobacco resulted in wilting sooner than wild-type and expression of GsTIP2;1 in Arabidopsis led to a reduction in germination and survival, in water stress conditions (Aharon *et al.* 2003, Wang *et al.* 2011). Here, we show that aquaporins from the same species can be expressed at atypical developmental time points to confer drought tolerance.

Seeds of 35S:TIP1;1-YFP and homozygous 35S:TIP3;1-YFP seeds and seedlings exhibit reduced drought tolerance, agreeing with Wang *et al.* (2011) and Aharon *et al.* (2003) who also employed the CaMV 35S promoter for constitutive expression. In contrast, lines overexpressing YFP-PIP1;2 and YFP-TIP3;2 under control of the TIP3;2 promoter, and seeds and seedlings heterozygous for 35S:TIP3;1-YFP exhibit enhanced drought tolerance. Therefore it can be proposed that there is an aquaporin dose dependency in the acquisition of drought tolerance, challenging the mixed opinions in the literature by considering the strength of promoters used. Seedling establishment was only affected by 35S overexpression due to the short window in which the TIP3;2 promoter is active (Gattolin *et al.* 2011, Vander Willigen *et al.* 2006, Schmid *et al.* 2005), whereas germination is affected by expression under both promoters. Aside from both promoters being active during germination, this could be due the necessity of water to drive and regulate this developmental stage (Bewley *et al.* 2013).

6.2 Expression of aquaporin isoforms localising to the plasma membrane in *Arabidopsis thaliana* embryos is beneficial for germination in drought conditions

During germination, the lines promoting expression of aquaporins localising to the PM and dual PM-tonoplast localisation exhibited drought tolerance, whereas those locating to tonoplast only did not. The importance of PM-localised PIPs in drought tolerance has previously been reported by using antisense inhibition of NtPIP1 in tobacco and AtPIP1 and AtPIP2 in Arabidopsis. These lines exhibited enhanced sensitivity to drought, and reduced recovery respectively (Siefritz *et al.* 2002, Martre *et al.* 2002). Aquaporins at the PM are beneficial to water uptake in the germinating seed, alluding to a fundamental role for native TIP3 at the PM of wild-type *Arabidopsis thaliana*. If PM localisation of aquaporins is increasing drought tolerance by increasing water uptake in the imbibing seeds, seed weight measurements prior to germination could reveal this difference, as described in Liu *et al.* (2007) who performed this experiment on rice embryos. Once the *tip3;1tip3;2* seeds are available, imbibed seed weight of this line will be compared to wild-type and MIP overexpressing lines (namely overexpressing YFP-tagged TIP3;1, TIP3;2, TIP3;2ΔC, TIP1;1 and PIP1;2 lines discussed in chapter 3), to identify any differences in water uptake prior to germination. For our hypothesis of plasma membrane localisation of MIP improving water uptake to be true, seeds overexpressing TIP3;1, TIP3;2 and PIP1;2 would all have a higher seed weight than other lines.

These results could now be transferred to crop species by performing the same assays on transgenic plants overexpressing the respective native isoforms. A good starting place would be within the *Brassica oleracea* species, given their 85% genome homology (Arabidopsis Genome Initiative 2000). *Brassica oleracea* (broccoli) has 11 PIP homologous to those found in *Arabidopsis thaliana* (which contains 13 PIP isoforms in total); whilst *Brassica rapa ssp. pekinensis* (Chinese cabbage) contains 6 Arabidopsis MIP genes with three corresponding orthologues, 15 with two orthologs, and 12 with a single ortholog (Tao *et al.* 2014). However, AtPIP2;8 and AtNIP1;1 had no syntenic orthologs in Chinese cabbage (Casado-Vela *et al.* 2010, Tao *et al.* 2014).

6.3 Generating a *tip3;1tip3;2* knockout line may help elucidate the physiological importance of TIP3 in germination

It has already been shown that blocking TIP3 activity with mercury decreases initiation of phase III of water uptake within the seed, causing a delay in germination time (Vander Willigen *et al.* 2006, Novikova *et al.* 2014). But the specificity and blocking ability of

mercury on aquaporins has recently been questioned (Li *et al.* 2014, Chaumont 2014, Maurel 2009). Therefore a knockdown or knockout line of TIP3 would enable precise identification of the roles these isoforms play in germination.

A knockdown strategy was attempted using the GATEWAY™ pFAST-RO3 silencing vector, with final TIP3 protein levels being lower than wild-type. However significant protein amounts remained, making phenotypic characterisation futile. Instead, efforts are now focussed on creating a double *tip3;1tip3;2* knockout line from single knockouts available from the Nottingham Arabidopsis Stock Centre (NASC). Up until very recently, the TDNA insertion line for TIP3;1 was not available and so this has only become a recent option. As discussed in section 1.5.1, blocking TIP3 with mercury has been shown to slow germination but not inhibit it, suggesting the important but not critical role for these aquaporins in this developmental stage (Vander Willigen et al. 2006, Veselova et al. 2003, Novikova et al. 2014). Based on this literature, I predict that *tip3;1tip3;2* seeds will exhibit a decrease in germination speed, but not complete inhibition. There is the possibility that removal of TIP3 could influence seed maturation, since these are the only aquaporins expressed at this time. However, T1 crosses have been made and are currently being brought to seed, therefore we do already know that the double TIP3 knockout is not lethal.

6.4 Overexpression of OLE1 alters oil body and PSV organisation

Overexpression of OLE1-tagRFP under the pFAST-RO3 vector alters both oil body size and PSV organisation in embryos. Oil body size is already known to be affected by both reduced expression and fluorescently tagged overexpression of OLE1 (Siloto *et al.* 2006, Shimada *et al.* 2010). Similarly, *ole1* knockdown lines exhibit irregular PSV shape, concurrent with our findings, and suggesting a link between oil bodies and vacuoles (Siloto *et al.* 2006). Interactions between oil bodies and vacuoles have previously been suggested based on the close and regular proximities of their membranes (Poxleitner *et al.* 2006, Naested *et al.* 2000). This raises the question of compatibility of using this vector to study vacuolar proteins, particularly as we found changes in TIP3 expression levels, hypothesised as an attempt to rescue deformed PSV shape. Despite these cellular changes, germination and growth are reported to be unaffected, although this was not rigorously tested (Shimada *et al.* 2010). Future work could therefore include testing seeds of lines expressing this vector using the same germination assay described in this thesis.

6.5 Homozygous 35S:TIP3;1-YFP seedlings present morphological alterations

In addition to the changes in cell morphology witnessed by overexpression of OLE1-tagRFP, changes were observed in homozygous seedlings overexpressing TIP3;1-YFP. Cells of 4 D.A.G seedlings were found to be significantly more rounded, with a higher degree of circularity and area:perimeter ratio, quantitatively describing the loss of curvature and digit prominence observed in these epidermal pavement cells. The observation that these seedlings struggle to develop beyond the two-cotyledon stage (data not shown) has led to two possible explanations; increased TIP3;1-YFP levels could lead to unconstrained water uptake, which in turn leads to cell waterlogging, therefore restricting the seedling from developing past this early stage of seedling establishment. Secondly, in an attempt to increase growth and establishment, cell wall elasticity may become relaxed to accommodate cell expansion caused by water uptake, which in turn leads to loss of cell shape (Schopfer *et al.* 2006). A confocal imaging time course from germination until mature plant stages of both leaves and roots from heterozygous and homozygous 35S:TIP3;1-YFP seeds could reveal the extent to which expression affects cell integrity and development. In addition, measuring Relative Water Content (RWC, %) and root and leaf hydraulic conductance between seedlings and plants of the different genetic backgrounds could reveal differences in water uptake (Bouchabke *et al.* 2008, Martinez-Ballesta *et al.* 2011).

6.6 DEX inducible expression of TIP3 in maturing seeds may help understand dual TIP3 sorting

Plasma membrane sorting of TIP3 is not a prerequisite for tonoplast localisation as TIP3;2ΔC successfully locates to the tonoplast only. On this basis, it unlikely that TIP3 targets first to the PM and then to the tonoplast, pointing towards a mechanism of dual targeting. It should now be possible to explore this using the DEX inducible TIP3;1-YFP system established here, by applying it to developing embryos. The importance of using embryonic tissues arises from the observation that TIP3;1-YFP localises only to the tonoplast in seedlings, both in this DEX system and under control of the 35S promoter. In addition, TIP3 promoter-driven expression of other TIP isoforms does not lead to them reaching the PM. Thus for the observed dual targeting, the C-terminus of TIP3 must contain a motif specific to PM localisation in embryonic tissues, which is only recognised by seed-specific sorting machinery, and a tonoplast-specific motif elsewhere in the protein, sending TIP3 only to the tonoplast at all other developmental stages. However, this does fail to address the fundamental complexity of how a protein with the same primary

sequence is differentially sorted at the same point in time. In order to understand PM targeting of TIP3, it will be necessary to study the C terminal sequence in depth, during seed maturation.

It is also worth considering that TIP3;1 may require the presence of TIP3;2 in order to reach the PM, just as ZmPIP1 requires hetero-oligomerization with ZmPIP2 for this targeting (Zelazny *et al.* 2007). Some ZmPIP2 and AtPIP2;1 contain the diacidic motif DxE, which PIP1 do not, this motif is required for ER export (Zelazny *et al.* 2009, Sorieul *et al.* 2011). More recently, an LxxxA motif identified in the third transmembrane domain of ZmPIP2 has been found to be required for PM localisation (Chevalier *et al.* 2014). However, TIP3;1 and TIP3;2 sequences are 85% homologous, therefore it is unlikely that there is a prerequisite for hetero-oligomerization based on sequence and although the LxxxA motif is found in some TIP, it is not found in TIP3 (Chevalier *et al.* 2014). So far we have not expressed TIP3;1-YFP in *tip3;2* background embryos to identify if the fluorescent protein fusion reaches PM and tonoplast in the absence of TIP3;2. However, once the double knockout *tip3;1tip3;2* is established, individual expression of fluorescently tagged TIP3;1 or TIP3;2 in this background could determine whether hetero-oligomerization is a requirement for trafficking. If expression of one TIP3 isoforms leads only to tonoplast localisation, it will reveal a requirement for hetero-oligomerization between TIP3;1 and TIP3;2 for PM trafficking.

6.7 TIP3 trafficking in embryos appears to be Golgi independent

In this project, we confirmed that TIP3 traffics Golgi independently using BFA treatment in *gnl1* Arabidopsis lines. This is in consensus with the literature, however these results are the first of their kind to be attempted on TIP3 in embryos, and in the light of dual PM-tonoplast localisation (Gomez *et al.* 1993, Rivera-Serrano *et al.* 2012, Park *et al.* 2004, Bottanelli *et al.* 2011). Imaging these constructs in an *ap-3* background (AP-3 has been reported to be part of the Golgi-independent trafficking pathway to the tonoplast in plants (Robinson 2004, Wolfenstetter *et al.* 2012), will enable us to test whether that is the route TIP3 takes to the tonoplast, by identifying TIP3-XFP constructs retained within the ER. In the context of Bottanelli *et al.* (2011) who found that TIP3;1 is trafficked through the MVB, we are closer to establishing the exact route, which is in agreement with the model described by Pedrazzini *et al.* 2013, shown in Figure 1.4 (Chapter 1: Introduction).

6.8 Conclusion

The unique dual localisation of TIP3;1 and TIP3;2 to the plasma membrane and tonoplast suggests a function for these MIP which may be different from other TIP isoforms. As these are the only aquaporins expressed in the maturing and germinating seed, a role for TIP3 during these developmental time points has previously been hypothesised (Vander Willigen *et al.* 2006, Gattolin *et al.* 2011, Novikova *et al.* 2014). This thesis concludes that overexpression of plasma membrane localised MIP, including TIP3 and PIP1;2, during germination, results in increased germination rates in drought conditions. Therefore, it is possible that plasma membrane localisation of aquaporins is key to this developmental stage. Thus, TIP3 may play a key role in water uptake within the imbibing and germinating seed. In addition, constitutive overexpression of TIP3;1 confers drought tolerance in seedlings, until a certain amount of TIP3;1 expression is reached; at which the effect is detrimental. Generation of a *tip3;1tip3;2* knockout line will help to further elucidate the physiological importance of TIP3 in germination.

The work contained in this thesis confirms the Golgi-independent trafficking pathway for TIP3 isoforms. However, the order of targeting to plasma membrane and tonoplast locations is yet to be revealed. With the successful generation of a transgenic line inducing expression of TIP3-YFP using dexamethasone, it will now be possible to decipher this dual sorting from as it is targeted following ER exit.

This project promotes a better understanding of the roles which aquaporins can play at important *Arabidopsis thaliana* developmental stages. In future, this may be applicable to Brassica species, and could stimulate research in using MIP family members to engineer crop drought resistance.

References

Abell B.M., Holbrook L.A., Abenes M., Murphy D.J., Hills M.J. and Moloney M.M. (1997) Role of the proline knot motif in oleosin endoplasmic reticulum topology and oil body targeting. *Plant Cell* **9**, 1481–1493

Aharon R., Shahak Y., Wininger S., Bendov R., Kapulnik Y., Galili G. (2003) Overexpression of a plasma membrane aquaporin in transgenic Tobacco improves plant vigour under favourable conditions but not under drought or salt stress. *Plant Cell* **15**, 439-447

Ahmed S.U., Rojo E., Kovaleva V., Venkataraman S., Dombrowski J.E., Matsuoka K., Raikhel N.V. (2000) The plant vacuolar sorting receptor AtELP is involved in transport of NH(2)-terminal propeptide-containing vacuolar proteins in *Arabidopsis thaliana*. *J. Cell Biol.* **149**, 1335-1344

Ainsworth E.A., Rogers A. (2007) The response of photosynthesis and stomatal conductance to rising [CO2]: mechanisms and environmental interactions. *Plant Cell Environ.* **3**, 258-270

Alexandersson E., Fraysse L., Sjovall-Larsen S., Gustavsson S., Fellert M., Karlsson M., Johanson U., Kjellbom P. (2005) Whole gene family expression and drought stress regulation of aquaporins. *Plant Mol. Biol.* **59**, 469-484

Alleva K., Niemietz C.M., Sutka M., Maurel C., Parisi M., Tyerman S.D., Amodeo G. (2006) Plasma membrane of *Beta vulgaris* storage root shows high water channel activity regulated by cytoplasmic pH and a dual range of calcium concentrations. *J. Exp. Bot.* **57**, 609-621

Anderberg H.I., Danielson J.A., Johanson U. (2011) Algal MIPs, high diversity and conserved motifs. *BMC Evol. Biol.* **110**, 1-15

Anderberg H.I., Kjellbom P, Johanson U. (2012) Annotation of *Selaginella moellendorffii* major intrinsic proteins and the evolution of the protein family in terrestrial plants. *Front. Plant Sci.* **33**, 1-14

(The) Arabidopsis Genome Initiative (2000) Analysis of the genome sequence of the flowering plant *Arabidopsis thaliana. Nature* **408**, 796-815

Aroca R., Ferrante A., Vernieri P., Chrispeels M.J. (2006) Drought, abscisic acid and transpiration rate effects on the regulation of PIP aquaporin gene expression and abundance in *Phaseolus vulgaris* plants. *Ann. Bot.* **98**, 1301-1310

Azad A.K., Sato R., Ohtani K., Sawa Y., Ishikawa T., Shibata H. (2011) Functional characterization and hyperosmotic regulation of aquaporin in Synechocystis sp. PCC 6803. *Plant Sci.* **180**, 375-382

Azad A.K., Yoshikawa N., Ishikawa T., Sawa Y., Shibata H. (2012) Substitution of a single amino acid residue in the aromatic/arginine selectivity filter alters the transport profiles of tonoplast aquaporin homologs. *Biochim. Biophys. Acta* **1818**, 1–11

Bansal A., Sankararamakrishnan R. (2007) Homology modeling of major intrinsic proteins in rice, maize and Arabidopsis: comparative analysis of transmembrane helix

association and aromatic/arginine selectivity filters. *BMC Struct. Biol.* **27**, 1-17

Barrieu F., Marty-Mazars D., Thomas D., Chaumont F., Charbonnier M., Marty F. (1999) Desiccation and osmotic stress increase the abundance of mRNA of the tonoplast aquaporin BobTIP26-1 in cauliflower cells. *Planta* **206**, 77-86

Bartisz G. (1997) Oxidative stress in plants. *Acta Phys. Plant.* **19**, 47-64

Baskin C.C., Baskin J.M. (2014) Seeds: ecology, biogeography and evolution of dormancy and germination. 2nd Ed. USA: Elsevier Academic Press.

Beebo A., Thomas D., Der C., Sanchez L., Leborgne-Castel N., Marty F., Schoefs B., Bouhidel K. (2009) Life with and without AtTIP1;1, an Arabidopsis aquaporin preferentially localized in the opposing tonoplasts of adjacent vacuoles. *Plant Mol. Biol*. **70**, 193-209

Bernstein E., Caudy A.A., Hammond S.M., Hannon G.J. (2001) Role for a bidentate ribonuclease in the initiation step of RNA interference. *Nature* **409**, 363-366

Besserer A., Burnotte E., Bienert G.P., Chevalier A.S., Errachid A., Grefen C., Blatt M.R., Chaumont F. (2012) Selective regulation of maize plasma membrane aquaporin trafficking and activity by the SNARE SYP121. *Plant Cell* **24**, 3463-3481

Bewley J.D., Bradford K., Hilhorst H. (2013) Seeds: Physiology of development, germination and dormancy. 3rd Ed. USA: Springer

Biela A, Grote K, Otto B, Hoth S, Hedrich R, Kaldenhoff R. (1999) *The Nicotiana tabacum* plasma membrane aquaporin NtAQP1 is mercury-insensitive and permeable for glycerol. *Plant J.* **5**, 565-70

Bienert G.P., Cavez D., Besserer A., Berny M.C., Gilis D., Rooman M., Chaumont F. (2012) A conserved cysteine residue is involved in disulfide bond formation between plant plasma membrane aquaporin monomers. *Biochem J.* **445**, 101-111

Bienert G.P., Chaumont F. (2011) Plant aquaporins: roles in water homeostasis, nutrition, and signaling processes. In Transporters and Pumps in Plant Signaling, Signaling and Communication in Plants. 7th Ed. Edited by Venema K. and Geisler M. Germany: Spinger-Verlag

Bienert G.P., Chaumont F. (2013) Aquaporin-facilitated transmembrane diffusion of hydrogen peroxide. *Biochim Biophys Acta*. **1840**, 1596-1604

Bonifacino J.S., Traub L.M. (2003) Signals for sorting of transmembrane proteins to endosomes and lysosomes. *Annu. Rev. Biochem.* **72**, 395-447

Bottanelli F., Foresti O., Hanton S., Denecke J. (2011) Vacuolar transport in tobacco leaf epidermis cells involves a single route for soluble cargo and multiple routes for membrane cargo. *Plant Cell* **23**, 3007–3025

Bouchabke O., Chang F., Simon M., Voisin R., Pelletier G., Durand-Tardif M. (2008) Natural variation in *Arabidopsis thaliana* as a tool for highlighting differential drought responses. *PLoS One* **3**, e1705

Bowman J.L., Mansfield S.G. (1993) Embryogenesis: Introduction. In *Arabidopsis*: An Atlas of Morphology and Development. *1st Ed.* Edited by Bowman J.L. New York: Springer

Chaumont F., Barrieu F., Wojcik E., Chrispeels M.J., Jung R. (2001) Aquaporins constitute a large and highly divergent protein family in maize. *Plant Physiol.* **125**, 1206-1215

Chaumont F, Tyerman SD. (2014) Aquaporins: highly regulated channels controlling plant water relations. *Plant Physiol.* **164**, 1600-1618

Casado-Vela J., Muries B., Carvajal M., Iloro I., Elortza F., Martinez-Ballesta M.C. (2010) Analysis of root plasma membrane aquaporins from *Brassica oleracea*: post-translational modifications, de novo sequencing and detection of isoforms by High Resolution Mass Spectrometry. *J. Prot. Res.* **9**, 3479–3494

Chevalier A.S., Bienert G.P., Chuamont F. (2014) A new LxxxA motif in the Transmembrane Helix3 of maize aquaporins belonging to the Plasma membrane Intrinsic Protein PIP2 group is required for their trafficking to the plasma membrane. *Plant Physiol.* **166**, 125–138

Choi W.G., Roberts D.M. (2007) Arabidopsis NIP2;1, a major intrinsic protein transporter of lactic acid induced by anoxic stress. *J. Biol. Chem.* **282**, 24209-24218

Cochard H., Venisse J.S., Barigah T.S., Brunel N., Herbette S., Guilliot A., Tyree M.T., Sakr S. (2007) Putative role of aquaporins in variable hydraulic conductance of leaves in response to light. *Plant Physiol.* **143**,122–133

Czechowski T., Stitt M., Altmann T., Udvardi M.K., Scheible W.R. (2005) Genome-wide identification and testing of superior reference genes for transcript normalization in Arabidopsis. *Plant Physiol.* **139**, 5-17

Da Ines O., Graf W., Franck K.L., Albert A., Winkler J.B., Scherb H., Stichler W., Schaeffer A.R. (2010) Kinetic analyses of plant water relocation using deuterium as tracer - reduced water flux of Arabidopsis *pip2* aquaporin knockout mutants. *Plant Biol.* **12**, 129-139

Danielson J.A., Johanson U. (2008) Unexpected complexity of the aquaporin gene family in the moss *Physcomitrella patens*. *BMC Plant Biol.* **8**, 1-15

Dekkers B.J., Willems L., Bassel G.W., van Bolderen-Veldkamp R.P., Ligterink W., Hilhorst H.W., Bentsink L. (2012) Identification of reference genes for RT-qPCR expression analysis in Arabidopsis and tomato seeds. *Plant Cell Phys.* **53**, 28-37

Dettmer J., Hong-Hermesdorf A., Stierhof Y.D., Schumacher K. (2006) Vacuolar H+-ATPase activity is required for endocytic and secretory trafficking in Arabidopsis. *Plant Cell* **18**, 715-730

Dhonuske P., Aniento F., Hwang I., Robinson D.G., Mravec J., Stierhof Y.D., Friml J. (2007) Clathrin-mediated constitutive endocytosis of PIN Auxin efflux carriers in Arabidopsis. *Curr. Biol.* **17**, 520–527

Di Sansebastiano G.P., Paris N., Marc-Martin S., Neuhaus J.M. (1998) Specific accumulation of GFP in a non-acidic vacuolar compartment via a C-terminal propeptide-mediated sorting pathway. *Plant J.* **15**, 449-457

Dixit R., Cyr R. (2003) Cell damage and reactive oxygen species production induced by fluorescence microscopy: effects on mitosis and guidelines for non-invasive fluorescence microscopy. *Plant J.* **36**, 280-290

Dunkel M., Latz A., Schumacher K., Müller T., Becker D., Hedrich R. (2008) Targeting of vacuolar membrane localized members of the TPK channel family. *Mol. Plant.* **6**, 938-949

Dynowski M., Mayer M., Moran O., Ludewig U. (2008) Molecular determinants of ammonia and urea conductance in plant aquaporin homologs. *FEBS Lett.* **582**, 2458-2462

Engelke D. (2004) RNA Interference (RNAi): The Nuts & Bolts of RNAi Technology Chapter 1: Targeted Gene Silencing in Plants using RNA interference. *1st Ed*. USA. DNA Press.

Epimashko S., Meckel T., Fischer-Schliebs E., Lüttge U., Thiel G. (2004) Two functionally different vacuoles for static and dynamic purposes in one plant mesophyll leaf cell. *Plant J.* **37**, 294-300

Fagard M., Boutet S., Morel JB., Bellini C., Vaucheret H (2000) AGO1, QDE-2, and RDE-1 are related proteins required for post-transcriptional gene silencing in plants, quelling in fungi, and RNA interference in animals. *Proc Natl Acad Sci* **97**, 11650-11654

Feeney M., Frigerio L., Kohalmi S.E., Cui Y., Menassa R. (2012) Reprogramming cells to study vacuolar development. *Front Plant Sci.* **493**, 1-9

Fetter K., Van Wilder V., Moshelion M., Chaumont F. (2004) Interactions between plasma membrane aquaporins modulate their water channel activity. *Plant Cell* **16**, 215-228

Fire A., Xu S., Montgomery M.K., Kostas S.A., Driver S.E., Mello C.C. (1998) Potent and specific genetic interference by double-stranded RNA in *Caenorhabditis elegans*. *Nature* **391**, 806-811

Finch-Savage W.E., Leubner-Metzger G. (2006) Seed dormancy and the control of germination. *New Phytol.* **171**, 501-523

Finch-Savage W.E., Phelps K. (1993) Onion (*Allium cepa* L.) Seedling emergence patterns can be explained by the influence of soil temperature and water potential on seed germination. *J. Exp. Bot.* **44**, 407-414

Finch-Savage W.E., Rowse H.R., Dent K.C. (2005) Development of combined imbibition and hydrothermal threshold models to simulate maize (*Zea mays*) and chickpea (*Cicer arietinum*) seed germination in variable environments. *New Phytol.* **165**, 825-838

Foresti O., daSilva L.L.P., Denecke J. (2006) Overexpression of the Arabidopsis Syntaxin PEP12/SYP21 inhibits transport from the Prevacuolar Compartment to the Lytic Vacuole *in vivo*. *The Plant Cell* **18**, 2275–2293

Fortin M.G., Morrison N.A., Verma D.P.S. (1987) Nodulin-26, a peribacteroid membrane nodulin is expressed independently of the development of the peribacteroid compartment, *Nucleic Acids Res.* **15**, 813–82

Foyer C.H., Lelandais M., Kunert K. (1994) Photooxidative stress in plants. *Phys.Planta.* **92**, 696-717

Francavilla C., Rigbolt K.T.G., Emdal K.B., Carraro G., Vernet E., Bekker-Jensen D.B., Streicher W., Wikstrom M., Sunstrom M., Bellusci S., Cavallaro U., Blagoev B., Olsen J.V. (2013) Functional proteomics defines the molecular switch underlying FGF receptor trafficking and cellular outputs. *Mol. Cell* **51**, 707-722

Fraysse L.C., Wells B., McCann M.C., Kjellbom P. (2005) Specific plasma membrane aquaporins of the PIP1 subfamily are expressed in sieve elements and guard cells. *Biol Cell* **97**, 519-534

Frigerio L., de Virgilio M., Prada A., Faoro F., Vitale A. (1998) Sorting of phaseolin to the **vacuole** is saturable and requires a short C-terminal peptide. *Plant Cell.* **10**, 1031-1042

Frigerio L., Hinz, G., Robinson, D. G. (2008) Multiple vacuoles in plant cells: rule or exception? *Traffic* **9**, 1564-1570

Fujimoto M., Ueda T. (2012) Conserved and plant-unique mechanisms regulating plant post-Golgi traffic. *Front. Plant Sci.* **3**, 1-10

Gambetta G.A., Fei J., Rost T.L., Knipfer T., Matthews M.A., Shackel K.A., Walker M.A., McElrone A.J. (2013) Water uptake along the length of grapevine fine roots: developmental anatomy, tissue-specific aquaporin expression, and pathways of water transport. *Plant Physiol.* **163**, 1254-1265

Gattolin S., Sorieul M., Hunter P.R., Khonsari R.H., Frigerio L. (2009) *In vivo* imaging of the tonoplast intrinsic protein family in Arabidopsis roots. *BMC Plant Biol.* **133**, 1-9

Gattolin S., Sorieul M., Frigerio L. (2010) Tonoplast intrinsic proteins and vacuolar identity. *Biochem. Soc. Trans.* **38**, 769-773

Gattolin S., Sorieul M., Frigerio L. (2011) Mapping of Tonoplast Intrinsic Proteins in maturing and germinating Arabidopsis seeds reveals dual localization of embryonic TIPs to the tonoplast and plasma membrane. *Mol. Plant* **4**, 180–189

Gerbeau P., Amodeo G., Henzler T., Santoni V., Ripoche P., Maurel C. (2002) The water permeability of Arabidopsis plasma membrane is regulated by divalent cations and Ph. *Plant J.* **30**, 71–81

Gerbeau P., Güçlü J., Ripoche P., Maurel C. (1999) Aquaporin Nt-TIPa can account for the high permeability of tobacco cell vacuolar membrane to small neutral solutes. *Plant J.* **18**, 577-587

Gomez, L., and Chrispeels, M.J. (1993) Tonoplast and soluble vacuolar proteins are targeted by different mechanisms. *Plant Cell* **5**, 1113–1124

Guenther J.F., Chanmanivone N., Galetovic M.P., Wallace I.S., Cobb J.A., Roberts D.M. (2003) Phosphorylation of soybean nodulin 26 on serine 262 enhances water permeability and is regulated developmentally and by osmotic signals. *Plant Cell.* **15**, 981–991

Gurskaya NG, Verkhusha VV, Shcheglov AS, Staroverov DB, Chepurnykh TV, Fradkov AF, Lukyanov S, Lukyanov KA. (2006) Engineering of a monomeric green-to-red photoactivatable fluorescent protein induced by blue light. *Nature Biotech.* **24**, 461-465

Hachez C., Besserer A., Chevalier A.S., Chaumont F. (2013) Insights into plant plasma membrane aquaporin trafficking, *Trends Plant Sci.* **18,** 344–352

Hachez C., Heinen R.B., Draye X., Chaumont F. (2008) The expression pattern of plasma membrane aquaporins in maize leaf highlights their role in hydraulic regulation. *Plant Mol. Biol.* **68**, 337-353

Hachez C., Laloux T., Reinhardt H., Cavez D., Degand H., Grefen C., De Rycke R., Inzé D., Blatt M.R., Russinova E., Chaumont F. (2014) Arabidopsis SNAREs SYP61 and SYP121 coordinate the trafficking of plasma membrane aquaporin PIP2;7 to modulate the cell membrane water permeability. *Plant Cell.* **26**, 3132-3147

Hachez C., Moshelion M., Zelazny E., Cavez D., Chaumont F. (2006) Localization and quantification of plasma membrane aquaporin expression in maize primary root: a clue to understanding their role as cellular plumbers. *Plant Mol. Biol.* **62**, 305-323

Hachez C., Veselov D., Ye Q., Reinhardt H., Knipfer T., Fricke W., Chaumont F. (2012) Short-term control of maize cell and root water permeability through plasma membrane aquaporin isoforms. *Plant Cell Environ.* **35**, 185-198

Hamilton A.J., Baulcombe D.C. (1999) A species of small antisense RNA in posttranscriptional gene silencing in plants. *Science* **286**, 950-952

Hammond S.M., Bernstein E., Beach D., Hannon G.J. (2000) An RNA-directed nuclease mediates post-transcriptional gene silencing in *Drosophila* cells. *Nature* **404**, 293-296

Hanba Y.T., Shibasaka M., Hayashi Y., Hayakawa T., Kasamo K., Terashima I., Katsuhara M. (2004) Overexpression of the barley aquaporin HvPIP2;1 increases internal CO(2) conductance and CO(2) assimilation in the leaves of transgenic rice plants. *Plant Cell Physiol.* **45**, 521-529

Heckwolf M., Pater D., Hanson D.T., Kaldenhoff R. (2011) The *Arabidopsis thaliana* aquaporin AtPIP1; 2 is a physiologically relevant CO2 transport facilitator. *Plant J.* **67**, 795–804

Henzler T., Waterhouse R.N., Smyth A.J., Carvaial M., Cooke D.T., Schaeffner A.R., Steudle E., Clarkson D.T. (1999) Diurnal variations in hydraulic conductivity and root pressure can be correlated with the expression of putative aquaporins in the roots of *Lotus japonicas*. *Planta* **210**, 50-60

Hofte H., Chrispeels M.J. (1992) Protein sorting to the vacuolar membrane. *Plant Cell* **4**, 995-1004

Hoh B., Hinz G., Jeong B.-K., Robinson D.G. (1995) Protein storage vacuoles form de novo during pea cotyledon development. *J. Cell Sci.* **108**, 299–310

Holm L.M., Jahn T.P., Moller A.L., Schjoerring J.K., Ferri D., Klaerke D.A., Zeuthen T. (2005) NH3 and $NH4^+$ permeability in aquaporin-expressing *Xenopus* oocytes. *Pflugers Arch.* **450**, 415–428

Holtorf S., Apel K., Bohlmann H. (1995) Comparison of different constitutive and inducible promoters for the overexpression of transgenes in *Arabidopsis thaliana*. *Plant Mol. Bio.* **29**, 637-646

Huang A.H. (1992) Oil bodies and oleosins in seeds. *Plant Physiol. Plant Mol. Bio.* **43**, 177–200

Huang A.H. (1996) Oleosins and oil bodies in seeds and other organs. *Plant Physiol.* **110**, 1055-1061

Huang L., Franklin A.E., Hoffman N.E. (1993) Primary structure and characterization of an *Arabidopsis thaliana* calnexin-like protein. *J Biol Chem* **268**, 6560–6566

Hunter P.R., Craddock C.P., Di Benedetto S., Roberts L.M., Frigerio L. (2007) Fluorescent reporter proteins for the tonoplast and the vacuolar lumen identify a single vacuolar compartment in Arabidopsis cells. *Plant Physiol.* **145**, 1371–1382

Isayenkov S., Isner J.C., Maathuis F.J.M. (2011) Rice two-pore K^+ channels are expressed in different types of vacuoles. *Plant Cell.* **23**, 756–768

Ishikawa F., Suga S., Uemura T., Sato M.H., Maeshima M. (2005) Novel type aquaporin SIPs are mainly localized to the ER membrane and show cell-specific expression in *Arabidopsis thaliana*. *FEBS Lett* **579**, 5814-5820

Jang H.Y., Yang S.W., Carlson J.E., Ku Y.G., Ahn S.J. (2013) Two aquaporins of *Jatropha* are regulated differentially during drought stress and subsequent recovery. *J. Plant Physiol.* **170**, 1028–1038

Janvier K., Bonifacino J. (2005) Role of endocytic machinery in the sorting of lysosome-associated membrane proteins. *Mol. Biol. Cell* **16**, 4231-4242

Jauh G.Y., Fischer A.M., Grimes H.D., Ryan C.A., Rogers J.C. (1998) δ-Tonoplast intrinsic protein defines unique plant vacuole functions. *Proc. Natl. Acad. Sci* **95**, 12995–12999

Jauh G.Y., Phillips T.E., Rogers J.C., (1999) Tonoplast intrinsic protein isoforms as markers for vacuolar functions. *Plant Cell* **11**, 1867-1882

Javot H., Lauvergeat V., Santoni V., Martin-Laurent F., Güçlü J., Vinh J., Heyes J., Franck K.I., Schaeffner A.R., Bouchez D., Maurel C. (2003) Role of a single aquaporin isoform in root water uptake. *Plant Cell* **15**, 509-522.

Jiang L., Rogers J.C. (1998) Integral membrane protein sorting to vacuoles in plant cells: evidence for two pathways. *J. Cell Biol.* **143**, 1183-1199

Johanson U., Karlsson M., Johansson I., Gustavsson S., Sjovall S., Fraysse L., Weig A.R., Kjellbom P. (2001) The complete set of genes encoding major intrinsic proteins in Arabidopsis provides a framework for a new nomenclature for major intrinsic proteins in plants. *Plant Physiol.* **126**, 1358-1369

Johansson I., Karlsson M., Shukla V.K., Chrispeels M.J., Larsson C., Kjellbom P. (1998) Water transport activity of the plasma membrane aquaporin PM28A is regulated by phosphorylation. *Plant Cell* **10**, 451-459

Johnson K.D., Herman E.M., Chrispeels M.J. (1989) An abundant, highly conserved tonoplast protein in seeds. *Plant Physiol.* **91**, 1006-1013.

Kaldenhoff R., Kolling A., Meyers J., Karmann U., Ruppel G., Richter G. (1995) The blue light-responsive AthH2 gene of *Arabidopsis thaliana* is primarily expressed in expanding as well as in differentiating cells and encodes a putative channel protein of the plasmalemma. *Plant J.* **7**(1), 87-95

Kaldenhoff R., Ribas-Carbo M., Sans J.F., Lovisolo C., Heckwolf M., Uehlein N. (2008) Aquaporins and plant water balance. *Plant Cell Environ*. **5**, 658-66

Kammerloher W., Fischer U., Piechottka G.P., Schaffner A.R. (1994) Water channels in the plant plasma membrane cloned by immunoselection from a mammalian expression system. *Plant J.* **6**, 187-199

Karimi M., Inze D., Depicker A. (2002) GATEWAY™ vectors for Agrobacterium-mediated plant transformation. *Trends in Plant Science* **7**, 194-195

Katsuhara M., Koshio K., Shibasaka M., Hayashi Y., Hayakawa T., Kasamo K. (2003) Over-expression of a barley aquaporin increased the shoot/root ratio and raised salt sensitivity in transgenic rice plants. *Plant Cell Phys.* **44**, 1378–1383

Kim H.U., Hsieh K., Ratnayake C. and Huang A.H. (2002) A novel group of oleosins is present inside the pollen of Arabidopsis. *J. Biol. Chem.* **277**, 22677–22684

Lewis L. (2012) PhD Thesis: Investigating the influence of phytopathogenic effectors upon host transcription, University of Warwick.

Li G., Santoni V., Maurel C. (2014) Plant aquaporins: Roles in plant physiology. *Biochim. Biophys. Acta* **1840**, 1574-1582

Li G.W., Peng Y.H., Yu X., Zhang M.H., Cai W.M., Sun W.N.. Su W.A. (2007) Transport functions and expression analysis of vacuolar membrane aquaporins in response to various stresses in rice. *J. Plant Physiol.* **165**, 1879-1888

Lian H.-L. Yu X., Ye Q., Ding X.-S., Kitagawa Y., Kwak S.-S., Su W.-A., Tang Z.-C. (2004) The role of aquaporin RWC3 in drought avoidance in rice. *Plant Cell Physiol.* **45**, 481–489

Liu P.-P., Koizuka N., Homrichhausen T.M., Hewitt J.R., Martin R.C., Nonogaki H.

(2005) Large-scale screening of Arabidopsis enhancer-trap lines for seed germination-associated genes. *Plant J.* **41**, 936-944

Liu H.Y., Yu X., Cui D.Y., Sun M.H., Sun W.N., Tang Z.C., Kwak S.S., Su W.A. (2007) The role of water channel proteins and nitric oxide signalling in rice seed germination. *Cell Res.* **17**, 638-649

Lopez F., Bousser A., Sissoeff I., Gaspar M., Lachaise B., Hoarau J., Mahe A. (2003) Diurnal Regulation of Water Transport and Aquaporin Gene Expression in Maize Roots: Contribution of PIP2 Proteins. *Plant Cell Physiol.* **44**, 1384-1395

Lopez F., Bousser A., Sissoëff I., Hoarau J., Mahé A. (2003) Characterization in maize of ZmTIP2-3, a root-specific tonoplast intrinsic protein exhibiting aquaporin activity. *J Exp Bot.* **396**, 539-541

Ludevid D., Höfte H., Himelblau E., Chrispeels M.J. (1992) The expression pattern of the tonoplast intrinsic protein γ-TIP in *Arabidopsis thaliana* is correlated with cell enlargement. *Plant Physiol.* **100**, 1633–1639

Luu D.T., Martiniere A., Sorieul M., Runions J., Maurel C. (2012) Fluorescence recovery after photobleaching reveals high cycling dynamics of plasma membrane aquaporins in *Arabidopsis* roots under salt stress. *Plant J.* **69**, 894-905

Ma J.F., Tamai K., Yamaji N., Mitani N., Konishi S., Katsuhara M., Ishiguro M., Murata Y., Yano M. (2006) A silicon transporter in rice. *Nature* **440**, 688–691

Maeshima M., Ishikawa F. (2008) ER membrane aquaporins in plants. *Pflugers Arch.* **456**, 709-716

Maitrejean M., Vitale A. (2011) How are tonoplast proteins degraded? *Plant Signal Behav.* **6**, 1809-1812

Maitrejean M., Wudick M.M., Voelker C., Bhakti Prinsi B., Mueller-Roeber B., Czempinski K., Pedrazzini E., and Vitale A. (2011) Assembly and sorting of the Tonoplast Potassium Channel AtTPK1 and its turnover by internalization into the vacuole. *Plant Physiol.* **156**, 1783–1796

Mahdieh M., Mostajeran A. (2009) Abscisic acid regulates root hydraulic conductance via aquaporin expression modulation in *Nicotiana tabacum*. *J. Plant Physiol.* **166**, 1993-2003

Mansfield S. G., Briarty, L. G. (1992) Cotyledon cell development in *Arabidopsis thaliana* during reserve deposition. *Can. J. Bot.* **70**, 151-164.

Martinez-Ballesta M.C., Rodriguez-Hernandez M.C., Alcaraz-Lopez C., Mota-Cadenas C., Muries B., Carvajal M. (2011) Chapter 6. Plant Hydraulic Conductivity: The Aquaporins Contribution. In Hydraulic Conductivity – Issues, Determination and Applications 1st Ed. Edited by Elango L. InTech

Martinière A., Lavagia I., Nageswarana G., Rolf D.J., Maneta-Peyret L., Luu D.T., Botchway S.W., Webb S.E.D., Mongrand S., Maurel C., Martin-Fernandez M.L.,

Kleine-Vehne J., Friml J., Moreau P., Runions J. (2012) Cell wall constrains lateral diffusion of plant plasma-membrane proteins. *Proc. Nat. Ac. Sci.* **109**, 12805-12810

Martre P., Morillon R., Barrieu F., North G.B., Nobel P.S., Chrispeels M.J. (2002) Plasma membrane aquaporins play a significant role during recovery from water deficit. *Plant Physiol.* **130**, 2101–2110

Marty F. (1999) Plant Vacuoles. *Plant Cell* **11**, 587-600

Mattana M., Vannini C., Espen L., Bracale M., Genga A., Marsoni M., Iriti M., Bonazza V., Romagnoli F., Baldoni E., Coraggio I., Locatelli F. (2007) The rice Mybleu transcription factor increases rolerance to oxygen deprivation in *Arabidopsis* plants. *Physiol. Plant* **131**, 106-121

Maurel C. (1997) Aquaporins and water permeability of plant membranes. *Annu. Rev. Plant Phys. Plant Mol. Biol.* **48**, 399–429

Maurel C. (2007) Plant aquaporins: novel functions and regulation properties. *FEBS Lett.* **581**, 2227-2236

Maurel C. Chrispeels M.J. (2001) Aquaporins. A molecular entry into plant water relations. *Plant Physiol.* **125**, 135-138

Maurel C., Kado R.T., Guern J., Chrispeels M.J. (1995) Phosphorylation regulates the water channel activity of the seed-specific aquaporin alpha-TIP. *EMBO J.* **14**, 3028–3035.

Maurel C., Reizer J., Schroeder J.I., Chrispeels M.J. (1993) The vacuolar membrane protein gamma-TIP creates water specific channels in *Xenopus* oocytes. *EMBO J.* **12**, 2241-2247

Maurel C., Santoni V., Luu D.T., Wudick M.M., Verdoucq L. (2009) The cellular dynamics of plant aquaporin expression and functions. *Curr. Opin. Plant Biol.* **12**, 690-698

Maurel C., Verdoucq L., Luu D.T., Santoni V. (2008) Plant aquaporins: membrane channels with multiple integrated functions. *Annu. Rev. Plant Biol.* **59**, 595–624

Mathur J., Radhamony R., Sinclair A.M., Donoso A., Dunn N., Roach E., Radford D., Mohaghegh M.P., Logan D.C. Kokolic K., Mathur N. (2010) mEosFP-based green-to-red photoconvertible subcellular probes for plants. *Plant Physiol.* **154**, 1573-1587

Meister G., Tuschl T. (2004) Mechanisms of gene silencing by double-stranded RNA. *Nature* **431**, 343-349

Mello C.C., Conte D. (2004) Revealing the world of RNA interference. *Nature* **431**, 338-342

Melroy D.L., Herman E.M. (1991) TIP, an integral membrane protein of the protein-storage vacuoles of the soybean cotyledon undergoes developmentally regulated membrane accumulation and removal. *Planta* **184**, 113-122

Michel B.E., Kaufmann M.R. (1973) The osmotic potential of polyethylene glycol. *Plant Physiol.* **51**, 914-6

Moshelion M., Becker D., Biela A., Uehlein N., Hedrich R., Otto B., Levi H., Moran N., Kaldenhoff R. (2002) Plasma membrane aquaporins in the motor cells of *Samanea saman. The Plant Cell* **14**, 727-739

Mitani-Ueno N., Yamaji N., Zhao F.J., Ma J.F. (2011) The aromatic/arginine selectivity filter of NIP aquaporins plays a critical role in substrate selectivity for silicon, boron, and arsenic. *J. Exp. Bot.* **62**, 4391–4398

Murata K., Mitsuoka K., Hirai T., Walz T., Agre P., Heymann J.B., Engel A., Fujiyoshi Y. (2000) Structural determinants of water permeation through aquaporin-1. *Nature* **407**, 599-605

Mizutani M., Watanabe S., Nakagawa T., Maeshima M. (2006) Aquaporin NIP2;1 is mainly localized to the ER membrane and shows root-specific accumulation in *Arabidopsis thaliana. Plant Cell Physiol.* **47**, 1420-1426

Naested H., Frandsen G.I., Jauh G.Y., Hernandez-Pinzon I., Nielsen H.B., Murphy D.J., Rogers J.C., Mundy J. (2000) Caleosins: Ca2+-binding proteins associated with lipid bodies. *Plant Mol Biol.* **44**, 463-76

Nagel O.W., Konings H., Lambers H. (1994) Growth rate, plant development and water relations of the ABA-deficient tomato mutant *sitiens. Phys. Plant*. **92**, 102-108

Nakabayashi K., Okamoto M., Koshiba T., Kamiya Y., Nambara E. (2005) Genome-wide profiling of stored mRNA in Arabidopsis thaliana seed germination: epigenetic and genetic regulation of transcription in seed. *Plant J.* **41**, 697-709

Nardini A., Salleo S. (2005) Water stress-induced modifications of leaf hydraulic architecture in sunflower: co-ordination with gas exchange. *J. Exp. Bot.* **56**, 3093–3101

Nebenfuhr A., Ritzenthaler C., Robinson D.G. (2002) Brefeldin A: deciphering an enigmatic inhibitor of secretion. *Plant Physiol.* **130**, 1102–1108

Nienhaus U.G. Nienhaus K., Holzle A., Ivanchenko S., Renzi F., Oswald F., Wolff M., Schmitt F., Rocker C., Vallone B., Weidemann W., Heilker R., Nar H., Wiedenmann J. (2006) Symposium-in-Print: Green Fluorescent Protein and homologs, photoconvertible fluorescent protein EosFP: biophysical properties and cell biology applications. *Photochem. and Photobiol.* **82**, 351-358

Novikova G.V., Tournaire-Roux C., Sinkevich I.A., Lityagina S.V., Maurel C., Obroucheva N. (2014) Vacuolar biogenesis and aquaporin expression at early germination of broad bean seeds. *Plant Phys. and Biochem.* **82**, 123-132

Nyblom M., Frick A., Wang Y., Ekvall M., Hallgren K., Hedfalk K., Neutze R., Tajkhorshid E., Tornroth-Horsefield S. (2009) Structural and functional analysis of SoPIP2;1 mutants adds insight into plant aquaporin gating. *J. Mol. Biol.* **387**, 653-668

Obroucheva N.V. (2013) Aquaporins in seeds. *Seed Sci. Res.* **23**, 213-216

Olbrich A., Hillmer S., Hinz G., Oliviusson P., Robinson D.G. (2007) Newly formed vacuoles in root meristems of barley and pea seedlings have characteristics of both protein storage and lytic vacuoles. *Plant Physiol.* **145**, 1383-1394

Olkkonen V., Stenmark H. (1997) Role of Rab GTPases in membrane traffic. *Int. Rev. Cytol.***176**, 1-85

Otegui M.S., Herder R., Schulze J., Jung R., Staehelin L.A. (2006) The proteolytic processing of seed storage proteins in Arabidopsis embryo cells starts in the multivesicular bodies. *Plant Cell* **18**, 2567-2581

Otegui M.S., Noh Y.S., Martínez D.E., Vila Petroff M.G., Staehelin L.A., Amasino R.M., Guiamet J.J. (2005) Senescence-associated vacuoles with intense proteolytic activity develop in leaves of Arabidopsis and soybean. *Plant J.* **41**, 831-844

Ouffatole M., Park J.H. Pozleitner M., Jiang L., Rogers J.C. (2005) Selective membrane protein internalization accompanies movement from the Endoplasmic Reticulum to the Protein Storage Vacuole pathway in Arabidopsis. *Plant Cell* **17**, 3066-3080

Palauqui J.C., Elmayan T., De Borne F.D., Crete P., Charles C., Vaucheret H. (1996) Frequencies, timing, and spatial patterns of co-suppression of Nitrate Reductase and Nitrite Reductase in transgenic tobacco plants. *Plant Physiol.* **112**, 1447-1456

Paris, N., Stanley, C.M., Jones, R.L. and Rogers, J.C. (1996) Plant cells contain two functionally distinct vacuolar compartments. *Cell* **85**, 563–572

Park M., Jin Kim S., Vitale A., Hwang I. (2004) Identification of the protein storage vacuole and protein targeting to the vacuole in leaf cells of three plant species. *Plant Physiol.* **134**, 625–639

Paudyal R., Jamaluddin A., Warren J.P., Doyle S.M., Robert S., Warriner S.L., Baker A. (2014) Trafficking modulator TENin1 inhibits endocytosis, causes endomembrane protein accumulation at the pre-vacuolar compartment and impairs gavitropic response in *Arabidopsis thaliana. Biochem J.* **460**, 177-185

Pedrazzini E., Komarova N.Y., Rentsch D., Vitale A. (2013) Traffic routes and signals for the Tonoplast. *Traffic* **14**, 622-628

Penfield S., Pinfield-Wells H.M., Graham I.A. (2006) Storage reserve mobilisation and seedling establishment in Arabidopsis. The Arabidopsis Book**:** e0100

Peng Y., Lin W., Cai W., Arora R. (2007) Overexpression of a *Panax ginseng* tonoplast aquaporin alters salt tolerance, drought tolerance and cold acclimation ability in transgenic Arabidopsis plants. *Planta* **226**, 729–740

Peret B., Li G., Zhao J., Band L.R., Voss U., Postaire O., Luu D.T., Da Ines O., Casimiro I., Lucas M., Wells D.M., Lazzerini L., Nacry P., King J.R., Jensen O.E., Schaffner A.R., Maurel C., Bennett M.J. (2012) Auxin regulates aquaporin function to facilitate lateral root emergence. *Nat. Cell Biol*. **14**, 991-998

Phillips A.L., Huttly A.K. (1994) Cloning of two gibberellin-regulated cDNAs from *Arabidopsis thaliana* by subtractive hybridization: expression of the tonoplast water channel, γ-TIP, is increased by GA3. *Plant Mol. Biol.* **24**, 603-615

Postaire O., Tournaire-Roux C., Grondin A., Boursiac Y., Morillon R., Schaeffner A.R., Maurel C. (2010) A PIP1 aquaporin contributes to hydrostatic pressure-induced water transport in both the root and rosette of Arabidopsis. *Plant Physiol.* **152**, 1418-30

Potenza C., Aleman L., Sengupta-Gopalan C. (2004) Invited review: targeting transgene expression in research, agricultural, and environmental applications: promoters used in plant transformation. *In Vitro Cell. Dev. Biol.—Plant* **40**, 1–22

Poxleitner M., Rogers S.W., Samuels A.L., Browse J. and Rogers J.C. (2006) A role for caleosin in degradation of oil-body storage lipid during seed germination. *Plant J.* **47**, 917–933

Prado K., Boursiac Y., Tournaire-Roux C., Monneuse J.M., Postaire O., Da Ines O., Schaeffner A.R., Hem S., Santoni V., Maurel C. (2013) Regulation of Arabidopsis leaf hydraulics involves light-dependent phosphorylation of aquaporins in veins. *Plant Cell.* **25**, 1029-1039

Prak S., Hem S., Boudet J., Viennois G., Sommerer N., Rossignol M., Maurel C., Santoni V. (2008) Multiple phosphorylations in the C-terminal tail of plant plasma membrane aquaporins: role in subcellular trafficking of AtPIP2;1 in response to salt stress. *Mol. Cell Prot.* **7**, 1019-1030

Preston G.M., Jung J.S., Guggino W.B., Agre P. (1993) The mercury-sensitive residue at cysteine 189 in the CHIP28 water channel. *J. Biol. Chem.* **268**, 17-20

Rath A., Glibowicka M., Nadeau V.G., Chen G., Deber C.M. (2009) Detergent binding explains anomalous SDS-PAGE migration of membrane proteins. *Proc. Nat. Ac. Sci.* **106**, 1760-1765

Raven P.H., Evert R.F., Eichorn S.E. (2005) Biology of Plants. 7th Ed. USA: W.H. Freeman and Company Publishers

Richter S., Geldner N., Schrader J., Wolters H., Stierhof Y.D., Rios G., Koncz C., Robinson D.G. Jurgens G. (2007) Functional diversification of closely related ARF-GEFs in protein secretion and recycling. *Nat. Lett.* **488**, 488-493

Rivera-Serrano E.E., Rodriguez-Welsh M.F., Hicks G.R., Rojas-Pierce M. (2012) A small molecule inhibitor partitions two distinct pathways for trafficking of Tonoplast Intrinsic Proteins in Arabidopsis. *PLOS ONE* **27**, e44735

Rivers R.L., Dean R.M., Chandy G., Hall J.E., Roberts D.M., Zeidel M.L. (1997) Functional analysis of nodulin 26, an aquaporin in soybean root nodule symbiosomes. *J Biol Chem.* **272**, 16256-16261

Robinson A.S. (2011) Production of membrane proteins: Strategies for expression and isolation. 1st Ed. USA. Wiley-VCH

Robinson D., Haschke H., Hinz G., Hoh B., Maeshima M. & Marty F. (1996) Immunological detection of tonoplast polypeptides in the plasma membrane of pea cotyledons. *Planta* **198**, 95-103

Robinson D.G., Langhans M., Saint-Jore-Dupas C., Hawes C. (2008) BFA effects are tissue and not just plant specific. *Trends Plant Sci.* **13**, 405-408

Robinson M.S. (2004) Adaptable adaptors for coated vesicles. *Trends Cell Biol.* **14**, 167–174

Rojas-Pierce M. (2013) Targeting of tonoplast proteins to the vacuole. *Plant Sci.* **211**, 132-136

Rojo E., Denecke J. (2008) What is moving in the secretory pathway of plants? *Plant Physiol.* **147**, 1493-1503

Rojo E., Gillmor C.S., Kovaleva V., Somerville C.R., Raikhel N.V. (2001) VACUOLELESS1 is an essential gene required for vacuole formation and morphogenesis in Arabidopsis. *Dev. Cell.* **1**, 303-310.

Ruiz-Lozano J.M., del Mar Alguacil M., Bárzana G., Vernieri P., Aroca R. (2009) Exogenous ABA accentuates the differences in root hydraulic properties between mycorrhizal and nonmycorrhizal maize plants through regulation of PIP aquaporins. *Plant Mol. Biol.* **70**, 565–579

Runions J., Brach T., Kuhner S., Hawes C. (2006) Photoactivation of GFP reveals protein dynamics within the endoplasmic reticulum membrane. *J Exp Bot* **57**, 43–50

Sakurai-Ishikawa J., Murai-Hatano M., Hayashi H., Ahamed A., Fukushi K., Matsumoto T., Kitagawa Y. (2011) Transpiration from shoots triggers diurnal changes in root aquaporin expression. *Plant Cell Env.* **34**, 1150-1163

Sakurai J., Ishikawa F., Yamaguchi T., Uemura M., Maeshima M. (2005) Identification of 33 rice aquaporin genes and analysis of their expression and function. *Plant Cell Phys.* **46**, 1568-1577

Sade N., Vinocur B.J., Diber A., Shatil A., Ronen G., Nissan H., Wallach R., Karchi H., Moshelion M. (2009) Improving plant stress tolerance and yield production: is the tonoplast aquaporin SlTIP2;2 a key to isohydric to anisohydric conversion? *New Phytol.* **181**, 651-661

Sade N., Gebremedhin A., Moshelion M. (2012) Risk-taking plants: Anisohydric behavior as a stress-resistance trait. *Plant Sig. & Behav.* **7**, 767–770

Sarda X., Tousch D., Ferrare K., Cellier F., Alcon C., Dupuis J.M., Casse F., Lamaze T. (1999) Characterization of closely related δ-TIP genes encoding aquaporins which are differentially expressed in sunflower roots upon water deprivation through exposure to air. *Plant Mol. Biol.* **40**, 179-191

Scarafoni A., Carzaniga R., Harris N., Croy R.D. (2001) Manipulation of the napin primary structure alters its packaging and deposition in transgenic tobacco (*Nicotiana tabacum L.*) seeds. Plant Mol. Biol. **46**, 727–739

Schmid M., Davison, T.S., Henz S. R., Pape U. J., Demar, M., Vingron, M., Scholkopf B., Weigel, D. & Lohmann, J.U. (2005) A gene expression map of *Arabidopsis thaliana* development. *Nat. Gen.* **37**, 501-506

Schopfer P. (2006) Biomechanics of plant growth. *Am. J. Bot.* **93**, 1415-1425

Schussler M.D., Alexandersson E., Bienert G.P., Kichey T., Laursen K.H., Johanson U., Kjellbom P., Schjoerring J.K., Jahn T.P. (2008) The effects of the loss of TIP1;1 and TIP1;2 aquaporins in *Arabidopsis thaliana*. *Plant J.* **56**, 756-767

Sheahan M.B., Staiger C.J., Rose R.J., McCurdy D.W. (2004) A green fluorescent protein fusion to Actin Binding Domain 2 of Arabidopsis Fimbrin highlights new features of a dynamic actin cytoskeleton in live plant cells. *Plant Phys.* **136**, 3968-3978

Shimada T.L., Shimada T., Hara-Nishimura I. (2010) A rapid and non-destructive screenable marker, FAST, for identifying transformed seeds of *Arabidopsis thaliana*. *Plant J.* **61**, 519-28

Shimada T.L., Shimada T., Takahashi H., Fukao Y. and Hara-Nishimura I. (2008) A novel role of oleosins in freezing tolerance of oilseeds in *Arabidopsis thaliana*. *Plant J.* **55**, 798-809

Siefritz F., Tyree M.T., Lovisolo C., Schubert A., Kaldenhoff R. (2002) PIP1 plasma membrane aquaporins in tobacco: from cellular effects to function in plants. *Plant Cell* **14**, 869–876

Siloto R.M., Findlay K., Lopez-Villalobos A., Yeung E.C., Nykiforuk C.L., Moloney M.M. (2006) The accumulation of oleosins determines the size of seed oilbodies in Arabidopsis. *Plant Cell* **18**, 1961-1974

Sliwinska E., Bassel G.W., Bewley J.D. (2009) Germination of *Arabidopsis thaliana* seeds is not completed as a result of elongation of the radicle but of the adjacent transition zone and lower hypocotyl. *J. Exp. Bot.* **60**, 3587-3594

Smart L.B., Moskal W.A., Cameron K.D., Bennett A.B. (2001) MIP genes are down-regulated under drought stress in *Nicotiana glauca*. *Plant Cell Physiol*. **42**, 686-693

Sorieul M., Santoni V., Maurel C., Luu D.T. (2011) Mechanisms and effects of retention of over-expressed aquaporin AtPIP2;1 in the endoplasmic reticulum. *Traffic* **12**, 473-482

Staff L., Hurd P., Reale L., Seoighe C., Rockwood A., Gehring C. (2012) The hidden geometrics of the *Arabidopsis thaliana* epidermis. *PLoS One 7*, e43546

Steudle E. (2001) The cohesion-tension mechanism and the acquisition of water by plant roots. *Ann. Rev. Plant Phys. Plant Mol. Biol.* **52**, 847-875

Steudle E., Peterson C.A. (1998) How does water get trough roots? *J. Exp. Bot.* **49**, 775-788

Suga S., Murai M., Kuwagata T., Maeshima M. (2003) Differences in aquaporin levels among cell types of radish and measurement of osmotic water permeability of individual protoplasts. *Plant Cell Phys*. **44**, 277-286

Sun M.-H., Xu W., Zhu Y.-F., Su W.-A., Tang Z.-C. (2001) A simple method for *In Situ* hybridization to RNA in guard cells of *Vicia Faba* L.: The expression of aquaporins in guard cells. *Plant Mol. Biol. Rep.* **19**, 129-135

Swanson S.J., Bethke P.C., Jones R.L. (1998) Barley aleurone cells contain two types of vacuoles. Characterization Of lytic organelles by use of fluorescent probes. *Plant Cell* **10**, 685-698

Tajkhorshid E., Nollert P., Jensen M.Ø., Miercke L.J., O'Connell J., Stroud R.M., Schulten K. (2002) Control of the selectivity of the aquaporin water channel family by global orientational tuning. *Science* **296**, 525-530

Takano J. Tanaka M., Toyoda A., Miwa K. Kasai K., Fuji K., Onouchi H., Naito S., Fujiwara T. (2010) Polar localization and degradation of *Arabidopsis* boron transporters through distinct trafficking pathways. *Proc. Nat. Ac. Sci.* **107**, 5220-5225

Takano J., Wada M., Ludewig U., Schaaf G., von Wirén N., Fujiwara T. (2006) The Arabidopsis major intrinsic protein NIP5;1 is essential for efficient boron uptake and plant development under boron limitation. *Plant Cell* **18**, 1498–1509

Tao P., Zhong X., Li B., Wang W., Yue Z., Lei J., Guo W., Huang X. (2014) Genome-wide identification and characterization of aquaporin genes (AQPs) in Chinese cabbage (*Brassica rapa ssp. pekinensis*). *Mol. Genet. Genomics.* [Epub ahead of print]

The O., Moore I. (2007) An ARF-GEF acting at the Golgi and in selective endocytosis in polarized plant cells. *Nat. Lett.* **488**, 493-497

Thompson A.J., Andrews J., Mulholland B.J., McKee J.M.T., Hilton H.W., Horridge J.S., Farquhar G.D., Smeeton R.C., Smillie I.R.A., Black C.R., Taylor I.B. (2007) Overproduction of abscisic acid in tomato increases transpiration efficiency and root hydraulic conductivity and influences leaf expansion. *Plant Physiol.* **143**, 1905-1917

Tornroth-Horsefield S., Wang Y., Hedfalk K., Johanson U., Karlsson M., Tajkhorshid E., Neutze R., Kjellbom P. (2006) Structural mechanism of plant aquaporin gating. *Nature* **439**, 688-694

Tournaire-Roux C., Sutka M., Javot H., Gout E., Gerbeau P., Luu D.T., Bligny R., Maurel C. (2003) Cytosolic pH regulates root water transport during anoxic stress through gating of aquaporins. *Nature* **425**, 393-397

Tuschl T., Zamore P.D., Lehmann R., Bartel D.P., Sharp P.A. (1999) Targeted mRNA degradation by double-stranded RNA in vitro. *Genes Dev.* **13**, 3191-7

Tyrrell M., Campanoni P., Sutter J.U., Pratelli R., Paneque M., Sokolovski S., Blatt M.R. (2007) Selective targeting of plasma membrane and tonoplast traffic by inhibitory (dominant-negative) SNARE fragments. *Plant J.* **51**, 1099-1115

Tzen J.T. and Huang A.H. (1992) Surface structure and properties of plant seed oil bodies. *J. Cell Biol.* **117**, 327–335.

Tzen J.T., Lie G.C., Huang A.H. (1992) Characterization of the charged components and their topology on the surface of plant seed oil bodies. *J. Biol. Chem.* **267**, 15626–15634.

Tzen J.T.C., Cao Y., Laurent P., Ratnayake C., Huang A.H.C. (1993) Lipids, Proteins, and Structure of Seed Oil Bodies from Diverse Species. *Plant Physiol.* **101**, 267-276

Uehlein N., Sperling H., Heckwolf M., Kaldenhoff R. (2012) The *Arabidopsis* aquaporin PIP1;2 rules cellular CO(2) uptake. *Plant Cell Environ.* **35**, 1077-1083.

Uehlein N., Lovisolo C., Siefritz F., Kaldenhoff R. (2003) The tobacco aquaporin NtAQP1 is a membrane CO2 pore with physiological functions. *Nature* **425**, 734-737

Uehlein N., Otto B., Hanson D.T., Fischer M., McDowell N., Kaldenhoff R. (2008) Function of *Nicotiana tabacum* aquaporins as chloroplast gas pores challeneged the concept of membrane CO_2 permeability. *The Plant Cell* **20**, 648-657

Valencia-Sanchez M.A. Liu J. Hannon G.J. (2006) Control of translation and mRNA degradation by miRNAs and siRNAs. *Genes and Dev.***20**, 151-524

Vallejo A.J., Yanovsky M.J., Botto J.F. (2010) Germination variation in *Arabidopsis thaliana* accessions under moderate osmotic and salt stresses. *Ann Bot.* **106**, 833–842

van der Weele C.M., Spollen W.G., Sharp R.E., Baskin T.I. (2000) Growth of *Arabidopsis thaliana* seedlings under water defecit studied by control of water potential in nutrient-agar media. *J. Exp. Bot.* **51**, 1555-1562

Vandeleur R.K., Mayo G., Shelden M.C., Gilliham M., Kaiser B.N., Tyerman S.D. (2009) The role of plasma membrane intrinsic protein aquaporins in water transport through roots: diurnal and drought stress responses reveal different strategies between isohydric and anisohydric cultivars of grapevine. *Plant Physiol.* **149**, 445-460

Vandeleur R.K., Sullivan W., Athman A., Jordans C., Gilliham M., Kaiser B.N., Tyerman S.D. (2014) Rapid shoot-to-root signalling regulates root hydraulic conductance via aquaporins. *Plant Cell Environ.* **37**, 520-538

Vander Willigen, C., Postaire, O., Tournaire-Roux, C., Boursiax, Y. & Maurel, C. (2006) Expression and inhibition of aquaporins in germinating *Arabidopsis* seeds. *Plant Cell Phys.* **47**, 1241-1250

Verdoucq L., Grondin A., Maurel C. (2008) Structure-function analysis of plant aquaporin AtPIP2;1 gating by divalent cations and protons. *Biochem J*. **415**, 409-416

Veselova T., Veselovskii V., Usmanov P., Usmanova O. (2003) Hypoxia and imbibition injuries to aging seeds. *Russ. J. Plant Physiol*. **50**, 835–842

Wallace I.S., Roberts D.M. (2004) Homology modeling of representative subfamilies of Arabidopsis major intrinsic proteins. Classification based on the aromatic/arginine selectivity filter. *Plant Physiol.* **135**, 1059–1068

Wang X., Li Y., Ji W., Bai X., Cai H., Zhu A., Sun X.L., Chen L.J., Zhu Y.M. (2011) A novel Glycine soja tonoplast intrinsic protein gene responds to abiotic stress and depresses salt and dehydration tolerance in transgenic *Arabidopsis thaliana. J. Plant Physiol.* **168**, 1241–1248

Weidemann J., Ivanchenko S., Oswald F., Schmitt F., Rocker C., Salih A., Spindler K.D., Nienhaus G.U. (2004) EosFP, a fluorescent marker protein with UV-inducible green-to-red fluorescence conversion. *Proc. Nat. Ac. Sci.* **101**, 15905–15910

Weitbrecht K., Mueller K., Leubner-Metzger G. (2011) First off the mark: early seed germination. *Journal Exp. Bot.* **62**, 3289-309

Welbaum G., Bradford K., Yim K.-O., Booth D., Oluoch M. (1998) Biophysical, physiological and biochemical processes regulating seed germination. *Seed Sci. Res.* **8**, 161–172

Wilkinson J.E., Twell D., Lindsey K. (1997) Activities of CaMV 35S and nos promoters in pollen: implications for field release of transgenic plants. *J. Exp. Bot.* **48**, 265-275

Wolfenstetter S., Wirsching P., Dotzauer D., Schneider S., Sauer N. (2012) Routes to the Tonoplast: the sorting of Tonoplast transporters in *Arabidopsis* mesophyll protoplasts. *Plant Cell* **24**, 215-32

Wudick M.M., Luu D.T., Tournaire-Roux C., Sakamoto W., and Maurel C. (2014) Vegetative and sperm cell-specific aquaporins of *Arabidopsis* highlight the vacuolar equipment of pollen and contribute to plant reproduction. *Plant Physiol.* **164**, 1697-1706

Zamore P.D., Tuschl T., Sharp P.A., Bartel D.P. (2000) RNAi: double-stranded RNA directs the ATP-dependent cleavage of mRNA at 21 to 23 nucleotide intervals. *Cell* **101**, 25-33

Zelazny E., Borst J.W., Muylaert M., Batako H., Hemminga M.A., Chaumont F. (2007) FRET imaging in living maize cells reveals that plasma membrane aquaporins interact to regulate their subcellular localization. *Proc. Natl. Acad. Sci.* **104**, 12359–12364

Zelazny E., Miecielica U., Borst J.W., Hemminga M.A., Chaumont F. (2009) An N-terminal diacidic motif is required for the trafficking of maize aquaporins ZmPIP2;4 and ZmPIP2;5 to the plasma membrane. *Plant J.* **57**, 346-355

Zhang C., Halsey L.E., Szymanski D.B. (2011) The development and geometry of shape change in *Arabidopsis thaliana* cotyledon pavement cells. *BMC Plant Bio* **11**, 1-13

Zhang L., Jiang D., Pang J., Chen R., Wang X., Yang D. (2013) The endoplasmic reticulum stress induced by highly expressed OsrAAT reduces seed size via pre-mature programmed cell death. *Plant Mol. Biol.* **83**, 153–161

Zheng H., Staehelin A. (2011) Protein Storage Vacuoles are transformed into Lytic Vacuoles in root meristematic cells of germinating seedlings by multiple, cell type-specific mechanisms. *Plant Physiol.* **155**, 2023–2035

Zhang J., Zhang X., Liang J. (1995) Exudation rate and hydraulic conductivity of maize roots are enhanced by soil drying and abscisic acid treatment. *New Phytol*. **131**, 329–336

Zhou S., Hu W., Deng X., Ma Z., Chen L., Huang C., Wang C., Wang J., He Y., Yang G., He G. (2012) Overexpression of the Wheat aquaporin gene, TaAQP7, enhances drought tolerance in transgenic Tobacco. *PLOS ONE* **7**, 1-14